Investigating the tumour promoting roles of complement membrane attack complex using global gene expression analysis.

By

Laurence David Towner

A thesis submitted to Cardiff University in candidature for the degree of Doctor of Philosophy.

Institute of Infection and Immunity,

School of Medicine,

Cardiff University,

Cardiff,

Wales, United Kingdom.

November 2013

Abstract

Activation of complement and its terminal pathway leads to the formation and insertion of the membrane attack complex (MAC) in the membranes of target cells. Complement is activated in tumours as is clear from the presence of complement activation products in cancer tissues. Over-expression of membrane bound complement regulators on tumour cells together with endogenous recovery mechanisms restricts complement activity and results in escape from lytic killing; nevertheless, sublytic MAC deposition is not without consequence. Sublytic MAC assembly on nucleated cells causes cell activation, secretion of extracellular matrix and pro-inflammatory cytokines and may cause protection from apoptosis. Signalling of these events is unclear.

The global effects of sublytic MAC were addressed in the murine colon carcinoma cell line (CT26) through the use of microarray technology. Cells were exposed to sublytic complement attack using pooled normal human serum (pNHS) and compared to MAC-inhibited controls generated using pNHS containing the C5 inhibitor OmCI. Total RNA was extracted at 0, 1 and 12 hours post-exposure and subjected to microarray analysis using the Illumina platform. Top statistically significant changes were then identified and a list of genes upregulated at both time points was uploaded to MetaCore and a gene network generated. From this a number of co-regulated genes which converged on the EGFR were highlighted. These were cxcl1, amphiregulin and matrix metalloproteinases (Mmp) 3 and 13. Both the top statistically significant and network derived genes were validated using qPCR. Changes in protein levels were then tested using western blot analyses for Mmp3 and Areg. Inhibition of the MEK/ERK, and to a lesser extent PI3K/Akt, signalling suppressed the gene upregulation that occurred in response to MAC but inhibition of p38 and JNK had no effect, implicating a MEK/ERK- PI3K co-activation. MAC deposition and not C5a/C5aR axis signalling was shown to be responsible for the mmp3 gene upregulation response.

Identification of MAC-mediated events and the signalling pathways involved may provide insight into the mechanisms by which complement activation influences tumour growth. In particular the data suggest that sublytic MAC deposition might promote a gene expression response which pushes the cells to a more aggressive phenotype by the upregulation of proliferative, survival, invasion and migratory signals. This in turn will inform strategies that seek to harness complement or complement regulation in tumour immunotherapy.

Acknowledgements

I would first like to thank my excellent supervisors, Dr Timothy Hughes and Professor B. Paul Morgan for their unending support, guidance, advice, encouragement, and help. Their scientific wisdom and experience, combined with their willingness to convey it, has been invaluable to this project. I will be forever grateful for their friendship and support through some difficult times, I couldn't hope to have done this without them.

I feel extremely fortunate to have worked with some fantastic scientists and great people in the lab. Special thanks to Dr. Martin Kolev, Dr. Meike Heurich, Dr. Svetlana Hakobyan, Dr. Daniella Cavalcante, Mrs Dawn Roberts and Dr. Jo Giles for instructing me in many of the techniques I used in this project as well as coaching me to think like a scientist. Thank you to Prof. Claire Harris for kindly providing several of her reagents as well as her help and advice. Thank you also to Dr. Carmen Van den Berg and Dr. Jack Ham for running the C5aR experiments for me.

Thank you to my long suffering girlfriend, Michelle, who has been through hell and back with me and my 'PhD'. This thesis is dedicated to her and her willingness to stick by me through the good times and the really bad! I would also like to thank my twin brother, Chris, who was always and forever will be on the other end of a phone. I owe my deepest gratitude to all my family, especially Mum and Dad, who have supported me in whatever I wanted to do and been there to help me whenever I have needed it.

I feel very lucky to have met some wonderful people and make some true friends during the last 4 years in Cardiff: Martin Kolev always had time for a good chat and was never one to refuse a trip to the pub; a trip to the canteen with Lana Hakobyan and Paul Mitchell was always a treat; tea and cake with Dawn Roberts, Jo Giles, Jo Welton, Meike heurich , Tim Hughes and Lana Hakobyan ensured that my blood sugar levels never dropped too low; Martin 'Magic' Scurr, Maria 'I'm the happiest Christmas tree' Stacey, Gabrielle Stack, Matthieu Besneux, and the rest of 3F04 are the most awesome bunch in all of UHW and the most Christmassy office in December of 2012! You'll miss my carols this year. What a great group of people, always something to laugh and joke about and never a dull moment.

Abbreviations

aa	Amino acid
AA	Arachidonic acid
ANOVA	Analysis of variance
AP-1	Activator protein 1
Areg/AR	Amphiregulin gene/protein
C	Complement
C5aR	C5a receptor
C5L2	C5a receptor like 2
C6D	C6 depleted serum
cAMP	Cyclic adenosine monophosphate
CDC	Complement dependent cytotoxicity
CM	Conditioned medium
COX	Cyclooxygenase
cPLA2	Phospholipase A2
Cxcl1/CXCL1	C-X-C motif ligand 1 (gene/protein)
d/upH_2O	De-ionized/ultrapure water
CD55	Decay accelerating factor
DAG	Diacyl glycerol
ECM	Extra-cellular matrix
EGF	Epidermal growth factor
EGFR	EGF receptor
ERK	Extracellular signal-regulated kinases
FBS	Fetal bovine serum
FDR	False discovery rate
Hb-egf/HB-EGF	Heparin binding-EGF (gene/protein)
IKKβ	IkappaB kinase beta
IL	Interleukin (1β, 6, 8, 11)
JNK1	c-Jun N-terminal protein kinases
LPS	Lipopolysaccharide

mAb	Monoclonal antibodies
MAC	Membrane attack complex of complement
MAPK	Mitogen activated protein kinase
mCRegs	Membrane-associated complement regulators
MIP-2	Macrophage inflammatory protein 2
Mmp/MMP	Matrix metalloproteinase (2, 9, 3, 13) (gene/protein)
mRNA	Messenger RNA
MW	Molecular weight
NADPH	Nicotinamide adenine dinucleotide phosphate
NALP-3	NACHT, LRR and PYD domains-containing protein 3
NFκB	Nuclear factor kappa B
OLG	Oligodendrocytes
OmCI	*Ornithodoros moubata* complement inhibitor
PCR	Polymerase chain reaction
PDGF	Platelet-derived growth factor
PI3K	Phosphoinositide 3-kinase
PKC	Protein kinase C
pNHS	Pooled normal human serum
qPCR	Quantitative PCR
RGC-32	Response gene to complement 32
RNS	Reactive nitrogen species
ROS	Reactive oxygen species
RPE	Retinal pigment epithelial cells
RTK	Receptor tyrosine kinase
ShEA	Activated sheep erythrocytes
TGFβ	Transforming growth factor
TNFα	Tumour necrosis factor α
WCE	Whole cell extract

Table of contents

1 Introduction

1.1 Complement System

1.1.1 Introduction

A bacteriolytic activity of serum first described by Hans EA Buchner had been extensively studied at the end of the 19th century and was shown to have heat labile and heat stable components. The heat labile component was later referred to as complement (C) by Paul Ehrlich in the late 1890s, a term deriving from its apparent 'complementation' of antibody action, but it is Jules Bordet who is generally credited with C's discovery (Morley & Walport, 2000). Bordet's observation was that heat treated immune serum (from an immunized animal) lost its bacteriolytic capacity but, when combined with a non-immune unheated serum, could cause bacteriolysis in the same way as unheated immune serum (Laurell, 1990).

C is a key part of innate immunity, providing an early warning signal and fast response upon encountering a foreign antigen. It is a system of proteins found in the serum which function as a proteolytic cascade amplifying an initial signal. The system is populated by roughly 30 proteins found in the fluid phase and on cell surfaces (Walport, 2001a).

The role that C plays in immunity is multifaceted and complex. It functions in infection control through cytolysis of invading pathogens, opsonization for phagocytosis and release of anaphylatoxins which recruit and activate immune cells (Walport, 2001a). It is also important in immune complex clearance (Schreibe.Ad & Frank, 1972). C can act as a bridge between innate and adaptive immunity helping to regulate B and T cell responses (Carroll, 2000; Dunkelberger & Song, 2010). Apart from these key immune functions it is implicated in processes including regulation during development of neuronal networks (Schafer et al, 2012).

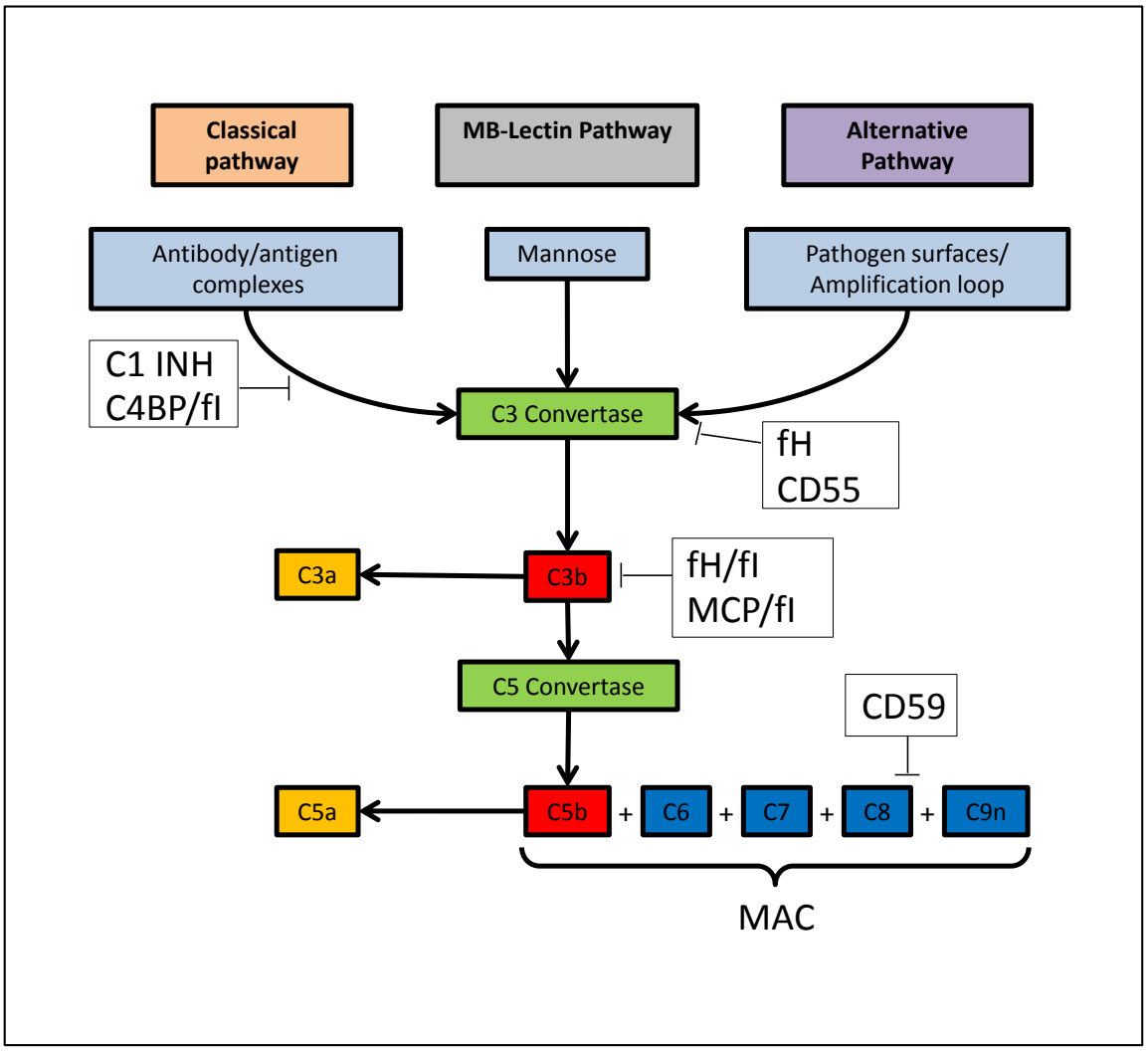

Figure 1.1.1.1 C cascade is activated through three triggering pathways which respond to antibody/antigen (classical), mannose sugars (MBL) and foreign surfaces/spontaneous tickover (alternative). The pathways converge on a C3 convertase which forms on the triggering surface and cleaves C3 into C3b and C3a. C3b deposits on local membrane allowing the further formation of C3-convertase enzymes and leading to the alteration of substrate specificity of the convertase from C3 to C5. C5 convertase then cleaves C5 into C5b and C5a. C5a is a potent anaphylatoxin capable of attracting and activating local immune cells. C5b is then able to bind C6 and be released from the surface. C5b6 once bound to C7 and C8 begins to deposit and puncture the membrane and allow C9 polymerisation and formation of a MAC pore.

1.1.2 **Activation**

C activates in response to several stimuli and is initiated by three activation pathways, the classical pathway which is primarily initiated by antibody:antigen complexes, the alternative pathway activated spontaneously by a tickover mechanism independently of antibody or as an amplification loop, and the mannose binding lectin pathway activated by mannose containing proteins or carbohydrates (Walport, 2001a).

1.1.2.1 Classical Pathway

Antibody bound with antigen is capable of binding the C1 complex which is then activated. The C1 complex is made up of the large collagen like C1q molecule interacting with a $C1r_2C1s_2$ oligomer. Once the C1q-$C1r_2C1s_2$ complex binds with an antibody-antigen complex it is activated; C1r molecules cleave each other in sequence and then cleave the neighbouring C1s molecules. Once cleaved and activated, C1s can extend out from the C1q scaffold allowing it to interact with the next molecules of the cascade, C4 and C2. C4 is cleaved by C1s releasing the C4a fragment and exposing an internal thioester moiety on the larger fragment C4b. This allows the C4b fragment to bind covalently with available amino or hydroxyl groups on local surfaces. C2 is then able to associate with the bound C4b in a metal-dependent manner where it is cleaved by C1s in an adjacent C1 complex, releasing the C2b fragment. The resulting C4b2a complex is the classical C3 convertase (Müller-Eberhard, 1988).

1.1.2.2 Lectin pathway

The lectin pathway is activated on the binding of either mannan binding lectin (MBL) to carbohydrate molecular patterns or one of three ficolins (L, M or H) to patterns of acetyl groups (Thiel, 2007). Activation is mediated, like the classical pathway, by serine proteases. There are three MBL associated serine proteases (MASPs) MASP-1, 2 and 3. Of these MASP-2 is key in the cleavage of C4 and C2, progressing in much the same way as the classical pathway (Vorup-Jensen et al, 1998). MASP-1 appears to activate MASP-2 in a homologous manner to C1r and C1s and recent evidence suggests that MASP-3 may activate fD thus regulating alternative pathway activation (Sekine et al, 2013).

1.1.2.3 Alternative pathway

The alternative pathway can be considered both an activating pathway and an amplification mechanism. A non-cleaved C3 molecule hydrolysed at the thioester bond, designated C3(H_2O), is capable of behaving like C3b and forming a C3 convertase thus

acting as a constantly activated tickover mechanism (Bexborn et al, 2008; Fishelson et al, 1984). C3(H_2O) binds factor B in the fluid phase, permitting factor B cleavage by the plasma enzyme factor D; Ba is released and the resulting C3(H_2O)Bb complex is an alternative pathway C3 convertase. When C3 is cleaved by C3 convertase or by proteases into C3b (and C3a), C3b can become covalently bound to surfaces and with the binding of factor B and its cleavage by factor D, C3bBb can form and create a surface-bound alternative C3 convertase enzyme (Fearon et al, 1973; Fishelson et al, 1984). The capability of C3b to form new convertase enzymes allows a small activation event to become amplified many fold thus forming a positive feedback amplification loop; properdin which binds and stabilizes the enzyme enhances amplification (Lachmann, 2009; Schwaeble & Reid, 1999).

1.1.2.4 C3

C3 is one of the most abundant proteins in plasma at 1.2 mg/mL (Kohler & Müller-Eberhard, 1967; Morley & Walport, 2000). Each of the activation pathways converge on the central C3 component which is cleaved into two fragments; the smaller C3a anaphylatoxin and the larger C3b opsonin (Walport, 2001a). C3b in plasma or deposited on target surfaces is rapidly cleaved in sequence by regulators to form, first iC3b, then C3c and C3dg (Liszewski et al, 2008). Surfaces enriched in deposited C3b and its cleavage products can adhere to and illicit signals to immune cells expressing relevant receptors, acting as tags (Lambris & Müller-Eberhard, 1986).

1.1.2.5 C5 convertase

Activation of C results in a C3 convertase enzyme being formed, generally the classical/lectin pathway enzyme is C4b2a and the alternative pathway enzyme is either C3bBb or C3(H_2O)Bb. For C activation to progress beyond this point the enzyme must alter specificity from cleavage of C3 to cleavage of C5. Alteration of specificity is dependent on the density of C3b deposited on the target surface, monomeric (C3bBb)

enzymes have a higher affinity for C3b only weakly interacting with C5, but when there is a high density of C3b this affinity shifts towards C5, thought to require the presence of more than one C3b and referred to as C3bBbC3b (Rawal & Pangburn, 2001). Cleavage of C5 into C5b (the larger fragment) and C5a (the smaller anaphylatoxic fragment) marks a key event in C progression (Walport, 2001a; Walport, 2001b). Both fragments have significant roles in C function and immunity. C5a is a potent anaphylatoxic protein released locally, attracting and activating immune cells which express the receptor, C5aR (Monk et al, 2007). C5b marks the start of the terminal pathway.

1.1.3 **Terminal Pathway**

C5b formed from cleavage of C5 is initially in its nascent form C5b*. This short-lived conformation binds to C6 in a stable hydrophilic interaction to form C5b6. The C5b6 complex remains loosely associated with C3b until it binds C7 to create C5b67 complex which initiates a hydrophilic-amphiphilic transition causing its release from the convertase and making it capable of forming a metastable interaction with surface phospholipids. Once bound to the surface, C5b67 recruits and binds C8 which begins the insertion into the membrane via its α chain. C8 now recruits and acts a catalyst for C9 polymerisation; C9 undergoes hydrophilic-amphiphilic transition, unfolding into the membrane and exposing fresh sites for further C9 binding. Polymerization of C9 results in the classical cylindrical pore of the membrane attack complex (MAC) (Müller-Eberhard, 1986).

1.1.4 **Anaphylatoxins and their receptors**

Activation of C results in the formation and release of three anaphylatoxic cleavage products, C4a, C3a and C5a, the smaller fragments of C4, C3 and C5 cleavage respectively. These proteins are each around 10 kDa in mass and have 74-77 amino acid (aa) sequence. They are rapidly inactivated by carboxypeptidases to their desarginine forms (DesArg). Hierarchically the potency of the anaphylatoxins are ordered C5a > C3a >C4a (Hugli, 1984; Zhou, 2012). The anaphylatoxins are named due to their induction of anaphylactic responses when generated in excess, they function on local tissue and cells

by causing contraction of smooth muscle, histamine release, increase in capillary permeability, adhesion of leukocytes to vascular endothelium, leukocyte chemotaxis, and aggregation of platelets and leukocytes (Vogt, 1986).

Specific roles of C3a on ligation to its receptor include eliciting histamine release from mast cells, eosinophils, neutrophils and basophils, thromboxane A release from macrophages, and the secretion of lysosomal enzymes from neutrophils (Lambris, 1988). C3a is capable of inducing vascular permeability and increasing contractility of vessels (Ember et al, 1992) as well as vasodilating activity (Schumacher et al, 1991). It has also been shown to trigger respiratory burst in neutrophils, releasing reactive oxygen species (ROS) and H_2O_2 in response to C3a exposure (Elsner et al, 1994b). C3a also causes respiratory burst in macrophages (Murakami et al, 1993) and eosinophils (Elsner et al, 1994a) and can act as a chemoattractant for eosinophils (Daffern et al, 1995) and mast cells (Nilsson et al, 1996). As a pro-inflammatory mediator, C3a is also capable of triggering cytokine release. In response to C3a *in vitro*, adherent PBMCs released interleukin (IL) -1β, tumour necrosis factor (TNF) -α and IL-6 (Takabayashi et al, 1998; Takabayashi et al, 1996). C3a can also exert influence on tissue cells, inducing IL-8 expression in epithelial cells and both IL-8 and IL-1β in endothelial cells (Monsinjon et al, 2003; Monsinjon et al, 2001).

C5a has influence on neutrophils and macrophages at nanomolar concentrations and is thus significantly more potent than C3a, though it shares many of its functions such as increasing vessel contractility (Ember et al, 1992). C5a has potent neutrophil chemoattractant activity, also influencing macrophages and monocytes (Marder et al, 1985). C5a has been shown to induce oxidative burst in neutrophils as well as enhancing phagocytosis of opsonised bacteria via C receptor (CR) type 3 upregulation (Mollnes et al, 2002; Sacks et al, 1978). It has also been described as having vasodilating activity in a canine model (Schumacher et al, 1991). C5a can modulate expression of cytokines such as macrophage inflammatory protein-2 (MIP-2) and monocyte chemoattractant protein-1

(MCP-1) induced by IL-6 in endothelial cells (Laudes et al, 2002) and TNF-alpha, MIP-2, and cytokine-induced neutrophil chemoattractant-1 (CINC-1) in epithelial cells response to LPS (Riedemann et al, 2002).

C3a and C5a effects are exerted via their ligation to receptors present on the surface of expressing cells. A receptor for C4a has not been described; although originally thought to exert effects through C3aR binding, it is now generally accepted that C4a does not have an important biological function. C3aR, C5aR (CD88) and C5L2 are the three receptors associated with anaphylatoxin responses. Both the C3aR and C5aR are members of the rhodopsin subfamily of G protein-coupled receptors (Gerard & Gerard, 1994). C5aR mediates the majority of responses attributed to C5a with C5L2, a structurally similar receptor but thought to lack signalling activity. C5L2 is only weakly phosphorylated upon binding but has a higher affinity for C5a than C5aR and thus may act as a decoy or scavenger receptor, regulating *in vivo* responses to C5a (Gao et al, 2005; Okinaga et al, 2003).

1.1.5 **Regulation**

C activation is a proteolytic cascade in continual tick-over and is thus capable of enormous amplification. With the powerful results of C activation mediated by the anaphylatoxins and potential for tissue damage mediated by MAC, there is a need for tight control. Around a third of all proteins belonging to the C system are regulatory in function.

1.1.5.1 Soluble regulators

The soluble regulators maintain fluid phase homeostasis, controlling release of inflammatory mediators and preventing depletion of the necessary components.

C1-Inhibitor (C1-INH) is a member of the serpin family of protease inhibitors and is the only classical pathway protease inhibitor present in serum (Ziccardi, 1981). C1-INH regulates activation of the classical pathway primarily by dissociating C1s and C1r from the activated C1 molecule (Davis et al, 2008). Apart from its classical pathway inhibition,

C1-INH is also capable of regulation of the lectin pathway via its inhibition of MASP-2, and has been suggested to cause a non-protease mediated inhibition of alternative pathway activation (Jiang et al, 2001; Kerr et al, 2008).

C4b-binding protein (C4BP) is a large glycoprotein of 500 kDa with regulatory activity for both the classical and lectin pathways (Blom et al, 2004). C4BP possesses factor I (FI) cofactor activity, inactivating soluble and surface bound C4b by catalysing its cleavage to C4c and C4d, thus regulating the formation of the classical C3-convertase enzyme (Fujita et al, 1978). C4BP binds C4b preventing the formation of the classical C3 convertase enzyme as well as acting as a decay accelerator to the forming C4b2a complex (Daha & van Es, 1980; Gigli et al, 1979).

FI is an 88 kDa serine protease and regulator of C3 convertase containing either C3b or C3(H_2O) (Davis, 1981; Hsiung et al, 1982). FI requires a co-factor to cleave C3b and C3(H_2O) into their inactivated forms iC3b and iC3(H_2O) through the cleavage of the α chain into a smaller and larger fragment which remain associated by a disulphide bridge (Pangburn & Müller-Eberhard, 1983). Co-factors, including factor H (FH), C4BP, membrane co-factor protein (MCP/CD46) and CR1 (CD35), direct substrate specificity to either C3b or C4b (Minta et al, 1998). iC3b can be further cleaved to C3c and C3dg when CR1 acts as cofactor (Ross et al, 1983)

FH is a 155 kDa glycoprotein with 20 repeated short consensus repeat (SCR) units making up its 1213 aa sequence (Ripoche et al, 1988; Sim & Discipio, 1982). FH functions as a regulator of the alternative pathway and its C3 convertase via its decay accelerating activity as well as its co-factor activity mediating FI cleavage of C3b as described above (Pangburn et al, 1977; Weiler et al, 1976; Whaley & Ruddy, 1976). FH functions as decay accelerator for alternative and classical C3-convertase enzymes as well as their corresponding C5 convertases (Heinen et al, 2009; Jokiranta et al, 1996).

1.1.5.2 Membrane associated regulators

CD46, also known as MCP is a membrane bound C regulatory protein ~ 60 kDa in size and comprised mainly of 4 SCRs. Variability in size is due to a number of splice variants and glycosylation patterns (Ballard et al, 1988; Post et al, 1991). MCP is widely distributed being expressed by platelets, granulocytes, Thelper, Treg, B-cells, NK cells and monocytes as well as fibroblasts, epithelial and endothelial cells but not by erythrocytes (McNearney et al, 1989; Seya et al, 1988). MCP was first described as a C3b/iC3b binding protein and later shown to possess co-factor activity for FI degradation of C3b and C4b into their inactivated forms (iC3b, iC4b) (Seya et al, 1986). Expression of MCP on the cell surface protects cells from C attack by intrinsic regulation, i.e. it is unable to act as co-factor for C3b deposited on bystander cells (Oglesby et al, 1992).

CD55, also known as decay accelerating factor (DAF), was first described as a 70 kDa glycoprotein isolated from human erythrocytes displaying decay acceleration of both the classical and alternative C3-convertases (Nicholsonweller et al, 1982). Membrane association of CD55 is dependent on its glycophosphatidyl (GPI) anchor which is attached during post-translational modification, the anchor allows it to be easily incorporated by exogenous addition and thus confers greater freedom of translocation on the outer leaflet of the membrane bilayer (Davitz et al, 1986; Medof et al, 1984; Thomas et al, 1987). The protein is expressed as a single aa chain containing a highly glycosylated region, GPI anchor site and 4 SCRs (Lublin & Atkinson, 1989). CD55 regulation is mediated partly by its binding of intrinsically bound C3b and C4b, preventing FB and C2 respectively from binding and forming the convertase enzymes, this happens without modification of either C3b or C4b (Medof et al, 1984). DAF is capable of dissociating C2a or Bb from preformed C3 convertases thereby rendering them inactive, this is achieved with no biochemical alterations to either C2a or Bb (Fujita et al, 1987).

CD35, also known as CR1, functions both as a receptor to C3b/C4b opsonised particles and as an efficient regulator of C. The CD35 protein is made up of 30 extracellular SCR

domains arranged into 4 long homologous repeats (LHRs) containing 7 SCRs each (Klickstein et al, 1987). Ligand binding sites for C3b and C4b are located in SCRs 8-9 and 1-2 respectively (Krych et al, 1991). The binding of each site to their respective ligands mediates both CR1 co-factor activity (Krych et al, 1994) and decay accelerating activity for both the C3 and C5 convertases of the alternative and classical pathways (Krych-Goldberg et al, 1999). Apart from its versatile regulatory functions, CD35 has important roles in C mediated phagocytosis and immune complex handling. CD35 is expressed on erythrocytes, polymorphonuclear leukocytes, B-cells T-cells, and monocytes (Fearon, 1980; Wilson et al, 1983). CR1 expressed on erythrocytes binds C3b/C4b labelled immune complexes so that they can be transported to the liver and cleared (Cornacoff et al, 1983). CR1 also causes adhesion of neutrophils to opsonised particles to promote their phagocytosis (Fallman et al, 1993).

CD59, once referred to as protectin, but now only known by its CD designation, was described as the antigen to which the antibody YTH 53.1 bound, potentiating lysis of cells to homologous C; the antigen was characterised as a 20 kDa glycoprotein with homology to Ly-6 antigens (Davies et al, 1989). CD59 is expressed as a 128 aa polypeptide chain which is processed to a 77 aa mature form. This mature protein is a single globular, cysteine rich extracellular domain, linked to the plasma membrane by a GPI anchor and has a single N-glycosylation site and several potential O-glycosylation sites (Holguin et al, 1990; Kimberley et al, 2007). CD59 regulates the terminal pathway of C; specifically inhibiting C9 polymerisation and membrane insertion by its binding of the C5b-8 complex and thus preventing MAC formation (Meri et al, 1990).

1.1.6 **Mouse complement**

The murine complement system shares much of the components of the human system albeit with varying degrees of homology. The mouse complement system is known to be significantly less active compared to its human counterpart. There are several molecular differences, both in the components of the cascade and regulators of the cascade. Murine

C4 is not capable of forming part of a classical C5 convertase i.e. C4bC2bC3b complex, as is known to occur in the human system, contributing a significant reduction in haemolytic activity (Ebanks & Isenman, 1996). With no C5 cleavage occurring during classical pathway activation the alternative pathway C5 convertase compensates for terminal pathway activation to occur. In fact the C5 component itself is lacking in 61% of in-bred mouse strains due to the synthesis of an abnormal protein through a post-translational defect (Ooi & Colten, 1979). Deficiency of the C8β sub-unit has also been recorded in MSM and Mae strains resulting in a severely reduced haemolytic activity which can be increased with supplementation with purified human C8 (Tanaka et al, 1991). A well known phenomenon has also been described pertaining to a difference between male and female haemolytic activity in mice. This difference is associated with lower titres of C4, C5 and C6 as well as C4BP in the serum of female mice comparing to males (Churchil.Wh et al, 1967; Ferreira et al, 1978; Shreffler, 1976). Some of this difference is due to androgen control of expression (Churchil.Wh et al, 1967; Shreffler, 1976).

Other than the differing serum activity, the murine system differs in its regulatory components. The mouse has structural and functional homologues for CR1, CD59, CD46 and CD55 (Holers et al, 1994; Kinoshita et al, 1985; Powell et al, 1997; Tsujimura et al, 1998). CD59 in the mouse exists in two forms, a and b, with differing tissue distribution; CD59a is widely distributed acting as the main terminal pathway regulator but CD59b is restricted to the testis with roles in spermatozoal acrosome activation(Baalasubramanian et al, 2004; Donev et al, 2008; Qian et al, 2000). There is also a duplication of the CD55 gene giving rise to a transmembrane and a GPI anchored form (Harris et al, 1999). In addition to these homologues mice also express the complement regulator complement receptor 1-related gene/protein-y (Crry) which is exclusive to rodents with the regulatory mechanisms of both MCP and CD55 (Kim et al, 1995; Molina, 2002).

Crry is considered the major complement regulator in mice, a fact which is demonstrated by the embryonic lethality of its deletion which can be reversed with C3 deficiency (Molina, 2002). Lethality could also be reversed with the treatment of the mother with anti-C5 Ab further demonstrating the importance of Crry as a complement regulator in mice (Ruseva et al, 2009). Given the mechanism by which Crry regulates complement it has been found to be a major contributor to the maintenance of complement homeostasis, controlling the constant turnover of C3 in tick-over (Wu et al, 2008).

1.2 Cancer and inflammation

1.2.1 Introduction

There has long been debate within the field of tumour immunology as to the role immunity has in tumour formation and progression. Infiltrating leukocytes within developing neoplasms were first described by Rudolf Virchow (Virchow & Chance, 1971) in the 19th century providing a key indicator of the link between inflammation and immunity in tumours. Over the last half century a great deal of progress has been made in understanding this link.

Inflammation in response to tissue damage is a normal physiological process. The process begins with the release of an array of inflammatory signals to initiate the early response. First responders to the site are neutrophils from the circulation, these release chemokines and cytokines required for recruitment and activation of effector cells. Monocytes arrive next and differentiate into macrophages upon activation becoming the main source of growth factor and cytokines. Released factors guide the remainder of the response, exerting influence on endothelial, epithelial and mesenchymal cells in the surrounding tissue (Coussens & Werb, 2002).

1.2.2 **Inflammatory tumour infiltrates**

Tumour tissue throughout its development has a significant infiltration of leukocytes, innate inflammatory cells including neutrophils, dendritic cells, macrophages, eosinophils and mast cells, and an adaptive immune cell infiltrate of lymphocytes (Coussens & Werb, 2002). A key mechanism responsible for recruitment of such cells is the tumour cell expression of chemokines and various chemoattractant factors like MCP-1 and CSF-1, thought to promote macrophage infiltration (Lin et al, 2001). Once recruited the diverse population provide a number of inflammatory factors including cytokines, chemokines, metallo/cysteine/serine-proteases, membrane perforating agents and mediators of cell death including TNFα, ILs, and IFNs (Coussens & Werb, 2001). The presence of immune infiltrates drives chronic inflammation which has the effect of triggering and promoting tumorigenesis through various mechanisms.

1.2.3 **Inflammation triggered cancer**

Chronic infections with a specific causative organism are known to be linked with cancer, accounting for at least 18% of all cases (Parkin, 2006). The common gastric infectious agent *H. Pylori* is closely associated with gastric adenocarcinomas (Franco et al, 2008). The best explanation for this association is its ability to drive a chronic inflammatory response given that infection with the more virulent cag-A/vacA expressing strains closely correlates with the incidence of pre-cancerous lesions (Plummer et al, 2007). Also, human patients suffering from colorectal tumours had a higher prevalence of the commensal enterotoxigenic *Bacteroides fragilis* bacterium (ETBF), an association supported by evidence suggesting a Th17 mediated inflammatory response is directly responsible for ETBF mediated tumour formation (Toprak et al, 2006; Wu et al, 2009). Other infectious agents with known links to cancer incidence include viral pathogens: Human papilloma virus (HPV) is linked to cervical cancer, Hepatitis B and C viruses (HBV and HCV) are linked to hepatocarcinoma and non-Hodgkin lymphoma, Epstein-Barr virus (EBV) is linked to Burkitt's lymphoma, nasopharyngeal carcinoma and Hodgkin's lymphoma, Human

herpes virus 8 (HHV-8) and Human T-cell leukaemia virus type I (HTLV-1) are linked to T-cell leukaemia (de Martel & Franceschi, 2009).

Chronic inflammation induced by environmental exposure to metals such as beryllium, chromium and nickel and to the fibrous agents making up asbestos, contribute to their known links to incidence of cancer (IARC, 2012). Exposure to asbestos leads to pleural mesothelioma an otherwise rare neoplasm. Asbestos fibre exposure and its carcinogenicity is proposed to be associated with inflammation via its biopersistence and induction of phagocytosis triggered activation of the NLRP-3 inflammasome and subsequent release of IL 1β (Dostert et al, 2008). Other environmental triggers of inflammation include tobacco smoke which can induce chronic inflammation via IKKβ and JNK1 and contribute to tumour promotion (Takahashi et al, 2010).

Conditions which are characterised by autoimmune mediated chronic inflammation are also associated with increased risk of cancer. Patients diagnosed with Crohn's disease have a higher risk of developing colorectal cancer and those diagnosed at a younger age were more at risk than those diagnosed later in life (Ekbom et al, 1990a). The same association was found in patients suffering from ulcerative colitis (Ekbom et al, 1990b).

Inflammatory mechanisms of tumour promotion are various. Primarily it is thought that activated cells in the leukocyte infiltrate release reactive oxygen and nitrogen species (RNS/ROS) which attack nucleic acids and mediate damage to DNA and other key molecules (reviewed (Hussain et al, 2003)). Briefly, activated cells release RNS; nitric oxide (NO•) and peroxynitrite (ONOO-) and ROS; hydroxyl radical (OH•) and superoxide (O2-•), via the activity of the enzymes myeloperoxidase, NADPH oxidase, and nitric oxide synthase. These cause oxidative damage and nitration of DNA bases leading to mutations in DNA sequence, error-prone repair and genetic instability (Rassool et al, 2007).

Tumour initiation via inflammation can be mediated by acquisition of p53 mutations which in ulcerative colitis patients was found to precede dysplasia and cancer formation, suggesting an inflammation associated genomic alteration (Lashner et al, 1999).

1.2.4 **Tumour promoting inflammation**

These associations represent a direct tumorigenic role for the inflammatory response with a clear mechanistic manifestation. It is, however, often the case that inflammation is secondary in tumour formation assisting in development, as in the case of chemically induced liver tumorigenesis mediated by diethylnitrosamine (DEN). DEN caused DNA damage and cell death but induced tumorigenesis through an indirect, IKKβ mediated inflammatory response which resulted in cytokine and growth factor induced compensatory proliferation and tumour development (Maeda et al, 2005). The role for IKKβ implicates NFκB in the inflammatory response. IL-1α release caused necrotic death and induced a proliferative response confirming the importance of cell death in inflammation driven tumorigenesis (Sakurai et al, 2008).

Cyclooxygenase (COX) 2 is upregulated in several human cancers and is responsible for the high levels of prostaglandin in the tumour microenvironment which in the case of neuroblastoma promote proliferation and survival of tumour cells (Rasmuson et al, 2012). Indeed, the key role this inflammatory mediator and other arachidonic acid (AA) pathway metabolites play in tumorigenesis is highlighted by the success in the use of the COX inhibitors. The non-steroidal anti-inflammatory drugs (NSAID) diclofenac, which increased apoptosis and inhibited tumour growth (Johnsen et al, 2004), and celecoxib which prevented tumour growth and increased cell susceptibility to chemotherapeutic drugs (Ponthan et al, 2007), were antitumour in *in vivo* models.

TNFα expression is thought to be key in the transition from chronic inflammation to tumorigenicity in the case of ulcerative colitis in which its increase was correlated with malignant transformation in a mouse model. This correlation was associated with

inflammatory cell trafficking and COX-2 expression. Blocking of TNFα signalling prevented transformation and could reverse progression of formed carcinomas (Popivanova et al, 2008). IL-6 trans-signalling (regulated by transforming growth factor (TNF) β), TNFα, IL-11 and IL-1β have each been implicated in colitis associated cancer tumorigenesis (Becker et al, 2004; Bollrath et al, 2009; Grivennikov et al, 2009).

Implication of IKKβ dependent NFκB activation in colitis associated cancer provides an indication of the molecular mechanisms of tumour promoting inflammation. Specific removal of IKKβ and thus NFκB activation in myeloid cells in a mouse model reduced tumour growth, correlating with reduced expression of IL-1α and β, IL-6, CXC motif ligand (CXCL) 1, macrophage inflammatory protein 2 (MIP-2), TNFα, COX-2, and intercellular adhesion molecule 1 (ICAM-1) in response to colitis induction (Greten et al, 2004).

1.2.5 **C and cancer**

1.2.5.1 Cancerous cells activate homologous C

When focussing on C in the context of cancer and transformed cells it is important to establish whether they are capable of activating endogenous C *in vivo*. Some of the first evidence of C activation by malignant transformed cells was found using immunohistochemistry of breast cancer tissue which showed deposition of the MAC and the components C3 and C4, in contrast to the lack of such components in adjacent benign breast tissue (Niculescu et al, 1992). These data indicate that transformed cells are capable of C activation as far as the terminal pathway and also suggest that this is due to classical pathway activation. Similar results were found in papillary thyroid carcinoma on which deposits of MAC, C3d, C4d, C5, IgG1 and IgG4 were detected (Lucas et al, 1996; Yamakawa et al, 1994). The concentration and activity of MBL in the plasma of colorectal cancer patients was higher when compared with normal controls, suggesting MBL may be activated in response to malignant transformation (Ytting et al, 2004). The presence of C3a and soluble MAC in the ascitic fluid taken from ovarian cancer patients also indicates activation of the alternative and classical pathways in this tumour type, supported by the

deposition of some activation products, for example C3d and C1q, on the surface of tumour cells (Bjorge et al, 2005). The exact trigger for C activation upon transformation is still not fully understood, although activation through immune complexes, antibody binding or direct C1q binding to necrotic/apoptotic cellular components are all possibilities. The relative contribution made by each activation pathway is unclear but data implicate all three pathways.

1.2.5.2 C in immunotherapeutic mAb

C activation is a contributor to the efficacy of a number of immunotherapeutic mAb used to treat cancers. C activation has been shown to contribute to tumour clearance for rituximab *in vitro* (Harjunpaa et al, 2000; Zhou et al, 2008), *in vivo* (Cragg & Glennie, 2004; Di Gaetano et al, 2003) and in treatment of patients (Kennedy et al, 2004). Taken together these data suggest a central role for C as an effector mechanism in therapeutic mAbs.

1.2.5.3 Cancer cell expression of mCRegs

It is widely thought that C activation on and around tumours is minimal due in part to the ubiquitous expression of C regulators (Fishelson et al, 2003; Jurianz et al, 2001). Most importantly, tumours abundantly express membrane bound C regulators (mCRegs).

The inhibition of C activation by the mCRegs expressed by cancer cells is in some cases bolstered by their upregulation on these cells, thus protecting the transformed cells from attack (McConnell et al, 1978). This interpretation is complicated by the apparent variability in expression levels of the mCRegs in several different cancers, but the overwhelming view is that in the majority of cancers investigated expression of one or more of the mCRegs is increased relative to healthy cells (Fishelson et al, 2003).

The possible role these regulators have in protecting tumours has been of great interest to those studying resistance to C fixing antibody in immunotherapy and can be demonstrated in *in vitro* studies in which mCReg protection is removed. The abrogation of regulatory activity invariably leads to significant increases in tumour cell sensitivity to C lysis (Yan et

al, 2008). Strategies include blocking with mAbs, for example with anti-CD55 in B-cell tumours, erythroleukaemic, melanoma, and renal tumour lines (Cheung et al, 1988; Gorter et al, 1996; Jurianz et al, 2001; Kuraya et al, 1992), and anti-CD59 in B-cell tumours, erythroleukaemic, mammary, ovarian, prostate, breast and renal cell lines (Donin et al, 2003; Ellison et al, 2007; Gorter et al, 1996; Jurianz et al, 2001; Kuraya et al, 1992).

The sensitization to killing by inhibiting mCRegs can be demonstrated *in vivo* giving results which reflect those in *in vitro* work. In an animal model, the human ovarian cancer cell line, A2780, was infected with recombinant retroviral particles containing a siRNA sequence designed to efficiently knock-down CD59 expression. Cells were then injected subcutaneously into nude mice. The CD59 knockdown cells formed significantly smaller xenograft tumours than a non-knocked-down infected cell control (Shi et al, 2009). Cells of the prostate cancer cell line PC-3 which demonstrate high expression of CD55 were transfected with the siRNA construct (CD55-3) targeted to knockdown CD55 expression. Cells were then injected into SCID mice. Mice injected with the PC-3 CD55-3 cells had significantly lower tumour burden compared to those injected with the PC-3 cells transfected with scrambled control (Loberg et al, 2006). Similar results were found when tumour cells isolated from breast cancer patients were xenotransplanted into SCID mice; mice injected with cells expressing high levels of CD59 developed larger tumours compared to those injected with cells expressing low levels of CD59 (Ikeda et al, 2008).

The level of CD55 expression in human breast cancers was found to correlate with disease prognosis; high CD55 expression correlated to a higher tumour size and poor outcome (Ikeda et al, 2008). Over-expression of CD55 in human cervical cancer tissue was shown to correlate with reduced deposition of C3b compared to surrounding tissue, suggesting C inhibition is relevant *in vivo* (Gao et al, 2009). In the same way levels of CD59 expression have been correlated with tumour grade and survival in colorectal cancer patients (Watson et al, 2006). The expression of both these mCRegs was also found to correlate to prognosis in non-small cell lung cancer (NSCLC) and contribute to

disease resistance to herceptin, an anti-Her2/neu mAb, treatment whose efficacy relies upon C activation (Zhao et al, 2009). The correlation between prognosis and expression of the mCRegs in multiple tumour types suggests a key role for C during tumorigenesis where levels are critical.

1.2.5.4 C activation influences tumour growth

Given the evidence that C activation occurs in tumour tissues and that C evasion strategies are used by tumour cells to avoid damage, it has long been thought that C activation is bad for tumours. This has fuelled recent work aimed at targeting antibodies for C fixation and dampening the inhibitory influence of expressed regulators.

There have, however, been a number of studies which suggest that C may promote cancer. A landmark study suggested a tumour promoting role for C5a (Markiewski et al, 2008). Growth of TC-1 injectable tumours was slower in C3, C4 and C5aR syngeneic knockout mice and the administration of a C5aR antagonist had a similar effect in the wild type mouse. Together, the data indicate that C, likely classical pathway activation, drives tumour progression and that the effect requires C5aR signalling. The principal finding of this study was that C5a released by C activation in the tumour micro-environment recruited myeloid derived suppressor cells (MDSCs) which once in the tumour worked to dampen a $CD8^+$ T-cell mediated immune response by releasing ROS and RNS.

C activation as a tumour promoting influence is a new but plausible idea given the well-known and powerful effect of inflammatory responses during tumour progression. A powerful effector of C activation is the MAC complex. Sublytic MAC effects may present a novel pro-tumour role for C.

1.3 Sublytic MAC

1.3.1 Mechanism of MAC induced lysis

The one-hit theory of cellular lysis by complement long held precedence because of kinetic and statistical studies which showed that a single C2 molecule could lead to lysis (Mayer et al, 1970). It is now understood that a single C2 does not restrict the number of terminal events because the formed C3 convertase showers the membrane with C3b (Müller-Eberhard et al, 1967). Cytolysis of an inert target, such as the aged erythrocyte, with a single MAC is theoretically possible as shown via C5b6 titrations (Yamamoto & Gewurz, 1978). It is however a different story with a metabolically active nucleated cell.

1.3.2 MAC resistance in nucleated cells

Deposition of the MAC on a nucleated cell can lead to disruption to membrane permeability as evidenced by calcium influx (Campbell et al, 1981; Michaels et al, 1976). However, nucleated cells display much greater resistance to MAC lysis compared to the aged erythrocyte, displaying multi-hit characteristics as shown in U937 cells exposed to C6 restricted serum (Koski et al, 1983). It was also apparent that this resistance to lysis was tightly associated with the cells metabolic activity, demonstrated by the increase in lipid synthesis induced in antibody sensitized tumour cells treated with C (Schlager et al, 1978). Beyond this association, previous observations had demonstrated that the phase of the cell cycle had a profound influence on susceptibility to MAC lysis; in general cells were least susceptible in their exponential phase and most susceptible in their stationary phase (Cikes & Friberg, 1971). Though this was associated with changes in antigen density the number of C components involved in activation was unrelated to susceptibility suggesting the effect was dependant on the cells metabolic status (Cooper et al, 1974; Ohanian & Borsos, 1975). Treatment with metabolic inhibitors enhanced susceptibility to MAC lysis (Ohanian & Schlager, 1981). These data implied that resistance was due to active mechanisms arising from within the cell.

Nucleated cells are protected from bystander damage by C activation via passive and active mechanisms. The first and primary defence is that of the membrane bound regulators including CD46, CD55 and CD59 (Morgan & Harris, 1999). CD59 is especially important as the last line of passive protection, inhibiting the formation of MAC (Meri et al, 1990). Protection from MAC beyond this involves internal processes which require expenditure of energy as evidenced by the effects of depletion of intracellular energy sources such as phosphocreatine and ATP (Tirosh et al, 1984). Ion pumps have even been implicated in the resistance of erythrocytes to MAC, activation of Ca^{2+} activated K^{+} pumps, counteracting the Na^{+} influx, was protective (Halperin et al, 1993b).

Nucleated cells are capable of removing MAC from their surface in order to survive an attack. Deposited MAC on U937 cells was shown in functional studies to have a half-life of 2 mins at 30°C and was increased to 2 hours at 2°C suggesting that the functional MAC was being removed from the membrane by an unknown mechanism (Ramm et al, 1983). The phenomenon was directly observed in Ehrlich cells where colloidal gold tagged complexes were internalised by endocytosis (Carney et al, 1985). In polymorphonuclear cells the MAC was shown to be removed by vesiculation (Campbell & Morgan, 1985). In 1987 Morgan et al. elegantly demonstrated both mechanisms to be involved in resistance of human neutrophils to homologous MAC. Supernatants of attacked cells were enriched with vesicles coated in MAC, accounting for 65% of the total. The remaining 35% of complexes remained on the cell but were not accessible to the detecting antibody and radio labelled C8 was found to be internalised for degradation (Morgan et al, 1987).

The phenomenon has since been reported to occur in many tumour and normal cells, including U937 monocytic cell line (Morgan et al, 1986), Ehrlich ascites tumour cells (Carney et al, 1985), K562 (Moskovich & Fishelson, 2007), glomerular epithelial cells (GECs) (Kerjaschki et al, 1989), blood platelets (Sims & Wiedmer, 1986) and oligodendrocytes (OLGs) (Scolding et al, 1989).

Using C9 labelled with AF488, Moskovich and colleagues were able to track deposited MAC on K562 cells, demonstrating outward emission of C9-AF488 via ectosomes and exosomes within 10 minutes (Moskovich & Fishelson, 2007). After 10 minutes, C9-AF488 entered the early endosomal compartment then later entered the perinuclear compartment where it co-localised with transferrin. The vesicles were then packed into multivesicular bodies and exocytosed or proteolytically degraded. The mitochondrial hsp70 chaperone known as mortalin promotes elimination of the MAC enriched vesicles on which it co-localises. When mortalin is blocked or silenced, the rate of vesiculation is reduced leaving the cell more sensitive to MAC lysis (Pilzer & Fishelson, 2005; Pilzer et al, 2010). The data suggests that mortalin could be involved in detection of MAC insertion and initiation of vesiculation.

1.3.3 **Resistance and signalling events**

Resistance to C is likely to be initiated by signalling cascades triggered at the surface. Levels of cyclic adenosine monophosphate (cAMP) the first second messenger to be discovered, are closely associated with levels of resistance with decreased levels being indicative of increased sensitivity (Lo & Boyle, 1979). Indeed, increased intracellular cAMP confers protection and can rescue cells from lysis (Boyle et al, 1976; Kaliner & Austen, 1974).

The first detectable event following MAC deposition is an immediate rise in intracellular free Ca^{2+} concentration ($[Ca^{2+}]i$). Calcium influx was first shown using pigeon erythrocyte ghosts containing obelin, demonstrating that MAC allowed Ca^{2+} to enter the cell along the marked gradient maintained across the membrane (Campbell et al, 1979). The rapid influx of Ca^{2+} increased intracellular concentrations from 0.3 µM to between 5 and 30 µM within 40 seconds (Campbell et al, 1981). Although first described in pigeon erythrocytes, a calcium influx upon MAC deposition was also shown in neutrophils. The study demonstrated using the Ca^{2+} chelator ethylene glycol tetra acetic acid (EGTA) that MAC deposition could induce release from intracellular stores in the absence of extracellular

Ca^{2+} and that rises in Ca^{2+} were key in the elimination of MAC from the membrane (Morgan & Campbell, 1985). Elimination of MAC from human platelets by exocytosis and from Ehrlich ascites by endocytosis are also Ca^{2+} dependent (Carney et al, 1986; Wiedmer et al, 1987).

K562 cells exposed to sublytic doses of C were subsequently exposed to what would otherwise would have been lytic doses, but were protected; a phenomenon known as induced protection (Reiter et al, 1992). The mechanisms mobilized to protect the cell from lysis in response to MAC deposition could protect the cell from subsequent lytic doses of MAC and other pore forming proteins; although the precise nature of these mechanisms remains uncertain, they were shown to be calcium dependent (Reiter et al, 1995).

The apparent importance of Ca^{2+} and cAMP suggested the mechanisms of recovery were dependent on signal transduction via either or both messengers and points to the potent influence MAC deposition has on host cells given the varied cellular processes regulated via these second messengers. This influence extends beyond cell protection and recovery.

1.4 Sublytic MAC effects

1.4.1 Introduction

What has become apparent is that MAC elimination and recovery are only the start of a huge range of cellular effects exerted by MAC. These effects also have important implications in the roles that C activation plays in disease. The effects of MAC which occur without lysis are known as nonlytic effects and doses of MAC which achieve this are considered sublytic. The next section will discuss the effects of sublytic MAC and create a picture of the signalling events involved.

1.4.2 **Expression**

Sublytic MAC is capable of profoundly influencing cell behaviour through cell activation and gene expression changes that can cause release of inflammatory mediators, cytokines, growth factors, adhesion molecules and extracellular matrix components and regulators.

1.4.2.1 Inflammatory mediators

The earliest described nonlytic effect of MAC was the release of reactive oxygen metabolites by neutrophils in response to doses of MAC which were below that required for lysis (Campbell et al, 1981; Campbell & Hallett, 1983).

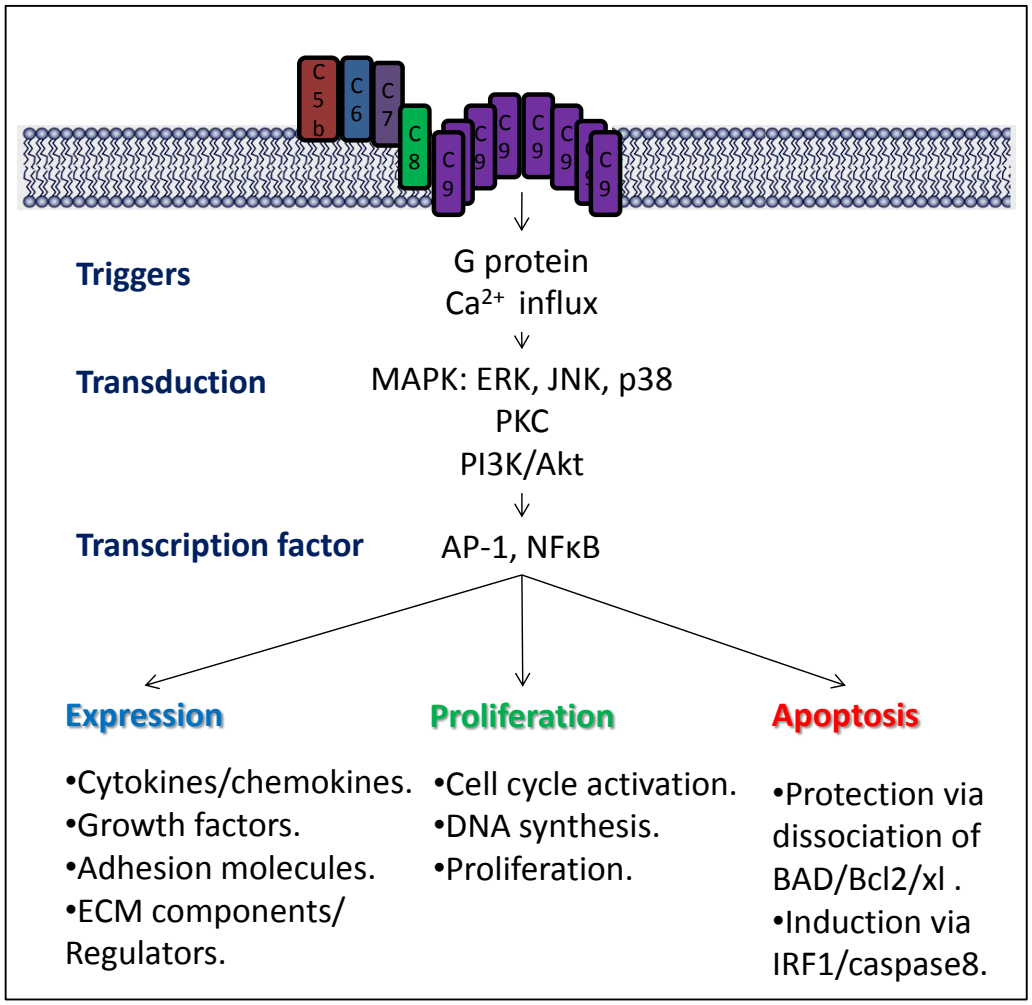

Figure 1.4.2.1 MAC assembly on nucleated cells has various effects on cellular processes. MAC deposition triggers signalling through Ca^{2+} and G-proteins at the cell surface leading to effects on expression; inflammatory mediators, adhesion molecules, extracellular matrix components and regulators, proliferation; triggering entry into the cell cycle, DNA synthesis and proliferation, apoptosis; protection from apoptosis via a BAD/Bcl2/xl mediated mechanism.

Beyond the oxidative burst, MAC can also affect the production and release of various AA metabolites, including leukotriene B4 by neutrophils and oligodendrocytes, thromboxane B2 by platelets and prostaglandin E2 by monocytes, glomerular epithelial (GECs) and mesangial (GMCs) cells and synoviocytes (Morgan, 1989).

MAC assembly on GECs results in a Ca^{2+} flux associated with release of AA and diacylglycerol (DAG) followed by prostaglandin F2α and thromboxane A2 production (Cybulsky, 1991). MAC activates phospholipase A2 (cPLA2) mediating the increase in free AA and thus prostaglandin E2 production via PKC signalling (Cybulsky et al, 1995; Cybulsky et al, 1998). Eicosanoid release by cultured GECs in response to MAC is thought to be driven by an upregulation of COX-2 protein although both COX-1 and -2 were involved *in vivo* (Takano & Cybulsky, 2000).

1.4.2.2 Cytokines

Sublytic MAC can also induce inflammatory cytokine production, the first example described was in monocytes which released IL-1(Hansch et al, 1987). In human GMCs, deposition of MAC caused the release of prostaglandin E2 along with IL-1 and TNFα (Schonermark et al, 1991). In response to MAC, HUVECs released IL-8 and MCP-1 with a detectable upregulation of both at mRNA and protein (Kilgore et al, 1996). It was later discovered this effect was dependant on the translocation of NFκB from the cytosol to the nuclear compartment (Kilgore et al, 1997). Transcription and release of IL-6 by human smooth muscle cells in response to MAC was induced by Gi-protein activation and mediated by NFκB and AP-1 although the effect was prevented upon treatment with an antioxidant suggesting a significant ROS contribution (Viedt et al, 2000).

1.4.2.3 Adhesion molecules

An example of the co-operative effect of MAC is the induction of neutrophil adhesion molecules in response to the combination of TNFα and MAC treatment of human umbilical vein endothelial cells (HUVECs) (Kilgore et al, 1995). MAC was demonstrated to enhance

the TNFα induced expression of E-selectin and intracellular adhesion molecule-1 (ICAM-1) and increase the neutrophil adhesion beyond that induced by TNFα and MAC alone. P-selectin has also been shown to be induced by MAC directly in HUVECs (Hattori et al, 1989). More recent work has suggested that inactive terminal C complex (iTCC), formed in fluid phase and often considered biologically inactive, is capable of upregulating expression of endothelial leukocyte adhesion molecule (ELAM)-1, ICAM-1 and vascular cell adhesion molecule (VCAM)-1 (Tedesco et al, 1997).

1.4.2.4 Growth factors

MAC has also been shown to effect the release of growth factors. Bovine aortic endothelial cell (AECs) and HUVECs released basic fibroblast growth factor (bFGF) and platelet-derived growth factor (PDGF) in response to MAC deposition and conditioned medium from these cells in turn caused increased proliferation rate in 3T3 cells (Benzaquen et al, 1994).

Assembly of MAC on human AECs induced release of a number of chemokines, cytokines and growth factors, including epidermal growth factor (EGF), CXCL5, CXCL1, IL-6, IL-8, MCP-1, placental growth factor 1 (PIGF), regulated on activation normal T cell expressed and secreted (RANTES) and angiogenin. IL-6, PIGF, and RANTES release were inhibited upon knockdown of Akt and FOXO1 suggesting their involvement in AAC-induced growth factor release (Fosbrink et al, 2006).

1.4.2.5 Extracellular Matrix (ECM) components and regulators

The earliest record of sublytic MAC effect on ECM expression was in GECs where it induced synthesis and release of collagen IV (Torbohm et al, 1990). GMCs also upregulated collagen IV as well as fibronectin in response to MAC (Wagner et al, 1994). Tubular epithelial cells were shown to up-regulate collagen IV coinciding with an increase in expression of its chaperone HSP47 (Abe et al, 2004). In retinal pigment epithelial cells

(RPEs) the ECM regulatory matrix metalloproteinases (MMP) 2 and 9 were upregulated in response to MAC deposition suggesting an opposing role in ECM degradation (Lueck et al, 2011).

1.4.3 **Cell fate**

Apart from altered gene expression and release of the various described factors and components, MAC deposition on nucleated cells can significantly alter their behaviour, for example, MAC can induce entry into cell cycle, alter rate of proliferation and modulate apoptosis.

1.4.3.1 Cell-cycle and proliferation

One of the first reports of a mitogenic activity for MAC was in Mouse Swiss 3T3 cells where MAC formed using purified C components induced significantly increased DNA synthesis when compared to controls. The MAC mitogenic effect also enhanced the effects of growth factors and could be demonstrated in their absence (Halperin et al, 1993a).

Further indication of a proliferative effect of MAC came from studying C6 deficient PVG rats which displayed reduced phenotype in experimental mesangioproliferative glomerulonephritis, including reduced proliferation of mesangial cells, an effect attributed to their inability to form MAC (Brandt et al, 1996).

C activation and sublytic MAC deposition on oligodendrocytes induced cell cycle entry marked by an increase of cdc2 activity in G1 progression and increased cdk4 complexed with cyclin D2 during G1/S transition. S phase entry was mediated by c-jun induction via JNK . MAC also induced the expression of the oncogenes junD and c-fos as well as increasing proliferation (Rus et al, 1996). Investigation of the mechanism revealed dependency on MAPK signalling pathways specifically activating ERK1 and JNK1. ERK1 activation was dependent on Raf-1 and MEK1 activity upstream (Rus et al, 1997). Activation of MAPK signal transduction was later shown to be triggered by Gβɣ subunits;

accompanied by increased GTPase-bound Pas and Ras in JY25 B cell line (Niculescu et al, 1997). In Schwann cells, a proliferative effect was mediated by ERK1, Gi proteins and PKC (Dashiell et al, 2000).

Activation of PI3K/Akt was responsible for a proliferative response to sublytic MAC in human aortic smooth muscle cells (ASMCs) (Niculescu et al, 1999). The PI3K/Akt proliferation response was shown to require phosphorylation and inactivation of forkhead transcription factor FOXO1 (Fosbrink et al, 2006)

The response gene to C 32 (RGC-32), first discovered by differential display analysis of gene expression response to C activation in oligodendrocytes, was associated with an increase in DNA synthesis pointing to its influence on the cell cycle (Badea et al, 1998). In ASMCs RGC-32 is upregulated in response to MAC and causes entry into the cell cycle by virtue of its binding and activation of $p34^{CDC2}$ kinase an association which is dependent on phosphorylation by $p34^{CDC2}$ itself (Badea et al, 2002).

1.4.3.2 Apoptosis

One of the more intriguing effects of sublytic MAC deposition in nucleated cells is its influence on the apoptotic fate of a cell.

OLGs undergo apoptosis subsequent to the removal of growth factors from defined media, a response which is ameliorated when OLG cells are exposed to sublytic MAC deposition; thus MAC rescues the cells from apoptosis (Rus et al, 1996). Apoptosis induced by growth factor withdrawal is thought to occur through the cytochrome c pathway initiated by mitochondrial dysfunction triggering caspase 3 and 9 activation. Protection of OLG from apoptosis by MAC was shown to be mediated by an increase in Bcl-2 protein which prevented cytochrome c release and inhibited the activation of caspase 3. The protection also extended to apoptosis induced by TNF-α suggesting the involvement of caspase 9 inhibition (Soane et al, 1999). Protection was reversed upon treatment with LY294002 and PTX pointing to a dependency of the effect on a Giα/PI3K/Akt signalling

pathway; PI3K phosphorylation of Bad resulted in its dissociation from the Bad/Bcl-xL which was dependent on Giα (Soane et al, 2001). This mechanism has also been shown to depend upon caspase 8 inhibition and increased levels of FLIP, thus suggesting that MAC interferes with Fas mediated apoptotic pathways (Cudrici et al, 2006). A Gβɣ mediated activation of the ERK1 pathway has also been implicated (Rus et al, 1997; Rus et al, 1996). A similar protective effect has been described for MAC in Schwann cells, protection from apoptosis subsequent to growth factor withdrawal, mediated by PI3K phosphorylation of BAD (Hila et al, 2001).

Conversely, MAC has been shown to induce apoptosis in GECs in the Thy-1N model, though the mechanism involved was not elucidated (Hughes et al, 2000). Later MAC induced apoptosis in GMCs was shown to be through upregulation of IRF1 which bound the caspase 8 promoter and upregulated it's expression (Liu et al, 2012).

1.5 Aims and Hypothesis

The view that C activation on and around tumours is anti-cancer in nature is under increasing scrutiny. The assumption relies heavily on the classical effector view of the system and its role as an immune defence; indeed in the case of mCReg over-expression in limiting the efficacy of treatment using anti-cancer mAb, it carries some truth. However, the inflammatory component in driving tumour development is now an accepted hallmark of cancer and the role that C, a major pro-inflammatory system, plays in this has largely been ignored. Recently, a limited number of studies have implicated some C components including C3 and C5a in tumour development but MAC has received limited attention, a situation which this thesis proposes to address.

The potent effects that MAC can exert on nucleated cells presents a mechanism by which C may influence tumour development and progression. This thesis will examine how a tumour promoting role for MAC may manifest as gene expression changes exerted by sublytic C on tumour cells.

The hypothesis to be tested is that tumour cells may respond to sublytic C by up-regulating genes which bestow upon the tumour a more metastatic and proliferative phenotype.

The key aims of the study are:

1. To optimise conditions for sublytic C membrane attack on selected cell lines and investigate suitable controls.
2. To identify, using microarray analysis, gene expression changes induced by exposure of tumour cells to sublytic C membrane attack, focussing on genes associated with tumour progression and metastasis.
3. To validate these gene expression responses at both the transcript and protein levels.
4. To determine the key C factor/s exerting the effect.

2 Materials and methods

2.1 Reagents

2.1.1 Antibodies

2.1.1.1 Primary antibodies

Name	Clonality	Species	Against	Purchased from	Technique	Working concentration
mCD59a7	Monoclonal	Rat IgG	Murine CD59a	In-house generated	FACS	10 µg/mL
αMCF-7 antiserum	Polyclonal	Rabbit	MCF-7 cell line	In-house generated	FACS/CDC	1/100
27d1	Monoclonal	Mouse IgG	Human C6	In-house generated	FPLC/WB	1 µg/mL
αMMP-3	Polyclonal	Goat IgG	Murine MMP-3	R&D	W/B	1 µg/mL
αMMP-13	Polyclonal	Rabbit IgG	Murine MMP-13	Abcam	W/B	1 µg/mL
αCXCL-1	Polyclonal	Rabbit IgG	Murine CXCL1	Abcam	W/B	1 µg/mL
αAR	Polyclonal	Goat IgG	Murine AR	R&D	W/B	1 µg/mL
αC5aR	Polyclonal	Rat IgG	Murine C5aR	AbD Serotec	W/B	1 µg/mL

2.1.1.2 Secondary antibodies

Name	Clonality	Species	Against	Purchased from	Conjugate	Technique	Working concentration
αRat FITC $F(ab)_2$	Polyclonal	Donkey	Rat IgG	Jackson	FITC	FACS	1/500
αRabbit FITC $F(ab)_2$	Polyclonal	Donkey	Rabbit IgG	Jackson	FITC	FACS	1/500
αMouse HRP	Polyclonal	Rabbit	Mouse IgG	Dako	HRP	WB	1/1000
αGoat HRP	Polyclonal	Rabbit	Goat IgG	Dako	HRP	WB	1/1000
αRabbit HRP	Polyclonal	Goat	Rabbit IgG	Dako	HRP	WB	1/1000

2.1.2 **Primers**

All primers were purchased from Biomers (Ulm, Germany) and upon arrival reconstituted in ultrapure (up) H_2O to a concentration of 100 µM. Reconstituted primers were stored at -20°C and when in use kept on ice at all times.

Name	For/Rev	Primer sequence	Length	Tm ˚C	Used for
Cd59a	Forward	ATATCTAGAGCCACCATGAGAGCTCAGAG	29	62	Cloning/PCR
	Reverse	CCGTCTAGATTAGAGATGACTTAAGAAAC	29	57	
pDR2	Forward	CAAGCCTCAGACAGTGGTTC	20	54	Sequencing/PCR
	Reverse	ATGTCTGGATCGGTGCGGGC	20	58	
Polr2a	Forward	CCCGCTGCGCACCATCAAGA	20	60.04	qPCR
	Reverse	GGGCGACCTCCCTCCGTTGT	20	60.53	
Actb	Forward	ACGGCCAGGTCATCACTATTG	21	60.13	qPCR
	Reverse	AGTTTCATGGATGCCACAGGAT	20	60.02	
OPN	Forward	ATTGCCTCCTCCCTCCCGGTGA	22	61.04	qPCR
	Reverse	GATGGGTCAGGCACCAGCCATG	22	59.79	
Ki67	Forward	TCAAGCGGAGCGGCGATGAC	20	59.84	qPCR
	Reverse	TGACACTACAGGCAGCTGGATACG	24	58.31	
uPA	Forward	AATGCTGTGTGCTGCGGACCCA	22	61.52	qPCR
	Reverse	GAGTTGGGCGGCCTTCGATGTT	22	59.73	
PCNA	Forward	TGCAAGTGGAGAGCTTGGCAATGG	24	59.94	qPCR
	Reverse	GAGCAAACGTTAGGTGAACAGGCT	24	57.67	
Rgs16	Forward	GGTACTTGCTACTCGCTTTTCC	22	60.9	qPCR
	Reverse	CAGCCGCGTCTTGAACTCT	19	62.3	
Fam110c	Forward	GGCCAAAGAAACCCCCAGCCAG	22	60.18	qPCR
	Reverse	GGCTCTGGAGTTTCAGACGCCTA	23	58.16	
Irf1	Forward	ATGCCAATCACTCGAATGCG	20	61.1	qPCR
	Reverse	TTGTATCGGCCTGTGTGAATG	21	60.4	
Hbb-bh1	Forward	GAAACCCCCGGATTAGAGCC	20	62	qPCR
	Reverse	GAGCAAAGGTCTCCTTGAGGT	21	61.4	
Mmp3	Forward	ACATGGAGACTTTGTCCCTTTTG	23	60.7	qPCR
	Reverse	TTGGCTGAGTGGTAGAGTCCC	21	62.9	
Mmp13	Forward	TGTTTGCAGAGCACTACTTGAA	22	60.1	qPCR
	Reverse	CAGTCACCTCTAAGCCAAAGAAA	23	60.2	
Areg	Forward	GGTCTTAGGCTCAGGCCATTA	21	61	qPCR
	Reverse	CGCTTATGGTGGAAACCTCTC	21	60.4	
Cxcl1	Forward	ACTGCACCCAAACCGAAGTC	20	60.04	qPCR
	Reverse	TGGGGACACCTTTTAGCATCTT	22	60.53	
C5aR	Forward	CAAGACGCTCAAAGTGGTGA	20	58.42	qPCR
	Reverse	TATGATGCTGGGGAGAGACC	20	58.28	

2.2 Cell Culture

Name	Contents
Serum free medium	1×RPMI 1640, 2mM L-glutamine, 50 U/mL penicillin G, 50 µg/mL streptomycin sulphate, 1mM sodium pyruvate.
Normal growth medium	Serum free medium + 10% (v/v) heat inactivated FBS.
Freezing medium	60% (v/v) serum free medium, 30% (v/v) FBS and 10% (v/v) DMSO.

2.2.1 Maintenance

CT26 mouse colon carcinoma cells were cultured in normal growth medium. For transfected cells, 100 µg/mL hygromycin (Invitrogen) was also included. Cells were maintained in 75cm^2 tissue culture flasks and kept in a humidified tissue culture incubator at 37°C, 5% CO_2. Cells were maintained in culture for 2 months, ~16 passages, before being discarded.

2.2.2 Initiating from liquid N_2 stocks

Frozen cells were thawed rapidly at 37°C in a water bath then gently transferred into 5 mL fresh, warmed normal growth medium. This suspension was pelletted by centrifugation at 300×g for 5 minutes at room temperature (RT) and the cells resuspended in 20 mL normal growth medium and placed into culture flasks.

2.2.3 Passaging for maintenance

For routine maintenance cells were passaged roughly twice a week. Cells were grown to 80% confluence in 75cm^2 flasks and the spent medium discarded. Monolayers were washed in saline and incubated with 0.05% trypsin, 0.53 mM EDTA (Gibco) solution until fully detached. Cell suspensions were diluted in saline and transferred to 20 mL universal containers. Cells were pelleted by centrifugation at 300×g for 5 minutes at RT and resuspended in normal growth medium. Routinely cells were seeded for maintenance cultures at a ratio of 1/20 into 15 mL normal growth medium in 75cm^2 flasks.

2.2.4 **Preparation of frozen stocks**

Cells were grown to 80% confluence in 175cm^2 tissue culture flasks and the spent medium discarded. Monolayers were then washed in saline and incubated with trypsin-EDTA (Gibco) solution until fully detached. Cell suspensions were diluted in saline and transferred to 20 mL universal container. Cells were pelleted by centrifugation at 300×g for 5 minutes at RT and re-suspended in 5 mL freezing medium so that cells were at a rough density of 1×10^7 per mL. Aliquots of 1 mL were prepared in cryo-vials and placed in an isopropanol freezer box which was stored at -80°C overnight to allow slow cooling (~1°C degree/min). Vials were then transferred to liquid nitrogen storage. Extensive frozen stocks were maintained so that experimental cells had undergone as few passages as possible.

2.2.5 **Trypan blue exclusion assay for cell counting**

Cell density was measured by trypan blue (TB) (Sigma-Aldrich, Dorset , UK) exclusion assay. To do this 20 µL of a cell suspension was diluted ½ in 0.4% (w/v) TB in PBS and mixed gently by repeat pipetting. The haemocytometer was assembled by affixing a glass coverslip. The cell suspension/trypan blue mixture was pipetted to the edge of the affixed coverslip and the mixture allowed to fill the area beneath the coverslip. The haemocytometer was placed under a microscope and the central grid located. Cells excluding the trypan blue dye were deemed viable and those that did not and stained blue were deemed non-viable. Viable cells within the grid were counted using a click counter and recorded. Cell density was calculated using the following formula:

$$cells\ mL^{-1} = cells\ in\ grid \times dilution\ factor \times 10^4$$

2.3 Serum preparation

For preparation of pooled normal human serum (pNHS) whole blood was collected from consenting volunteers and placed in 20 mL glass vials. Blood was allowed to clot at RT for

1 hour and then placed on ice for 1 hour to contract the clot. The clotted blood was transferred to a 50 mL falcon tube and centrifuged at 800×g for 10 minutes at 4°C with no braking. The serum was then transferred to a second falcon tube and centrifuged at 800×g for a further 10 minutes then supernatants pooled and mixed. Serum was decanted carefully to a fresh tube and sterile filtered through 0.22 µm syringe filter. Filtered serum was kept on ice while making appropriate aliquots for storage at -80°C.

2.4 Sublytic C experiments

In sublytic C experiments the required cells were seeded onto plates and allowed to form a monolayer over 20 hours in normal growth conditions. For sublytic attack experiments cells were grown to 80% confluence and spent media discarded. The monolayers were then washed in saline and incubated with trypsin-EDTA (Gibco) solution until fully detached. Cells were washed twice in 5 mL warmed serum free medium and cell density ascertained using the trypan blue exclusion assay. Cells were then diluted to a density of 5×10^5 per mL in normal growth medium and seeded in culture plates so that 1.6×10^3 cells were present per mm^2 of available culture area. Seeded cells were incubated under normal growth conditions for 20 hours. Aliquots of pNHS were thawed placed in sterile tubes and incubated with or without *Ornithodoros moubata* C inhibitor (OmCI) added at 10 µg/mL at RT for 20 minutes. Serum aliquots were then diluted to a final concentration of 5% (v/v) in serum free medium. Cells were removed from the incubator and washed twice in serum free medium then serum dilutions decanted into relevant wells. The plate was then incubated in normal growth conditions for required time.

2.5 RNA extraction from cultured cells

2.5.1 **RNA Handling**

All procedures involving RNA handling were conducted in an ethanol cleaned tissue culture hood with surfaces treated with a solution of 100 mM NaOH + 0.1% SDS to

destroy RNases. Pipette tips were RNase/DNase free. Extracted RNA was placed on ice immediately and stored long term at -80°C. During experiments RNA was thawed and kept on ice at all times.

2.5.2 **Extraction**

RNA extraction was performed using the Genelute Mammalian Total RNA Miniprep Kit (Sigma-Aldrich, Dorset, UK). Lysis solution was prepared by adding 10 µL β-mercaptoethanol (βME) per mL of supplied lysis reagent containing guanidine thiocyanate. Cell monolayers were washed in saline and 250 µL lysis solution added and incubated at RT for 2 minutes followed by repeat pipetting to homogenize the sample. The homogenate was then transferred to the blue filtration column and centrifuged at 9,500×g for 1 minute (RT) to remove cell debris and shear chromosomal DNA. An equal volume of 70% ethanol was added to the filtrate then mixed using a vortexer. RNA was bound to the silica membrane of the nucleic acid binding column by centrifugation for 15 seconds and the flow through discarded. Bound RNA was washed by centrifugation (9,500×g, RT, 15 seconds) using 500 µL guanidine thiocyanate wash buffer and the column transferred to a fresh tube. Bound RNA was washed twice by centrifugation, 15 seconds then 2 minutes, in ethanol containing wash buffer. To avoid ethanol contamination the nucleic acid binding column was centrifuged dry for one minute before being transferred to a fresh tube. RNA was eluted by the addition of 50 µL of elution buffer which was incubated at RT for 1 minute followed by centrifugation at 9,500×g, RT for 1 minute.

2.5.3 **Quantitation of RNA**

In order to measure concentration, RNA was diluted 1/20 in ultrapure H_2O. The absorbances at 260nm and 280nm of this dilution were measured by spectrophotometry using a nanodrop (Thermo Scientific, DE, USA) spectrophotometer. The machine was initialized and blanked with ultrapure H_2O. RNA dilutions (2 µL each) were placed on the pedestal and measured. Absorbances were noted and the ratio calculated between absorbance at 260 and 280 nm. Values calculated as 2.0 ±0.2 were deemed pure and of

high quality. Concentration was then calculated from the absorbance reading at 260 nm using Beers law given that RNA has an extinction co-efficient of 38 (µg/mL)$^{-1}$ cm^{-1}:

$$RNA\ concentration\ \mu g\ \mathrm{mL}^{-1} = Absorbance\ A_{260} \times 38 \times dilution\ factor$$

2.5.4 **Reverse Transcription**

Reverse transcription of RNA to generate first strand cDNA was carried out using the TaqMan Reverse Transcription Reagents (Applied Biosystems/Life Technologies Ltd, Paisley, UK). Master-mixes were prepared for the number of RNA samples with 10% excess to allow for pipetting errors then mixed using a vortexer (Figure 2.5.4.1A). Aliquots of 6.15 µL were shared to fresh tubes, 1 µg of RNA added and the volume made up to 10 µL with ultrapure H_2O. Reaction mixes were placed in a DNA Engine Dyad PCR thermo-cycler machine (MJ Research, MA, USA) and the programme shown in Figure 2.5.4.1B used for the reverse transcription reaction. Reaction mixes containing cDNA were either diluted directly in ultra-pure (up) H_2O for qPCR or placed directly at -80°C for storage.

A.

	1x
Rtbuffer	1
Oliogo d(t)	0.5
MgCL2	2.2
DNTPs	2
RNAse Inh	0.2
Rtase	0.25
Total	6.15

B.

Step	Temperature	Time
2	37°C	1hour
3	95°C	5min
4	4°C	∞

Figure 2.5.4.1 Reverse transcription protocol. A. reaction mix using the TaqMan kit reagents (Applied Biosystems), volume was made up to 10 µL with 1 µg RNA plus upH_2O. B. Thermocycler program set on Dyad DNA Engine machine (MJ Research).

2.6 Quantitative polymerase chain reaction (qPCR)

2.6.1 **Primer design**

QPCR primers were either sourced from PrimerBank, taken from published research or designed using PrimerBLAST. PrimerBank is a comprehensive database of human and mouse qPCR primer pairs designed using NCBI transcript sequences, a primer designing algorithm, plus a number of specifically designed filters (Spandidos et al, 2010). The algorithm used is based upon the oligopicker algorithm proposed for microarray probe design which takes a non-redundant protein coding sequence and by sorting all sequences satisfying a pre-defined T_m by rejection using criteria designed to ensure specificity to target, good sequence complexity and accessibility (Wang & Seed, 2003b). The algorithm was refined for qPCR by testing for specificity to the target transcript using BLAST and chances of secondary structure formation minimized by testing for primer self-complementarity (Wang & Seed, 2003a). The algorithm creates primers with T_m values of ~60°C and GC content between 35% and 65% preferring oligonucleotide lengths of between 19-23 nucleotides. The PrimerBank database has at least one primer pair for each known coding transcript in mice and in many cases primer pairs have been experimentally validated for efficacy.

Primers which had been validated were selected preferentially. Those which had not were selected based upon product length, between 90-200 nucleotides, and inclusion of exon/exon boundaries within product sequence to target transcript over non-transcript RNA/cDNA or contaminating genomic material.

PrimerBLAST is an online primer design tool which combines the pre-existing design tool primer3 and the BLAST global sequence alignment tool to assess the possibility of unintended amplification. Primer 3 is a popular primer designing tool provided by the NCBI which suggests possible primer sequences for the amplification of a desired sequence which satisfy a number of user defined constraints including T_m, primer length and product

length (Rozen & Skaletsky, 2000). BLAST or basic local alignment search tool uses an algorithm which compares a user defined amino acid or nucleotide sequence to database sequences by calculating an MSP score to describe the similarity and therefore the alignment (Altschul et al, 1990). Combining these two modules creates a powerful primer design tool with enormous flexibility. For the designing of validation primers of which there were two, the refseq accession codes for target transcripts were inserted as template and the following restrictions applied-

1. 90-200 nucleotide product size
2. 57 min, 60 opt, 63 max T_m range
3. Primer must span an exon/exon junction
4. Enable search for primer pairs specific to the intended PCR template ticked- Mus musculus.

PrimerBLAST generated a list of suitable primer pairs along with possible unintended annealing sites within the mouse refseq database.

2.6.2 **QPCR expression analysis**

To analyse the relative expression of genes of interest, real-time qPCR was used. Reverse transcription reaction mixes containing first strand cDNA representative of RNA material was diluted 1/10 in upH_2O. QPCR was performed using 1× SYBR Green Jump Start Readymix (Sigma-Aldrich, Dorset, UK) and master-mixes sufficient for triplicates were prepared for each primer pair (Figure 2.6.2.1A). For experiments with several samples, master-mixes were prepared without cDNA addition until shared into fresh tubes. Reaction mixes were aliquoted into white 48-well PCR plates, then the plates sealed with optical flat 8-cap strips (Bio-Rad, Hertfordshire, UK). Plates were mixed using a vortexer, briefly spun down by centrifugation and placed on the plate of a MiniOpticon Real-Time PCR Detection System (Bio-Rad) controlled by PC using the Opticon Monitor 3.1 software (Bio-Rad). Themocycling protocol shown in Figure 2.6.2.1B was used as

standard. The calculation used for relative expression was the $\Delta\Delta C_t$ method Figure 2.6.2.1C+D). C_t values were the cycle number at which fluorescence crossed a threshold level chosen as the point at which the PCR expansion was linear in all samples (Figure 2.6.2.1C). The mean C_t values for β-actin and Polr2A as the housekeeping genes were calculated and referred to as the C_t[HKG] and the value for target gene was referred to as C_t[sample]; ΔC_t was calculated by subtracting HKG from sample (Figure 2.6.2.1Di). $\Delta\Delta C_t$ was calculated from the ΔC_t using the formula in (Figure 2.6.2.1Dii). Control sample was included as baseline and so a % relative expression value was calculated (Figure 2.6.2.1Diii).

A.

	1×	3.2×
SyBR Green	10	32
upH_2O	7.6	24.32
For	0.2	0.64
Rev	0.2	0.64
RM Total	18	57.6
1/10 cDNA	2	6.4
Total	20	64
Transferred total	-	20

B.

Step	Temperature	Time
1	95°C	15 min
2	95°C	15 sec
3	65°C	1 min 10 sec
4	Plate Read	-
5	Cycle 2 ×40	-
6	70-90°C	15 sec every 0.3C read
	end	

C.

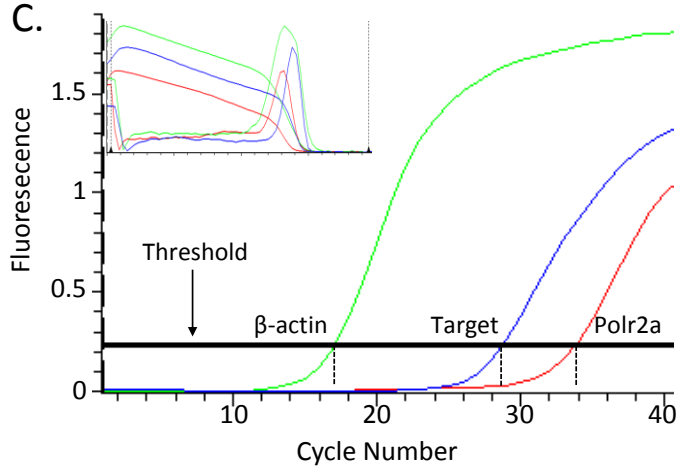

D.

i. $\Delta C_t = C_t[sample] - C_t[HKG]$

ii. $\Delta\Delta C_t = (2^{-\Delta C_t}) \cdot 100$

iii. $\%RE = \frac{\Delta\Delta C_t\,[Sample]}{\Delta\Delta C_t\,[Control]} \cdot 100$

Figure 2.6.2.1 qPCR gene expression analysis protocol. A. Reaction mix for qPCR using SYBR Green reagent (Sigma) showing for reaction volumes of 20 µL and in triplicate with excess (×3.2). B. Thermocycler program set on MiniOpticon machine (Bio-Rad) for qPCR including PCR amplification (steps 1-5) and melt curve (step 6). C. Calculation of Ct values through the setting of a threshold; threshold is set as the earliest point where amplification is linear and Ct values taken as cycle number at which the threshold is reached. D. Equations for the calculation of i=ΔCt, ii=ΔΔCt, iii=% (RE) relative expression from Ct values from sample (Ct[sample]) and the mean Ct of housekeeping genes (Ct[HKG]).

2.7 Protein separation SDS-PAGE

Name	Contents
Sodium Dodecyl Sulphate (SDS) Stacking gel buffer	0.5 M Tris, 0.4% (w/v) SDS, pH6.8
SDS resolving gel buffer	1.5 M Tris, 0.4% (w/v) SDS, pH8.8
Non-reducing loading buffer	0.1 M Tris, 10% (v/v) glycerol, 2% (w/v) SDS 0.01% bromophenol blue, pH 6.8
Running buffer	25 mM Tris, 191 mM glycine 1% (w/v) SDS
Coomassie Blue Stain	0.2% (w/v) coomassie blue R250 in 45% (v/v) methanol, 8% (v/v) acetic acid in dH_2O
De-staining buffer	20% (v/v) methanol, 8% (v/v) acetic acid in dH_2O

2.7.1 Gel Casting

Sodium dodecyl sulphate polyacrylamide gel electrophoresis (SDS-PAGE) was performed using the Mini-PROTEAN Tetra Cell system (Bio-Rad).

	Stacking (mL)	Resolving (mL)	
Gel Percentage	**5%**	**15%**	**10%**
Upper buffer mL	1.2	3.75	3.75
40% Acrylamide/Bis mL	0.625	5.625	3.75
dH_2O mL	3.12	5.46	7.335
10% Ammonium persulphate mL	0.05	0.15	0.15
TEMED mL	0.005	0.015	0.015
Total	5 mL	15 mL	15 mL

Gel casts were assembled according to the manufacturers instructions. Stacking and lower gel mixes were prepared according to the above recipes, ammonium persulphate was added immediately prior to pouring into casts to initiate polymerisation. Lower gels were poured first filling three quarters of the volume and butanol used to level and protect the top from air which inhibits the polymerisation process. Once polymerised, the butanol was removed and the upper compartment washed with dH_2O. Ammonium persulphate was added to the stacking gel mix and this was poured on top of the set lower gel. The comb was then quickly inserted taking care to avoid introducing air bubbles. Once set the

cast containing the gel was clamped into the running tank, running buffer was filled to the appropriate levels to cover the anode and cathode.

2.7.2 **Sample preparation**

Protein samples were prepared by diluting the required quantity in 6× loading buffer. This was mixed using a vortexer and placed on heat block at 90°C for 10 minutes to thoroughly de-nature the sample with the exception of serum samples which were incubated at RT for 30 minutes. Samples were mixed using a vortexer and loaded into the wells of prepared polyacrylamide gels. The molecular weight marker well was loaded with 8 µL Seeblue Plus2 Protein Standards (Invitrogen/Life Technologies Ltd, Paisley UK). The tank was connected to the power pack and gels electrophoresed at 100 V for 1h (or until dye front reached 0.5 cm from edge of the gel).

2.7.3 **Coomassie stain**

Polyacrylamide gels were stained with coomassie blue stain for the detection and visualisation of separated proteins. Gels were rinsed in dH_2O to remove surface running buffer and bathed in coomassie stain for 3 hours on a rocker. Coomassie blue stain was removed, the gel rinsed then bathed in destain buffer and incubated for an hour on a rocker. The destain solution was removed and replaced with fresh destain and the process repeated until bands appeared blue against a clear background. Coomassie stained gels were then scanned.

2.8 Western Blot

Name	Contents
Transfer buffer	25 mM Tris, 191 mM glycine, 20% (v/v) methanol
Phosphate buffered saline (PBS)	8.2 mM Na_2HPO_4, 1.5 mM KH_2PO_4, 137mM NaCl, pH7.4, 0.22 µm filtered
Blocking buffer	5% (w/v) dried milk in PBS
Wash buffer	0.1% (v/v) Tween 20 in PBS

2.8.1 **Transfer by wet electroblotting**

Transfer of protein from SDS-PAGE gels to nitrocellulose membrane for western blotting, was carried out using the Mini Trans-Blot Electrophoretic Transfer Cell system (Bio-Rad). Polyacrylamide gels containing separated proteins were removed from their glass sandwich and equilibrated in transfer buffer for 5 minutes on a rocker. A transfer cassette was prepared in the following order; pad, blotting paper, nitrocellulose membrane. All components had been thoroughly soaked in transfer buffer prior to cassette assembly. The gel was placed on top of the membrane and the sandwich completed with a second sheet of blotting paper and pad, the sandwich was placed in the cassette and air bubbles expelled using a roller. The complete cassette and transfer sandwich was clamped shut and placed in the electrode housing in the transfer tank along with an ice block for cooling and a magnetic stirrer. The tank was filled with transfer buffer and connected to power pack. Transfer was carried out over 1 hour at 100V.

2.8.2 **Probing of membrane**

Membranes with transferred protein were placed in a 50mL falcon tube and blocked in blocking buffer (as above) either overnight at 4°C or for 1 hour at RT on a roller. Proteins of interest were detected with a primary antibody added to 5 mL of blocking buffer at dilutions optimized for the individual antibody (normally between 1/500 -1/2000). Primary antibodies were incubated with the membranes at 4°C overnight or 0.5-2 hour at RT. Membranes were washed 3 × 5 minutes in wash buffer (as above). The HRP conjugated secondary antibody was added in 5 mL of blocking buffer at dilutions appropriate to the individual secondary antibody (normally between 1/1000 and 1/2000) and the membranes incubated for between 30 minutes and 1 hour at RT. The probed membrane was washed as above, followed by a final wash with PBS.

2.8.3 **Membrane development**

Membranes were developed using the ECL Prime western blotting detection reagent (GE Healthcare Life Sciences, Buckinghamshire, UK) as per the manufacturers instructions. Briefly, reagents A and B were mixed 1:1 allowing 750 µL per membrane and incubated on the membrane for 3 minutes. Excess solution was shaken off and luminescence detected by exposing X-ray film (GE Healthcare Life Sciences, Buckinghamshire, UK) to the membrane in a dark room for between 30 seconds to 3 hours. Films were developed in a SRX-101A autodeveloper machine (Konica Minolta, NJ, USA) and the results noted.

3 Optimization of sublytic C conditions

3.1 Introduction

3.1.1 Sublytic C

Sublytic C attack is defined as C activation in the absence of lysis. In practice this means that activation occurs on nucleated cells leading to MAC assembly on the membrane but at a level that cells can survive. Surviving cells are activated in a number of ways which results in downstream effects on gene expression and protein synthesis. The term sublytic is often defined experimentally as levels resulting in lysis below 10%, but throughout the literature there is some variation; ranging from below 5% up to 15% lysis (Qiu et al, 2012; Reiter et al, 1992).

3.1.2 CT26 cells

CT26 cells are a chemically induced transplantable colon carcinoma cell line derived form BALB/c mice (Corbett et al, 1975). They were developed to study colorectal cancers and selected as highly proliferative and metastatic (Brattain et al, 1980). Using CT26 as a model cell line *in vitro* will enable the overall findings of these investigations to be confirmed *in vivo* in the BALB/c mouse.

3.1.3 C fixation

Activation of C on allogeneic nucleated cells *in vitro* is often reliant on a trigger for fixation. For this cells are coated in antibody often raised against the cells or an abundantly expressed antigen. For example the Thy-1.1 antibody is used to coat GMCs binding Thy1 antigen, this model is derived from the mesangioproliferative glomerulonephritis model in rats termed Thy1N (nephritis) (Lu et al, 2012). In the case of the erythroleukaemic cell line K562 a heat inactivated antiserum is used for C fixation (Jurianz et al, 2001). In these protocols normal human serum (NHS) is used for the C source and heat inactivation of this serum used to control for lytic activation and MAC formation. In a heterologous

system where serum C source and cell target are derived from differing mammalian species, the need for a targeting antibody is dependant on the efficiency of C activation. This is determined by a number of factors including most obviously the expression of regulators on the surface of the target cell membrane and robustness of the serum C source. Other factors include charge and features of the target surface which will dictate the pathway initiated (for example, natural antibodies in serum can initiate the classical pathway), stability of the convertase formed, and efficiency of MAC assembly (Morgan et al, 2005).

3.1.4 **Strategies for isolating MAC mediated effects**

3.1.4.1 Heat inactivation of serum

Heating serum at 56°C for ~30 minutes, removes C activity by inactivating its heat labile components C2 and factor B as well as C1q and others to a lesser degree (Joisel et al, 1983; Lozada et al, 1995; Lynen et al, 1973). Heat treatment also destroys the activity of a multitude of heat labile non-C factors such as growth factors, vitamins, amino acids, and hormones. This non-specific destruction of serum growth factor and hormone content make it a poor control for the cell activating sublytic effects of C.

3.1.4.2 Depletion of C6

Inhibition of the terminal pathway is also possible by depletion of individual components needed to generate the MAC complex. This can be achieved by depletion of any one of the terminal components, C6 (Gao et al, 2007), C7, C8 and in some cases C9 (Fosbrink et al, 2006). Depleted serum can be used to allow generation of C5b and incomplete terminal complexes, C5b-6, C5b-7, C5b-8; the latter two are capable of depositing on cell surfaces and causing disruption in membrane integrity (Podack et al, 1980). Depletion is usually achieved by passage of sera over columns containing antibodies against the specific components. Reconstitution of depleted components restores the serum lytic capacity.

C6 occupies a crucial point linking activation to the terminal pathway and thus represents an ideal target for removal. Removal of C6 allows activation to progress up to and including cleavage of C5 but prevents continuation of terminal pathway because C5b is prevented from binding C6, a key step in the pathway towards formation of the MAC . C6 depleted serum is therefore an ideal reagent for controlling MAC mediated sublytic effects.

3.1.4.3 OmCI

Inhibition of terminal pathway selectively can also be achieved using inhibitors such as the OmCI which is a saliva protein derived from the *Ornithodoros moubata* tick. OmCI is a 17 kDa non-glycosylated protein expressed as a single polypeptide chain, a member of the lipocalin family of barrel-forming proteins. OmCI has been shown to act at the C5 stage of activation blocking the activity of both the alternative and classical C5 convertase enzymes and thus preventing C5 cleavage to C5a and C5b. Excess of C5 but not C3 removed this inhibitory activity suggesting a direct action on C5 and not the convertase enzyme (Nunn et al, 2005). Biochemical analyses has shown that OmCI binds directly to C5. Upon binding to C5 away from the cleavage site, OmCI stabilized the global protein structure, preventing it's cleavage into C5b and C5a (Fredslund et al, 2008). Binding of C5 by OmCI effectively acts as a terminal pathway/MAC inhibitor by blocking progression of C activation beyond C5. This makes it an ideal tool as a control for MAC induced effects.

3.1.5 **CD59**

CD59 is the only membrane bound regulator of MAC expressed by human cells. Over-expression of CD59 by tumour cells is purported to be one of the evasion mechanisms tumour cells use to avoid C mediated damage (Fishelson et al, 2003). The presence of CD59 at the site of MAC deposition makes it a molecule at the frontier of sublytic attack and therefore its role is of great interest. CD59 is linked to the outer leaflet of the membrane by a GPI lipid anchor. Cross-linking of CD59 via antibodies on haematopoietic cells triggers signalling events such as calcium flux and tyrosine kinase activation leading

to ROS release (Morgan et al, 1993; Vandenberg et al, 1995). These events bear resemblance to that activated by sublytic MAC. This resemblance was given credence by work showing Src family protein tyrosine kinases activation through CD59 cross-linking could be induced by C8 (Murray & Robbins, 1998). These observations raise the possibility that CD59 may act as a receptor for MAC and mediate some of its sublytic effects.

3.1.6 **Putative sublytic C response genes**

3.1.6.1 Osteopontin (OPN)

Work published by Wai et al in 2005 presented an association between OPN and other markers with metastatic and proliferative phenotype in CT26 cells. Si-RNA knockdown of OPN decreased the metastatic potential of the cells when injected into syngeneic BALB/C mice. *In vitro* analysis of the cells showed that OPN suppression resulted in significant reduction in MMP-2 expression combining to lower their migration and invasion index compared to wild type and mismatch controls. This was reflected by *in vivo* work where knock down of OPN resulted in dramatic reduction of hepatic nodules in an injected tumour metastasis model (Wai et al, 2005).

The metastatic potential of OPN is driven through the PI3K pathway. Analysis of a highly active 38bp segment of the OPN promoter sequence revealed potential binding sites for several transcription factors including the AP-1 consensus binding sequence. Further investigations demonstrated that this site was utilised by the c-jun homo-dimer of AP-1. Inhibition of PI3K resulted in lowered levels of c-jun together with phosphorylated forms of JNK-1 and 2 and these changes correlated with a reduction in OPN expression. Both pharmacological inhibition and knock down of JNK suppressed adhesion migration and invasiveness to a level similar to that of cells with low OPN expression (Mi et al, 2004).

The impact of PI3K on the metastatic potential of cancer cells has been shown to involve, through Akt, cell proliferation and OPN expression. HepG2 cells treated with EGF showed

increased expression in OPN at both mRNA and protein levels, an effect which was abrogated on inhibition of PI3K with wortmannin treatment (Zhang et al, 2004).

The proposed link between sublytic C, OPN expression and an influence on metastasis is based on the common initiation of the PI3K pathway and involvement of Akt and c-jun, implicated in both protective mechanisms of the cell during sublytic C attack and over-expression of OPN and the resulting increase in metastatic potential. A link between OPN expression and sublethal MAC has not been described.

In the work defining a role for OPN in metastases using the CT26 cell line, other characterising markers were used to assess metastatic and proliferative potential - uPA, PCNA and Ki67 (Wai et al, 2005).

3.1.6.2 Urokinase-type plasminogen activator (uPA)

Urokinase-type plasminogen activator (uPA) expressed by cancer cells has been linked to metastasis both in animal models and in patients where it serves as a predictor of survival (Andreasen et al, 1997). The MAPK pathway has been implicated in uPA expression involving activation of ERK1 and promoter binding of fos and junD to an AP-1 site on uPA promoter (Lengyel et al, 1996).

3.1.6.3 Ki67 antigen

Ki67 antigen is present in all active phases of the cell cycle but completely absent in resting phases. Its function is not understood but it is clear that without Ki67, proliferation is not possible, indeed upon proliferation it is synthesised and degraded in a tightly controlled manner (Scholzen & Gerdes, 2000). Ki67 expression was demonstrated to be regulated through the binding of Sp-1 to its promoter (Tian et al, 2010). The signalling pathways regulating its expression are unknown. Because Ki67 is exclusively expressed by proliferative cells it has become a common marker for cells undergoing this process and thus is used as a diagnostic tool for neoplasms (Scholzen & Gerdes, 2000).

3.1.6.4 proliferating cell nuclear antigen (PCNA)

PCNA antigen is also found to be expressed in proliferating cells and is an accessory protein to DNA polymerase δ and DNA polymerase ε. This means it has functions in DNA synthesis, recombination, repair and metabolism. It has also been associated with cell cycle regulation and check-point controls (Kelman, 1997).

Ki67 and PCNA, are often used as proliferative markers and the presence of these markers is strongly linked with the aggressiveness of cancer and correlate with patient survival (Ben-Izhak et al, 2002).

3.1.7 **Chapter aims**

The aim of the work described in this chapter is to optimize the reagents, conditions and controls for sublytic C experiments on tumour cells. Furthermore, preliminary experiments are detailed which were carried out to ascertain detectable effects of sublytic C and inform time points used for the microarray experiment. To achieve these aims the practical goals were:

1. Clone Cd59a plasmid and transfect into CT26 cell line.
2. Assess sensitivity of CT26 to C lysis to ascertain their sublytic threshold and confirm the functionality of the transfected Cd59a protein product.
3. Explore terminal pathway control systems for use in sublytic C experiments.
4. Explore possible candidates for gene expression changes in response to sublytic attack using qPCR.

3.2 Methods

3.2.1 **Molecular Biology**

Name	Contents
Lauria-Bertani (LB amp.) broth	1% (w/v) bacto-tryptone, 0.5% (w/v) yeast extract, 1% (w/v) NaCl, 269 µM sodium ampicillin, in H_2O
LB amp. Agar	LB amp. broth plus 0.7% (w/v) agar
SOC medium	2% (w/v) bacto-tryptone, 0.5% (w/v) yeast extract, 0.05% (w/v) NaCl, 2.5 mM KCl, 10 mM $MgCl_2$, and 20 mM glucose
80% Glycerol	80% (v/v) glycerol in H_2O
TAE	40 mM Tris, 40 mM acetic acid, 1 mM EDTA, pH7.2
Loading buffer (agarose gel electrophoresis)	20% glycerol (w/v) in 10×TAE with 0.2% (w/v) bromophenol blue.

3.2.1.1 LB agar plate preparation

LB amp agar was prepared using the recipe in reagent list. Mixture excluding ampicillin was autoclaved. Molten LB agar was allowed to cool (56°C), mixed with ampicillin then poured into petri dishes to give a 5 mm deep layer (~5 mL). These plates were allowed to set in an air flow hood and covered and sealed in plastic packaging for storage at 4°C.

3.2.1.2 Bacterial transformation

Electro-competent *E.coli* NEB5α cells (New England Biolabs, Hertfordshire, UK) were transformed as per manufacturer's instructions. Briefly, an aliquot was thawed and 50 µL of the cell suspension placed in a sterile tube on ice. Plasmid DNA, ~100 ng in 5 µL was added directly and gently mixed then incubated on ice for 2 minutes. The mixture was then heat shocked by placing in a water bath set to 42°C for exactly 30 seconds, followed by removal to ice for 2 minutes. SOC medium (950 µL, warmed to 37°C) was added directly to the cell suspension which was then incubated at 37°C for 1 hour before 100 µL aliquots were spread on LB amp agar plates. Plates were incubated overnight at 37°C.

3.2.1.3 Bacterial culture for glycerol stocks and plasmid isolation

Single colonies from LB amp agar plates were picked and placed in individual sterile 50 mL falcon tubes each containing 5 mL of LB amp broth. Inoculated cultures were placed in

an orbital incubator (Gallenkamp, Leicestershire UK) and set to mix at 180 rpm overnight at 37°C.

3.2.1.4 Glycerol stock preparation

Glycerol stocks were used to store positive transformants for long periods. Positive plasmid colonies were picked and expanded overnight at 37°C as above. Cell culture volumes were mixed 1:1 with 80% glycerol to give a 40% final concentration and 1 mL aliquots prepared. Aliquots were labelled and stored at -80°C.

3.2.1.5 Plasmid purification

Bacterial cultures created as above were harvested by centrifugation at 4600×g for 10 minutes, supernatant was discarded and cell pellet processed. Plasmid DNA was purified using the QIAprep Miniprep kit (QIAGEN, West Sussex, UK) as per the manufacturer's instructions. Briefly, cell pellets were resuspended in 250 µL of alkaline lysis buffer. Lysates were neutralised with a high salt buffer for adsorption of DNA onto a silica solid phase membrane by centrifugation. Adsorbed DNA was washed with 80% ethanol in wash buffer and eluted in tris buffer (10 mM TrisHCl, pH 8.5). Concentration of purified plasmid DNA was determined by absorbance at 260 nm using a Nanodrop Spectrophotometer, then stored at -20°C in aliquots.

3.2.1.6 Gel extraction PCR product recovery

PCR products separated by electrophoresis on agarose gels were extracted using the QIAquick Gel Extraction Kit (QIAGEN) as per manufacturer's instructions. Briefly, bands of interest were excised, weighed and melted at 50°C in 300 µL guanidine thiocyanate buffer per 100 mg of gel. To this, 100 µL isopropanol per 100 mg of gel was added and the mixture applied to a solid phase silica membrane spin column by centrifugation. Bound DNA was washed in guanidine thiocyanate buffer followed by 80% ethanol wash buffer then eluted in tris buffer (10 mM TrisHCl, pH 8.5).

3.2.1.7 DNA agarose gel electrophoresis

DNA was separated on agarose gels of between 1-2% (w/v). Larger DNA fragments or plasmids were separated on lower (1%) percentage gels and smaller fragments on higher (1.5-2%) percentage gels. Agarose powder (Life Technologies Ltd, Paisley, UK) was weighed out in a conical flask and diluted in 1×TAE buffer then heated in a microwave until dissolved. Molten agarose was cooled and ethidium bromide added to a final concentration of 0.5 µg/mL. The agarose was poured into a casting tray containing a comb to create loading wells. The gel was allowed to set then placed in an electrophoresis tank containing 1×TAE running buffer. DNA samples were mixed 1 in 6 with glycerol loading buffer and 20 µL loaded into wells alongside a base pair marker of appropriate size, i.e. 100 bp for smaller fragments or 1000 bp for larger fragments. DNA was electrophoresed at 100V for between 15 minutes to an hour. DNA bands were visualised under a UV lamp.

3.2.1.8 Polymerase chain reaction (PCR) for cloning and screening

PCR reactions were carried out in a DNA Engine Dyad PCR thermo-cycler machine (MJ Research, MA, USA) using Platinum Blue super mix 1.1 × (Invitrogen, Paisley, UK); forward and reverse primers were added to a final concentration of 1 µM and template added along with upH_2O to create a final volume of 25 µL.

3.2.1.9 Restriction digest

Restriction digestion of plasmid or fragment DNA was conducted using XbaI (NEB) in buffer 3 (NEB supplied restriction digest buffers) for 1 hour at 37°C.

3.2.1.10 Dephosphorylation

Dephosphorylation was achieved using Antarctic phosphatase (NEB). To target DNA (linearized plasmid DNA), 10× Antarctic phosphatase reaction buffer (NEB) was added to a final concentration of 1×. Antarctic phosphatase (10 units) was then added to the

volume and the reaction mixture incubated at 37°C for 30 minutes. The phosphatase was inactivated by incubation at 65°C for 10 minutes.

3.2.2 **Cloning of mouse Cd59a into the pDR2 expression vector**

3.2.2.1 pDR2ΔEF1α expression vector

The pDR2ΔEF1α plasmid referred to as pDR2 hereafter, is a mammalian expression vector (Figure 3.2.2.1). The construct carries an ampicillin resistance gene for selection in prokaryotic organisms and a hygromycin resistance gene for selection in eukaryotic, mammalian cells. Inserted genes are expressed under the control of the human elongation factor 1a promoter (EF1α), a constitutive promoter taken from elongation factor 1A gene. The presence of the SV40 polyA sequence for polyadenylation improves expression levels in mammalian cells (Gimmi et al, 1988). pDR2 contains a large polylinker sequence containing amongst others an XbaI restriction enzyme site: TCTAGA.

3.2.2.2 Cloning of the Cd59a gene

Cloning of the Cd59a gene required the designing of specific primers directed to the sequence with the addition of the recognition site for the endonuclease restriction enzyme XbaI at both the 3 and 5 prime ends (Figure 3.2.2.2A). The forward primer was designed to accommodate the XbaI site, plus the consensus Kozak GCCACC sequence and the first 14 nucleotides of the target sequence (Figure 3.2.2.2A+B). Kozak proposed that a consensus sequence flanking the initiator codon was required for eukaryotic ribosomal recognition of the correct initiator codon, the sequence had GCC repeating units with -3 sequence A or G then CC in relation to initiating AUG (Kozak, 1987). The reverse primer also contained an XbaI site plus the last 20 nucleotides of the target sequence (Figure 3.2.2.2A+B).

Total RNA was extracted from 20 mg of fresh mouse liver as described in section 2.5.2. This was quantified (section 2.5.3) and 1 µg added to a pre-prepared reverse transcription

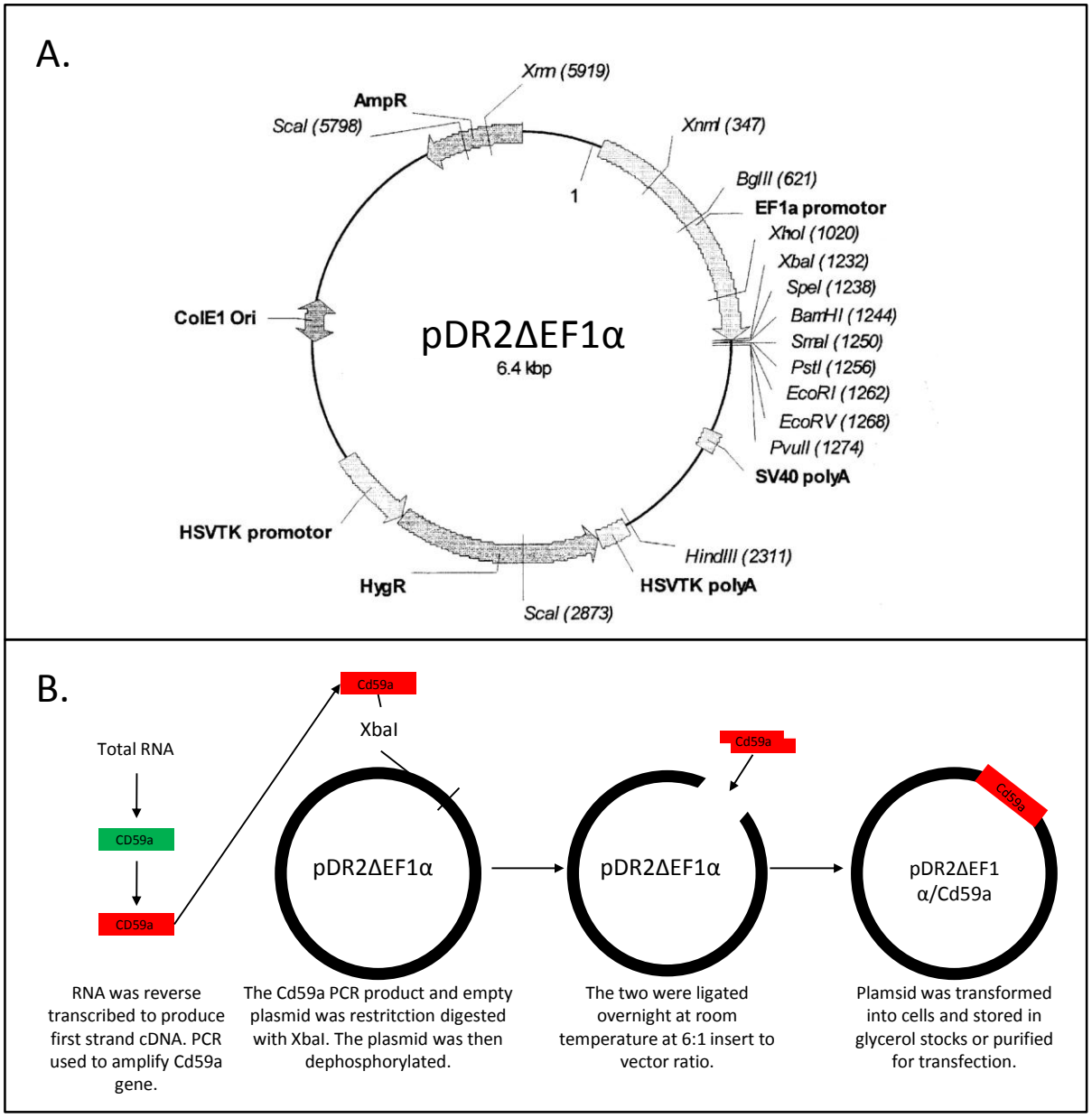

Figure 3.2.2.1 pDR2 plasmid vector and cloning strategy. A. Schematic representation of the pDR2 plasmid showing positions for EF1α promoter, SV40 polyA, polylinker and resistance genes for hyg. and amp. B. Cloning strategy for insertion of Cd59a gene into polylinker region by a non-directional cloning strategy. cDNA reverse transcribed form liver total RNA was used to PCR amplify the Cd59a gene. pDR2 and Cd59a PCR product were restriction digested using XbaI and plasmid dephosphorylated and the two ligated.

A.

Cd59a primers

For: ATA*TCTAGA*GCCACCATGAGAGCTCAGAG (62°C)

Rev: CCG*TCTAGA*TTAGAGATGACTTAAGAAAC (57°C)

Cd59a PCR product 397bp

ATA*TCTAGA*CGCCACCATGAGAGCTCAGAGGGGACTCATCTTACTCCTGCTGCTTCTGGCTGTGTTCTGTTCCA
CAGCTGTTAGCCTCACATGCTACCACTGTTTCCAACCGGTGGTTTCTTCATGCAATATGAACAGCACTTGCTCTC
CTGACCAGGATTCCTGTCTCTATGCTGTAGCCGGAATGCAAGTGTATCAAAGGTGTTGGAAACAATCAGATTG
TCATGGTGAGATCATTATGGACCAATTAGAAGAGACAAAATTAAAATTCAGATGCTGCCAGTTTAACTTGTGT
AACAAAAGTGACGGATCCTTGGGGAAGACACCATTGCTGGGGACCTCGGTTCTGGTGGCCATTTTGAATCTTT
GTTTCTTAAGTCATCTCTAA*TCTAGA*CGG

B.

Step	Temperature	Time
1	95°C	5min
2	95°C	30sec
3	38°C	30sec
4	72°C	1min
5	Cycle to step 2	7times
6	95°C	30sec
7	54°C	30sec
8	72°C	1min
9	Cycle to step 6	×30
10	4°C	∞

C.

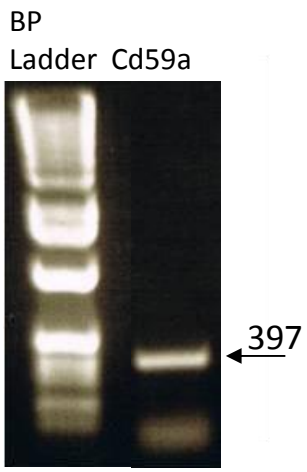

Figure 3.2.2.2 PCR amplification of mouse Cd59a gene. A. Forward and reverse primers specific for the 5 and 3 prime sequence of Cd59a transcript (RefSeq NM_001111060.1). Primers contain XbaI recognition site (green), Kozak sequence (underlined), overlap Cd59a transcript sequence (yellow) and start/stop codons (red). Fragment sequence is labelled in the same way and primers highlighted in brown. B. PCR thermocycling programme for expansion of Cd59a gene. C. PCR product was separated on 1% TAE agarose gel for 30 minutes at 100V, band at 397bp represents the amplified Cd59a gene, lower band comprises primer dimers.

(RT) reaction mix then placed on a thermocycler plate and program set as described in section 2.5.4. Once completed, resulting first strand cDNA was placed on ice.

PCR amplification of mouse Cd59a coding sequence from cDNA was done using specific primers shown in Figure 3.2.2.2A. A stepped PCR program was utilised with an initial low annealing temperature of 38°C for the first 7 cycles followed by annealing at 54˚C for the remaining 30 cycles (Figure 3.2.2.2B). Each PCR reaction contained 1.5 µL of cDNA from first strand RT reaction mixture.

The PCR products were electrophoresed in TAE agarose (section 3.2.1.7) and a band of 396bp corresponding to the expected size for the Cd59a coding region was excised while viewing on a UV transilluminator (Figure 3.2.2.2 C). The PCR fragment was then purified from the gel using a QIAquick kit as described in section 3.2.1.6 and eluted DNA quantified by Nanodrop measurement of absorbance at 260 nm.

3.2.2.3 Recombination of Cd59a into pDR2 expression plasmid

pDR2 plasmid DNA was purified from 5 mL cultures using the QIAprep Spin Miniprep Kit as described in section 3.2.1.5. The purified pDR2 plasmid and Cd59a fragment were both separately digested with XbaI to generate complementary ends for ligation. Figure 3.2.2.3 shows an example of linearized pDR2 plasmid by XbaI digestion compared to uncut and restriction digestion with enzyme for which no recognition site exists on the plasmid. Plasmid DNA linearized by a single restriction digest is liable to re-circularize or become ligated with itself during ligation reaction. To reduce the possibility of plasmid re-circularization, linearized plasmid DNA was dephosphorylated by treatment with Antarctic phosphatase (NEB) added directly to restriction digest reaction mix.

The digested Cd59a fragment was cleaned with the QIAquick PCR Purification Kit (QIAGEN) and ligated with the linearized plasmid using 6:1 and 10:1 insert : vector ratios. Ligation mixes were transformed into NEB5α competent cells and colonies selected after overnight incubation on ampicillin selective agar plates.

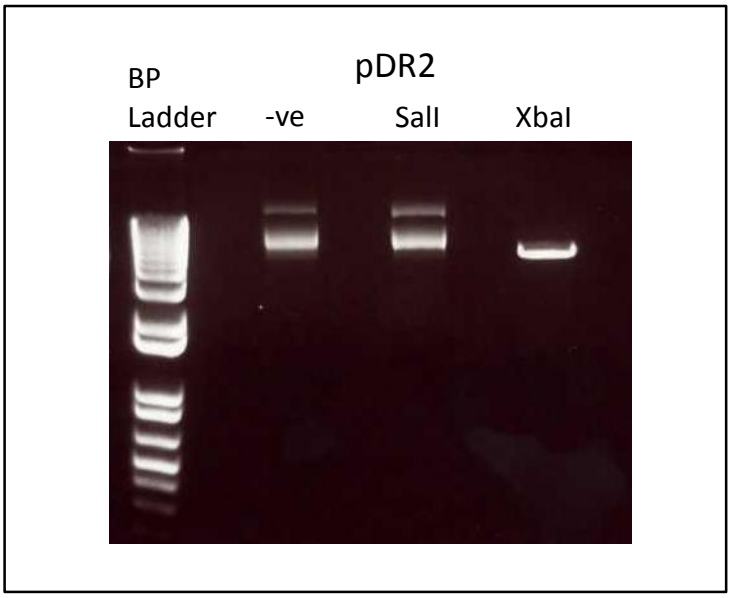

Figure 3.2.2.3 Single restriction digest of pDR2 vector. Plasmid DNA was incubated for 1 hour at 37°C in NEB buffer 3 containing no enzyme (-ve), SalI, and XbaI. Uncut and SalI 'digest' control plasmid DNA ran with two distinct bandings roughly 12 and 8 Kb in size representing uncoiled/relaxed plasmid and supercoiled plasmid respectively. XbaI cut the plasmid at a single site resulting in linear plasmid as shown by the band running to roughly 6Kb, SalI digestion did not linearize the plasmid, confirming the absence of a recognition site.

Insertion of the gene into the vector digested with XbaI alone allowed the possibility of insertion in two orientations. To select colonies containing the Cd59a gene ligated in the correct orientation, a direction specific primer pair was used for PCR based screening (Figure 3.2.2.4A). The forward primer used was specific for the plasmid sequence up-stream from the polylinker site and the reverse primer was specific for Cd59a terminal sequence (Figure 3.2.2.4A). Colonies formed on agar amp. plates after transformation from ligation were picked at random (6 and 7 for 6:1 and 10:1 ligation ratios respectively) and diluted directly in the pre-prepared PCR mix and placed on thermocycler for screening. PCR program was set as shown in Figure 3.2.2.4 B then products separated on 1% TAE agarose gel by electrophoresis. As shown in Figure 3.2.2.4C, 4 colonies for each of the ligation ratios were shown to contain plasmid containing correctly oriented Cd59a gene. Corresponding colonies were used to inoculate LB broth for expansion and plasmid purified using the QIAprep Spin Miniprep Kit (QIAGEN).

Purified plasmid DNA was sequenced by Cardiff University Central Biotechnology Services via the dye-terminator method and capillary electrophoresis using Genetic

A.

pDR2ΔEF1α PCR primers

For: CAAGCCTCAGACAGTGGTTC (54°C)

Rev: CCG*TCTAGA*TTAGAGATGACTTAAGAAAC (57°C)

pDR2ΔEF1α /CD59a (correctly orientated) 506 bp

CAAGCCTCAGACAGTGGTTCAAAGTTTTTTTCTTCCATTTCAGGTGTCGTGAGGAATTC*TCTAGA*GCCACCATG
AGAGCTCAGAGGGGACTCATCTTACTCCTGCTGCTTCTGGCTGTGTTCTGTTCCACAGCTGTTAGCCTCACATG
CTACCACTGTTTCCAACCGGTGGTTTCTTCATGCAATATGAACAGCACTTGCTCTCCTGACCAGGATTCCTGTCT
CTATGCTGTAGCCGGAATGCAAGTGTATCAAAGGTGTTGGAAACAATCAGATTGTCATGGTGAGATCATTATG
GACCAATTAGAAGAGACAAAATTAAAATTCAGATGCTGCCAGTTTAACTTGTGTAACAAAAGTGACGGATCCT
TGGGGAAGACACCATTGCTGGGGACCTCGGTTCTGGTGGCCATTTTGAATCTTTGTTTCTTAAGTCATCTCTAA
*TCTAGA*CGG

B.

Step	Temperature	Time
1	95°C	5min
2	95°C	30sec
3	60°C	55sec
4	72°C	1min
5	Cycle to step 2	× 40
6	72°C	5min
7	4°C	∞

C.

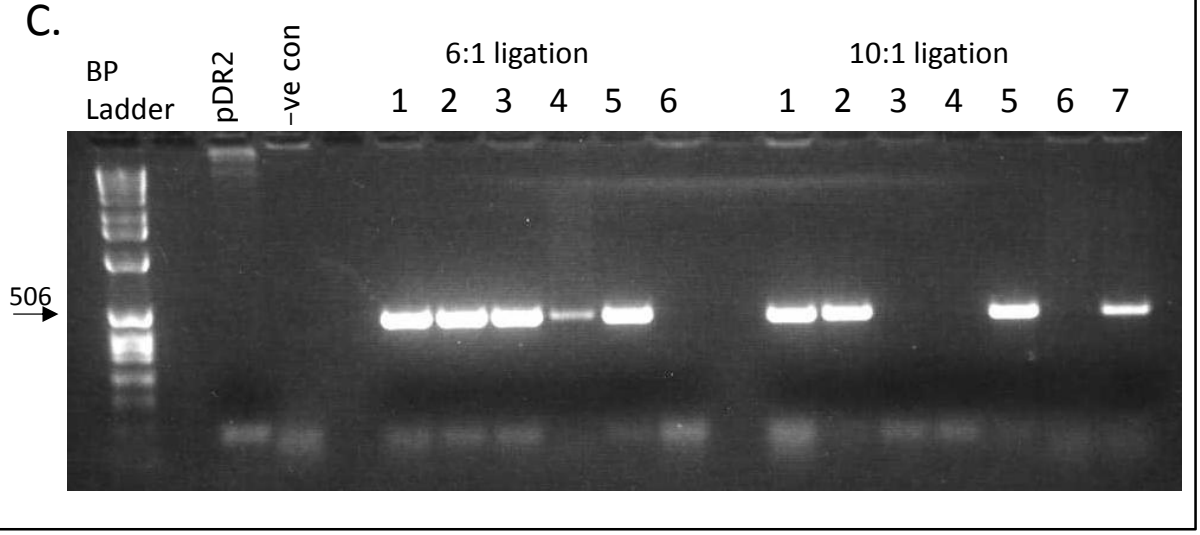

Figure 3.2.2.4 Screening PCR of colonies transformed with ligation reaction mixes. A. Forward primer specific for a region upstream of pDR2 polylinker and reverse primer specific for 3 prime region of the Cd59a gene, fragment length is 506bp. B. PCR program for screening of colonies. C. PCR products were separated on a 1% TAE agarose gel for 30 minutes at 100V. 4 colonies were positive in 6:1 ratio and 4 in 10:1.

A.

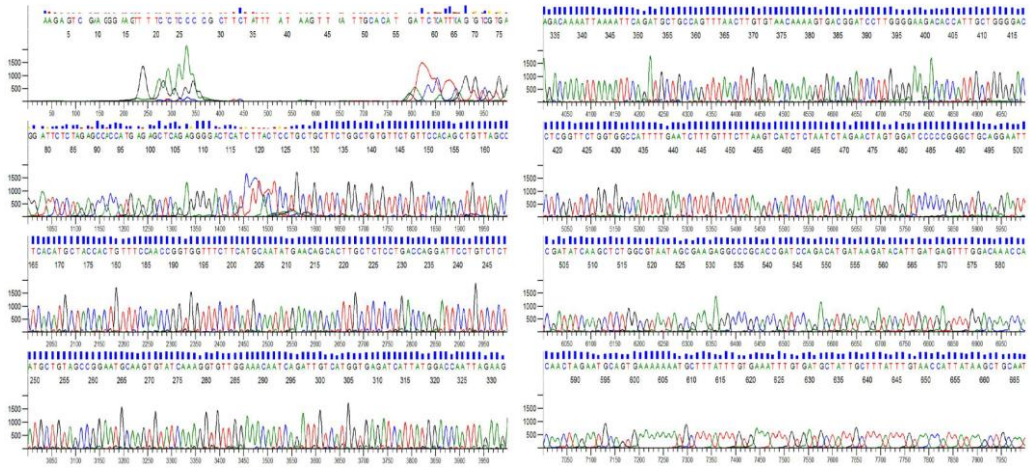

B.

>ref|NM_001111060.1| Mus musculus CD59a antigen (Cd59a), transcript variant 1, mRNA
Length=1823

GENE ID: 12509 Cd59a | CD59a antigen [Mus musculus] (Over 10 PubMed links)

Score = 688 bits (372), Expect = 0.0
Identities = 372/372 (100%), Gaps = 0/372 (0%)
Strand=Plus/Plus

```
Query  1    ATGAGAGCTCAGAGGGGACTCATCTTACTCCTGCTGCTTCTGGCTGTGTTCTGTTCCACA  60
            ||||||||||||||||||||||||||||||||||||||||||||||||||||||||||||
Sbjct  266  ATGAGAGCTCAGAGGGGACTCATCTTACTCCTGCTGCTTCTGGCTGTGTTCTGTTCCACA  325

Query  61   GCTGTTAGCCTCACATGCTACCACTGTTTCCAACCGGTGGTTTCTTCATGCAATATGAAC  120
            ||||||||||||||||||||||||||||||||||||||||||||||||||||||||||||
Sbjct  326  GCTGTTAGCCTCACATGCTACCACTGTTTCCAACCGGTGGTTTCTTCATGCAATATGAAC  385

Query  121  AGCACTTGCTCTCCTGACCAGGATTCCTGTCTCTATGCTGTAGCCGGAATGCAAGTGTAT  180
            ||||||||||||||||||||||||||||||||||||||||||||||||||||||||||||
Sbjct  386  AGCACTTGCTCTCCTGACCAGGATTCCTGTCTCTATGCTGTAGCCGGAATGCAAGTGTAT  445

Query  181  CAAAGGTGTTGGAAACAATCAGATTGTCATGGTGAGATCATTATGGACCAATTAGAAGAG  240
            ||||||||||||||||||||||||||||||||||||||||||||||||||||||||||||
Sbjct  446  CAAAGGTGTTGGAAACAATCAGATTGTCATGGTGAGATCATTATGGACCAATTAGAAGAG  505

Query  241  ACAAAATTAAAATTCAGATGCTGCCAGTTTAACTTGTGTAACAAAAGTGACGGATCCTTG  300
            ||||||||||||||||||||||||||||||||||||||||||||||||||||||||||||
Sbjct  506  ACAAAATTAAAATTCAGATGCTGCCAGTTTAACTTGTGTAACAAAAGTGACGGATCCTTG  565

Query  301  GGGAAGACACCATTGCTGGGGACCTCGGTTCTGGTGGCCATTTTGAATCTTTGTTTCTTA  360
            ||||||||||||||||||||||||||||||||||||||||||||||||||||||||||||
Sbjct  566  GGGAAGACACCATTGCTGGGGACCTCGGTTCTGGTGGCCATTTTGAATCTTTGTTTCTTA  625

Query  361  AGTCATCTCTAA  372
            ||||||||||||
Sbjct  626  AGTCATCTCTAA  637
```

Figure 3.2.2.5 Sequencing data and gene alignment for positive plasmid. Plasmid DNA expanded from colony 2 of 6:1 ligation was sequenced using the pDR2 5 and 3 prime primers specific for either side of the polylinker site. A. Chromatogram showing 5 prime sequencing with 100% coverage of the ligated Cd59a gene. B. BLAST alignment of sequence demonstrated the Cd59a gene had been cloned with high fidelity, without introduction of base changes or mutations.

Analyzer 3130xl (Applied Biosystems, Warrington, UK). Sequencing was carried out using forward and reverse primers specific for pDR2 polylinker region:

For: CAAGCCTCAGACAGTGGTTC

Rev: ATGTCTGGATCGGTGCGGGC

The sequencing data provided 100% coverage of the Cd59a plasmid insert and use of the NCBI basic alignment search tool (BLAST) confirmed that the inserted fragment was 100% identical to the sequence published for mus musculus Cd59a antigen (Cd59a), transcript variant 1, mRNA (RefSeq NM_001111060.1) Figure 3.2.2.5. Positive colonies were cultured in 5 mL aliquots of LB broth and cells used to generate sufficient plasmid DNA for further work, purified using the QIAprep Spin Miniprep Kit (QIAGEN), and for glycerol stock preparation, which were stored at -80°C.

3.2.2.4 Transfection of CT26 cells with pDR2 and pDR2/Cd59a

Transfection of CT26 cells with the prepared plasmids was achieved with either Effectene (QIAGEN) or Nanofectin (PAA, Somerset, UK) transfection reagents. For each transfection cells were seeded at 2×10^5 cells per well of a six well plate and incubated overnight in normal growth conditions.

For complex formation when using the effectene reagent 2 µg of pDR2/Cd59a plasmid DNA were diluted in DNA-condensation buffer (EC) to a volume of 100 µL. A volume of 16 µL of enhancer was then added and mixed using vortexer. This was incubated at room temperature for 5 minutes then spun down and 40 µL effectene reagent added (1:20, DNA:effectene). The final volume was mixed using a vortexer and incubated at room temperature for 7 minutes.

For complex formation, when using the nanofectin reagent, 3 µg pDR2 plasmid DNA and 9.6 µL nanofectin reagent (1:3.2, DNA:nanofectin) were both placed in 100 µL of diluent in separate tubes and mixed using a vortexer. The nanofectin containing solution was added

to the DNA containing solution and mixed using a vortexer. The resulting mixture was incubated for 20 minutes at room temperature.

To add the complex to seeded cells, spent medium was aspirated from the 6 well-plate, the cells washed and 1600 µL fresh full growth medium added. The transfection complex containing mixtures were diluted in 600 µL full growth medium and added dropwise to cells.

To allow for complex settling and cell uptake, the plates were incubated in normal growth conditions for 24 hours before selection antibiotic was added. For effective selection fresh medium with selection antibiotic Hygromycin (hyg.), at a concentration of 250 µg/mL, was added daily until colony formation was observed. Selection took 13 and 20 days for pDR2 and pDR2/Cd59a respectively for colony formation at which point cell numbers were adequate for expansion.

3.2.2.5 PCR for confirmation of transfection

In order to demonstrate and optimize a method for transfection screening, a PCR was developed using primers specific for the polylinker region of pDR2 (Figure 3.2.2.6). Fragment sizes depended on presence of the Cd59a gene in transfected plasmid and are shown in Figure 3.2.2.6A. PCR reaction mixes were prepared as in section 3.2.1.8 and 50 and 100 ng pDR2 and pDR2/Cd59a plasmid added. Reaction mixes were placed on thermocycler plate and program shown in Figure 3.2.2.6 run. PCR products were separated by electrophoresis on 1% agarose TAE gel (Figure 3.2.2.6C) showing product size for pDR2 as 143bp and pDR2/Cd59a as 527 bp.

This system is therefore useful in distinguishing the two plasmids and can be used to identify the presence of plasmid in transfected cells.

A.

pDR2ΔEF1α PCR primers

For: CAAGCCTCAGACAGTGGTTC
Rev: ATGTCTGGATCGGTGCGGGC

pDR2ΔEF1α 145 bp

CAAGCCTCAGACAGTGGTTCAAAGTTTTTTTCTTCCATTTCAGGTGTCGTGAGGAATTCT
CTAGAACTAGTGGATCCCCCGGGCTGCAGGAATTCGATATCAAGCTCTGGCGTAATAG
CGAAGAGGCCCGCACCGATCCAGACAT

pDR2ΔEF1α /CD59a 529 bp

CAAGCCTCAGACAGTGGTTCAAAGTTTTTTTCTTCCATTTCAGGTGTCGTGAGGAATTCT
CTAGAGCCACCATGAGAGCTCAGAGGGGACTCATCTTACTCCTGCTGCTTCTGGCTGT
GTTCTGTTCCACAGCTGTTAGCCTCACATGCTACCACTGTTTCCAACCGGTGGTTTCTT
CATGCAATATGAACAGCACTTGCTCTCCTGACCAGGATTCCTGTCTCTATGCTGTAGCC
GGAATGCAAGTGTATCAAAGGTGTTGGAAACAATCAGATTGTCATGGTGAGATCATTAT
GGACCAATTAGAAGAGACAAAATTAAAATTCAGATGCTGCCAGTTTAACTTGTGTAACAA
AAGTGACGGATCCTTGGGGAAGACACCATTGCTGGGGACCTCGGTTCTGGTGGCCATT
TTGAATCTTTGTTTCTTAAGTCATCTCTAATCTAGAACTAGTGGATCCCCCGGGCTGCAG
GAATTCGATATCAAGCTCTGGCGTAATAGCGAAGAGGCCCGCACCGATCCAGACAT

B.

Step	Temperature	Time
1	95°C	5min
2	95°C	30sec
3	60°C	55sec
4	72°C	1min
5	Cycle to step 2	× 40
6	72°C	5min
7	4°C	∞

C.

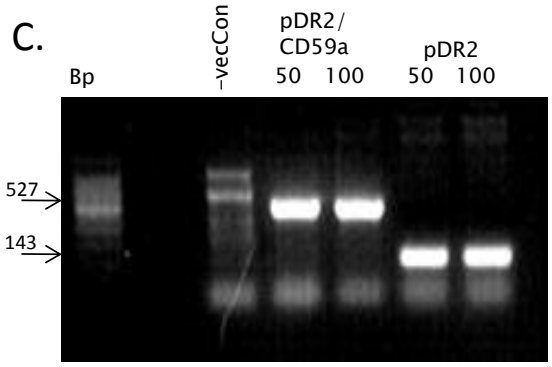

Figure 3.2.2.6 Development of transfection screening PCR. A. 5 and 3 prime pDR2 primers (brown) flanking the polylinker site expand PCR products of 143bp and 527bp for pDR2 and pDR2/Cd59a plasmids respectively. B. PCR thermocycler programme with 60°C annealing temperature and 40 cycles. C. 50 and 100 ng of purified plasmid was used for PCR reaction and the volumes separated by agarose gel electrophoresis (1% in TAE at 100V for 30 minutes), fragments predicted are clearly visible for pDR2/Cd59a and pDR2 plasmids, the negative control was clean.

3.2.3 **Flow cytometry**

For detection of surface antigens expressed by cells flow cytometry of antibody stained cells was used. Cells were detached in PBS+EDTA (5 mM) to protect protein from tryptic digestion and washed in FACS buffer - PBS+1% bovine serum albumin (BSA). Cell were incubated with a primary antibody for 1 h at 4°C. The cells were washed three times, and incubated with a FITC labelled secondary antibody for 30 min at 4°C in the dark. The stained cells were washed three times then analysed on a FACSCalibur (Becton Dickinson, Heidelberg, Germany) and the data analysed with Summit 4.3.1 software and plotted as a fluorescence intensity histogram.

3.2.4 **Haemolysis C activity assay**

3.2.4.1 Preparation of activated sheep erythrocytes (ShEA)

Haemolysis assays were conducted using aged sheep erythrocytes (ShE) which were required to be activated by coating in antibody for C activation. C fixation diluent (CFD) was freshly prepared from CFD tablets (Oxoid, Basingstoke, England) and kept on ice throughout. ShE were washed by placing 1 mL of sheep blood in Alsever's (TCS Biosciences, Buckingham, UK) in 20 mL CFD and centrifugation at 860×g (low braking) for 5 minutes. Supernatant was discarded and cells re-suspended in 20 mL CFD and centrifuged again. This was repeated until supernatant was clear, then 400 µL of the pelleted ShE were transferred to 10 mL warmed at 37°C CFD, this was mixed with 10 mL of warmed CFD containing 1/2000 amboceptor anti-ShE (Siemens Healthcare Diagnostics, Forchheim, Germany). The mixture was incubated for 30 minutes at 37°C on a rotator/roller. Cells were then washed by centrifugation as before until the supernatant was clear, the final pellet resuspended in 20 mL CFD creating a 2% activated ShE (ShEA) suspension that was stored on ice.

3.2.4.2 Haemolytic assay

ShEA prepared as described above were utilised to determine the haemolytic activity of various batches of human sera. Controls representing non-specific haemolysis (min) and 100% haemolysis (max) were prepared with 100 µL CFD or 0.2% triton-X-100 respectively. Serum samples were serial diluted ½ in CFD and placed in rows of a 96 well-plate, including a row for serum only to control for absorbance caused by serum. To experimental and min/max control volumes, 50 µL of the 2% ShEA suspension was added and to serum only controls CFD was added, then all wells made up to 150 µL and plates incubated for 1 hour at 37°C. To measure haemolysis, release of haemoglobin was measured in the supernatant. Plates were spun at 350×g for 3 minutes at 4°C, 80 µL of the supernatant was transferred to a flat bottomed 96 well-plate and absorbance measured at 410 nm using a FLUOstar OPTIMA plate reader (BMG Labtech, Aylesbury, UK). Percentage haemolysis was calculated using the following equation:

$$\%\, Lysis = \left(\frac{A^{complement\ release} - A^{spontaneous\ release}}{A^{detergent\ release} - A^{spontaneous\ release}} \right) \times 100$$

3.2.5 **Calcein release C dependent cytotoxicity (CDC) assays**

CDC assays were developed using the fluorescent labelling reagent calceinacetoxymethyl (AM). Calcein AM is a cell-permeant dye molecule, non-fluorescent in its precursor form, with its lipophilic blocking AM groups. Upon entry into a live cell the blocking groups are removed through acetoxymethyl ester hydrolysis by non-specific intracellular esterases. Hydrolysis converts the molecule into a less lipophilic moiety preventing its exit from the cell. The calcein molecule also becomes strongly fluorescent making it an excellent cell dye for use in lysis assays. For CDC assays all buffers and reagents, with the exception of serum dilutions, were pre-warmed to 37°C.

3.2.5.1 CDC assay

To measure the sensitivity of CT26 cells to CDC lysis the following protocol was followed. Cells grown to 80% confluency were washed in saline and detached using 10mM EDTA PBS. Cells were washed in serum free RPMI and live cell density measured by trypan blue exclusion assay as described in section 2.2.5. Cells were diluted to a density of 5×10^5 cells per mL, 100 µL placed in a flat-bottomed 96 well-plate, and the plate incubated for 16 hours at 37°C, 5% CO_2. Adherent cells were washed in serum free medium and 100 µL complete growth medium + 2 µg/mL calcein AM was dispensed into each well. The plate was then incubated for 1 hour at 37°C, 5% CO_2. Loaded cells were then washed twice in RPMI no additives and serum dilutions dispensed directly into wells and incubated for 1 hour at 37°C, 5% CO_2. For testing of C fixation, cells were incubated with or without 1/100 αMCF-7 antiserum in serum free RPMI for 1 hour at 4°C then washed twice. Serum dilutions were prepared by mixing human serum in serum free RPMI and 100 µL added per well of cells then incubated for 1 hour at 37°C, 5% CO_2.

3.2.5.2 Calcein release measurement

After exposure to serum, supernatant was transferred from plates either after centrifugation in detached cell experiments or directly from plates in monolayer experiments, to flat-bottomed 96-well plates and the fluorescence measured at excitation 485nm and emission 520nm using a FLUOstar OPTIMA plate reader (BMG Labtech, Aylesbury, UK). Remaining cells were lysed by addition of 100 µL 0.2 % Triton-X-100 RPMI solution per well and incubated for 15 minutes then, the plate was then spun and the supernatant transferred to a fresh flat-bottomed 96-well plate and fluorescence measured as above to quantify the total releasable calcein for each sample. Percentage lysis was calculated with the formula below. Values were then plotted using Graphpad Prism.

$$\%\, Lysis = 100 \times (FI^{complement\ release} / (FI^{complement\ release} + FI^{detergent\ release}))$$

3.2.6 **Affinity purification of Human C6 from serum**

3.2.6.1 Anti-C6 column preparation

Name	Contents
Phosphate buffered saline (PBS)	8.2 mM Na_2HPO_4, 1.5 mM KH_2PO_4, 137mM NaCl, pH7.4, 0.22µm filtered
Phosphate buffered saline (PBS) Azide	As above + 0.01% (w/v) NaN_3
Coupling buffer	0.2 M $NaHCO_3$, 0.5 M NaCl, pH 8.3, 0.22µm filtered
Wash buffer A	0.5 M ethanolamine, 0.5 M NaCl pH 8.3, 0.22µm filtered
Wash buffer B	0.1 M sodium acetate, 0.5 M NaCl, pH 4.0, 0.22µm filtered

An in-house generated mouse IgG anti-human C6 antibody, 27d1 was dialyzed overnight at 4°C in coupling buffer. Dialysed antibody was filtered through a 0.22 µm syringe filter and the concentration determined by absorbance at 280nm. 43.5 mg of antibody was coupled to a 5 mL Hi Trap column (GE Healthcare, Little Chalfont, UK), pre-washed with 1 mM HCl, by repeated (3×) passage at 1 mL/min. Free active binding sites on the column were blocked by application of buffer A (3×10 mL); followed by buffer B (3×10 mL). The column was then incubated in buffer A for 30 min at RT followed by a repetition of the first wash sequence. The finished column with bound antibody was washed into PBS azide and stored at 4°C.

To assess the coupling efficiency the antibody concentration in the retained flow-through coupling buffer was determined by absorbance at 280nm. Coupling efficiency was calculated as ~70%, equivalent to 33 mg of IgG coupled to the column.

3.2.6.2 Fast Protein Liquid Chromatography (FPLC) Purification of Human C6

Name	Contents
Glycine Elution buffer	100 mM Glycine in H_2O, pH 2.5, 0.22 µm filtered
Tris Neutralising buffer	1 M Tris, pH 10.5
H_2O	0.22 µm filtered

Purification of human C6 by affinity chromatography from plasma was carried out on an Akta Prime FPLC machine controlled with UNICORN 2.11 software (GE Healthcare, Little Chalfont, UK). The machine fluidics, normally stored in 20% ethanol, were washed with H_2O before washing into running buffer. The affinity column was attached, avoiding introduction of air bubbles. For first use the column was washed in elution buffer (0.3 mL/min) to remove any unbound or weakly attached antibody and re-equilibrated in running buffer (2 mL/min). Pooled, 0.22 µm filtered normal human serum (pNHS) was injected using a 50 mL Akta 'superloop' (GE Healthcare) installed on the injection valve. The column was washed in 4 column volumes (CV) running buffer and bound protein eluted in 2 CV of elution buffer. Eluted protein was collected in 1 mL fractions using a frac-950 (GE Healthcare) into 12 mm tubes containing 100 µL tris neutralising buffer to adjust the pH of the elution buffer to neutral and thus protect the integrity of the eluted protein. The column was re-equilibrated in 4 CV of running buffer.

3.2.6.3 Generation of C6 depleted Pooled Human Serum

Name	Contents
CFD run buffer (made from tablets, 1 per 100 mL)	4 mM Na barbitone, 145 mM NaCl, 0.83 mM $MgCl_2$, 0.25 mM $CaCl_2$, pH 7.2, 0.22 µm filtered
Diethylamine Elution buffer	50 mM Diethylamine, 10 mM Tris, 150 mM NaCl, pH11, 0.22 µm filtered
Tris Neutralising buffer	1 M Tris, pH 7

Serum, freshly prepared as described (section 2.3) was filtered through a 0.22 µm syringe filter and kept on ice. The 5 mL HiTrap column prepared as described in section 3.2.6.1 was attached to a FPLC, as described (section 0). Running buffer used for serum

preparations was CFD so that serum dilution would not interfere with C activity as is the case for PBS. Serum was injected by superloop as described in (section 0) and flow-through collected in 5 mL fractions. Flow-through was immediately placed on ice, pooled and filtered. C6 was eluted from the column and fractions neutralised with 1 M tris (pH 7), the column was then washed and re-equilibrated in running buffer. Where repeat injections were required the flow-through serum was injected by superloop and the method repeated. At every opportunity the serum was kept on ice. Depleted sera was tested to confirm lack of C lytic activity by haemolysis assay (section 3.2.4), aliquoted appropriately and stored at -80°C.

3.3 Results

3.3.1 **Confirmation of transfection**

The CT26 mouse colon carcinoma cell line does not express the CD59a antigen, the primary regulator of the MAC in mice (Baalasubramanian et al, 2004). In order to understand the role CD59a plays in sublytic MAC responses, CT26 cells were transfected with pDR2/Cd59a and pDR2 as an empty plasmid control. Transfection was conducted as described in 3.2.2.4 and cells tested for uptake of plasmid by PCR using the protocol described in section 3.2.2.5. PCR reactions confirmed the presence of pDR2 and pDR2/Cd59a in respective transfected cells corresponding in fragment sizes to purified pDR2 and pDR2/Cd59a positive controls (Figure 3.3.1.1A). To establish that the plasmid present was functional and driving constitutive expression of the CD59a antigen the cells were stained for CD59a, and analysed by flow cytometry (Figure 3.3.1.1B). CT26 cells confirmed by PCR as containing pDR2 and pDR2/Cd59a constructs were compared with untransfected cells. Untransfected and pDR2 transfected cells gave no signal above the background represented by secondary only control confirming that CT26 cells do not express the CD59a; however pDR2/Cd59a transfected cells had a much higher signal, a broad distribution of expression with >90% positive of total population.

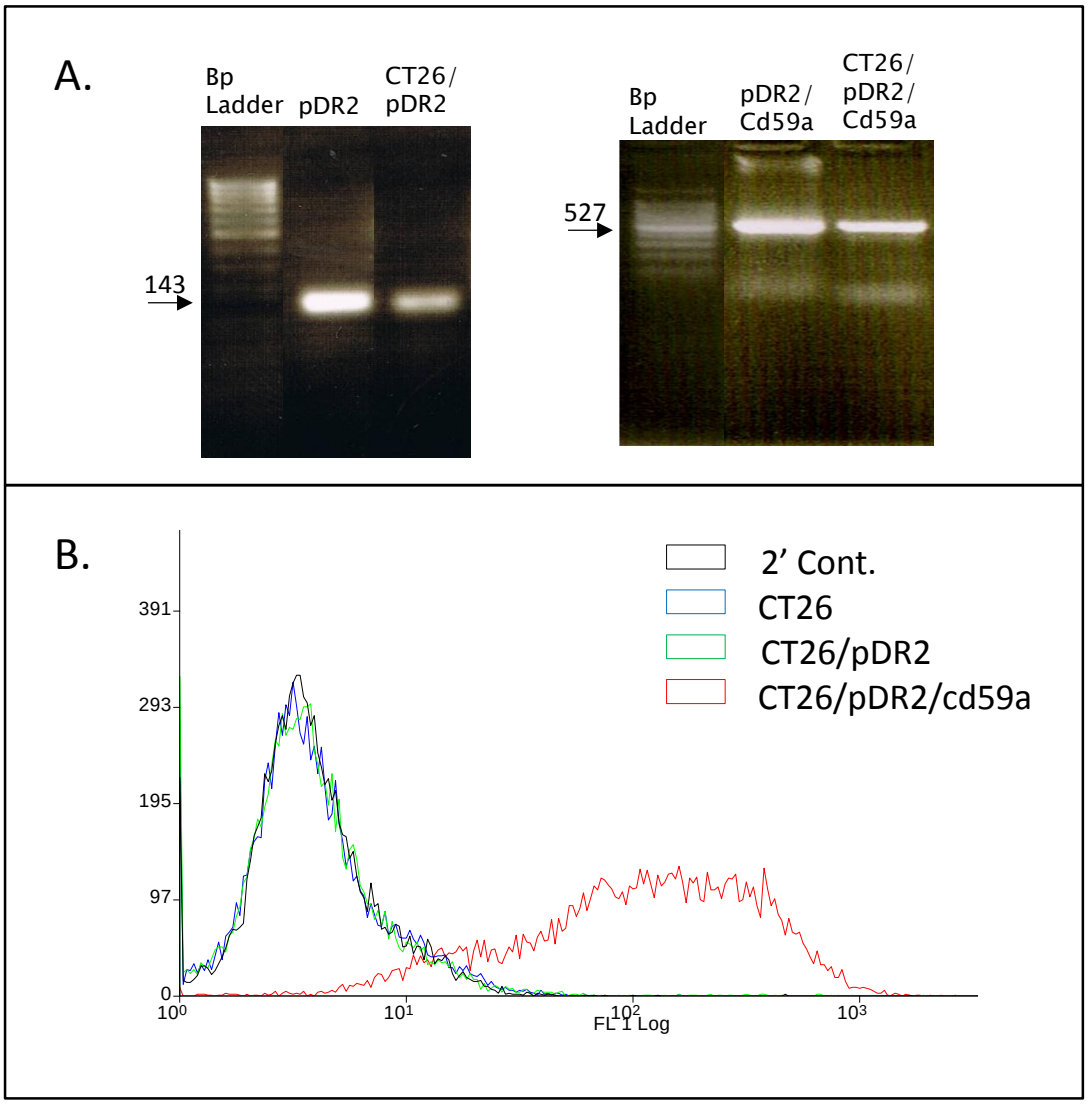

Figure 3.3.1.1 A. Screening of transfected CT26 cells using PCR. 50 ng of plasmid DNA isolated from cells designated CT26/pDR2 and CT26/pDR2/Cd59a (expanded colonies formed following hygromycin selection), was screened using the developed PCR. Fragments at 143 bp and 527 bp confirmed presence of pDR2 and pDR2/Cd59a plasmids in respectively. B. FACS staining for CD59a protein expression on transfected cells. CT26/pDR2 and CT26/pDR2/Cd59a were expanded and detached using EDTA then stained with mCD59a7 and an anti-mouse IgG FITC conjugated secondary antibody. FACS plot lines: Green; CT26/pDR2 secondary (2') control, Blue; CT26/pDR2 1' and 2', Red; CT26/pDR2/Cd59a 2' control and Pink; CT26/pDR2/Cd59a 1' and 2'.

3.3.2 **C susceptibility of CT26 cells**

3.3.2.1 C fixation using antiserum

To assess whether CT26 cells required antibody binding for C fixation, an antiserum raised against MCF-7 breast cancer cell line was used. The antiserum was shown by FACS analysis to bind CT26 cells (Figure 3.3.2.1A). CT26 cells were treated with anti serum and CDC lysis during incubation with 0-10% serum concentrations measured as described in section 3.2.5.2

Lysis profiles for cells incubated with and without antiserum were roughly similar, demonstrating an increase from 0 to 40% lysis with serum increasing 0 to 10% (Figure 3.3.2.1B). Addition of the αMCF-7 antiserum resulted in no significant increase in lysis compared to without its addition suggesting CT26 cells were capable of activating the C cascade spontaneously or through serum-natural antibody against expressed surface antigens. Note that the target cells are of mouse origin and serum from human. Binding of antibodies present in the antisera as shown by FACS did not contribute to increased C activation.

3.3.2.2 Sensitivity of CT26 cells to C

To assess the sensitivity of CT26 cells to C lysis, determine sublytic conditions and demonstrate that transfected CD59a was functionally capable of MAC regulation in these cells a CDC lysis assay was performed Figure 3.3.2.1C. CT26, CT26/pDR2 and CT26/pDR2/Cd59a cultured in a monolayer were loaded with calcein-AM and exposed to 0-40% pNHS concentrations for 1 hour, then lysis was calculated as described in section 3.2.5.2. Sensitivity of cells to C lysis was dependent on serum concentration, a clear effect of serum titration showed 40% pNHS resulted in the highest levels of lysis of around 50%. Lysis rose rapidly between 0 and 10% but increased less rapidly between 10 and 40% though not reaching a plateau. CT26 and CT26/pDR2 cells were roughly similar in CDC susceptibility with CT26 being marginally more susceptible.

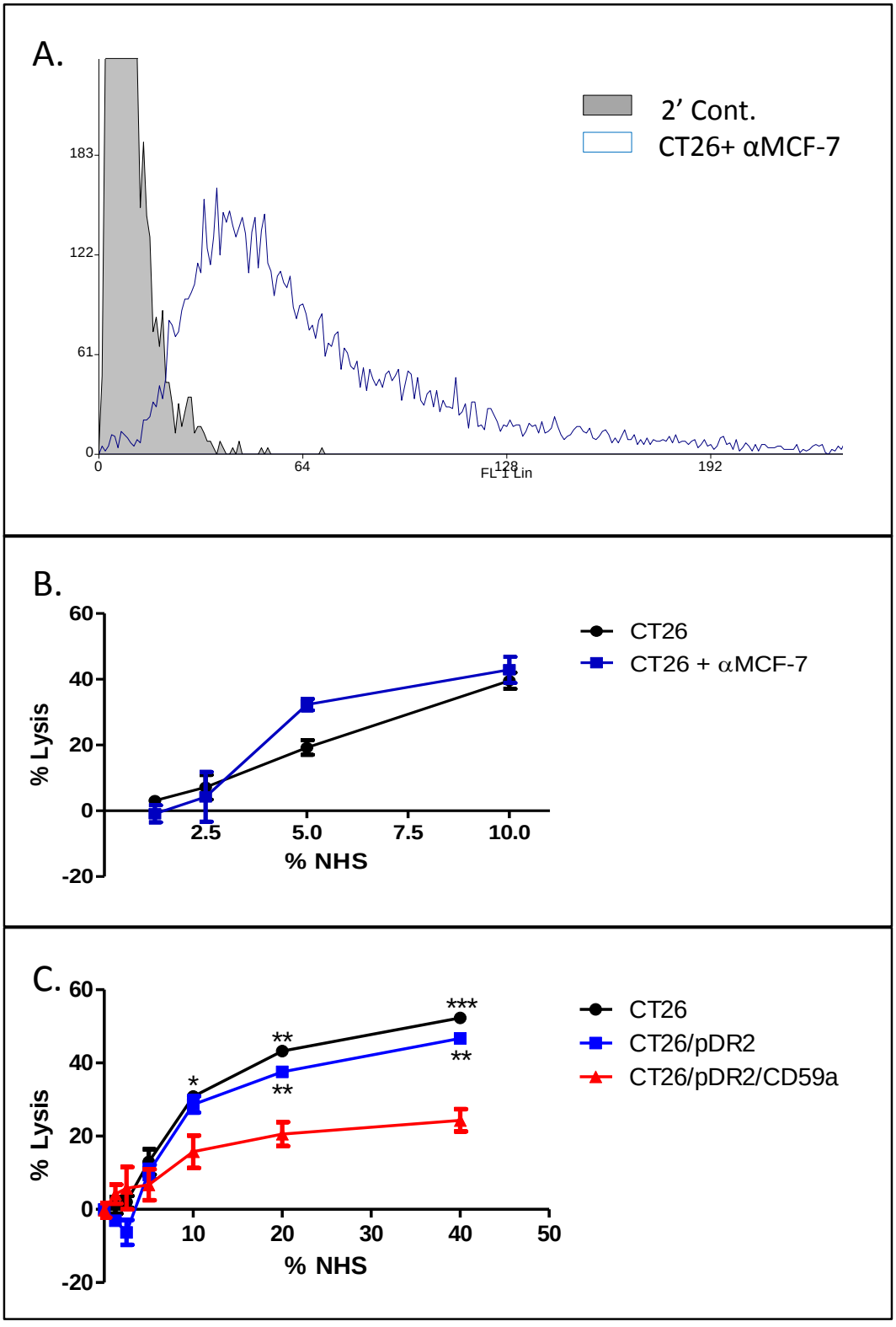

Figure 3.3.2.1 C dependent cytotoxicity (CDC) of CT26 cells using calcein release assays. A. FACS analysis of cells incubated with αMCF-7 anti-sera to assess binding of antibody to cell antigens. B. Comparison of detached CT26 cell susceptibility to C mediated lysis with and without αMCF-7 anti-sera pre-treatment. C. Susceptibility of CT26, CT26/pDR2 and CT26/pDR2/Cd59a cells in a monolayer to C lysis. In each CDC assay cells were loaded with calcein AM then exposed to serum for 1h at 37°C. Fluorescence was measured in the supernatant together with the residual released from the cells by 0.2% triton-X-100 treatment. % lysis was calculated as described in section 3.2.5.2. Results are mean n=3 +/- SEM (ns= not significant, *p<0.05, **p<0.01, ***p<0.001).

In contrast, CT26/pDR2/Cd59a cells were protected from C lysis with cell killing reaching a maximum of 20% when exposed to 40% serum. Indeed, the lytic profile showed a less rapid increase in lysis between 0 and 10% compared to CT26 and CT26/pDR2. CD59a expressing cells were significantly protected from lysis compared to CT26 and CT26/pDR2 at all serum doses between 10 and 40%.

At the lower serum concentrations (1.25, 2.5 and 5%) lysis was similar in each of the cells types irrespective of the presence of transfected CD59a, resulting in 10% lysis and below. C activation which achieves 10% lysis or less can be considered sublytic. The serum concentration which achieved this sublytic level in all cells was 5%.

3.3.3 **C6 depletion of serum**

To generate a control reagent for MAC induced sub lytic effects it was initially decided to prepare serum depleted of C6 since C6 is an essential component of the terminal pathway and the MAC. All purifications and depletions of C6 from plasma or serum were performed using the anti-C6 Hi TRAP column (section 3.2.6.1).

3.3.3.1 C6 purification: C6 activity

To test the column performance, capacity and also to ensure that purified C6 was active for use in future add-back experiments, C6 was purified from frozen plasma stocks. Plasma was thawed and filtered with a 0.2 µm syringe filter and 50 mL injected onto the column (FPLC setup and column attached as described in section 0). Protein was eluted in glycine buffer pH 2 and fractions corresponding to the elution peak (Figure 3.3.3.1A) were pooled and dialysed overnight against PBS at 4°C. Purified C6 was analyzed by SDS-PAGE on 10% polyacrylamide gels under reducing and non-reducing conditions and the gels coomassie stained (section 2.7.3) (Figure 3.3.3.1B). C6 ran faster on the gel under non-reducing conditions compared to reduced, bands appearing ~100 kDa according to molecular weight markers. C6 contains 32 internal disulphide bonds making it a highly stable protein and thus insensitive to SDS linearization (Discipio & Hugli, 1989).

However, under reducing conditions the covalent linkages are broken and the protein unravels to its fully linearized length.

Activity of purified C6 was confirmed using serum from $C6^{-/-}$ rats (Figure 3.3.3.1C+D). Haemolysis was conducted as in section 3.2.4. Deficient serum was titrated with or without addition of 50 µg/mL of C6 and ShEA added to each well. A serum only titration was used to control for signal caused by serum. The plate was incubated at 37°C for 1 hour and percentage haemolysis calculated from maximum and minimum controls. C6 deficient serum from knockout rats was haemolytically inactive until the addition of human C6 protein restored haemolytic activity to the serum (Figure 3.3.3.1C). Further experiments showed that as little as 10 µg/mL of human C6 was capable of restoring full haemolytic activity to the serum (Figure 3.3.3.1D).

3.3.3.2 C6 purification: column capacity

To test the capacity of the column to deplete plasma of C6, 50 mL plasma was run through the column and the flow-through collected then C6 eluted from the column (run 1). The diluted 60 mL flow-through was passed back over the column, eluted (run 2) and the 100 mL flow-through collected. This was passed over a third time and the remaining C6 protein eluted (run 3). Fractions were collected and pooled so that a C6 sample was retained after each run, elution peaks are shown in Figure 3.3.3.2 A. The C6 protein was analyzed on 7.5% polyacrylamide gels which were coomassie stained and western blotted (Figure 3.3.3.2B+C). Coomassie gels and western blots showed that the first pass extracted the greatest quantity of C6 with a little in the second run. None could be detected in the elution from the final pass by either coomassie or western blot. The data suggested that complete depletion of C6 from 50 mL plasma required at least 2 passes through the column.

3.3.3.3 C6 depletion from serum: single injections

The next step was to investigate the capability of the column to deplete serum with a single pass of the column since it is desirable to reduce the negative impact of passing serum through an antibody coupled column on C activity. Separate injections of 5 and 10 mLs serum (runs 1 and 2 respectively) were made and depleted serum collected (Figure 3.3.3.3A). Coomassie stain and western blot of eluted fractions demonstrated C6 recovery (Figure 3.3.3.3B+C). However, when haemolytic activity of the depleted serum from runs 1 and 2 was compared to that of pNHS (Figure 3.3.3.3D) the seras retained significant lytic activity showing less than a log decrease in activity. Depletion of 5 mL serum was marginally more effective than 10 mL injection. Thus, trace amounts of residual C6 were sufficient for significant haemolytic activity suggesting that MAC formation remains possible because of incomplete depletion.

3.3.3.4 C6 depletion: triple injection

Having demonstrated that single injections even of low volumes of sera were not able to achieve complete depletion of C6, repeated injections were performed starting with 20 mL volumes of pNHS. Collected flow-through was passed over the column twice more after original inject so that in total the serum had been thrice through the column (runs 1-3) (Figure 3.3.3.4A). To reduce any dilution of serum flow-through, only the most concentrated fractions were pooled as judged by UV trace post-injection. Depleted serum was then tested for its haemolytic activity compared to pNHS and showed a log reduction in activity which could be restored to that of pNHS with the addition of C6 to a final concentration of 50 µg/mL (Figure 3.3.3.4B). Apart from demonstrating a reduction of haemolytic activity by the near-total removal of C6, this also demonstrates that there is no loss of haemolytic potential subsequent to the passing of serum three times through a HiTrap column.

3.3.3.5 C6 depletion: quad injection

Although a log reduction in haemolytic activity was achieved after three passes of the serum, it was thought that a further reduction in activity could be achieved with a fourth pass. Western blot of serum after each run shows that C6 is undetectable after first run (Figure 3.3.3.5A). However, haemolytic activity remained in the final depleted serum, albeit reduced by more than a log compared to that of pNHS, and was fully restored upon the addition of C6 at a final concentration of 50 µg/mL (Figure 3.3.3.5B). Reduction of haemolytic activity of this depleted serum represented the closest to depletion thus far. CDC lysis assays conducted as in section 3.2.5, show that the depleted sera had significantly reduced lytic activity against CT26 cells compared to pNHS (Figure 3.3.3.5C). Addition of C6 to a final concentration of 50 µg/mL increased CDC activity but could not restore lytic activity of C6 depleted sera to that of pNHS. At this point, although C6D showed reduced haemolytic activity and very low CDC activity the failure to achieve complete inhibition of MAC formation capacity and restore CDC activity by C6 add-back, it was concluded that total C6 depletion as a sublytic C reagent presented a significant challenge that could not be overcome with the available tools and methods.

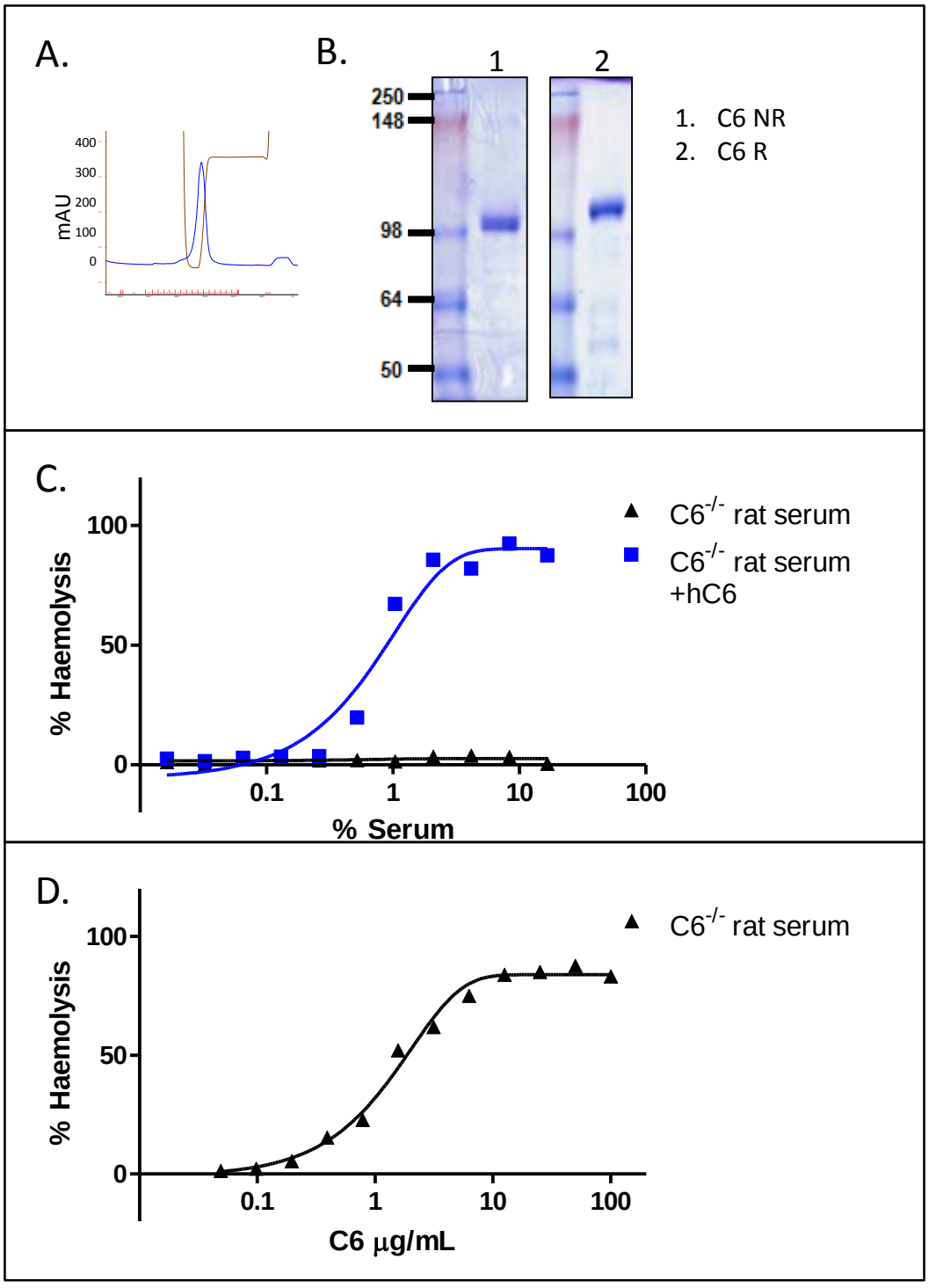

Figure 3.3.3.1 C6 purification from plasma using Hi-trap column coupled with 27d1 anti-human C6 antibody. A. UV absorbance at 280 nm profile of eluted protein. B. coomassie stain of pooled eluted fractions (1; non-reduced, 2; reduced). C. Haemolysis of $C6^{-/-}$ rat serum plus eluted fraction at 50 µg/mL of serum reconstituted lytic activity. D. Reconstitution of haemolytic activity in rat serum over protein concentrations from 100 µg/mL down to 0.

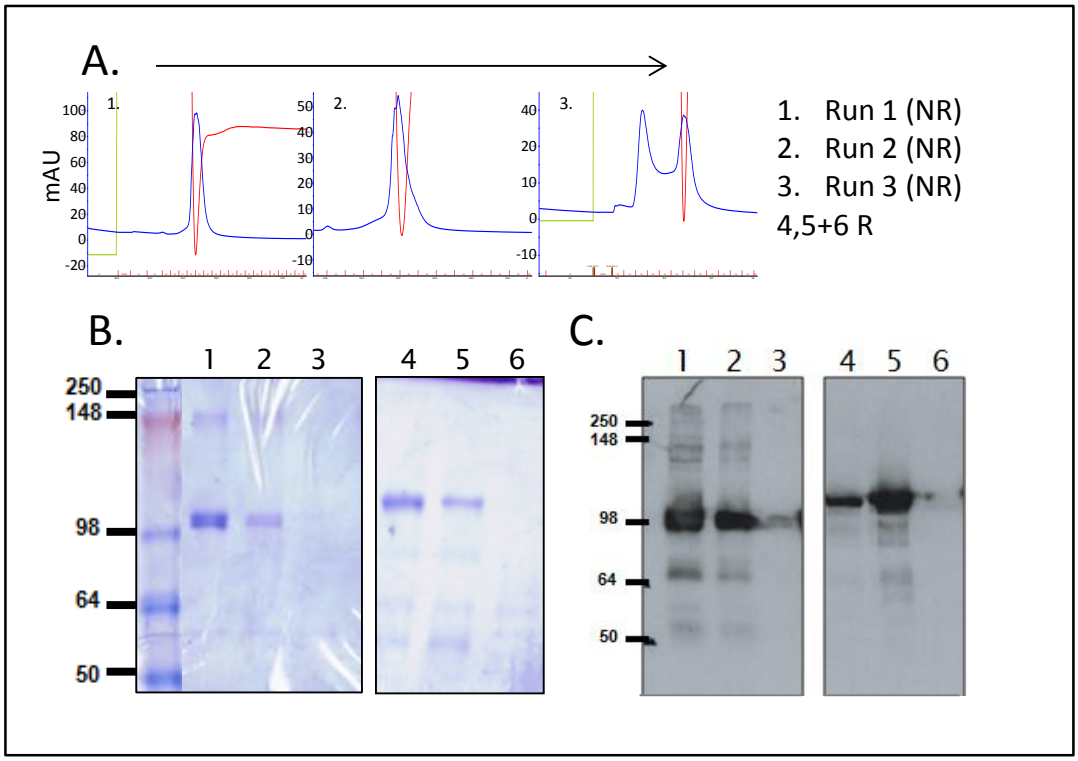

Figure 3.3.3.2 C6 depletion from 50 mL plasma. A. UV absorbance profile of eluted protein from sequential elutions (1-3, left to right). B coomassie stain and C. western blot; of pooled eluted fractions: 1+4; first, 2+5; second, 3+6; third run(1-3 non-reduced, 4-6 reduced).

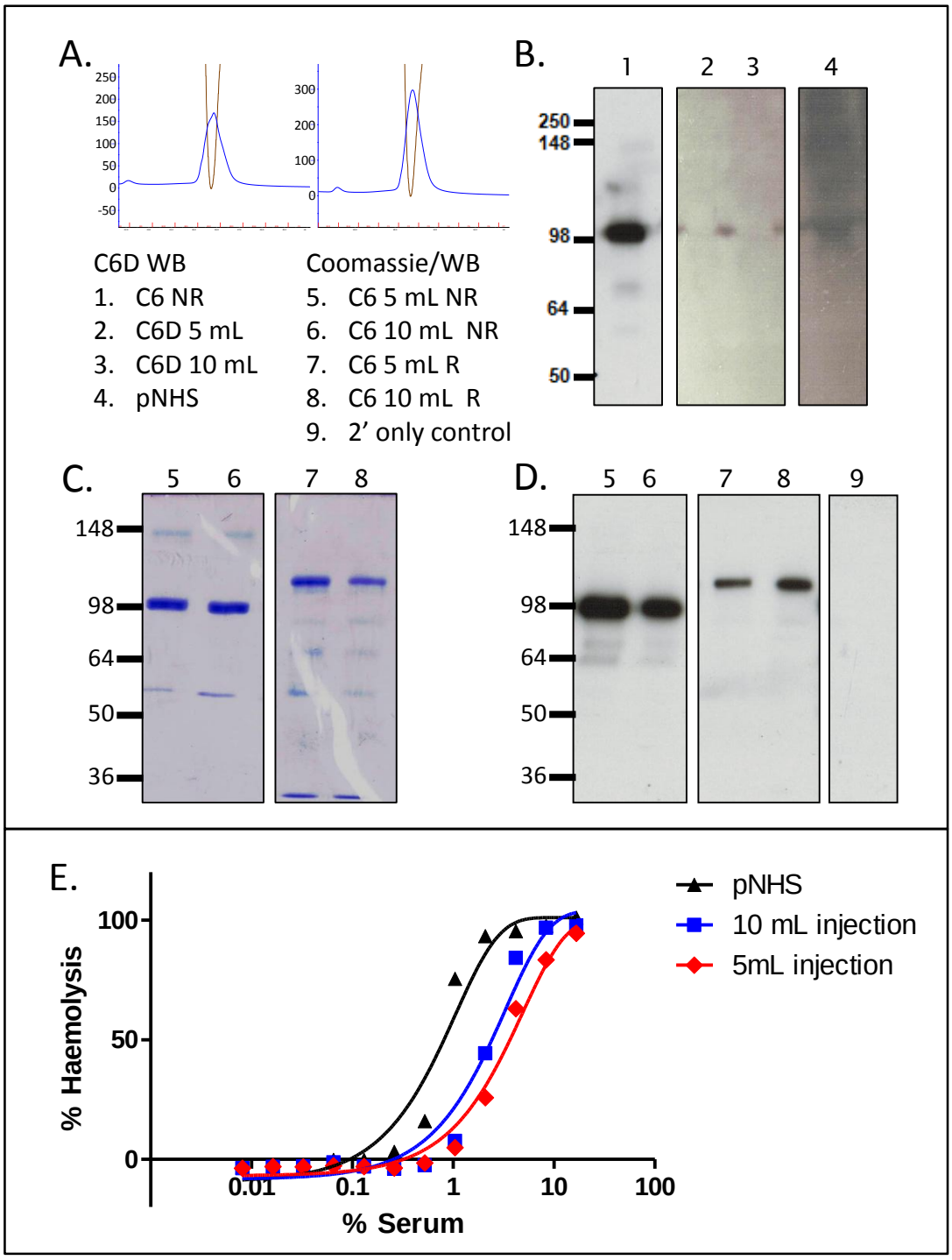

Figure 3.3.3.3 C6 depletion of 5 and 10 mL single injections of serum. A. UV absorbance at 280 nm profile of eluted protein from run 1 and run 2 (left to right). B. coomassie stain and C. western blot of eluted fractions 1+3; Run 1, 2+4; Run 2 (1-2; non-reduced, 3-4 ;reduced, 5; 2' control WB). D. Haemolytic activity of depleted sera from runs 1 and 2 compared to pNHS.

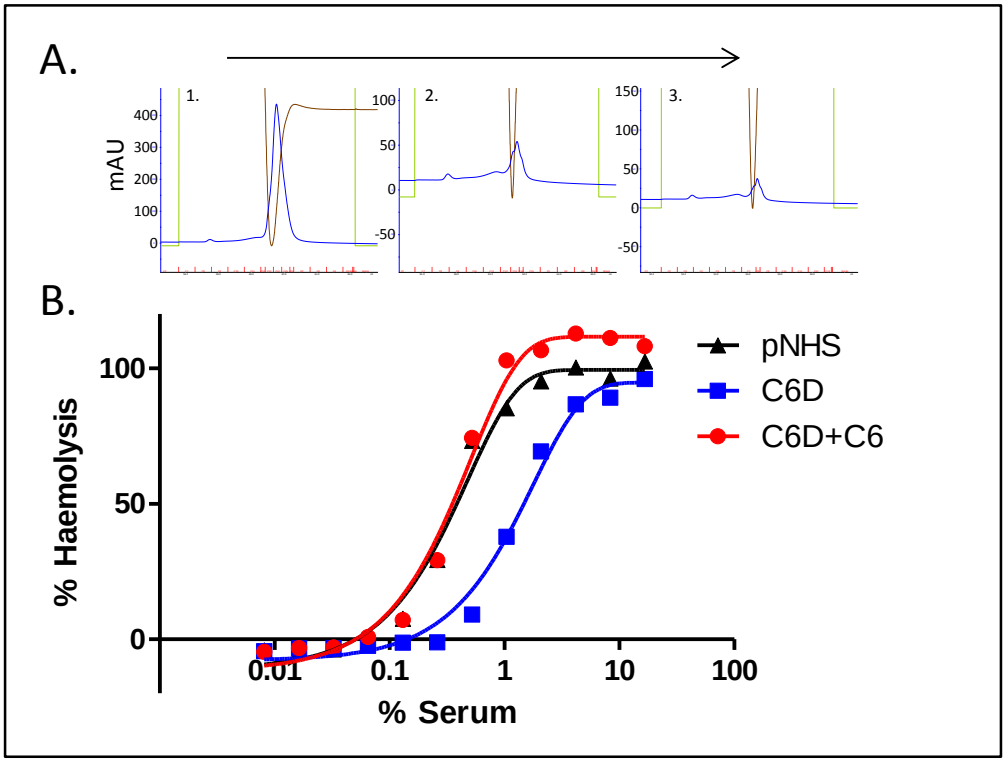

Figure 3.3.3.4 Serum depletion of C6, triple injections. A. UV absorbance at 280 nm profile of eluted protein from 3 sequential injections (left to right). B. Haemolytic activity of depleted sera with and without supplementation of C6 at 50 µg/mL serum compared to pNHS.

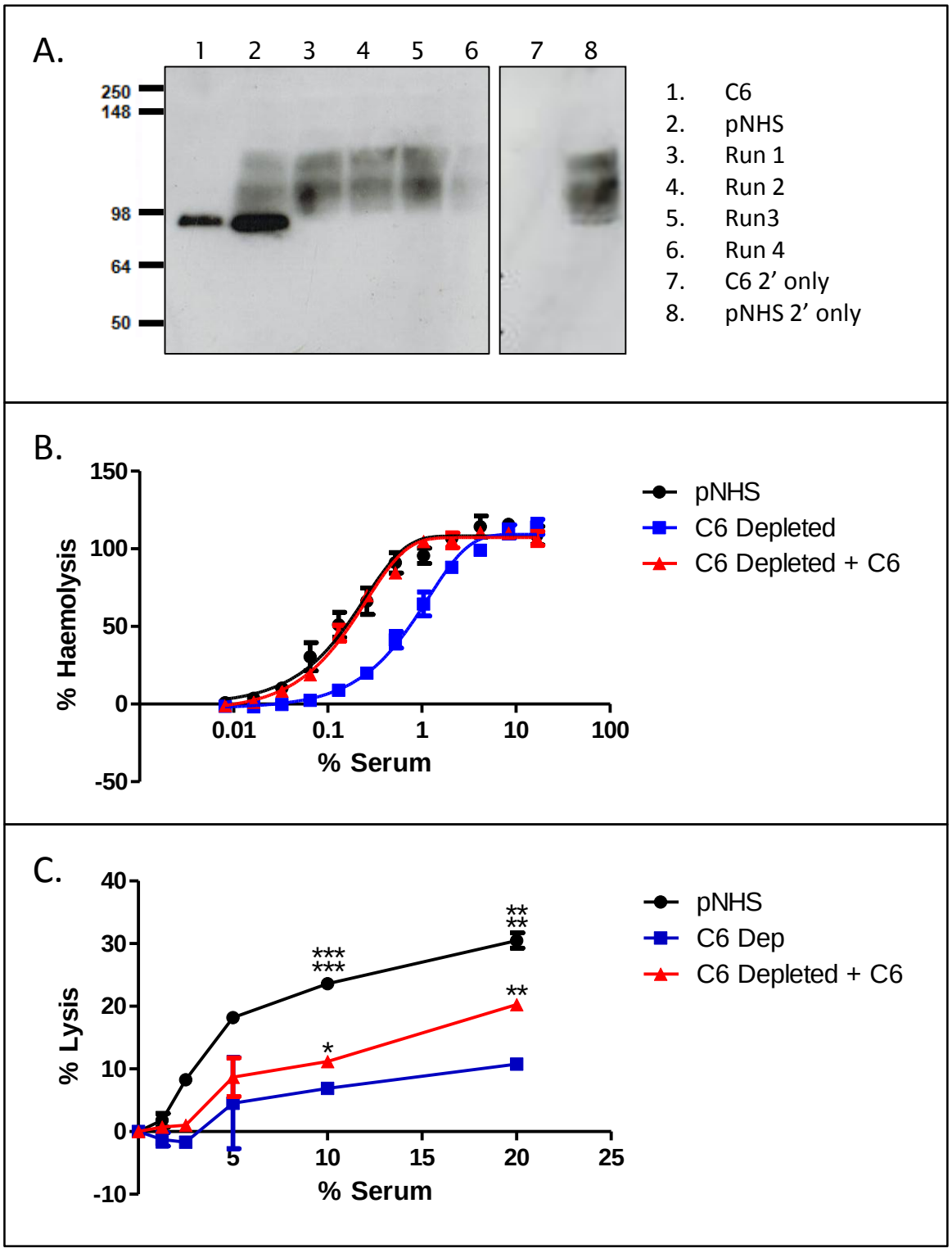

Figure 3.3.3.5 Serum depletion of C6, four injections with high pH elution conditions. A. Western blot of depleted sera probed with 27d1 (1') and HRP conjugated α-mouse IgG (2') (1;C6 protein, 2; pNHS, 3-6; depleted sera 1-4 injections, 7;C6 2' control, 8; pNHS 2' only control). B. Haemolytic activity of depleted sera with and without supplementation with C6 at 50 µg/mL serum compared to pNHS. C. CDC lytic activity (against CT26 cells) of C6D serum with and without supplementation with C6 at 50 µg/mL compared to pNHS. Results are mean n=3 +/- SEM (*p<0.05, **p<0.01, ***p<0.001).

3.3.4 **OmCI**

The failure of C6 depletion to provide a haemolytically inactive serum necessitated the use of a new strategy. I thus next explored the possibility of using inhibiting reagents to remove/block haemolytic activity. One such available reagent was OmCI, a C5 inhibiting protein isolated from the *Ornithodoros moubata* tick (Nunn et al, 2005).

3.3.4.1 OmCI Haemolysis

The concentration of OmCI required for complete inhibition of C activity was determined by haemolysis assay. A dilution series of OmCI concentrations ranging from 20 to 0.02 µg/mL in 50 µL was prepared in CFD. To each well 50 µL of a 50% serum solution was added and the plate incubated for 15 minutes at room temperature. Fifty microlitres of a pre-prepared 4% ShEA cell suspension was then added to each well. Maximum and minimum release wells were prepared as described (section 3.2.4.2) and the plate incubated for an hour at 37°C. Haemoglobin release was measured by absorbance and percentage haemolysis calculated using maximum and minimum release controls as in section 3.2.4. The concentration of OmCI required to achieve complete inhibition of C activity was found to be 10 µg/mL (0.6 µM) of serum (Figure 3.3.4.1A). Inhibition of serum using this dose was further confirmed by haemolysis comparing pNHS with pNHS treated with OmCI in serial titration (Figure 3.3.4.1B). Inhibition of CT26 CDC using OmCI was tested by calcein release as described in section 3.2.5 (Figure 3.3.4.1C). CDC was significantly inhibited by OmCI at both 5 and 10% pNHS ($p<0.01$ and 0.05 respectively) with OmCI treated serum diluted to 10% (v/v) achieving little over 5% lysis. The sublytic threshold level of 5% pNHS achieved just under 7% lysis and OmCI treated serum about 1% confirming it as a suitable control for assessing sublytic C.

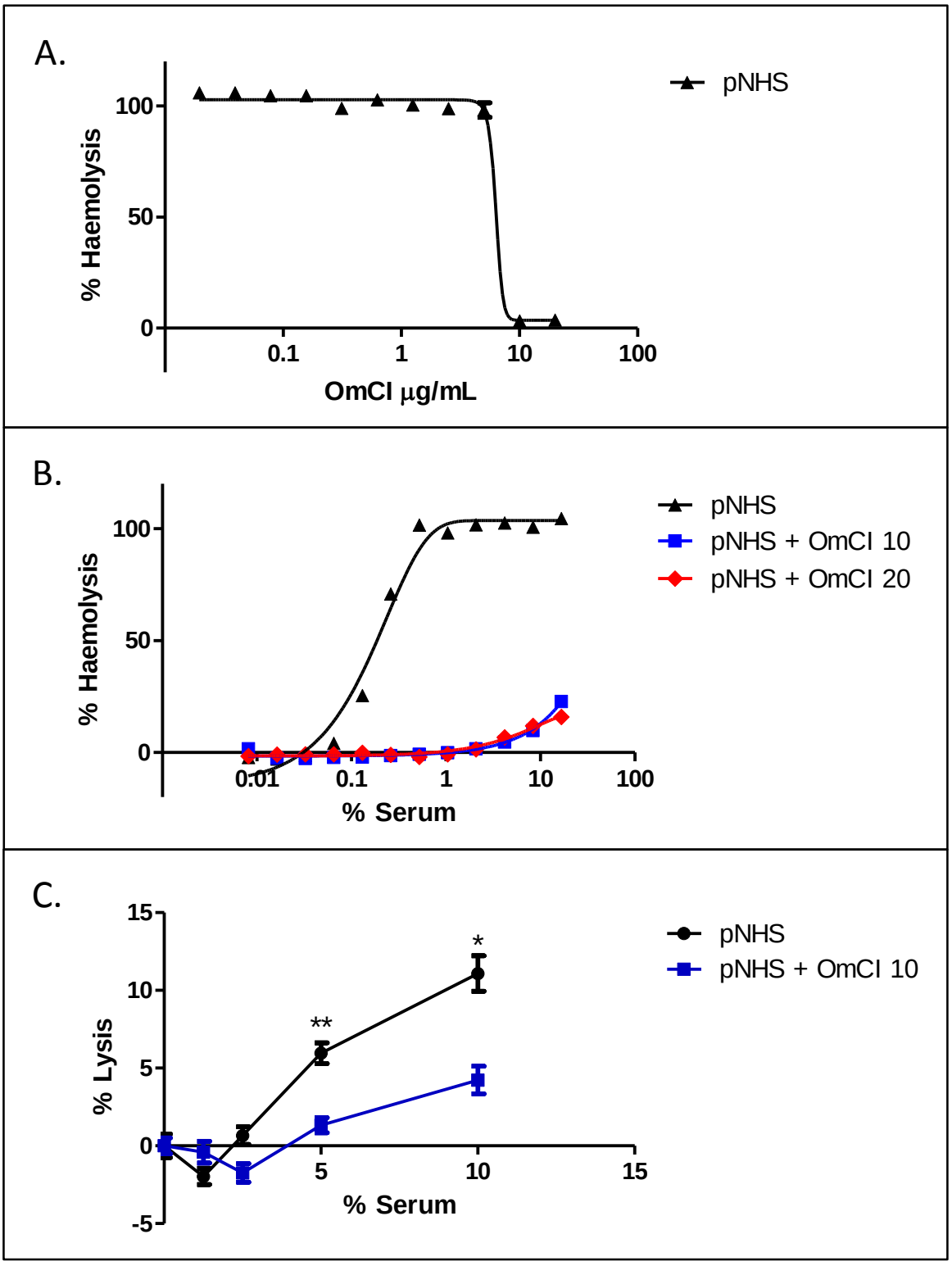

Figure 3.3.4.1 OmCI inhibition of the lytic potential of human serum. A. Haemolytic assay of serum treated with different doses of OmCI. B. Haemolytic activity of serum treated with or without 10+20 µg/mL OmCI, serum was titrated from 16% down to 0. C. OmCI inhibition of pNHS mediated CDC of CT26 cells. CDC assay showing lysis of cells exposed to 0-10% pNHS with or without 10 µg/mL OmCI treatment, results are mean n=3 +/- SEM (*p<0.05, **p<0.01) .

3.3.5 **Sublytic attack**

Section 3.3.2 described the sensitivity of CT26 mouse colon carcinoma cells to C lysis as defined in CDC calcein release assays. CT26 cells seeded to generate a monolayer of 1.6×10^3 per mm^2 of available culture surface area, exposed to 5% pNHS for 1 hour, resulted in less than 10% lysis and can be considered sublytic. Section 3.3.4 described the use of the terminal pathway inhibitor, OmCI as a control in sublytic experiments. Complete terminal pathway inhibition of serum was achieved by pre-treatment with 10 µg/mL OmCI for 15 minutes at room temperature shown both in haemolysis and CDC lysis assays (Figure 3.3.4.1). Looking carefully at the data, the conditions chosen for sublytic experiments were as follows: Cell monolayers 1.6×10^3 per mm^2 exposed to 5% pNHS, treated with or without 10 µg/mL OmCI and incubated in normal culture conditions (37°C, 5% CO_2) for 1 hour.

With conditions optimized, preliminary experiments could be performed to ascertain the best possible design for analysis of sublytic C effects and the role of the MAC. To do this measurable outputs were required to show that CT26 cells were indeed responding to sublytic C.

The first possible markers representing a response by tumour cells to sublytic C to be examined were informed by literature associations. Particular focus was placed on genes which had been shown to influence metastasis and proliferation acting as markers for tumour aggression. Proliferative markers chosen were Ki67 and PCNA. Metastatic markers chosen were OPN and uPA (Wai et al, 2005).

3.3.5.1 qPCR analysis

To determine whether expression of these marker genes was responsive to sublytic C, real time qPCR analysis was used to give gene expression relative to β-actin as a housekeeping control. Briefly, CT26, CT26/pDR2 and CT26/pDR2/Cd59a cells were cultured in the absence of hygromycin for 24 hours prior to seeding overnight at the stated

density (section 3.2.5.2) in normal growth conditions. Serum was treated with or without OmCI for 15 minutes at room temperature then diluted to 5% in serum free medium. The monolayers were then washed in serum free medium and 5% serum dilutions added. Cells were exposed for 1 hour and total RNA extracted directly from the monolayers using the Genelute extraction kit (Sigma). Concentration of extracted total RNA was measured and 1 µg reverse transcribed (section 2.5.4). PCNA, Ki67, uPA and OPN expression was measured relative to β-actin by qPCR analysis as described in section 2.6.2.

Expression data from the qPCR analyses of the proliferative markers PCNA and Ki67 revealed contradictory changes in gene expression with PCNA increasing strongly while Ki67 was decreased in un-transfected cells (Figure 3.3.5.1A and B). PCNA expression was significantly upregulated in response to pNHS compared to pNHS+OmCI in untransfected ($p<0.01$) and to a lesser extent in CD59a expressing cells ($p<0.05$) but not in empty vector controls which could indicate a proliferative response by CT26 cells to sublytic C; however, the effect was diminished in transfected cells suggesting perhaps that the presence of a transfected plasmid and hygromycin selection pressure interfered with this response (Figure 3.3.5.1A).

Relative expression of Ki67 in CT26 cells was significantly decreased in response to sublytic C ($p<0.05$), however in empty vector transfection controls gene expression increased significantly ($p<0.05$), whilst CD59a transfected cells showed no response to sublytic attack but had higher basal expression levels. Overall expression values for Ki67 calculated relative to β-actin were very low suggesting very low abundance compared to the housekeeping gene. This may make it difficult to interpret expression values.

The metastasis associated markers uPA and OPN were both increased in response to sublytic C when compared to the OmCI control (Figure 3.3.5.2A+B respectively).

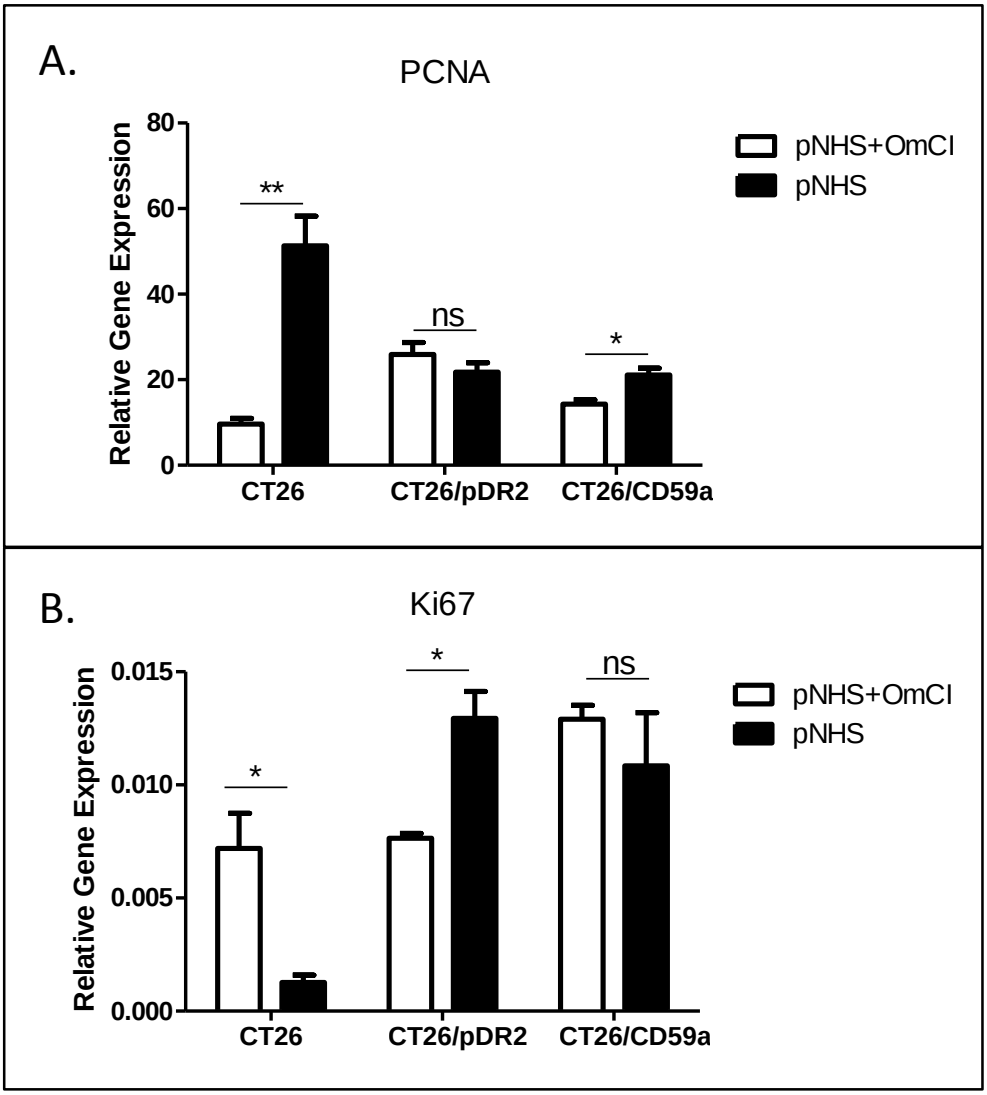

Figure 3.3.5.1 qPCR expression analysis of PCNA and Ki67 in response to sublytic C. Total RNA was extracted from CT26, CT26/pDR2 and CT26/pDR2/Cd59a cells exposed to 5% serum with or without OmCI treatment, reverse transcribed and subjected to qPCR analysis using primers specific for PCNA (A.) and Ki67 (B.) relative to β-actin calculated using the ΔΔCt calculation outlined in section 2.6.2. Results are mean n=3 +/- SEM (ns= not significant, *p<0.05, **p<0.01).

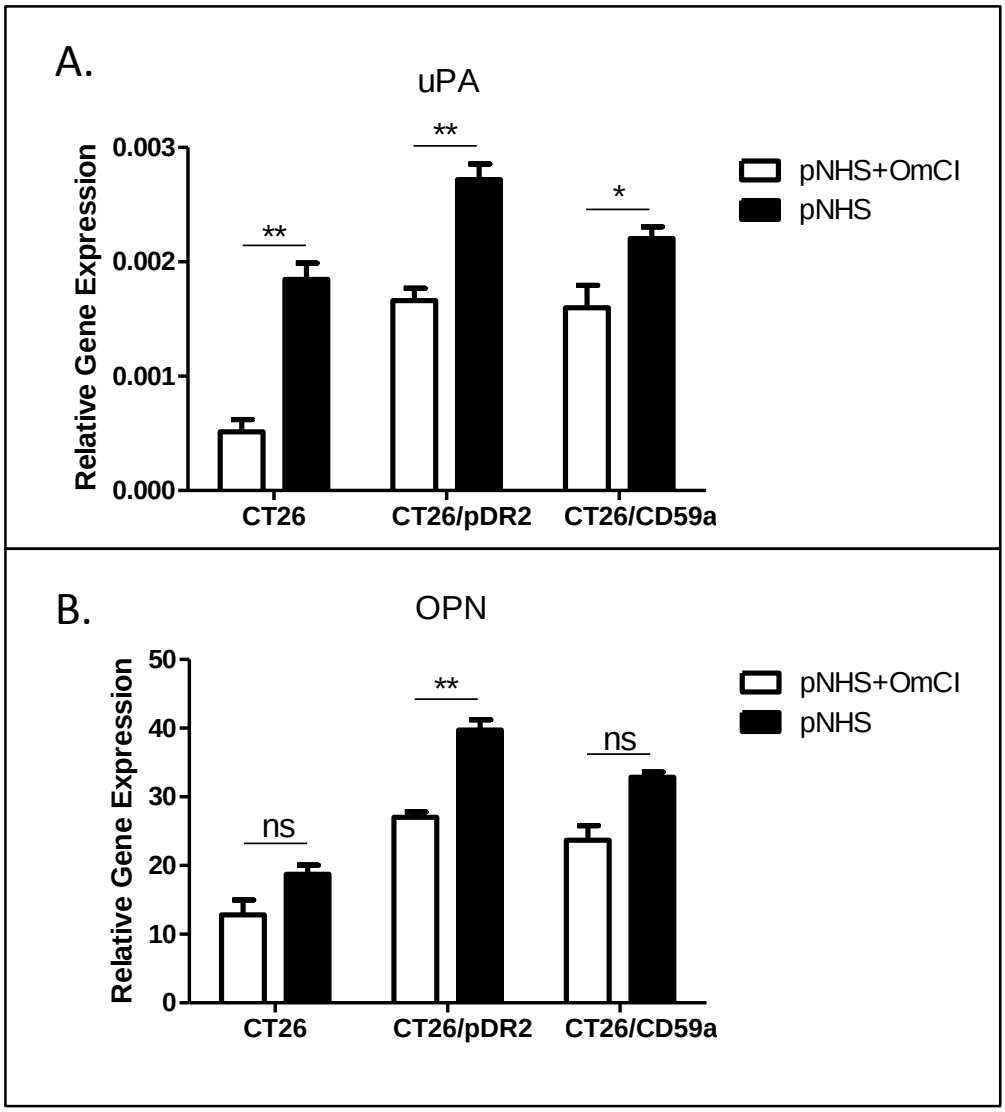

Figure 3.3.5.2 Expression analysis of uPA and OPN in response to sublytic C. Total RNA was extracted form CT26, CT26/pDR2 and CT26/pDR2/Cd59a cells exposed to 5% serum with or without OmCI treatment, reverse transcribed and subjected to qPCR analysis using primers specific for uPA (A.) and OPN (B.) relative to β-actin calculated using the ΔΔCt calculation outlined in section 2.6.2. Results are mean n=3 +/- SEM (ns= not significant, *p<0.05, **p<0.01).

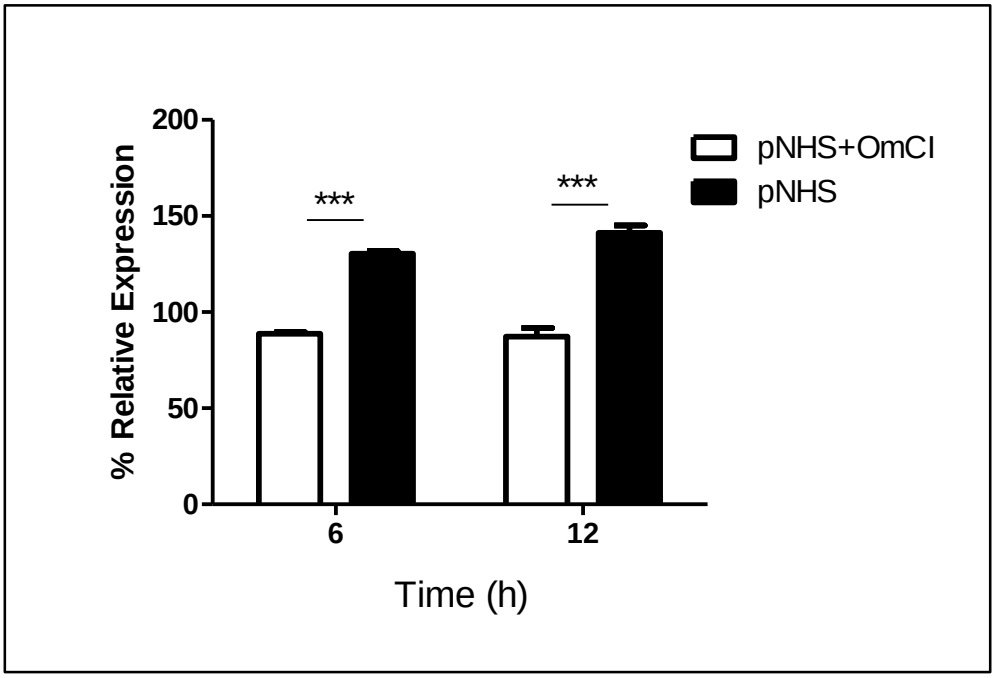

Figure 3.3.5.3 Expression analysis of OPN in response to exposure to sublytic C over a 12 hour time course. CT26 cells were exposed for 6 and 12 hours to 5% serum treated with or without OmCI then total RNA extracted and reverse transcribed. OPN gene expression was analysed by qPCR and calculated as relative to β-actin using the ΔΔCt calculation outlined in section 2.6.2 then presented as a % of untreated control . Results are mean n=3 +/- SEM (*p<0.001).**

The effect was mirrored in all three cell lines suggesting expression of CD59a had little impact on the expression levels although basal expression for both genes was higher in transfected cells and upregulation somewhat less in CD59a expressing cells compared to transfection controls. Upregulation of uPA was significant in all three cell lines (CT26 and CT26/pDR2 $p<0.01$, CT26/pDR2/Cd59a $p<0.05$) but OPN upregulation was only significant in pDR2 ($p<0.01$) cells although relative expression values were greater in OPN compared to uPA which suggests, as was the case for Ki67, that uPA was in deficit compared to the housekeeping gene. For this reason OPN was used as an indicative gene for gene expression changes in response to sublytic C and was investigated further.

To understand the time frame during which the upregulation of OPN occurred the experiment was repeated with only untransfected CT26 cells looking at expression levels at 6 and 12 hours post exposure. Cell monolayers were exposed to serum dilutions for 6 and 12 hours along with an untreated control. Total RNA was extracted and reverse transcribed for qPCR analysis of OPN. Expression levels were analysed relative to β-actin and calculated as a % of the untreated control as described in section 2.6.2.

Significant upregulation of OPN occurred at 6h ($p<0.001$) and 12h ($p<0.001$) hours showing a steady increase over the time course (Figure 3.3.5.3). Expression in OmCI control cells remained roughly the same as untreated cells at both time points. This data demonstrated a sustained gene expression change in response to sublytic C over a 12 hour period.

3.4 Discussion

The aims of the work described in this chapter were to develop and optimize the reagents and conditions for sublytic C experiments. Specifically, I sought to determine the concentration of pNHS required to achieve a sublytic threshold when used as a source of C on CT26 cells and investigate systems which could be used as controls for comparison against C terminal pathway activation as well as assess the influence of CD59a in any observed effects.

3.4.1 **Cd59a transfection**

For investigations into the role of CD59 in sublytic C effects on CT26 murine colon carcinoma cells a plasmid construct containing the murine homologue Cd59a was engineered. Cells were transfected with this construct (or its empty vector control) and transfection confirmed by PCR and expression of Cd59a protein product by flow cytometry. A feature of the expression profile revealed by flow cytometry was a broad spread of expression levels ranging from 1 log up to 3. To remove this spread CD59a expression could be sorted by serial dilutions to single cells and cloned out then screened to isolate high, middle and low expressors which could be used to further characterise the influence of MAC on cellular responses.

3.4.2 **Susceptibility of CT26 cells to CDC**

Calcein release CDC assays were used to demonstrate the functionality of expressed CD59a and define conditions for subsequent investigations into the cellular consequences of sublytic C attack.

CT26 cells were capable of triggering C activation in the absence of a fixing antibody. The mechanism for this activation is likely to be classical pathway activation via natural antibodies present in human sera. In a heterologous system such as this where a murine cell line is exposed to human serum, one possible explanation is that activation is

mediated by the natural presence in human serum of antibodies reactive to HMAg, a foetal bovine antigen incorporated in cell surfaces during culture with FBS (Richter et al, 1977).

Assays were initially developed using cells in suspension, as in antibody C fixation tests, but these were adapted for adherent cells which was the preferred format for sublytic experiments. CD59a expressing cells demonstrated significant protection from lysis compared to both the transfection control and untransfected cells. Overexpressed CD59a was therefore functionally active and capable of influencing susceptibility to lysis. In all cases the lytic profiles showed the cells had roughly similar sublytic thresholds revealing that the serum concentration which resulted in below 10% lysis was 5% for all three cell lines. It is from these assays that the cell density and sublytic threshold were derived for subsequent sublytic C experiments.

3.4.3 **C6 depletion of serum**

Detection of a cellular response to sublytic C is dependent on a comparison with a control, the choice of control is key in it's interpretation. Sublytic experiments which use serum as a C source require careful consideration because of the many growth factors and hormones present. These will inevitably activate cells and induce signalling events which must be controlled for. In addition to this, the use of serum as a C source to study the non-lethal effects of the MAC is further complicated by the release of the anaphylatoxins (C3a, C5a) prior to activation of the terminal pathway and formation of MAC.

It is therefore not sufficient to simply inactivate C completely as is the case in heat treatment of serum. A better strategy aimed at focussing on MAC formation is to remove the ability of serum to form MAC by depleting sera of factors required for its sequential formation. Terminal pathway progression and MAC formation can be restored by addition of the removed component. C6 depletion of serum was achieved by affinity chromatography using a Hi-trap column to which had been coupled a monoclonal

antibody reactive against human C6. The column had a dual purpose in that it allowed C6 to be purified for reconstitution of the haemolytic activity of C6 depleted serum.

C6 purification from 50 mL plasma by repeated passages suggested the column capacity was sufficient to deplete this volume with 3 passes (with elution of bound C6 between runs). However, it was desirable to keep the number of passes down to reduce the risks of on-column activation and dilution of the sera. Single runs of 5 or 10 mLs of serum suggested that complete depletion was achievable according to coomassie and western blot. However, the "depleted" sera retained significant haemolytic activity despite increasing the number of repeat passages of serum over the column from 1 to 4 and an alteration of elution conditions from low to high pH, it became clear that complete removal of haemolytic activity, despite the apparent removal of C6 as tested by western blot.

Haemolytic activity in serum "depleted" of C6 can be explained by trace amounts of residual C6. It is apparent that serum with extremely low quantities of C6 retains the ability to form MAC. This feature is perhaps not unexpected because subtotal C6 deficient individuals have been described with serum C6 concentrations as low as 0.74 µg/mL (compared to the normal ~45 µg/mL) but with relatively normal terminal pathway activation capacity (Wurzner et al, 1991). C6 is abundant in serum and it is clear that inhibition of terminal pathway activation and lysis requires it to be completely depleted. Formed C5b remains associated with the C5 convertase enzyme and is only released when it binds C6, this might explain why C6 does not limit activation because the C5b essentially 'waits', although briefly, for binding. With the excess C7 in C6 depleted serum any C5b6 that does form can readily bind C7 and the pathway continues. A more effective method might have been depleting of C7 because of its known rate limiting properties during terminal pathway activation (Silversmith & Nelsestuen, 1986). If C7 levels are restricted C5b6 accumulates in the fluid phase but is less likely to encounter C7. Binding of C7 allows it to associate with membrane and recruit C8 and C9. Depletion of C8 or C9 was not used because of

the reported cell activating properties of C5b-7 and C5b-8, though this activity is significantly less compared C5b-9 (MAC) (Niculescu et al, 1999).

A less likely explanation for the retention of haemolytic activity by C6 depleted sera is that the 27d1 antibody did not recognise a polymorphic variant of C6 such as that reported previously by Orren at al (1992). In that case a C6 protein, of 86% the molecular weight of the wild type, was isolated in patients with subtotal C6 deficiency. Serum containing this C6 subtotal deficiency (C6SD) protein retains haemolytic activity (Orren et al, 1992).

3.4.4 **OmCI treatment of serum**

In the search for a suitable control for MAC formation the C5 binding tick protein OmCI was tested. OmCI inhibited haemolytic activity of serum at 10 µg/mL of neat serum. C5 is present in serum at roughly 75 µg/mL equivalent to 0.39 µM, with OmCI inhibiting at 10 µg/mL or 0.6 µM the C5:OmCI molar ratio equates to 1:1.5. This is close to the hypothetical 1:1 ratio required for complete inhibition (Hepburn et al, 2007). OmCI concentrations above 10 µg/mL did not achieve improved inhibition indicating that saturation of available C5 had been reached. This is in agreement with concentrations determined by Hepburn et. al. (2007). Assays with human serum showed OmCI inhibited haemolysis completely at 14 µg/mL and to 92% at 9.4 µg/mL (Hepburn et al, 2007).

The use of a single reagent to inhibit the terminal pathway as a control has many advantages compared to depleted serum approaches. OmCI can be used to treat serum at the optimised concentrations determined in previous experiments; whereas depleted sera would likely require further optimization because of reduction in activity and a requirement for C6 supplementation for sublytic C activation. It has further advantages because it allows the use of pooled normal human serum (pNHS) which can be readily prepared in large quantities compared to C6 depleted sera which would require multiple depletion protocols to be undertaken.

3.4.5 **Sublytic C influence on putative marker genes**

With sublytic conditions optimized the next key objective was to develop the protocol on which a microarray experiment could be conducted. From the literature several genes were chosen representing key processes in tumour development and metastases in which a role for sublytic C attack could be hypothesised. The metastatic associated genes OPN and uPA, and the proliferation associated PCNA and Ki67 were found to be expressed by CT26. OPN expression by CT26 is directly linked to metastatic potential in both *in vitro* and *in vivo* studies (Wai et al, 2005). The remaining genes serve as surrogate markers of proliferative potential.

The metastatic markers OPN and uPA proved to be the most reliable markers. Both were upregulated in response to sublytic C and to similar degrees. Upregulation was reflected in each transfected cell line apart from an increase in basal expression. CD59a expression slightly suppressed the effect of upregulation probably by reducing functional MAC deposition and abrogating to some extent any sublytic effect. A C mediated upregulation of either of these genes has not been described previously. OPN was upregulated over a 12 hour time course in which the response was tested in CT26 cells.

The effect was mirrored in all three cell lines suggesting expression of CD59a had little impact on the expression levels although basal expression for both genes was higher in transfected cells and upregulation somewhat less in CD59a expressing cells compared to transfection controls.

3.4.6 **Murine cells , human serum**

The system optimized for the investigation of sublytic C effects makes use of human serum but the model cell line is of murine origin. This has some advantages but some important implications which should be considered.

The system has several practical advantages compared to the alternatives. The lack of a requirement for a complement fixing antibody means that there is no need to develop a

cell/antibody model where the recognised antigen is suitable, lacking signalling capacity. Also, human serum is plentiful making it easy to prepare large homogeneous batches for freezing compared to murine which is difficult to source in any great quantity. Finally, as discussed in section 1.1.6 murine serum is less haemolytically active than human and notoriously difficult to work with.

Though the system has these benefits it is clearly not advantageous to use a mixed species model. Cells bathed in non-homologous serum may respond differently to the stimulus intended and therefore may present a challenge when extrapolating results.

3.4.7 **Summary and conclusion**

Conditions for sublytic C attack were optimized in this chapter including cell density, format and serum concentration. Attempts to generate a non-lytic C6 depleted serum to control for MAC were unsuccessful and so the C5 inhibiting tick protein, OmCI, was used in its stead. Out of the four genes analysed by qPCR OPN and possibly uPA were upregulated in serum conditions compared to the OmCI treated control, demonstrating that sublytic C, and specifically the terminal pathway, could induce expression of genes associated with metastasis. OPN was shown to significantly increase over a 12 hour period in response to sublytic C attack from serum. These results allowed the construction of a 12h based sublytic attack experiment wherein RNA obtained from attacked CT26 cells would be subject to whole genome microarray analysis.

4 Global gene expression microarray

4.1 Introduction

4.1.1 Microarray gene expression analysis

4.1.1.1 Microarray principles

Microarray analysis allows the expression levels of many genes to be determined simultaneously. In recent years it has become commonplace to use microarray technology for various applications due to the democratisation of the available platforms through proliferation of information, access and reduction in cost. All microarray technologies are based on the hybridisation of DNA or RNA, a unique phenomenon first predicted by Watson and Crick, where sequences with high levels of complementarity are able to bind with high levels of specificity and affinity (Marmur & Doty, 1961; Watson & Crick, 1974). Microarray, as its name suggests, is a miniaturised version of the hybridisation technique allowing the number of queried entities to be increased by many thousands of times. Thus, the technology can be described as thousands of parallel dot blot experiments (Kafatos et al, 1979; Saiki et al, 1989; Southern, 2001).

4.1.1.2 Microarray technology

Principally, the technologies are based upon immobilization of specific nucleotide sequence onto a platform; these sequences are referred to as probes. Spots containing many identical immobilized probes are arranged so that their specific location is defined. An RNA or DNA sample, referred to as the target, is labelled, usually with a fluorescent moiety and incubated with the immobilized probes to allow for hybridisation of complementary sequence. After washing, each probe location is scanned for fluorescent signal. Fluorescent signal from each spot corresponds to the quantity of a DNA or RNA sequence hybridised with its specific probe, revealing the comparative quantity of a specific sequence in the starting material (Miller & Tang, 2009).

The technological underpinnings for the many platforms vary in three key aspects; the probe size, the method of manufacture and number of samples that can be accommodated (Tarca et al, 2006). A major advancement in the development of microarray technology was the move to rigid impermeable support materials from the flexible porous membrane (such as nitrocellulose) used in the dot blot technique; glass and in some cases silicon have been used, the impermeable quality of the material allows probes to be directly immobilized or synthesised in situ on the surface of the support with a high degree of accuracy. An impermeable support also promotes hybridisation by allowing improved access of probe to target (Southern, 2001). Printing of probes onto a glass support using inkjet technology or a contact printing method accurately places spots on the surface to create 10,000-30,000 separate and probe enriched 100-150 µm sized spots.

Early arrays used probes or complementary DNAs (cDNA) which were synthesised as dsDNA by PCR. Larger probes up to 1 KB in length have the advantage of specificity (Tarca et al, 2006). Immobilization of large dsDNA probes is achieved either through electrostatic forces or by UV cross-linking (Cheung et al, 1999; Ehrenreich, 2006). Covalent linkages can also be achieved with 5 prime amino group modification which is then linked to an available aldehyde or epoxy group present on a coated surface. The method of 'printing' dsDNA probes onto a glass support was the first microarray to be successfully used in a lab setting (Schena et al, 1995). Technology now more often use shorter oligonucleotide probes of between 25-70 nucleotides in length which give greater sensitivity and are more often chemically synthesised (Tarca et al, 2006).

4.1.1.3 In situ synthesis

The relative simplicity of placing a pre-synthesised probe on to a support then immobilizing it has given way to the much more specific and complex process of *in situ* synthesis where probes are 'built' base by base directly on to the support. *In situ* synthesis for modern microarrays is achieved by one of three strategies, photolithographic, digital

mask or inkjet methods. Photolithography is a system which uses bases coupled with a photo labile protecting group which will only allow chemical attachment of bases when the group is removed by exposure to UV. Bases are made available sequentially and a lithographic mask used to selectively expose spots for attachment. Over several cycles of A, T, G and C each probe is synthesised to a pre-programmed sequence. This is the method used by Affymetrix to create its quartz based GeneChips. Digital mask utilises a similar strategy replacing the lithographic mask with a virtual mask or digital micro mirror device (DMD). This technology is used by Roche to produce its NimbleGen chips which are also based upon quartz platforms. In contrast to these mask utilising approaches, Agilent uses inkjet technology to place nucleotides one by one in sequence specific to each probe onto a glass support (Hughes et al, 2001).

4.1.2 **Bead array**

4.1.2.1 Introduction

A novel system, known as bead array, substitutes the chip based substrate onto which the probes are attached, with 3µm silica beads which are allowed to self-assemble randomly onto a platform etched with micro-wells as shown in Figure 4.1.2.1 (Michael et al, 1998). Bead arrays allow for a greater density of features compared to conventional spotted arrays but necessitate a method of identifying the probes on randomly arranged beads. An ingenious method was devised to decode the location of beads using hybridisation with fluorescently labelled decoder sequences. In addition to the gene specific sequence of each probe a unique 29-mer identifier sequence or address is also included (Figure 4.1.2.1). Defined pools of oligonucleotide decoders labelled with one of four ‘colours’ are hybridised and scanned and then the Beadchip washed. Repetition of this sequence with several decoder pools builds a unique code for each bead based on the colour status after each hybridisation (Gunderson et al, 2004). This method also has the advantage of validating hybridisation and providing quality control for every bead on the array.

4.1.2.2 BeadChip

In its current form, Illumina BeadChips are manufactured by immobilizing 10s of thousands of unique synthesised oligonucleotides of 50 nucleotide bases in length onto beads in separate reactions to create a bead type for each probe. For every unique probe there are roughly 30 separate beads on any given chip which arrange randomly resulting in a Poisson distribution of beads per type and chip, a fact which is compensated for by the abundance of beads per probe. This abundance also adds an extra level of data quality due its inherent redundancy, controlling for outliers and read problems which in conventional single probe features can confound results (Kuhn et al, 2004).

For murine expression studies the MouseRef-8 v2.0 Expression BeadChip is suitable. It includes expression probes for 25600 refseq transcripts of which 19100 are unique genes. Probe content is informed by the National Centre for Biotechnology Information Reference Sequence (NCBI refseq) database, build 36 release 22, and is supplemented with content derived from the Mouse Exonic Evidence Based Oligonucleotide (MEEBO) and RIKEN FANTOM2 databases. Construction of the BeadChip accommodates 8 samples which when paired allows interrogation of 16 samples in total.

4.1.2.3 RNA Sample preparation

For the detection of gene expression, abundance of hybridised material must be measured easily. Historically this has meant the labelling through various means of target with fluorescent probe, usually Cy3 or Cy5. Many early microarray methods relied on the labelling of cDNA during reverse transcription of mRNA samples, through incorporation of

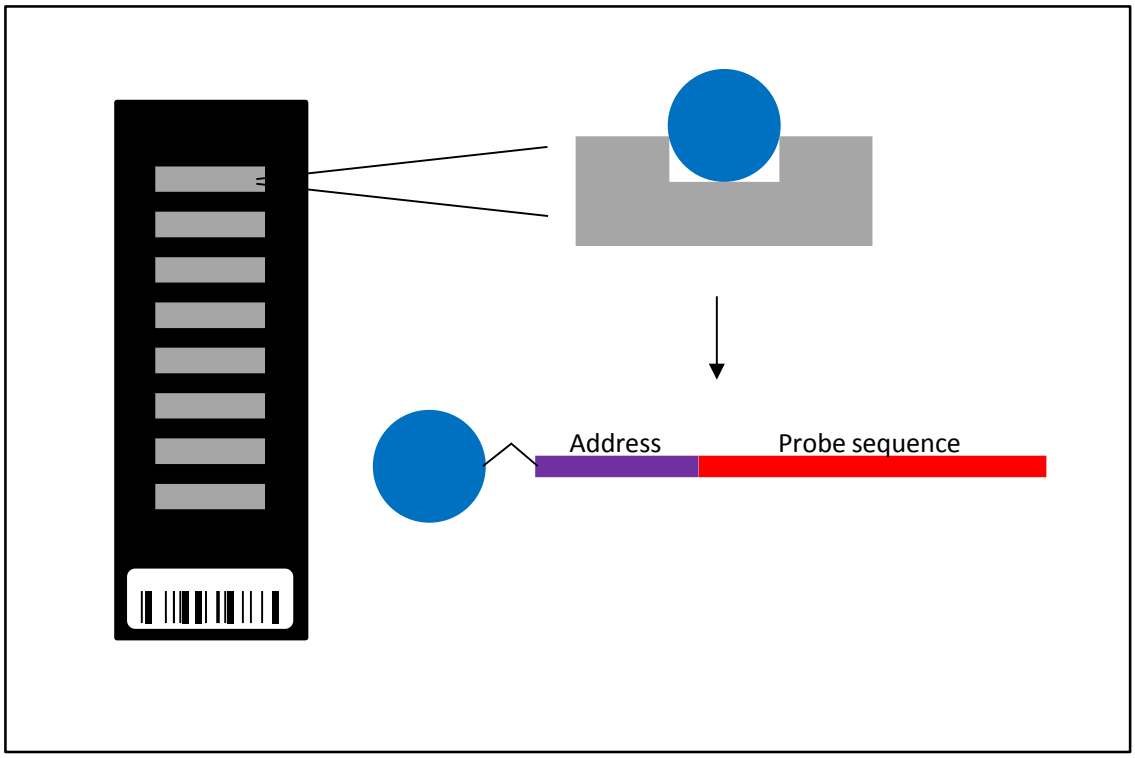

Figure 4.1.2.1 Mouse ref8v2 BeadChip array. Plasma etched wells are populated with 3 µm silica beads coated in conjugated nucleotide sequence containing both an address and probe sequence. Address sequence is used for localisation of randomly distributed beads. Probe sequence is 50 nucleotide bases in length and complementary to target sequence. Each BeadChip contains 8 arrays to accommodate 8 separate samples, and chips are shipped in pairs to accommodate 16 samples.

dye labelled nucleotides. RNA quantity is a key consideration in the success of a hybridisation experiment; with some starting materials yielding tiny amounts of RNA it is often necessary to amplify the signal. A now common method to achieve amplification of RNA uses T7 polymerase to achieve a linear amplification (Figure 4.1.2.2) . Firstly, mRNA is specifically reverse transcribed using oligo(dT) primers with an incorporated T7 promoter sequence, then second-strand DNA synthesis is performed using DNA polymerase creating double stranded cDNA strands. Double stranded cDNA is then used as a template for *in vitro* transcription by T7 polymerase which recognises the promoter sequence and generates many cRNA strands from the template (Vangelder et al, 1990). T7 amplified RNA was shown to give reliable expression data when compared with unamplified RNA prepared using standard techniques, giving similar differential expression ratio values (Pabon et al, 2001). T7 amplified cRNA can also be produced with incorporated labelling such as biotin labelled nucleotides. Inclusion of a biotinylated uridine (16-UTP) in the mixture allows the incorporation of biotin in all new cRNA strands. Cyanine 3 conjugated to streptavidin is used for detection through binding to biotin labelled cRNA post hybridisation.

4.1.2.4 Hybridisation procedure and data collection

Direct hybridisation of biotinylated cRNA with BeadChip probes is achieved by incubation overnight in HYB buffer. Fluorescence is detected by the iScan system which uses a laser confocal system to scan the BeadChip and generate an image from which spot locations can be defined and signal assigned. Signal intensity represents relative abundance of complementary cRNA sample which directly correlates with mRNA transcript and thus gene expression.

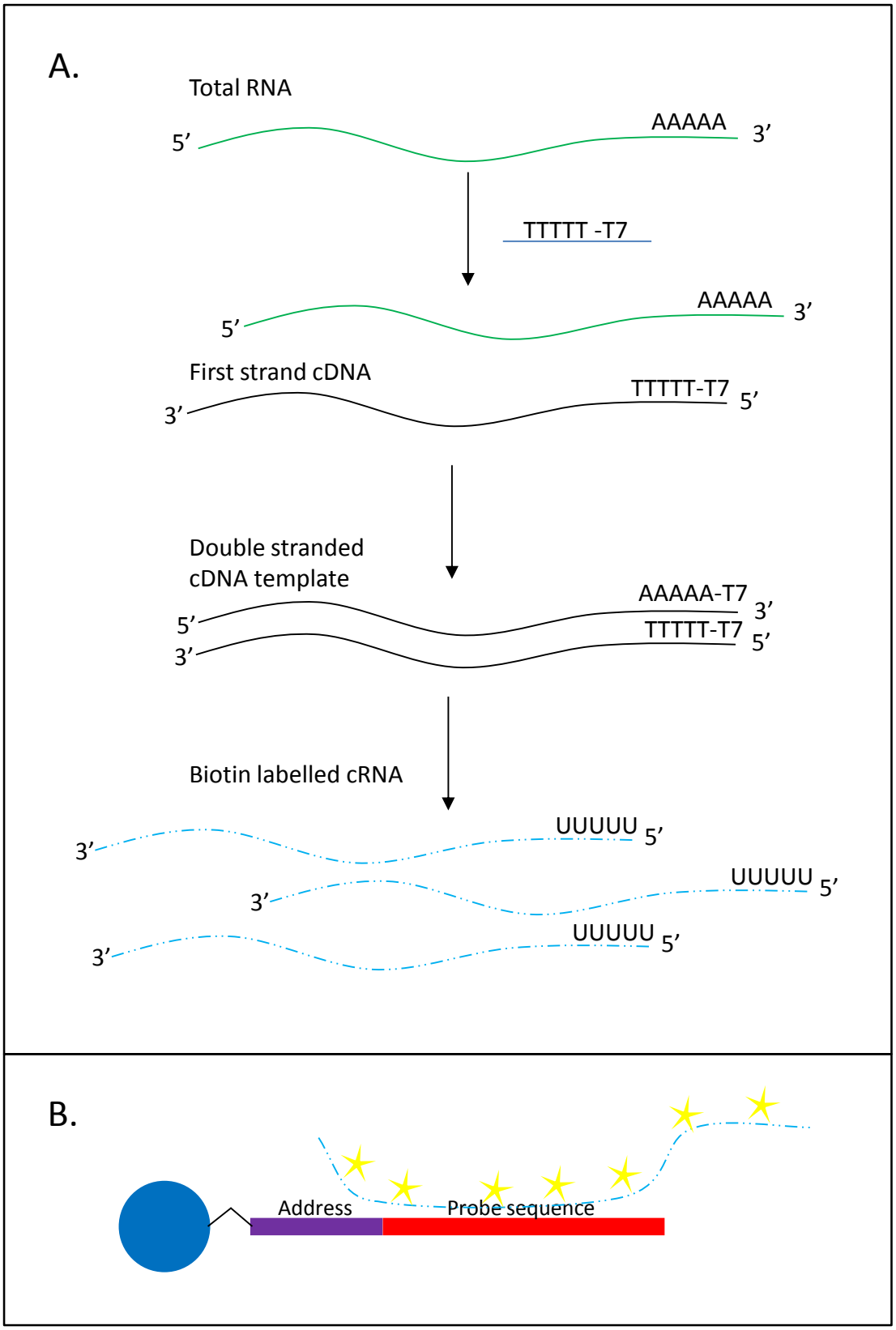

Figure 4.1.2.2 T7 polymerase amplification method for RNA sample amplification and labelling. A. Starting material is reverse transcribed with poly d(T) primers containing the T7 promoter sequence then a second DNA strand is synthesised using a DNA polymerase leaving dsDNA. T7 polymerase then creates cRNA from biotin labelled 16-UTP to produce amplified and biotin labelled cRNA strands. B. Hybridisation of labelled cRNA sample to probe sequence conjugated beads.

4.1.3 **Chapter aims**

The aim of this chapter is to explore the use of global gene expression analysis to determine the effects of sublytic C attack on CT26 cells under the experimental conditions optimized in chapter 3. To best understand the impacts of sublytic C on tumour cells the expression analysis will seek to determine changes in genes which would confer an advantage to developing tumours. To achieve these aims the practical objectives are:

1. Conduct a sublytic C experiment and interrogate gene expression using microarray technology.
2. Conduct quality control analysis of acquired data using principal components analysis and other exploratory techniques.
3. Ascertain differentially expressed genes by statistical analysis to create gene lists and heatmaps.
4. Use pathway and network analysis tools to mine for possible implicated pathways or processes and define a set of genes of interest which can be proceeded by further experimental investigation.

4.2 Results

4.2.1 **Microarray experiment**

4.2.1.1 Sublytic C attack

In order to understand the influence of sublytic C on tumour cells a microarray experiment was proposed as a means to identify the gene expression signature of cells exposed to sublytic C. Microarray allows the interrogation of gene expression for tens of thousands of genes and their transcript variants.

For the generation of good quality data it is vital that the experiment be well designed and thus it was carefully planned. Conditions for sublytic C were as set out in chapter 3 and performed on CT26 cells seeded from a 5×10^5 per mL suspension (at 1.6×10^3 cells per mm^2) into a 12 well plate and incubated under normal growth conditions for 20 hours and exposed to C attack conditions for 1 and 12 hours from initial addition, RNA was then extracted directly from the cell monolayers. Cell detachment during sublytic attack was controlled for by centrifugation of medium at 800×g then adding lysis buffer to cell pellet. Cell pellet and monolayer lysates were pooled before continuing with RNA extraction. Each experimental condition was run in quadruplicate and arranged as shown in Figure 4.2.1.1 giving a total of 20 RNA samples extracted. Eluted RNA was placed immediately on ice and stored at -80°C.

4.2.1.2 RNA quantitation and quality control

Extracted RNA was analysed using the Agilent 2100 Bioanalyzer (Agilent Technologies, Cheshire, UK) by Megan John at Cardiff University's in-house central biotechnology services (CBS). Briefly, 1 µL of sample was applied to an RNA 6000 Labchip which was then placed in the 2100 Bioanalyzer and a voltage applied so that the sample was drawn through microfluidic channels passing through a sieving polymer and a fluorescent dye. Detection of fluorescently labelled RNA during its migration and mass separation was

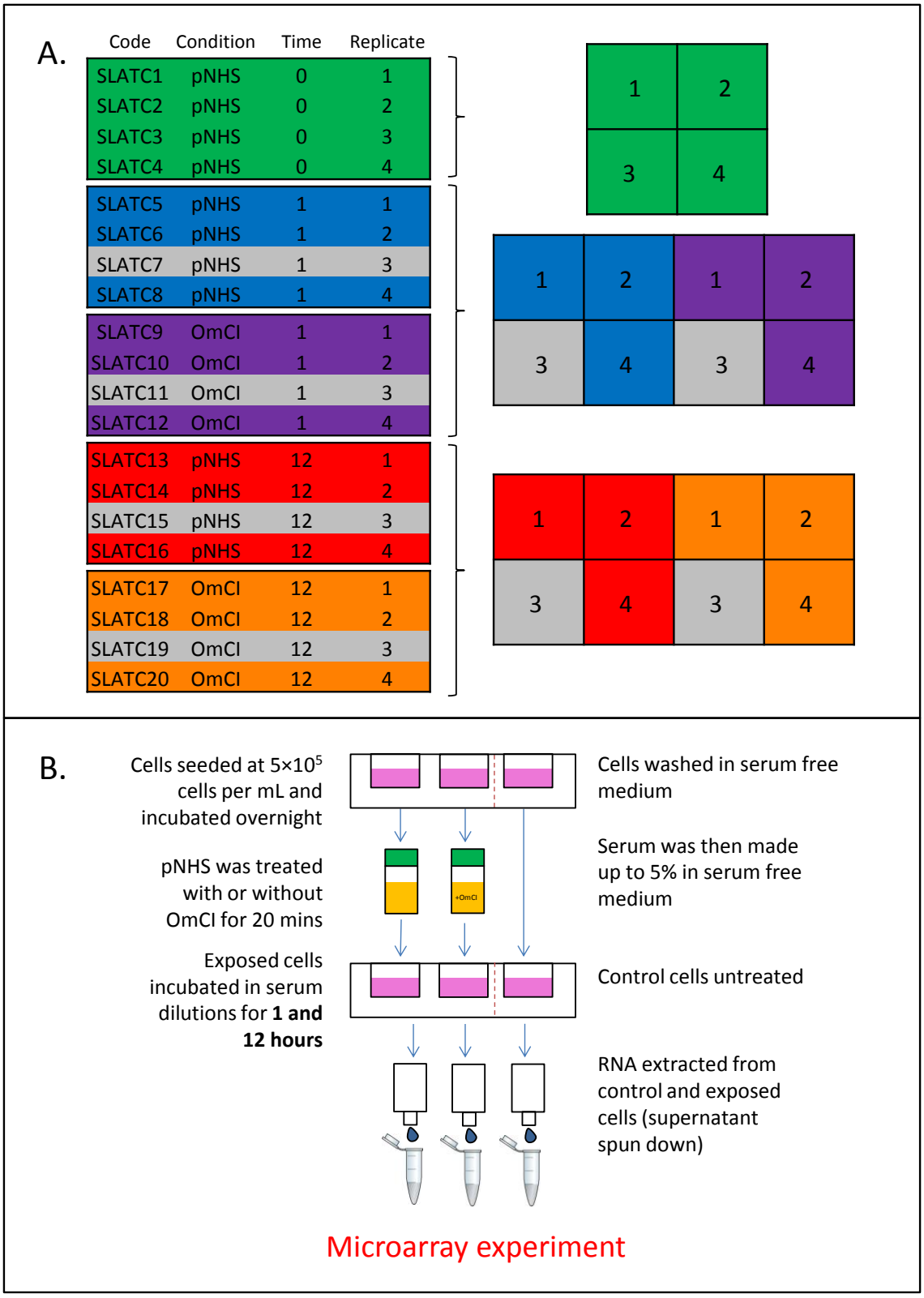

Figure 4.2.1.1 Sublytic C experimental design and protocol. A. Colour coded sample arrangement on 3×12 well culture plates outlining the experimental design, green=control, blue/purple=pNHS/pNHS+OmCI 1 hour, red/orange=pNHS/pNHS+OmCI 12 hour, grey=samples excluded from microarray for later validation. B. Schematic diagram of sublytic C protocol: cells seeded overnight at 5×10^5; pNHS treated with or without 10 µg/mL OmCI for 20 minutes; cells washed then serum dilution added and incubated under normal growth conditions for 1 and 12 hours, leaving one as untreated control; RNA extracted from cell monolayer.

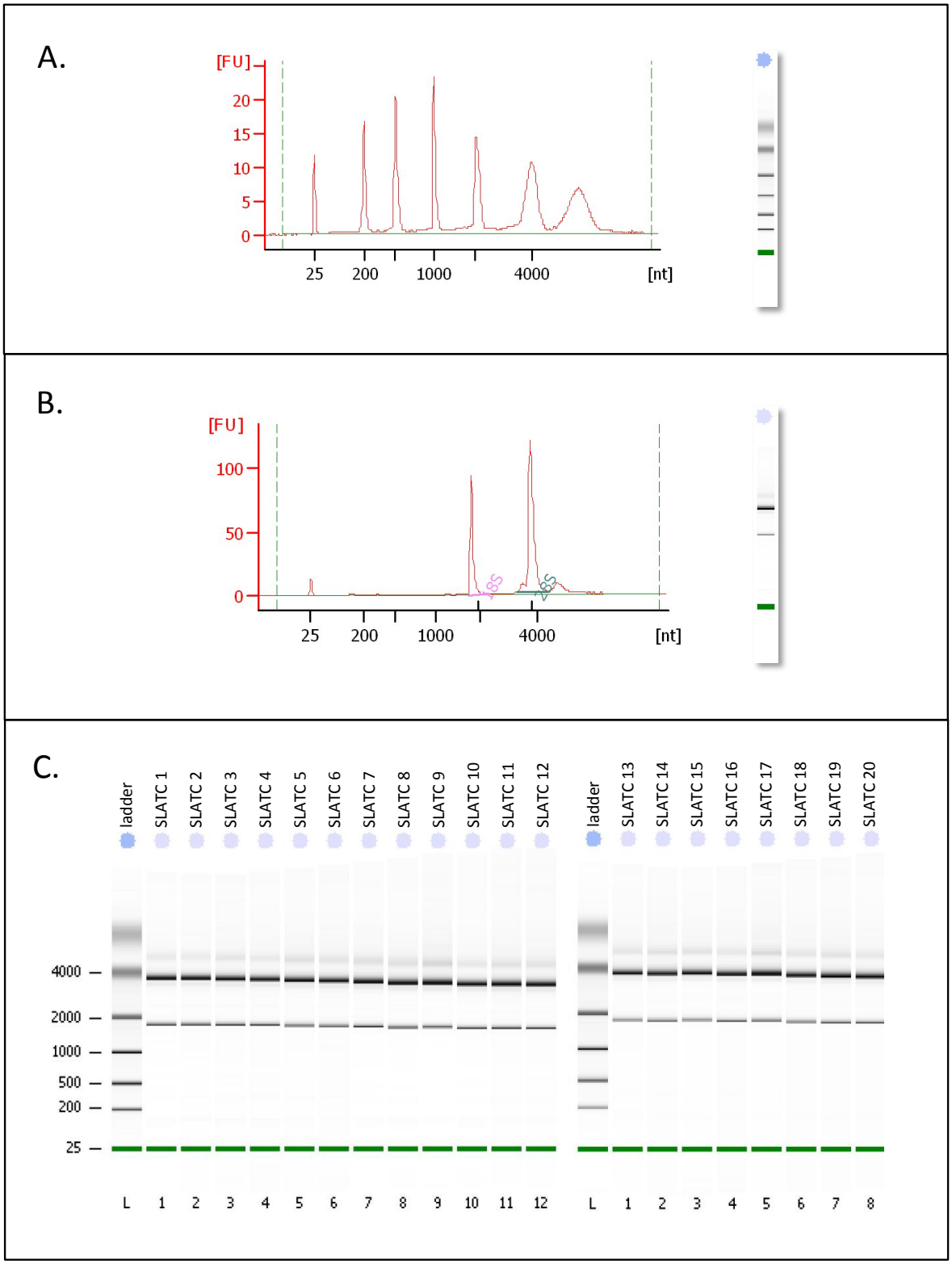

Figure 4.2.1.2 RNA quality and quantification analysis using Agilent 2100 Bioanalyzer. A. RNA mass ladder electropherogram and band pattern 5606, 4000, 2000, 1000, 500, 200, 25 nucleotide peaks. B. Example electropherogram and band pattern of sample RNA 28s and 18s peaks are labelled. C. Sample RNA band patterns of 28s and 18s ribosomal RNA presented alongside RNA size ladders.

recorded as an image similar to agarose gel separations and plotted on an electropherogram. An RNA 6000 ladder was run alongside the samples for identification of mass. RNA integrity was assessed using the ratio of the ribosomal 18s and 28s RNA (rRNA), this gives an indication of RNA degradation status. RNA quality was scored using the RNA integrity number (RIN) calculated by the proprietary software as a function of the electropherogram trace.

Extracted RNA intended for microarray analysis was of high quality with each sample achieving RIN scores of 10. Electropherograms showed minimal degradation and ribosomal peaks 18s:28s were between 1.8 and 2.5. Concentrations varied from 210 to 594 ng/µL (Figure 4.2.1.2).

4.2.1.3 Microarray

Having generated high quality RNA it was possible to proceed to the microarray experiment. Protocols for RNA labelling hybridisation and BeadChip scanning were conducted as per manufacturer's instructions by Megan John at Cardiff University's in house central biotechnology services (CBS). All equipment, reagents and materials were purchased from Illumina (Illumina UK, Essex, UK).

The mouse ref8v2 BeadChips can accommodate 8 samples per chip and were purchased as a pair. 16 of the 20 samples extracted were used excluding 1 sample per test condition except the control as highlighted in grey in Figure 4.2.1.1. Biotinylated cRNA was produced from RNA samples using the process outlined in section 4.1.2.3. 750 ng of Biotin-cRNA were prepared in HYB buffer, pipetted into sample ports of BeadChips and groups were distributed equally over the two chips to minimize batch effects. The samples were hybridised for 14 hours at 58°C in a rocking Illumina Hybridisation Oven. BeadChips were then washed at 55°C for 10 minutes in a high temperature wash buffer, then at room temperature in E1BC buffer for 5 minutes with shaking. BeadChips were washed in 100%

EtOH for 10 minutes and then for a further 2 minutes in E1BC buffer. BeadChips were blocked on a rocker for 10 minutes by incubation in 4 mL block E1 buffer.

A 1 µg/mL Cy3-Streptavidin solution was prepared by dilution in E1 block buffer and the BeadChips incubated on a rocker for 10 mins at room temperature followed by washing shaking in E1BC buffer for 5 minutes. BeadChips were dried by centrifugation at 1400 rpm for 4 minutes to prevent evaporation which might leave residue and interfere with scanning.

BeadChips were scanned by laser excitation using the iScan Reader controlled by iScan Control Software (Illumina). Fluorescence detected by this procedure allowed the generation of an image from which signal intensity data was calculated for defined positions on the chip. GenomeStudio Expression Module software (lllumina) was used to convert the signal intensity data into expression data.

4.2.1.4 Quality control

Contained within the HYB buffer are a comprehensive set of control oligonucleotides corresponding to probes located on the BeadChip which allow various qualitative aspects of the process to be monitored within the experiment. Hybridisation controls are 6 directly Cy3 labelled oligonucleotides complementary to 6 probes on the chip in defined concentrations of low, medium and high yielding a signal gradient (Figure 4.2.2.1A). Stringency controls are 4 probes each with mismatched bases at 2 positions (Figure 4.2.2.1B). Each mismatched probe has a perfect matched counterpart complementary to a hybridisation control oligonucleotide. Occurrence of signal on mismatch probe indicates low stringency. To check the quality of streptavidin staining, there are 2 probes complementary to biotin labelled oligonucleotides present in the HYB buffer present on the BeadChip. Detected signal indicated that Cy3-streptavidin labelling had been successful and high stringency conditions could remove the hybridised biotin oligo (Figure 4.2.2.1C) Negative controls are probes which do not have a complementary target in the

sample, thus any signal detected represents the background level from which the detection limits can be calculated in conjunction with standard deviation (Figure 4.2.2.1D.). Housekeeping controls include a set of 14 probes on the chip targeted to 7 housekeeping gene sequences in the sample which indicate the intactness of transcript (Figure 4.2.2.1E). The GenomeStudio software produced a QC report summarizing the signal from the various internal controls.

QC data from the BeadChips averaged across the dataset showed good hybridisation demonstrating tight titration in low, medium and high abundance Cy3 oligonucleotides and good stringency able to differentiate mismatch and perfect match control probes. In the experiment, Cy3-streptavidin labelling was shown to have been successful. Signal from negative controls was about 120 AU (arbitrary units) and thus very low with a small amount of noise, which was about 10 AU. A good signal was gained from housekeeping genes demonstrating the quality of the transcript and confirming its murine origin.

4.2.2 **Data handling and primary analysis**

4.2.2.1 Data normalization

Once the GenomeStudio software had generated signal intensity data from scan images data were normalized using the quantile method. The fundamental aim of normalisation is to ensure that the signal from each chip is equivalent overall. Normalization is necessary to remove unwanted variability, an inevitable product of a large number of parallel arrays. Sources of bias include differences in starting RNA quantity, quality, labelling efficiency, and systematic bias (Quackenbush, 2002). Quantile normalization aims to match the distribution of probe intensity values across each array. To do this each array's probe intensity values are ranked in order (regardless of probe identity) and then adjusted so that if plotted against each other they would produce a straight line. In practice this is done through sorting columns (sample) in order then calculating the mean from each row and substituting it to each entry in the row, the data is then re-sorted to its original order,

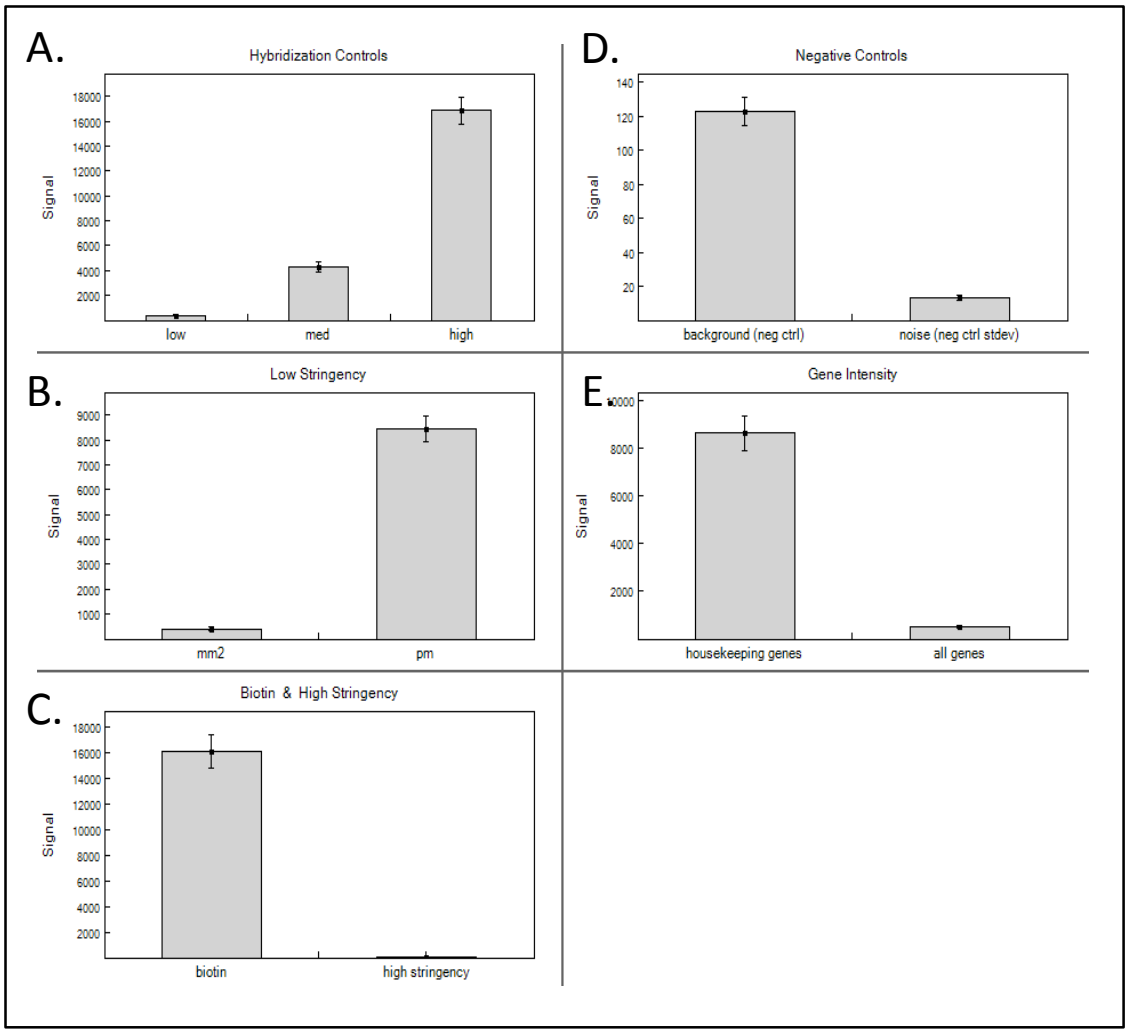

Figure 4.2.2.1 Microarray hybridisation quality control output. Oligonucleotides present in HYB buffer and probes present on the chip allowed the assessment of A. hybridisation specificity. B. hybridisation robustness under low stringency, C. streptavidin labelling success and high stringency signal removal D, negative control background and noise levels and E. signal form housekeeping gene controls.

resulting in normalized values (Bolstad et al, 2003). Normalized data were presented in a tab delimited text file for entry into analysis software.

4.2.2.2 Partek and GeneSpring

Empirical data processing, which included entity exploration and statistical analysis, was performed using GeneSpring 12.0 GX (Agilent Technologies, Cheshire, UK) and PartekGenomics Suite version 6.6 (build 6.13.0213, Partek Incorporated, Missouri, USA). Data input in both software applications required the data to be presented in a tab delimited text file (probes by row, sample by column) with a corresponding annotation file (also in tab delimited text to define probe identities, gene codes, chromosomal locations, gene ontology information and other pertinent details). The file used was the Illumina-provided MouseRef-8_V2_0_R2_11278551_A.txt. Normalized data were given a threshold of 1 to eliminate missing values and transformed by a logarithm base 2 to scale down the raw signal values as is standard practice for microarray data. In the case of GeneSpring, in addition to log2 transformation, the baseline was adjusted according to the median taken across the dataset. This adjustment allowed simple data representation and could be used for downstream analysis as will be described later.

4.2.2.3 Principal components analysis (PCA) and batch removal

Initial analysis was aimed primarily at exploratory description of the data. In order to ascertain the spread of the data and determine the possible contributors to variation a principal components analysis (PCA) was performed using Partek.

PCA aims to reduce a multivariate dataset containing large numbers of correlated variables to a small number of uncorrelated variables whilst retaining much of the original information. To arrive at the key components the data are transformed and compressed to derive the ‘principal components’ (Jolliffe, 2002). Plotting the data summarized from each sample by its top 3 principle components results in a 3D map, on which the position of each sample describes the influence of each component.

The PCA map in Figure 4.2.2.2 A. describes the separation of the dataset as functions of principal components 1,2 and 3; assigning contributions of 14.1, 9.37 and 7.99% of overall variation respectively. Sample spheres were colour coded by condition, red=control, blue=pNHS+OmCI and green=pNHS. Centroids were added, linked and colour coded by sample groupings; black=control, light blue/green=1 hour and dark blue/green=12 hours. Centroid groupings clearly show that the data are well separated by experimental conditions. However, grouping based on batch number, i.e. the chip number on which the samples were placed, revealed a clear batch effect.

Batch effects are due to experimental differences caused by processing of samples on separate chips or, in some cases, at different times. Batch effects in this experiment were probably due to the spread of 16 samples across 2 chips. Effects exerted by batch in this experiment are unlikely to have influenced the biological interpretation of the data due to the careful design of the experiment.

Batch effects were removed from the data via the batch removal tool in the Partek software by including chip location information as a variable and selecting remove batch effect by factor. Figure 4.2.2.2 B shows the PCA map post batch removal showing tight groupings with greatly improved separation. Percentage of variation accounted for by PCs #1(14.8%) , 2 (9.78%) and 3 (8.37%) are largely in agreement between plots suggesting that the batch effect was small.

Batch removal was not maintained in further statistical and downstream analysis due to its influence on p-values. The analysis of variance (ANOVA) function within Partek is capable of adjusting for batch effects so that batch removal was not necessary during further analyses.

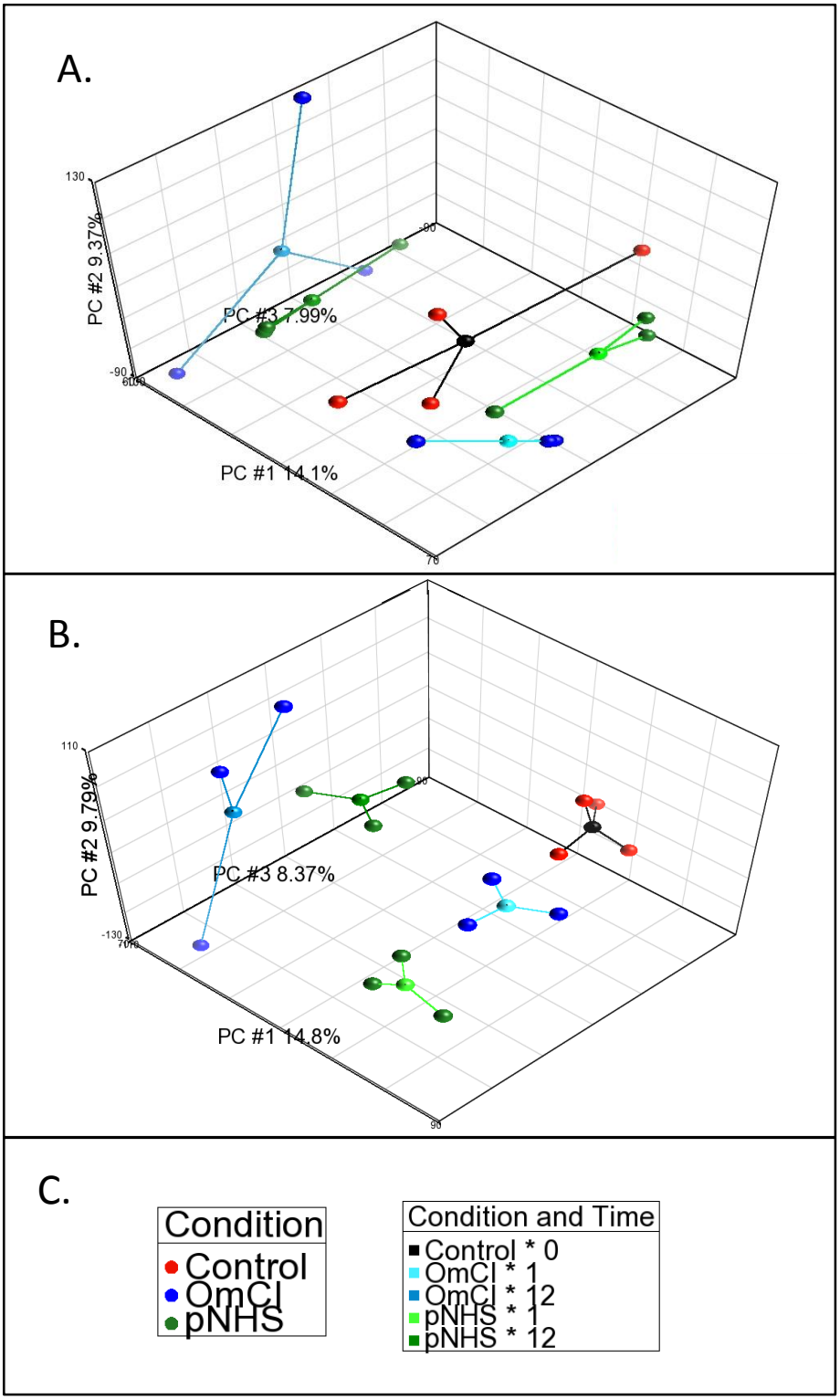

Figure 4.2.2.2 Principal component analysis (PCA) plots. A. 3D PCA plot displaying the top 3 principal components before batch removal and B. after batch removal. C. PCA plot key, left box; red=control, blue=pNHS+OmCl, green=pNHS, right box centroids; black=control, blue=pNHS+OmCl, green=pNHS, light=1 hour, dark=12 hour.

4.2.2.4 Gene expression change scatter plots

Linear scatter plots were created using GeneSpring comparing the mean gene expression values between sample groups. Serum conditions pNHS and pNHS+OmCI were compared at each exposure time point, 1 and 12 hours, on two separate plots. Normalized and transformed gene expression values taken from pNHS conditions were used to colour code the data; red=upregulation (above median baseline), yellow=no expression change (on or close to median baseline) and blue=down regulation (below median baseline). Plotted data represents the comparative gene expression levels of pNHS against the control condition containing OmCI. Because the data is plotted between sample groups, genes with no difference in expression levels will fall upon a central line, this line represents a fold change of 1. Differences between sample groups will fall either side of this line. In addition to this central line, parallel lines are drawn above and below which represent a boundary of 1.3 fold change. Genes up or down regulated by more than 1.3 fold when compared to their control fall beyond these boundaries.

Cells exposed for 1 hour to pNHS compared to the OmCI treated control had a large number of differentially expressed genes changing by more than 1.3 fold and marginally more genes appeared to be upregulated in the pNHS condition compared to pNHS+OmCI. A great many genes fell between the 1.3 fold change boundaries representative of an equal effect across the groups. Exposure for 12 hours resulted in far fewer differentially expressed genes and were more tightly distributed.

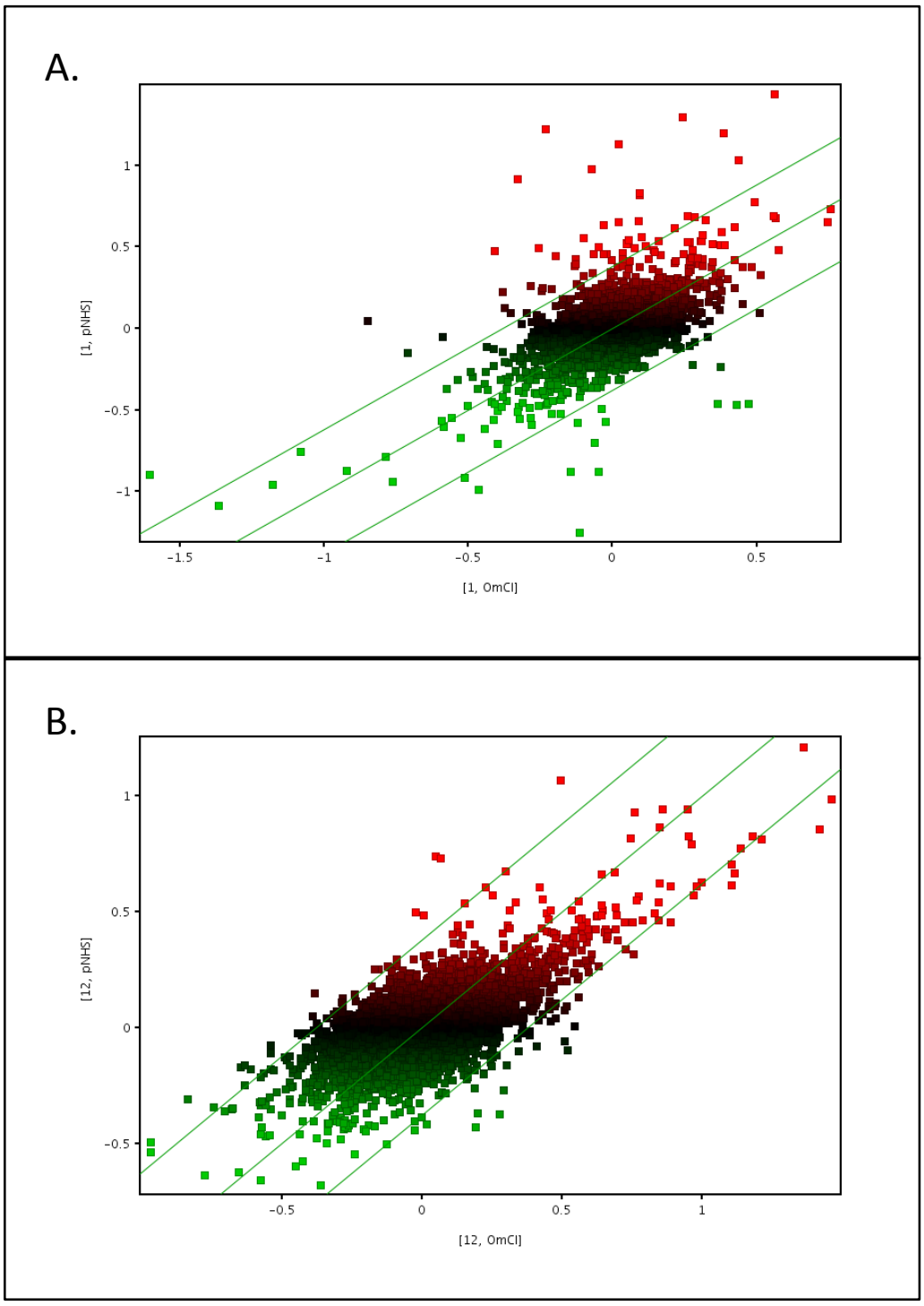

Figure 4.2.2.3 Scatter plot comparisons between samples. Log2 transformed, median baseline adjusted data and means calculated for sample groups. Data is plotted comparing pNHS and pNHS+OmCI at 1 hour (A.) and 12 hours (B.) post exposure. Correlation of points along a central line represent no gene expression change between samples i.e. 1 fold change (FC), parallel lines represent 1.3 FC.

4.2.2.5 ANOVA analysis

To analyse the data properly it is necessary to perform statistics for the detection of differentially expressed genes. This was done using Partek by analysis of variance analysis (ANOVA). A 2-way ANOVA model was applied using method of moments (Eisenhart, 1947).

Contrasts were prepared by comparing serum condition (pNHS vs. OmCI), exposure time (1 vs. 12), serum conditions after 1 hour (pNHS * 1 vs. OmCI * 1) and serum conditions at 12 hours (pNHS * 12 vs. OmCI * 12) using Fisher's Least Significant Difference (LSD) test (Tamhane & Dunlop, 2000).

ANOVA results output included p-values for significance, ratios and fold-change values of expression. The comparisons also allow the calculation of effect sizes for each of the defined factors including time, serum condition and both time and serum conditions. Figure 4.2.2.4 shows the mean F ratio, which is the signal to noise ratio; noise (error) is defined as the remaining variation not explained by the defined factors. Values above the error are above background noise and thus important. A hierarchy of effect size is clear, time having the largest effect size with a mean F ratio of 6.18. Serum condition contributed a much smaller effect size of 1.54 times the background and time tabulated with serum condition (i.e. pNHS at 1 or 12 hours compared with pNHS+OmCI at 1 or 12 hours etc.) slightly greater with 1.7.

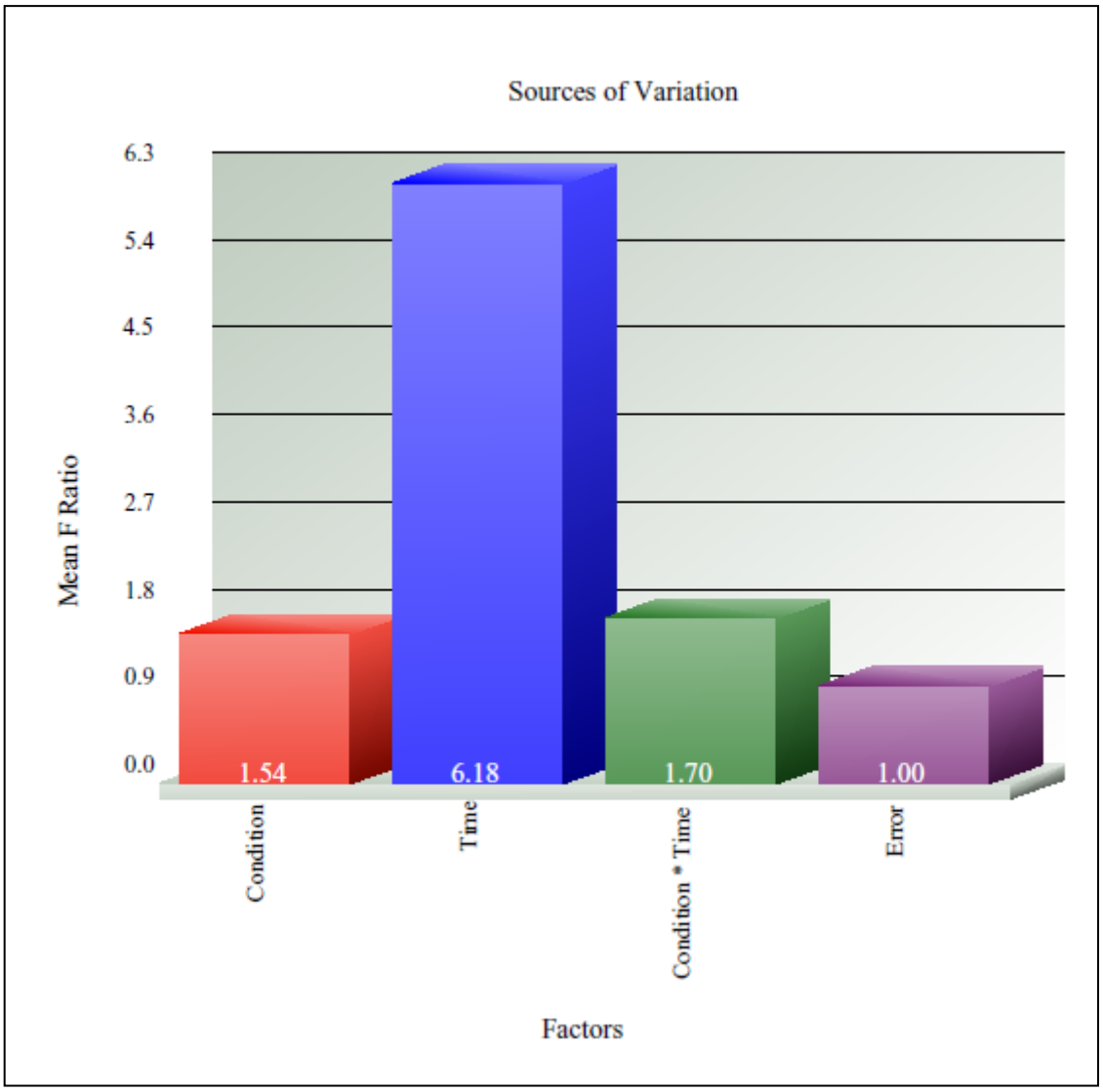

Figure 4.2.2.4 Sources of variation from experimental factors. Mean F ratio plotted for serum condition (pNHS, pNHS+OmCl) , time (1 hour, 12 hours) , cross tabulation (pNHS 1 h or 12h, pNHS+OmCl 1h or 12h) and error.

4.2.3 **Gene list generation from ANOVA statistics**

4.2.3.1 Gene list criteria

ANOVA statistics applied to the dataset allowed lists to be created of differentially expressed genes following specified patterns. Gene lists were generated on comparisons set by the LSD test and further refined by expression status; increase, decrease, any change or no change. Once these were selected, lists were sorted by fold change and p-value, with or without false discovery rate (FDR). Inclusion of the FDR applies a restriction on the rejection of the null hypotheses based upon a calculated false discovery rate (Benjamini & Hochberg, 1995). FDR increases the stringency by predicting the rate of false rejections based on the number of tests then altering the p-value cut-off accordingly thus reducing the number of apparently significant differences.

4.2.3.2 Heatmap generation

In order to present gene lists as clustered heatmaps, data (log 2 transformed) were standardized by shifting to a mean of zero and scaled to a standard deviation of one. Clustering of ANOVA gene lists was achieved through the 'clustering of significant genes' option in Partek. Gene lists created as described above were organised by hierarchical clustering of gene expression patterns and heatmaps generated. Hierarchical clustering groups genes displaying similar expression patterns together and organises them into a hierarchy described by dendrograms. Clustering by this method is unsupervised, taking no account of sample and experimental condition information. Heatmaps were organised by clustered genes in rows with expression values (standardized and scaled) colour coded so that genes decreased were represented by green, no change by black and increased by red.

4.2.3.3 Serum and time point comparison heatmaps

Heat maps were generated using Partek to summarize the lengthy gene lists created from the macro comparisons, i.e. pNHS vs. pNHS+OmCI serum treatment and 1 hour vs. 12

hour time points. The criteria applied to create the time point comparison lists were as follows: any change, any fold change, FDR adjusted p-value of <0.01 generating 1429 entities, and to the serum condition comparison: any change with an unadjusted p-value of <0.01 generating 529 entities.

Figure 4.2.3.1 shows the heatmap generated from clustering of genes in the time point comparison list. A clear separation can be seen between the sample groupings. As was shown by mean F ratio plot of variation, time point is responsible for much of the variation in the dataset. Two clearly defined groupings of genes are revealed displaying expression increase at either 1 hour and not 12 or 12 hours and not 1 hour with marginally more genes upregulated in the 1 hour time point. Controls were more similar to both serum conditions at 1 hour compared to 12 hours as would be expected.

Figure 4.2.3.2 is the heatmap generated from clustering of genes in the serum condition comparison gene list. Clustering is much less defined. Dendrogram linkage shows that controls are most similar to pNHS+OmCI at 1 hour and the next level of hierarchy is occupied by pNHS at 1 hour with pNHS at 12 hours.

4.2.3.4 Direct comparison gene list

Smaller lists were generated focussing on the differentially expressed genes comparing pNHS with pNHS+OmCI at each time point. Genes with any significant change at these time points were selected using an FDR adjusted p-value <0.05 and no fold change restrictions to create gene lists of 49 and 26 entities for 1 and 12 hour time points respectively. These were then used to create hierarchically clustered heatmaps showing grouping of genes up and down regulated at 1 and 12 hours.

Gene lists were also created using the most stringent restrictions to give the most statistically significant changes at each comparison. P-value was FDR adjusted ($p<0.05$) and pNHS versus pNHS+OmCI comparison with FC>2 (up) or -2 (down) at 1 and 12 hours (except up at 12 hours FC>1.5).

At 1 hour there was a clear set of differentially regulated genes both up and downregulated (Figure 4.2.3.3 and Figure 4.2.3.4). Genes associated with signal transduction such as Rgs16, Dusp2 and Itprip were upregulated. Regulator of G-protein signalling 16 (Rgs16) is a GTPase activating protein which limits G-protein activation by GPCRs (G-protein coupled receptors), it has also been described as important in controlling GPCR induced Ca^{2+} oscillation in conjunction with IP3 (Berman et al, 1996; Luo et al, 2001). Dual specificity phosphatase 2 (Dusp2) is a MAPK phosphatase acting to regulate MAPK signalling cascades through dephosphorylation at serine/threonine and tyrosine residues (Owens & Keyse, 2007). Dusp2 is a nuclear inducible regulator of MAPK activation thus is expressed upon signal activation (Owens & Keyse, 2007). Inositol 1,4,5-trisphosphate receptor interacting protein (Itprip is also referred to as DANGER) is involved in altering the Ca^{2+} sensitivity of IP3R increasing the potency of Ca^{2+} mediated inhibition of Ca^{2+} release (van Rossum et al, 2006). Involvement of Ca^{2+} signalling is indicated by these hits as well as Gα-protein mediated signalling and MAPK kinase activation. Each hit was upregulated and had regulatory functions suggesting an inducible self-regulation.

Genes with transcription regulatory functions which were upregulated at 1 hour were Egr1, Egr2 and Fos (Figure 4.2.3.3). Early growth response 1 and 2 (Egr1/2) gene products are both zinc finger containing transcription factors members of the immediate early response genes (Joseph et al, 1988; Lau & Nathans, 1987). Egr1 follows similar kinetics to c-fos induction responding to mitogen stimulation, cell differentiation and cell de-polarization (Sukhatme et al, 1988). Egr1 gene product regulates gene expression of transcription regulators, signalling proteins, cell-cycle regulatory proteins, extracellular matrix proteins, ion channel proteins, growth factors and cytokines (Fu et al, 2003). FOS is the gene product of c-fos gene expression and is like Egr1/2 in its status as an immediate early response gene. It can form heterodimers with jun or atf-2 of the AP-1

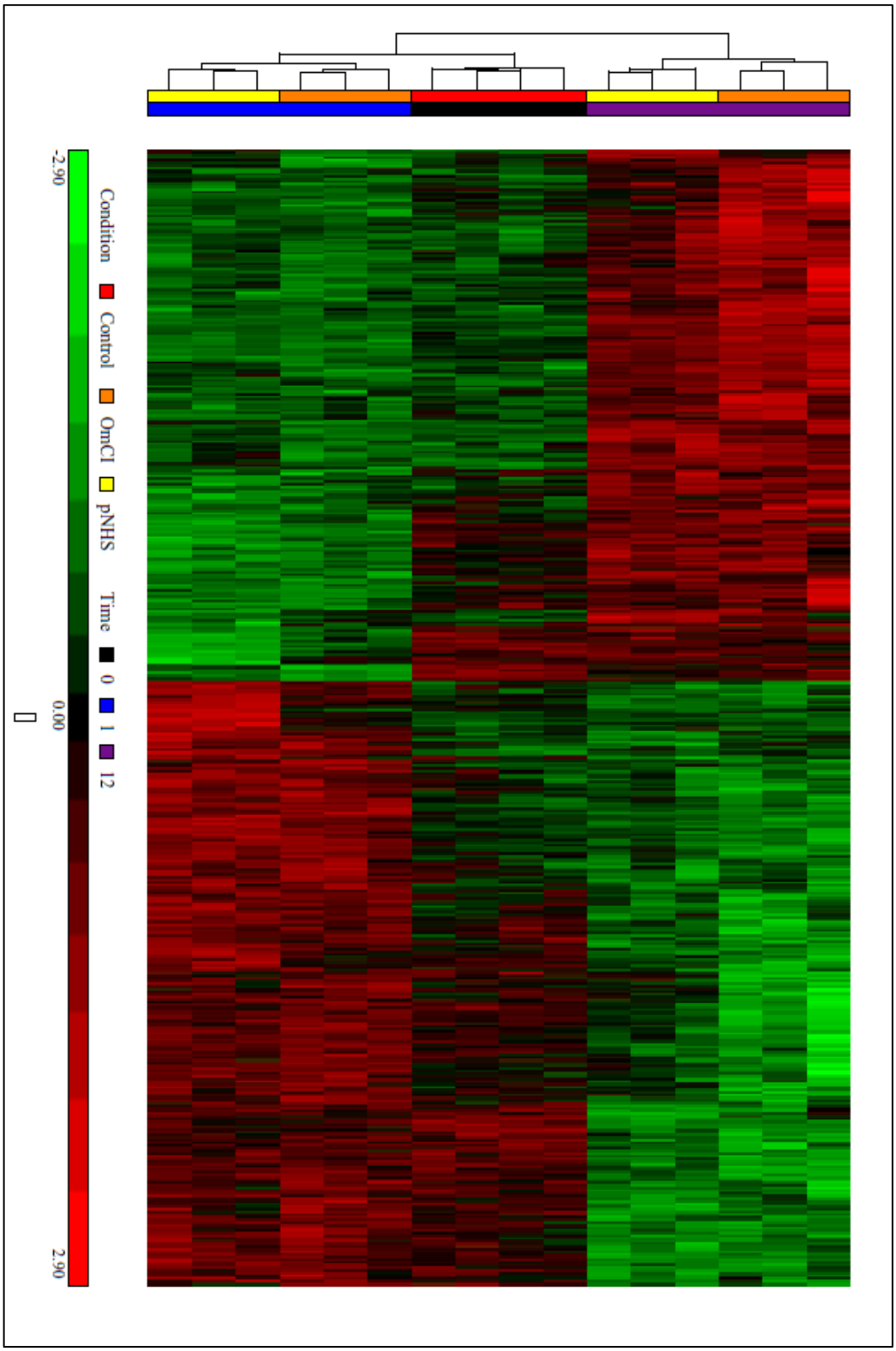

Figure 4.2.3.1 Hierarchical clustering heatmap of time point comparison. 1 hour relative to 12 hour. Gene list criteria: any change, 0 FC, FDR adjusted p-value <0.01 = 1429 entities. Dendrograms clustering sample bar: Serum condition; red=control, orange=OmCI, yellow=pNHS Time point; black=0, blue=1 hour, purple=12 hour. Gene expression values(log2 transformed, 0 mean shifted, scaled to SD=1) for clustered entities: green=downregulated, black=no change, red=upregulated.

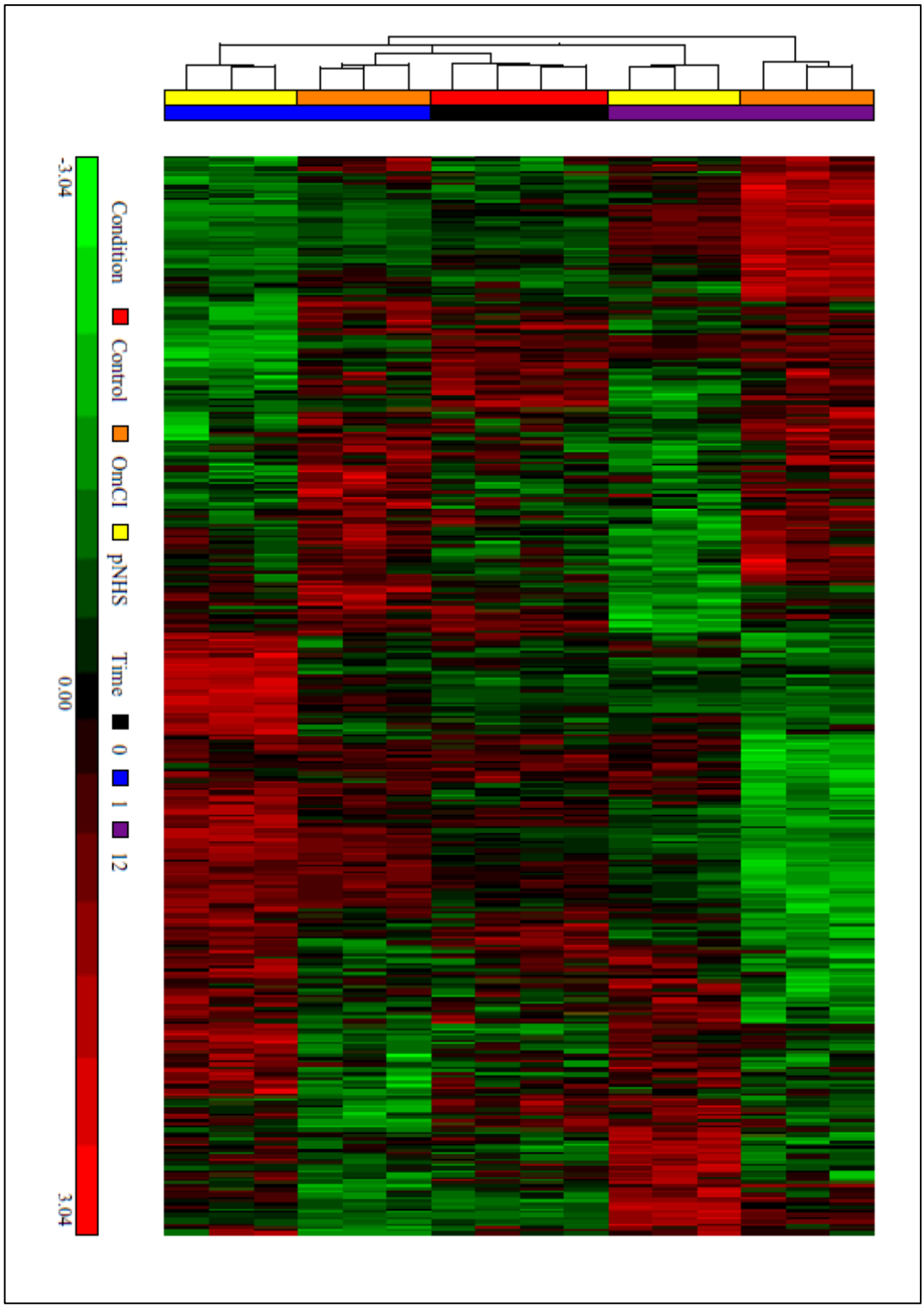

Figure 4.2.3.2 Hierarchical clustering heatmap of serum condition comparison pNHS relative to pNHS+OmCl. Gene list criteria: any change, 0 FC, unadjusted p-value <0.01 = 529 entities. Dendrograms clustering sample bar: Serum condition; red=control, orange=OmCl, yellow=pNHS Time point; black=0, blue=1 hour, purple=12 hour. Gene expression values(log2 transformed, 0 mean shifted, scaled to SD=1) for clustered entities: green=downregulated, black=no change, red=upregulated.

	Probeset ID	Symbol	Transcript	p-value(pNHS * 1 vs. OmCl * 1)	Fold-Change(pNHS * 1 vs. OmCl * 1)
4	ILMN_2600744	Rgs16	ILMN_209950	3.03E-09	2.74759
18	ILMN_2662926	Egr1	ILMN_215729	9.47E-08	2.37517
11	ILMN_2995794	Itprip	ILMN_242056	6.49E-08	2.16089
1	ILMN_2623983	Egr2	ILMN_212209	4.57E-11	2.08117
19	ILMN_2757634	Fam110c	ILMN_222981	1.89E-07	2.07236
29	ILMN_1216764	Ier3	ILMN_223302	2.47E-07	1.86804
47	ILMN_2698449	Hbegf	ILMN_218639	3.40E-05	1.84976
13	ILMN_3009243	Dusp2	ILMN_212470	1.14E-06	1.83362
6	ILMN_1242406	Dusp2	ILMN_212470	3.54E-08	1.7654
44	ILMN_1243862	Il11	ILMN_215774	4.13E-07	1.68709
25	ILMN_2790357	Sema7a	ILMN_210076	1.36E-05	1.66959
42	ILMN_2617468	Chac1	ILMN_211596	8.14E-05	1.63399
26	ILMN_3105417	Bdnf	ILMN_241360	8.49E-07	1.59235
39	ILMN_2714031	Errfi1	ILMN_246139	2.60E-05	1.57705
10	ILMN_2636403	Axud1	ILMN_213373	2.16E-07	1.56266
9	ILMN_2737685	Mmp13	ILMN_210384	4.96E-07	1.52378
34	ILMN_3162407	Zfp36	ILMN_188430	3.28E-05	1.51643
20	ILMN_2742075	Cd14	ILMN_221922	1.50E-05	1.48833
49	ILMN_2763002	Eno2	ILMN_223357	3.66E-07	1.47919
22	ILMN_1216335	Cttnbp2nl	ILMN_252976	4.68E-07	1.47526
45	ILMN_2595732	LOC100046232	ILMN_310357	1.59E-06	1.45961
28	ILMN_2776909	Irx3	ILMN_224225	2.34E-05	1.43995
21	ILMN_1238547	Areg	ILMN_217903	8.00E-05	1.43899
36	ILMN_2744138	BC003236	ILMN_191936	8.74E-05	1.4349
23	ILMN_2619330	Plk3	ILMN_211765	5.73E-05	1.39709
33	ILMN_2736471	Ccno	ILMN_239687	5.61E-05	1.39025
15	ILMN_2750515	Fos	ILMN_222500	2.37E-06	1.38727
16	ILMN_3161263	Fzd5	ILMN_260431	4.47E-06	1.37462
43	ILMN_1221429	Mllt11	ILMN_209038	3.46E-05	1.36678
40	ILMN_2825817	Spry4	ILMN_220989	8.02E-05	1.34179
27	ILMN_3162369	Fbxo33	ILMN_234957	8.27E-05	1.32069
30	ILMN_3031099	Coq10b	ILMN_235389	1.84E-05	1.31654
24	ILMN_2775307	Lamc2	ILMN_210712	4.16E-05	1.27519
12	ILMN_1249426	Socs4	ILMN_216527	1.72E-05	1.24619
5	ILMN_1240323	Dnajb1	ILMN_222931	1.06E-07	1.23503
32	ILMN_1235006	Slc14a1	ILMN_246276	6.52E-05	1.20163
31	ILMN_1242054	Bard1	ILMN_212214	6.02E-05	1.17755
48	ILMN_2883414	Cenpl	ILMN_236103	3.91E-05	-1.14079
41	ILMN_1221886	Zfp3	ILMN_220772	2.44E-05	-1.21309
38	ILMN_1228568	Irf2bp1	ILMN_213448	7.76E-06	-1.259
37	ILMN_3109491	6430527G18Rik	ILMN_230817	8.64E-05	-1.37081
46	ILMN_2672190	Id1	ILMN_216536	8.74E-05	-1.52188
7	ILMN_2737713	Edn1	ILMN_221606	2.40E-07	-1.55358
3	ILMN_2599782	Irf1	ILMN_209850	1.50E-08	-1.65858
14	ILMN_2759365	Angptl4	ILMN_259520	2.30E-08	-1.7643
8	ILMN_1239294	Cdc42ep2	ILMN_235254	4.58E-08	-1.77185
17	ILMN_2903945	Gadd45g	ILMN_222120	3.26E-08	-1.85834
35	ILMN_2744890	Gadd45g	ILMN_222120	3.53E-06	-1.90128

Figure 4.2.3.3 Gene list of significantly differential genes 1 hour post exposure; pNHS 1 hour relative to pNHS+OmCl 1 hour. List criteria: any change, 0 FC, FDR adjusted p-value <0.05 = 49 entities. Entities are sorted by p-value and fold change displayed (pNHS relative to OmCl).

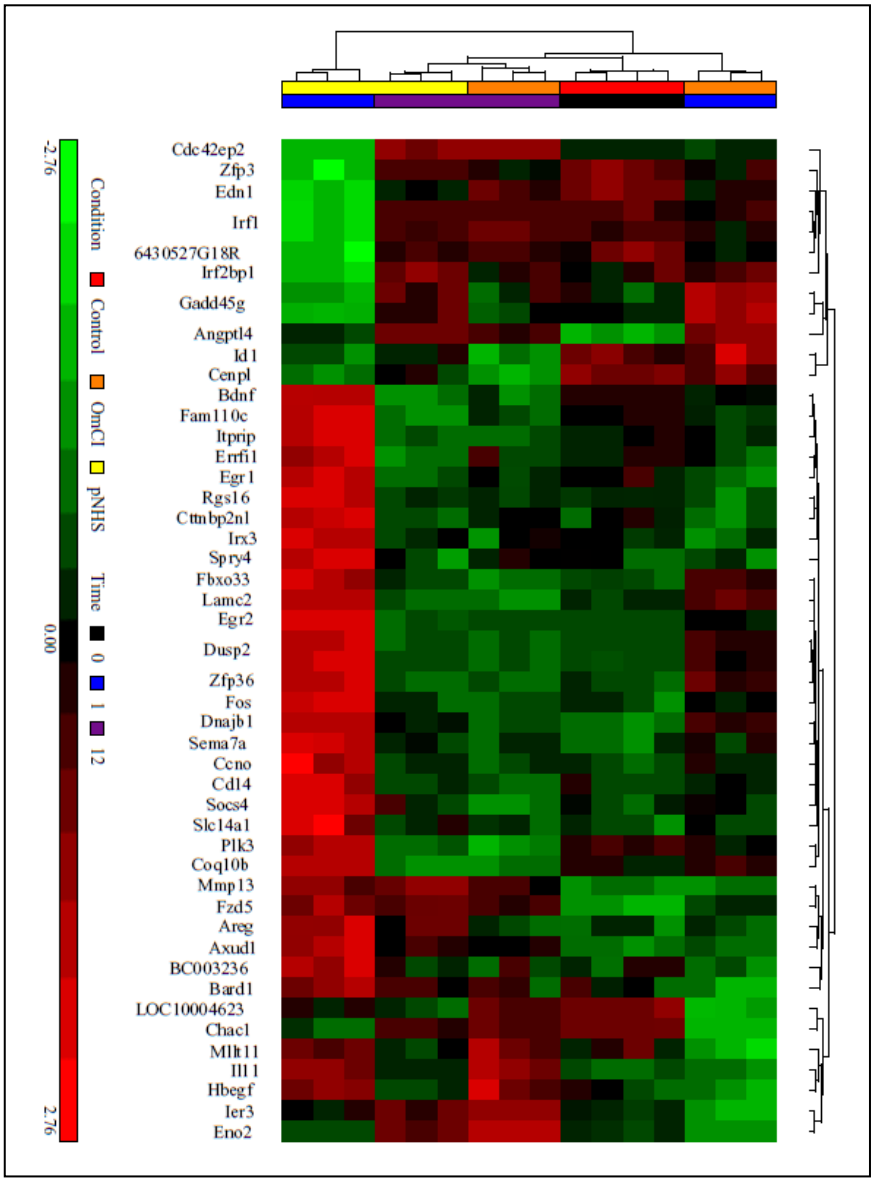

Figure 4.2.3.4 Hierarchical clustering heatmap of 1 hour serum condition comparison. pNHS 1 hour relative to pNHS+OmCI 1 hour. Gene list criteria: any change, 0 FC, FDR adjusted p-value <0.05 = 49 entities. Dendrograms clustering sample bar: Serum condition; red=control, orange=OmCI, yellow=pNHS Time point; black=0, blue=1 hour, purple=12 hour. Gene expression values (log2 transformed, 0 mean shifted, scaled to SD=1) for clustered entities: green=downregulated, black=no change, red=upregulated.

	Probeset ID	Symbol	Transcript	p-value(pNHS * 12 vs. OmCI * 12)	Fold-Change(pNHS * 12 vs. OmCI * 12)
1	ILMN_1260323	Akr1c18	ILMN_215518	4.16E-07	1.61755
2	ILMN_1225816	Hbb-bh1	ILMN_216390	1.99E-07	1.58676
3	ILMN_3024416	Lca5	ILMN_228057	1.15E-05	-1.21942
4	ILMN_1215755	Grwd1	ILMN_217875	6.54E-06	1.35417
5	ILMN_1233461	Irf9	ILMN_213365	3.30E-05	-1.2958
6	ILMN_1248415	Tgoln1	ILMN_217106	8.19E-06	1.20895
7	ILMN_2834379	Tgfbi	ILMN_259309	1.18E-05	1.22264
8	ILMN_2730003	Ccdc86	ILMN_259483	6.87E-06	1.44565
9	ILMN_2726931	Blnk	ILMN_220791	4.48E-05	1.23898
10	ILMN_2851735	Ankrd13d	ILMN_218809	2.67E-05	-1.14059
11	ILMN_2650915	Jmjd2b	ILMN_214701	2.32E-05	-1.19633
12	ILMN_2840082	P2ry12	ILMN_234920	1.76E-05	1.11138
13	ILMN_2980858	Lpcat3	ILMN_210660	2.49E-05	-1.24422
14	ILMN_2862379	Rhod	ILMN_213115	4.10E-06	1.30125
15	ILMN_2591632	Gtf2e1	ILMN_209005	1.10E-05	1.226
16	ILMN_2595283	Rrp1b	ILMN_231400	1.22E-05	1.39104
17	ILMN_2855315	Hist1h1c	ILMN_235246	3.91E-05	1.31188
18	ILMN_2742152	Gadd45a	ILMN_221926	1.58E-05	-1.47492
19	ILMN_2689138	2310044G17Rik	ILMN_226732	1.06E-05	1.28768
20	ILMN_3104025	Asb13	ILMN_236715	4.87E-06	1.26694
21	ILMN_1252745	Gtf2h2	ILMN_256180	2.49E-05	1.19023
22	ILMN_2664686	Chaf1b	ILMN_215876	4.77E-05	1.3061
23	ILMN_1243862	Il11	ILMN_215774	1.29E-05	-1.44406
24	ILMN_2595732	LOC100046232	ILMN_310357	5.16E-05	-1.29817
25	ILMN_2807665	2010003O18Rik	ILMN_250737	3.22E-05	1.21124
26	ILMN_2763002	Eno2	ILMN_223357	3.91E-07	-1.47538

Figure 4.2.3.5 Gene list of significantly differential genes 12 hours post exposure; pNHS 12 hours relative to pNHS+OmCI 12 hours. List criteria: any change, 0 FC, FDR adjusted p-value <0.05 = 26 entities. Entities are sorted by p-value and fold change displayed (pNHS relative to OmCI).

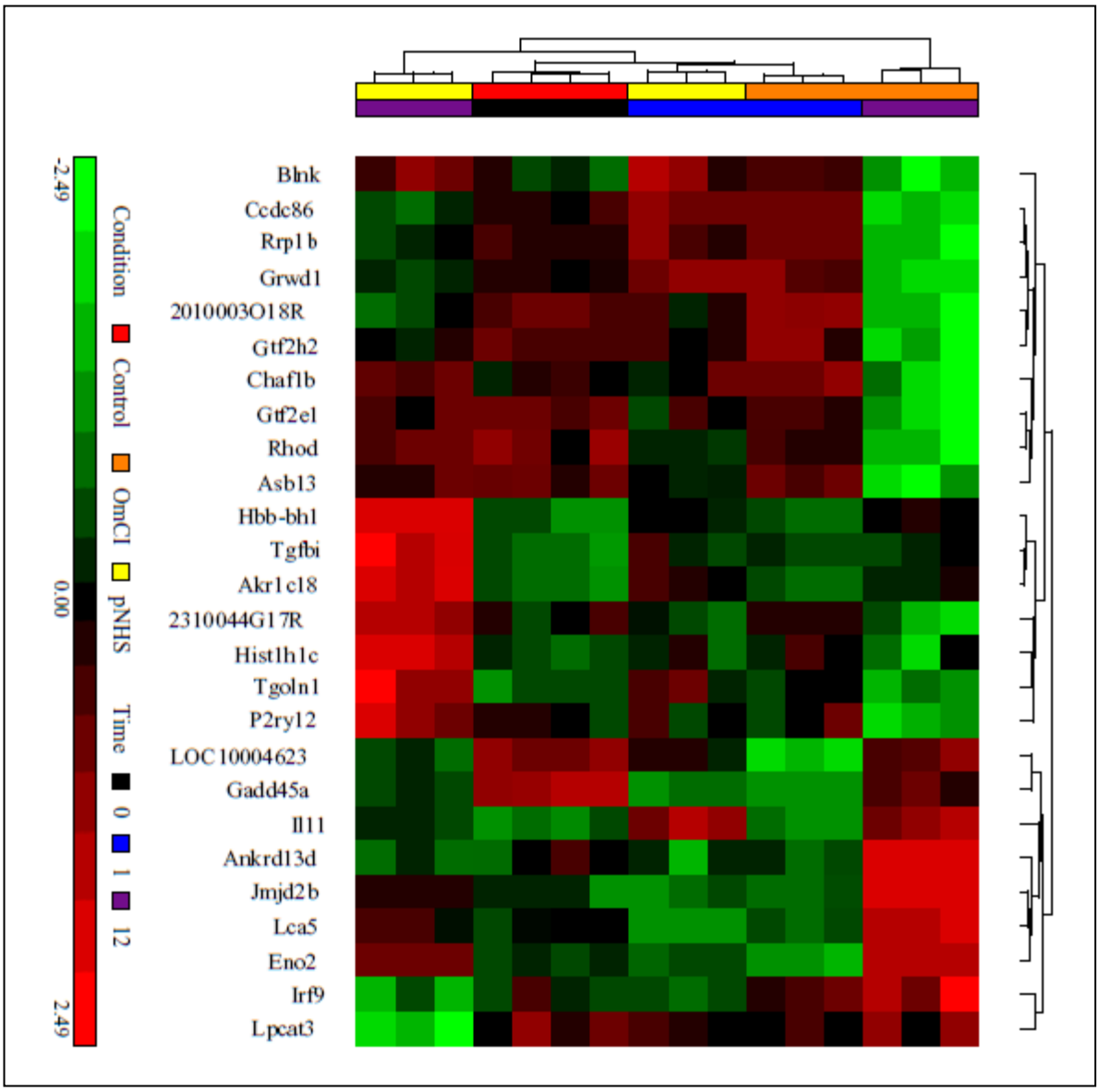

Figure 4.2.3.6 Hierarchical clustering heatmap of 12 hour serum condition comparison pNHS 12 hour relative to pNHS+OmCI 12 hour. Gene list criteria: any change, 0 FC, FDR adjusted p-value <0.05 = 26 entities. Dendrograms clustering sample bar: Serum condition; red=control, orange=OmCI, yellow=pNHS Time point; black=0, blue=1 hour, purple=12 hour. Gene expression values (log2 transformed, 0 mean shifted, scaled to SD=1) for clustered entities: green=downregulated, black=no change, red=upregulated.

A.

	Probeset ID	Symbol	Transcript	p-value(pNHS * 1 vs. OmCI * 1)	Fold-Change(pNHS * 1 vs. OmCI * 1)
1	ILMN_2623983	Egr2	ILMN_212209	4.57E-11	2.08117
2	ILMN_2600744	Rgs16	ILMN_209950	3.03E-09	2.74759
3	ILMN_2995794	Itprip	ILMN_242056	6.49E-08	2.16089
4	ILMN_2662926	Egr1	ILMN_215729	9.47E-08	2.37517
5	ILMN_2757634	Fam110c	ILMN_222981	1.89E-07	2.07236

B.

	Probeset ID	Symbol	Transcript	p-value(pNHS * 1 vs. OmCI * 1)	Fold-Change(pNHS * 1 vs. OmCI * 1)
1	ILMN_2834777	Irf1	ILMN_209850	5.15E-10	-2.19138

C.

	Probeset ID	Symbol	Transcript	p-value(pNHS * 12 vs. OmCI * 12)	Fold-Change(pNHS * 12 vs. OmCI * 12)
1	ILMN_1260323	Akr1c18	ILMN_215518	4.16E-07	1.61755
2	ILMN_1225816	Hbb-bh1	ILMN_216390	1.99E-07	1.58676

D.

Gene Symbol	Gene Name	function
Egr2	Early growth response 2 (Egr2), mRNA.	Sequence-specific DNA-binding transcription factor. Binds to two specific DNA siteslocated in the promoter region of HOXA4. E3 SUMO-protein ligase helping SUMO1 conjugation to its coregulators NAB1 and NAB2, whose sumoylation down-regulates EGR2 own transcriptional activity.
Rgs16	Regulator of G-protein signaling 16 (Rgs16), mRNA.	Inhibits signal transduction by increasing the GTPase activity of G protein alpha subunits thereby driving them into their inactive GDP-bound form. Binds to G(i)-alpha and G(o)-alpha, but not to G(s)-alpha. May play a role in regulating the kinetics of signaling in the phototransduction cascade.
Itprip	Inositol 1,4,5-triphosphate receptor interacting protein (Itprip), mRNA.	Enhances Ca(2+)-mediated inhibition of inositol 1,4,5-triphosphate receptor (ITPR) Ca(2+) release
Egr1	Early growth response 1 (Egr1), mRNA.	Transcriptional regulator. Recognizes and binds to the DNA sequence 5'-CGCCCCCGC-3'(EGR-site). Activates the transcription of target genes whose products are required for mitogenesis and differentiation.
Fam110c	Family with sequence similarity 110, member C (Fam110c), mRNA.	May play a role in microtubule organization
Irf1	Interferon regulatory factor 1 (Irf1), mRNA.	Transcriptional regulator which displays a remarkable functional diversity in the regulation of cellular responses. These include the regulation of IFN and IFN-inducible genes, host response to viral and bacterial infections, regulation of many genes expressed during hematopoiesis, inflammation, immune responses and cell proliferation and differentiation, regulation of the cell cycle and induction of growth arrest and programmed cell death following DNA damage.
Akr1c18	Aldo-keto reductase family 1, member C18 (Akr1c18), mRNA.	Converts progesterone to its inactive form, 20-alpha-dihydroxyprogesterone (20-alpha-OHP). In the liver and intestine, may have a role in the transport of bile. May have a role in monitoring the intrahepatic bile acid concentration. Has a low bile-binding ability. May play a role in myelin formation
Hbb-bh1	Haemoglobin Z, beta-like embryonic chain (Hbb-bh1), mRNA.	amma chains make up the fetal hemoglobin F, in combination with alpha chains

Figure 4.2.3.7 Gene list of top most significant expression changes when comparing pNHS with pNHS+OmCI at 1 hour and 12 hours. List criteria: FDR adjusted p-value <0.05 A. pNHS 1 hour relative to OmCI 1 hour 1FC> 2 (upregulated) and B. FC< -2 (down regulated), C. pNHS 12 hour relative to OmCI 12 hour FC> 1.5. Entities are sorted by p-value and fold change displayed (pNHS relative to OmCI) D. Egr2, Rgs16, Itprip, Egr1, Fam110c, Irf1, Akr1c18, Hbb-bh1 genes are identified and function summary taken from UniProt database general annotation.

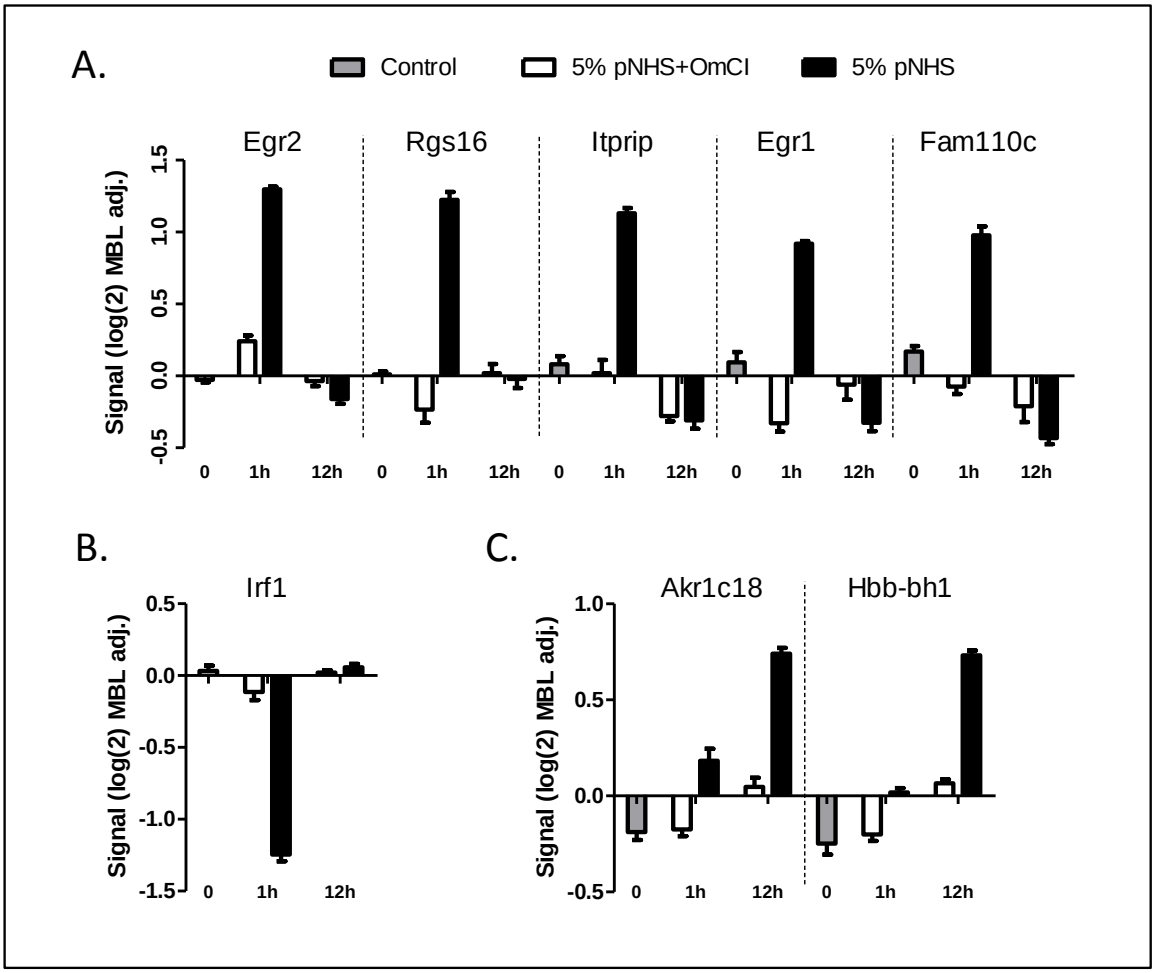

Figure 4.2.3.8 Microarray data bar charts for top most significant expression changes when comparing pNHS with pNHS+OmCl at 1 hour and 12 hours. Data is displayed as log2 transformed, median baseline adjusted and mean calculated for sample groups ± SEM. Baselines therefore represents median of values taken across the dataset. A. upregulated after 1 hour; B. Down regulated at 1 hour; C. upregulated at 12 hours.

transcription factor family (Karin et al, 1997). C-fos is regulated by the MAPK pathway ERKs which stimulate its expression and regulate its activation (Monje et al, 2005).

Genes that have products with growth factor functions which were upregulated by pNHS after 1 hour (Figure 4.2.3.3) were Bdnf and Areg. Brain derived neurotrophic factor (Bdnf) gene product is a neuronal growth factor involved in regulation neuronal cell differentiation and survival of neuronal cells (Barde et al, 1982). Amphiregulin (Areg) gene product codes for an EGF like growth factor which works via the EGFR receptor to either stimulate or suppress proliferation depending on cell type, hence the 'amphi' prefix (Shoyab et al, 1989).

The suppressor of cytokine signalling 4 (Socs4), upregulated at 1 hour (Figure 4.2.3.3) gene product is associated with EGFR signalling through its role as a negative regulator. It performs this role via promoting ubiquitination of the receptor, tagging it for degradation (Bullock et al, 2007). Interferon regulatory factor 1 (Irf1) was down regulated at 1 hour, gene product is a nuclear transcription factor involved in regulation of interferon responsive genes (Miyamoto et al, 1988). It can be induced in response to IFNα and β, IL-1, IL-6 and Ca^{2+} ionophores (Nguyen et al, 1997). In addition to this Irf9 was also down regulated in pNHS at 12 hours. In response to interferon stimulated JAK/STAT signalling a heterotrimeric complex of STAT1/STAT2/IRF9 forms and translocates to the nucleus to regulate interferon responsive genes (Qureshi et al, 1995). Irf1 is thought to be a tumour suppressor gene through its role in apoptosis induction and regulation of cell growth (Kim et al, 2004). Irf1 gene expression has been shown to mediate influence on apoptosis via transcription induction of caspase-8 (De Ambrosis et al, 2007).

Genes upregulated at 12 hours (Figure 4.2.3.5 and Figure 4.2.3.6) included Hbb-bh1, Tgbi, Akr1c18. Haemoglobin Z, beta-like embryonic chain (Hbb-bh1) gene product is involved in oxygen transport and is expressed by yolk sac-derived erythroid cells during early embryonic development (Farace et al, 1984). This haemoglobin has been shown to

be upregulated in gemcitabine resistant colon tumour tissue which was likely due to high-level amplification rather than gene function through amplification of the 7E1 chromosomal location. This may also explain olfactor gene (olf prefixed) upregulation in the microarray which also clusters to this region (van de Wiel et al, 2005). Transforming growth factor β-induced (Tgfbi), upregulated at 12 hours, gene product is an extracellular matrix protein induced by TGFβ1 involved in cell adhesion, migration and integrin signalling in keratinocytes (Jeong & Kim, 2004; Skonier et al, 1992). It also interacts with fibronectin and collagen I and is tightly co expressed with the fibronectin gene involved in microtubule stabilization (Ahmed et al, 2007; Billings et al, 2002). Aldo-ketoreductase family 1, member C18 (Akr1c18) gene product is a hydroxysteroid dehydrogenases (HSD) and NADP(H)-dependent oxidoreductase which belongs to the AKR super family, it functions as an enzyme in progesterone inactivation (Ishida et al, 1999).

The top most statistically significant genes are summarized in figures Figure 4.2.3.7 and Figure 4.2.3.8.

4.2.4 **Gene enrichment analysis**

4.2.4.1 Introduction

Having gained an insight into the genes most responsive to the various experimental conditions through ANOVA statistics and gene list creation it was necessary to apply more complex methods to gain more biologically relevant interpretations of these data. There are many strategies that allow the gene expression patterns to be mined to assign interpretations based upon information regarding each gene's expression, regulation and interactions. These are further supplemented by gene product information regarding function and protein interactions i.e. enzyme activation or inhibition. Generically this type of analysis is termed pathway analysis.

Pathway analysis relies on annotation information for the probes used by the technology. There are a plethora of systems which categorise gene information to facilitate pathway

analysis, including Gene Ontology (GO), Kyoto Encyclopaedia of Genes and Genomes (KEGG) and GenMAPP (Curtis et al, 2005).

The Gene Ontology (GO) project was created by a collaboration of gene databases in 1998 aiming to standardize a set of controlled and structured vocabulary which describes key molecular biology characteristics of a gene, including sequence and product function. GO annotations include stable identifiers which are organised into 4 over-arching categories; molecular function (MF), biological process (BP), cellular component (CC) and sequence ontology (SO) (Harris et al, 2004).

By labelling of genes with a standardized vocabulary, gene lists created from expression information can reveal mechanistic information by enrichment of gene ontology terms allowing greater insights into the biology of the gene expression changes than would be possible with manual investigations of large gene lists. This is the basic premise upon which all pathway analysis sits, different methods and software rely on various statistical techniques and ontology information databases to determine likelihood of involvement of a process or pathway (Curtis et al, 2005).

The KEGG pathway database intends from the outset to create literature informed pathways integrating information regarding the role played by each gene. Pathways are represented by genes and molecules linked by wiring diagrams linking them by interaction to create a network (Kanehisa et al, 2004).

Pathway analysis is now, after 2 decades of development, becoming an invaluable tool in modern day biological research allowing far greater inferences from data than could ever have been achieved before. Responsibility for this lies with the expansion of knowledge in various fields of biology allowing a platform of collated databases containing large amounts of literature confirmed information on gene linkages, interactions and much more. This explosion makes possible a greater degree of integration between the various

information including genetic, proteomic, transcriptomic and metabolomic interactions. This integrative approach is known as systems biology (Cavalieri & De Filippo, 2005).

MetaCore (GeneGo, Encinitas, CA) is a comprehensive online systems biology database with a proprietary collection of metabolic and cell signalling pathway based upon primary literature sources created by a dedicated team. MetaCore software relies on the mapping of data upon prebuilt pathway maps and networks to calculate a p-value based upon the alignment between the two (Bugrim et al, 2004). The online environment offers several analysis tools for mining of datasets using these comprehensive databases including enrichment analysis of pathway maps, process networks, diseases (by biomarkers), metabolic pathways and GO processes.

4.2.4.2 Enrichment analysis using MetaCore

Gene enrichment analysis was conducted, aligning the database held within MetaCore pathway maps, process networks and disease by biomarkers with gene expression data from the sublytic C microarray experiment. The dataset was uploaded via the general parser upload wizard as 5 sample means of log2 transformed median baseline altered data. Experiments were activated in the software window and enrichment analysis selected. Enrichment analysis using the extensive pathway maps ontology databases of MetaCore provided a revealed a spectrum of pathways which sublytic C influenced and activated. For this analysis, data was presented as mean gene expression changes about the median so that up or down regulation could be detected using a threshold of -/+ 0.1 and a p-value filter of 0.1. Samples were colour coded as shown in Figure 4.2.4.1. Presented p-values represent the probabilities of a particular enrichment being by chance and are displayed as –log histograms.

Charts displaying greatest enrichments of gene expression changes in pNHS conditions compared to OmCI inhibited (red=1 hour and brown=12 hours) are of greatest interest. These include the following implicated pathway maps: Reproduction GnRH signalling,

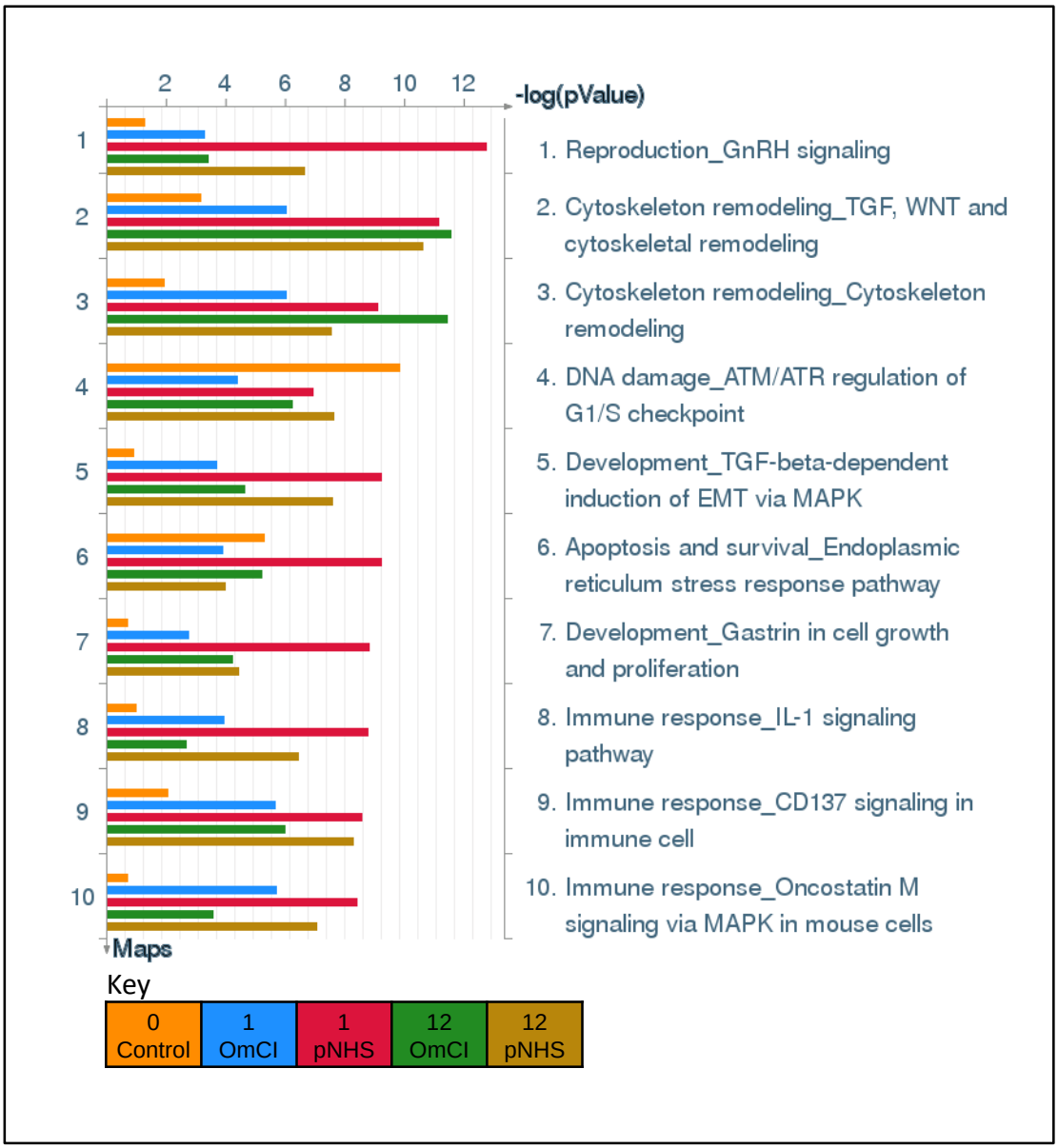

Figure 4.2.4.1 Pathway map enrichment score histograms. The 10 most enriched pathway maps detected by the number of differentially expressed entities within the uploaded dataset. Each bar represents a sample group and coloured as in key, giving the –log p-value score for enrichment of pathway maps.

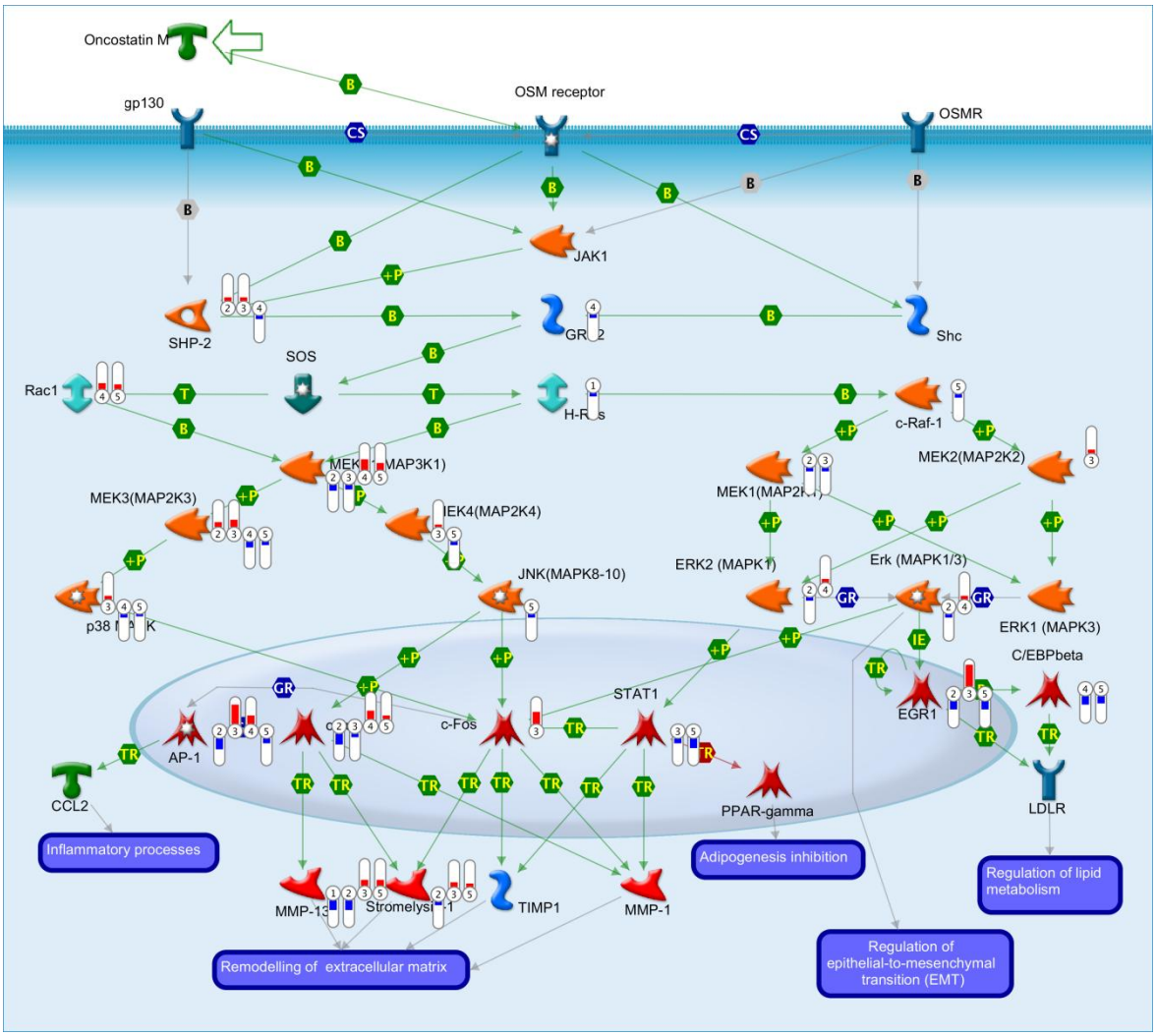

Figure 4.2.4.2 Pathway map- Immune response: Oncostatin M signalling via MAPK in mouse cells. Map displays the collated linkages of the oncostatin M signalling pathway describing the cell signalling and transcriptional changes in response to receptor ligation. Linkages are shown by slender lines with description of linkage displayed in hexagonal symbols, B=binding, +P= phosphorylation, T=transformation IE=influence on expression, TR=transcription regulation. Expression data is presented as thermometer like symbols, red=above median expression, blue=below median expression.

TGFβ induction of EMT via MAPK, IL-1 signalling, CD137 signalling in immune cells, oncostatin M signalling via MAPK (Figure 4.2.4.1).

Enrichment analysis data show influences exerted by serum as discussed in previous sections; hence the influence exerted by sublytic C could be viewed. Interpretation of maps required focussing on genes dysregulated upon pNHS treatment at 1 and 12 hours, either up or down, ignoring those that are similarly dysregulated in both pNHS and pNHS+OmCI conditions which would indicate a serum response independent of C. TGFβ, IL-1, CD137 and oncostatin M signalling pathways were implicated. Epithelial to mesenchymal transition and apoptosis-endoplasmic stress response processes were also implicated. Common within these pathways were expression changes in components of MAPK signalling pathways including suggestion of MKK7 and MEK1 phosphorylation of JNK, c-Raf1 phosphorylation of MEK2 and p38α phosphorylation and activation of ATF-2 or STAT1 transcription factors. TRAF6 binding or modification of TAB1/2 or SITPEC is implicated as involved in signal transduction through MEK4/JNK exerting transcription influence through the AP-1 monomer c-fos. TRAF2 may be involved in MEK3/p38 or MEK4/JNK influencing transcription through ATF-2 or AP-1 respectively. Many of the implicated gene expression changes are upregulated at 1 and downregulated at 12 hours suggesting feedback mechanisms.

The oncostatin M signalling pathway map contains implicated objects outside of the signalling and transcription regulating components (Figure 4.2.4.2). The extracellular matrix regulating genes Mmp3 and Mmp13 were each upregulated by pNHS at both time points giving a clear indication that p38, JNK and MEK/ERK MAPK pathways may be activated by exposure to sublytic C regulating gene expression via AP-1 transcription factor.

4.2.5 **Network analysis**

The work described in this chapter has identified the gene expression signatures given by sublytic C attack under the conditions used. Enrichment analysis has indicated the involvement of various processes including the immune response and apoptosis modulation in cell responses to sublytic C. However the aim to identify specific genes which may confer an advantage to a forming tumour has been confounded by the lack of convincing pathway related genes on which to focus. The strong influence that the chosen time point has on the data variation can potentially mask the effects of sublytic C attack the experiment is designed to explore. Using the power and flexibility of Partek statistics and gene list generation a more focussed strategy can be employed to determine the specific influence of sublytic C.

4.2.5.1 Overlap gene list generation

Partek statistics provide the opportunity to focus in on gene sets which present a very specific pattern of expression within the dataset. A gene list was collated to better represent the influence of sublytic C on CT26 cells. Genes responsive to sublytic C were selected as upregulated at both 1 hour and 12 hours post exposure to the conditions. This was reasoned to highlight those genes which were consistently upregulated over the period of the experiment. Firstly two lists were created from ANOVA statistics with the following filters applied: Increase in pNHS * 1 relative to OmCI * 1 with p value < 0.05 and increase in pNHS * 12 relative to OmCI * 12 with p value < 0.05. It was necessary to generate large gene lists initially in order to create a sufficiently large (but not too large) overlap list and so a lower level of stringency was applied; no FDR adjustment and no fold change restriction. Created lists were populated with 781 and 1148 entities respectively. From these lists an overlap was taken as the intersecting region of a Venn diagram comparison, this contained 66 entities (Figure 4.2.5.1). Clustering of the genelist as shown in Figure 4.2.5.2 demonstrates the list contains genes upregulated in response to pNHS

	Probeset ID	Symbol	Transcript	p-value(pNHS * 1 vs. OmCI * 1)	Fold-Change(pNHS * 1 vs. OmCI * 1)	p-value(pNHS * 12 vs. OmCI * 12)	Fold-Change(pNHS * 12 vs. OmCI * 12)
1	ILMN_1240323	Dnajb1	ILMN_222931	1.06E-07	1.23503	0.00185733	1.07348
2	ILMN_2737685	Mmp13	ILMN_210384	4.96E-07	1.52378	0.00650418	1.14512
3	ILMN_1249426	Socs4	ILMN_216527	1.72E-05	1.24619	0.00157409	1.13555
4	ILMN_1238547	Areg	ILMN_217903	8.00E-05	1.43899	0.0180413	1.18086
5	ILMN_2860804	Tfrc	ILMN_211824	0.000125388	1.40674	0.00247263	1.25972
6	ILMN_2753809	Mmp3	ILMN_219123	0.000159494	1.23906	0.0462792	1.08968
7	ILMN_1260323	Akr1c18	ILMN_215518	0.000200139	1.281	4.16E-07	1.61755
8	ILMN_2762380	Enpp4	ILMN_223315	0.000207995	1.16497	0.000395452	1.15143
9	ILMN_2631994	Hexim1	ILMN_212955	0.000249227	1.16175	0.000532145	1.14598
10	ILMN_3033753	Fndc5	ILMN_244553	0.000438051	1.10563	0.0426112	1.04763
11	ILMN_2600646	Mia3	ILMN_209942	0.000524624	1.16672	0.0249163	1.08631
12	ILMN_2757617	Il1rl1	ILMN_215312	0.000608952	1.19425	0.000550805	1.19704
13	ILMN_2798753	Gnl2	ILMN_250623	0.000681798	1.20127	0.00371376	1.15482
14	ILMN_1237058	Cnga3	ILMN_221213	0.000714416	1.06946	0.0117395	1.0446
15	ILMN_2705604	Ppp1r15b	ILMN_186016	0.000855383	1.19491	0.00154355	1.17839
16	ILMN_2619848	Tfrc	ILMN_211824	0.0015468	1.28305	0.00240607	1.26335
17	ILMN_2759415	Cenpe	ILMN_227180	0.00219871	1.05983	0.0103522	1.04622
18	ILMN_1225816	Hbb-bh1	ILMN_216390	0.00329093	1.16353	1.99E-07	1.58676
19	ILMN_2666018	Mgp	ILMN_215984	0.0034199	1.26867	6.50E-05	1.48997
20	ILMN_1241657	Cnot2	ILMN_219105	0.00532856	1.07852	0.00877129	1.07192
21	ILMN_2797928	Mustn1	ILMN_215350	0.00610923	1.15646	0.00182066	1.19161
22	ILMN_2875251	Ang	ILMN_244375	0.00619403	1.1171	0.0457869	1.07665
23	ILMN_2923285	Rnf32	ILMN_213506	0.0063251	1.09164	0.0418454	1.06186
24	ILMN_2502596	Nmnat1	ILMN_232308	0.00654942	1.07596	0.0237638	1.05908
25	ILMN_2907499	Tatdn2	ILMN_244008	0.00667741	1.17943	0.0071941	1.17698
26	ILMN_3143227	Tmem183a	ILMN_249013	0.00730189	1.12779	0.000514444	1.19426
27	ILMN_2720786	Scmh1	ILMN_247166	0.00732057	1.07901	0.0263702	1.0612
28	ILMN_2763245	Cxcl1	ILMN_223377	0.00831195	1.55636	0.0206054	1.45109
29	ILMN_2720763	BC025546	ILMN_220336	0.00841115	1.17742	0.00525206	1.19349
30	ILMN_2751090	Cep68	ILMN_222538	0.00965334	1.08604	0.00840214	1.08827
31	ILMN_2671344	Adamts12	ILMN_242188	0.0106427	1.05428	0.0215408	1.04715
32	ILMN_3097726	Gnl3	ILMN_250637	0.0117709	1.11868	0.000137441	1.23639
33	ILMN_2716558	LOC669251	ILMN_235418	0.0125271	1.05613	0.0190704	1.05159
34	ILMN_2724942	Ptgis	ILMN_220660	0.0131669	1.11756	0.0109388	1.12193
35	ILMN_2791578	Gspt1	ILMN_216927	0.0146217	1.10004	0.0229139	1.09097
36	ILMN_1231287	Msi1	ILMN_217693	0.0156498	1.05121	0.00793649	1.05822
37	ILMN_1224651	2810405J04Rik	ILMN_217867	0.0156769	1.11424	0.00414044	1.14635
38	ILMN_2703748	Luc7l	ILMN_219060	0.0186717	1.11708	0.0366221	1.10023
39	ILMN_2634768	Olfr78	ILMN_213211	0.0199231	1.082	0.0265471	1.07697
40	ILMN_2605096	Rsl1d1	ILMN_210385	0.0207247	1.14149	0.0437253	1.11818
41	ILMN_2659644	Map2k3	ILMN_215446	0.0209027	1.07477	0.00842064	1.08952
42	ILMN_2650439	Galnt1	ILMN_212372	0.0212788	1.10417	0.00272697	1.15253
43	ILMN_2935998	Tmeff2	ILMN_194817	0.0213607	1.07636	0.0018916	1.11779
44	ILMN_2598050	1700049K14Rik	ILMN_256176	0.0221217	1.06819	0.0293862	1.06398
45	ILMN_2872058	Ctsh	ILMN_241653	0.0223128	1.10535	0.0273958	1.10056
46	ILMN_1236889	Selp	ILMN_216201	0.0253795	1.12538	0.0328451	1.11795
47	ILMN_1216854	Zfp787	ILMN_242380	0.0289459	1.05575	0.000742605	1.10493
48	ILMN_3161571	Olfr104	ILMN_249555	0.0294168	1.05714	0.0280145	1.05779
49	ILMN_2600627	Noc4l	ILMN_209940	0.0305599	1.09742	0.00628803	1.13449
50	ILMN_1228590	Ogfod2	ILMN_221240	0.0308091	1.08774	0.00901813	1.11346
51	ILMN_2593774	1190002H23Rik	ILMN_209224	0.0311035	1.07557	0.000476638	1.15525
52	ILMN_1239947	Hnf4g	ILMN_221613	0.0319447	1.04848	0.0234694	1.05199
53	ILMN_2829129	Dcpp1	ILMN_240826	0.0335684	1.05797	0.027549	1.0607
54	ILMN_1239345	Asf1a	ILMN_214517	0.034306	1.04164	0.0388347	1.04041
55	ILMN_1240933	Ambn	ILMN_217978	0.0367144	1.04166	0.0118774	1.05304
56	ILMN_1258977	Tmem33	ILMN_225515	0.0384204	1.08152	0.0391759	1.08112
57	ILMN_2653081	Prkab1	ILMN_214884	0.0391979	1.07229	0.0409149	1.07151
58	ILMN_2836664	Polr1a	ILMN_260912	0.0394424	1.05206	0.00427644	1.081
59	ILMN_3151503	C130032J12Rik	ILMN_222501	0.0408503	1.10148	0.000261866	1.24628
60	ILMN_2792809	Arpc5	ILMN_218989	0.0425289	1.06436	0.0470318	1.0627
61	ILMN_2679037	LOC100046883	ILMN_310789	0.0448332	1.11185	0.00110273	1.22763
62	ILMN_2856457	Krtap16-3	ILMN_208768	0.0449878	1.05583	0.00357391	1.09265
63	ILMN_2737479	Slc12a9	ILMN_215442	0.0450887	1.06685	0.0217535	1.07948
64	ILMN_1245139	Scamp3	ILMN_218241	0.0455026	1.07573	0.038499	1.07905
65	ILMN_1227235	Timm10	ILMN_216641	0.046028	1.15605	0.0173915	1.19764
66	ILMN_2698361	Ars2	ILMN_217819	0.0474577	1.0767	0.00713001	1.11537

Figure 4.2.5.1 List of genes significantly upregulated at both 1 and 12 hours; pNHS 1 and 12 hour relative to pNHS+OmCI 1 and 12 hours. List criteria: unadjusted p-value <0.05; pNHS 1 hour relative to OmCI 1 hour UP, 0 FC; pNHS 12 hour relative to OmCI 12 hour, UP, 0 FC. Entities are sorted by p-value (1 hour) and fold change displayed (pNHS relative to OmCI).

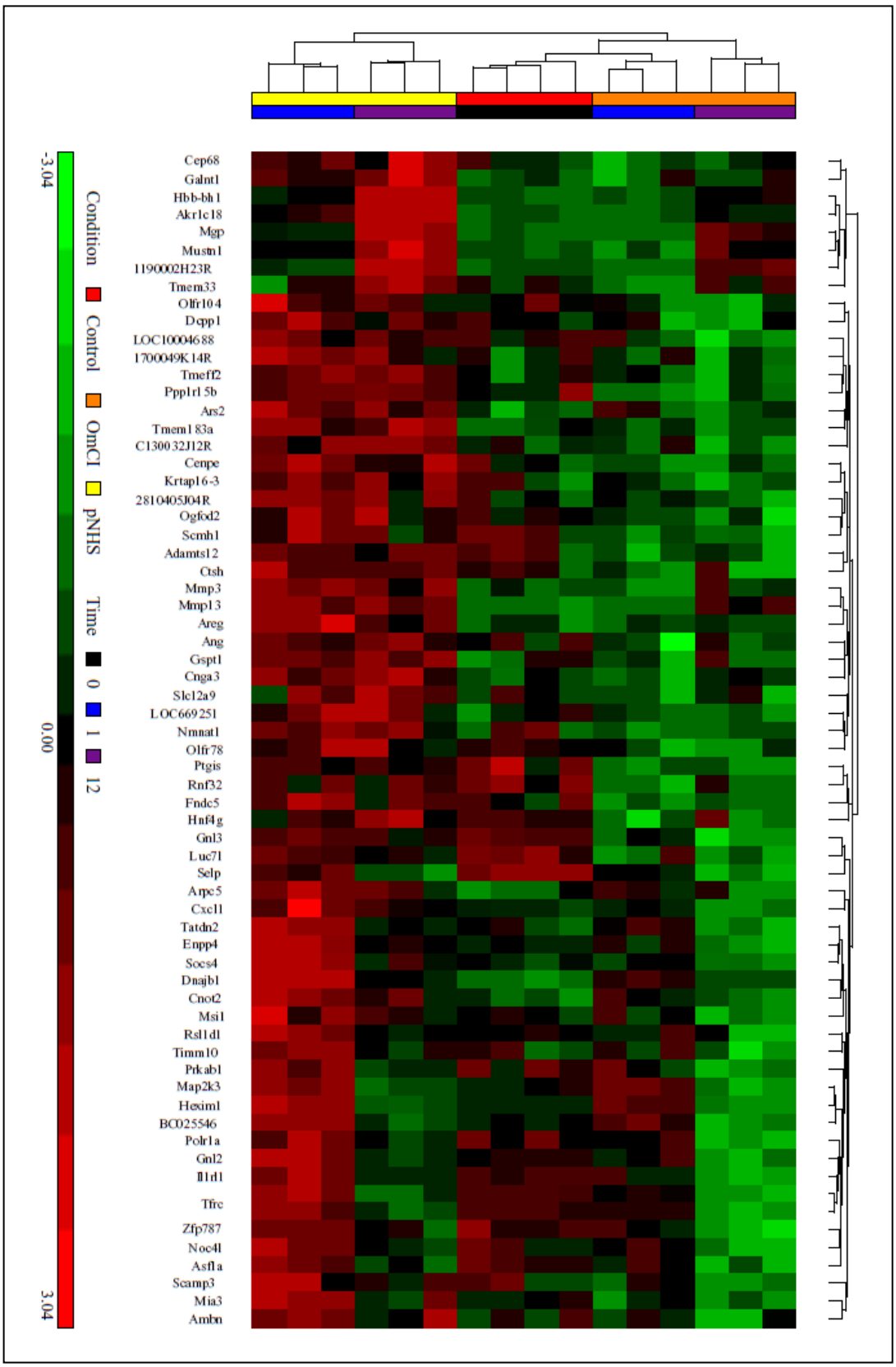

Figure 4.2.5.2 Hierarchical clustering heatmap of overlap gene list. PNHS 12 hour relative to pNHS+OmCI 12 hour. Gene list criteria: unadjusted p-value <0.05; pNHS 1 hour relative to OmCI 1 hour UP, 0 FC; pNHS 12 hour relative to OmCI 12 hour, UP, 0 FC. Overlap list=66 entities. Dendrograms clustering sample bar: Serum condition; red=control, orange=OmCI, yellow=pNHS Time point; black=0, blue=1 hour, purple=12 hours. Gene expression values (log2 transformed, 0 mean shifted, scaled to SD=1) for clustered entities: green=downregulated, black=no change, red=upregulated.

compared to pNHS+OmCI at either 1 hour only, 12 hour only and crucially at both time points.

4.2.5.2 Network building form overlap gene list

The gene list generated in section 4.2.5.1 was uploaded into GeneGo as a custom entity list. It was then used to explore the possible linkages by building a network from the custom entities. The network was built using the list as seed 'nodes' and the algorithm for linkage based upon standard Dijkstra's shortest path. This algorithm plots the shortest pathway between nodes by the addition of up to 2 steps based upon 'from' - 'to' pathways between seed nodes. Additional nodes are therefore added as linkages. Canonical pathways are considered as 1 linkage and so multiple nodes are added in this case. It is important to note that generated networks are created using the curated ontologies contained within MetaCore. This means that each connection between nodes derive from confirmed biological interactions taken from literature citations.

Once generated the network was explored at length. For clarity, nodes were manually moved to determine the key seed nodes and their overlapping connections. Nodes unconnected to the main network were removed. Node groups displaying little connectivity to the main network were pruned to reveal the most interrelated nodes. With the network reduced to its most connected nodes it was organised by cellular location from left to right: the extracellular space representing gene products which are secreted, cytoplasmic where much of the signalling is transduced, and nuclear from which gene expression is regulated.

Out of the network seed nodes derived from the gene list, generated as described in section 4.2.5.1, four key downstream genes; matrix metalloproteinases (Mmp) 3 and 13, C-X-C motif ligand 1 (Cxcl1) and amphiregulin (Areg) were highlighted. These genes were co-regulated by a network of putative signalling events and cascades including Ca^{2+} release, PI3K, various MAPK pathways, PKC and JAK/STAT pathways via a number of

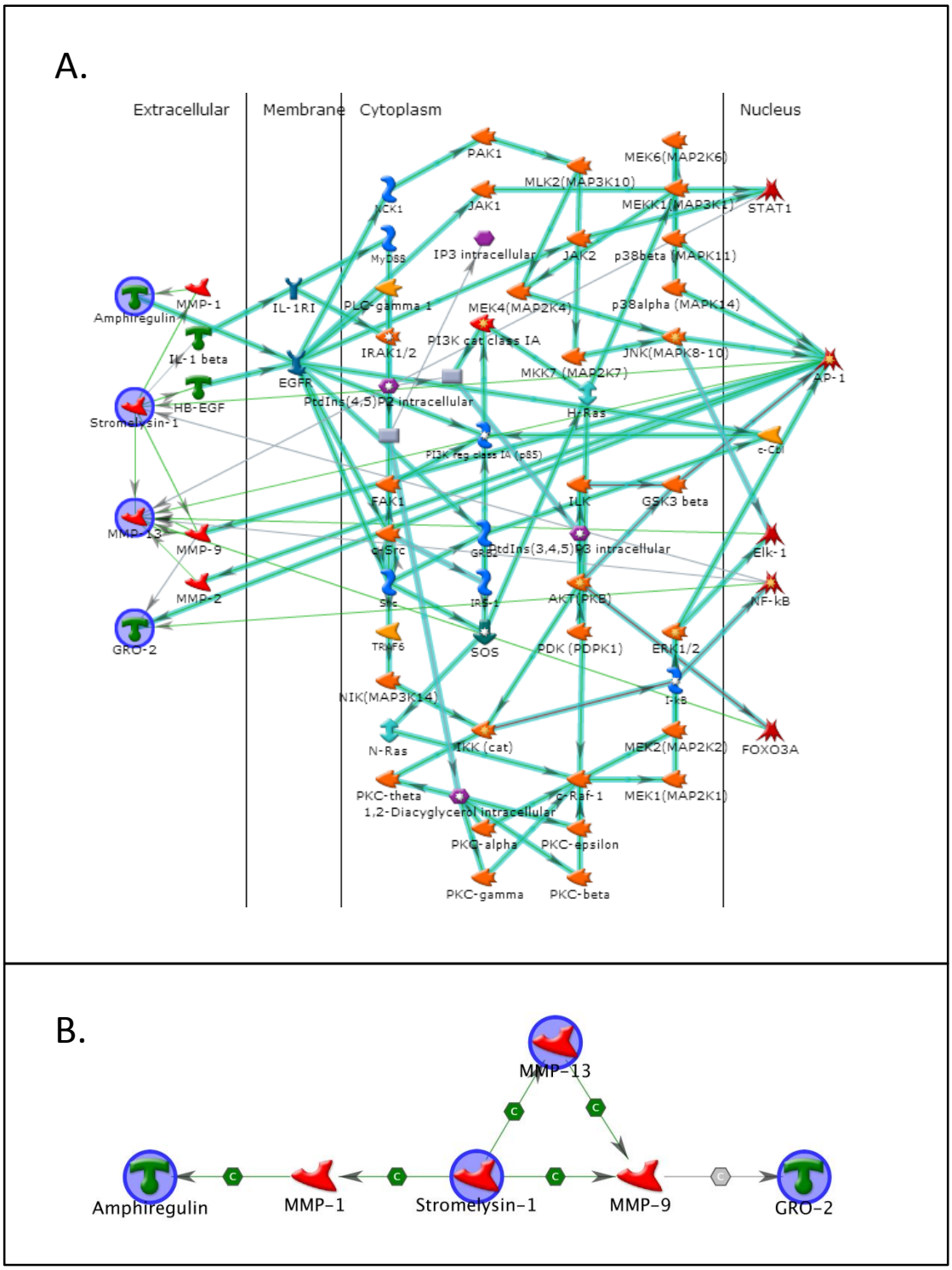

Figure 4.2.5.3 Gene linkage analysis of overlap gene list. Networks describing the interconnected regulation of four key downstream effector genes, generated: shortest path, max 2 steps, either inclusion of (A) or exclusion of canonical linkages (B). Network is organised to cellular localization of gene product. Seed nodes are circled in navy blue. Thick light blue lines describe canonical pathways of signal transduction and transcription regulation. Thin lines are non-canonical interactions either transcriptional regulation or protein association e.g. enzymatic regulation/cleavage. Hexagonal labels represent mechanism of interaction, c=cleavage, green=positive activation, grey=unspecified.

A.

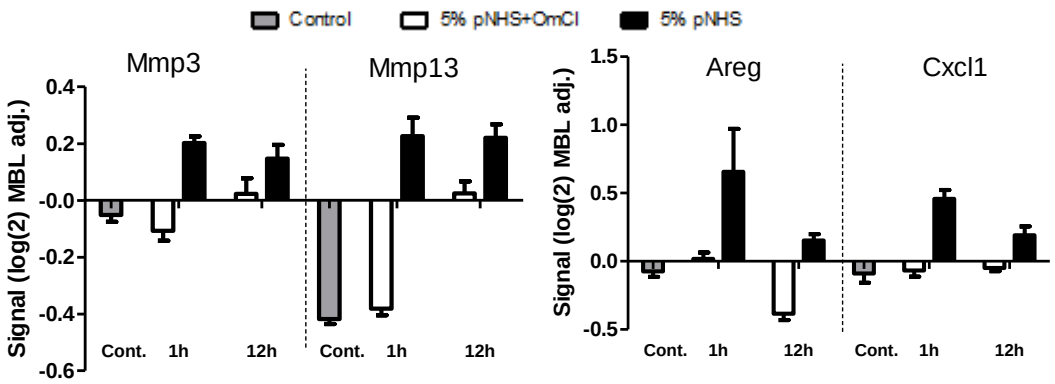

B.

	Probeset ID	Symbol	Transcript	p-value(pNHS * 1 vs. OmCI * 1)	Fold-Change(pNHS *1 vs. OmCI * 1)	p-value(pNHS * 12 vs. OmCI * 12)	Fold-Change(pNHS * 12 vs. OmCI * 12)
1	ILMN_1238547	Areg	ILMN_217903	2.31E-06	1.43899	0.00185142	1.18086
2	ILMN_2737685	Mmp13	ILMN_210384	1.06E-06	1.52378	0.0100312	1.14512
3	ILMN_2753809	Mmp3	ILMN_219123	9.89E-05	1.23906	0.00367792	1.08968
4	ILMN_2763245	Cxcl1	ILMN_223377	8.74E-03	1.55636	0.0215031	1.45109

C.

Gene Symbol	Gene Name	function
Areg	amphiregulin (Areg), mRNA.	Ligand of the EGF receptor/EGFR. Autocrine growth factor as well as a mitogen for a broad range of target cells including astrocytes, Schwann cells and fibroblasts.
Cxcl1	chemokine (C-X-C motif) ligand 1 (Cxcl1), mRNA.	Has chemotactic activity for neutrophils. Contributes to neutrophil activation during inflammation. Hematoregulatory chemokine, which, in vitro, suppresses hematopoietic progenitor cell proliferation. KC(5-72) shows a highly enhanced hematopoietic activity
Mmp3	matrix metallopeptidase 3 (Mmp3), mRNA.	Can degrade fibronectin, laminin, gelatins of type I, III, IV, and V; collagens III, IV, X, and IX, and cartilage proteoglycans. Activates procollagenase.
Mmp13	matrix metallopeptidase 13 (Mmp13), mRNA.	Degrades collagen type I.

Figure 4.2.5.4. Network derived hits. A. Microarray data bar charts for network analysis derived hits, data is displayed as log2 transformed, median baseline adjusted and calculated mean for sample groups. Baselines therefore represents median across the expression values taken for each probe. B. Gene list entities are sorted by p-value (1 hour) and fold change displayed (pNHS relative to OmCI). C. Areg, Cxcl1, Mmp3, Mmp13 genes are identified and function summary taken from UniProt database general annotation.

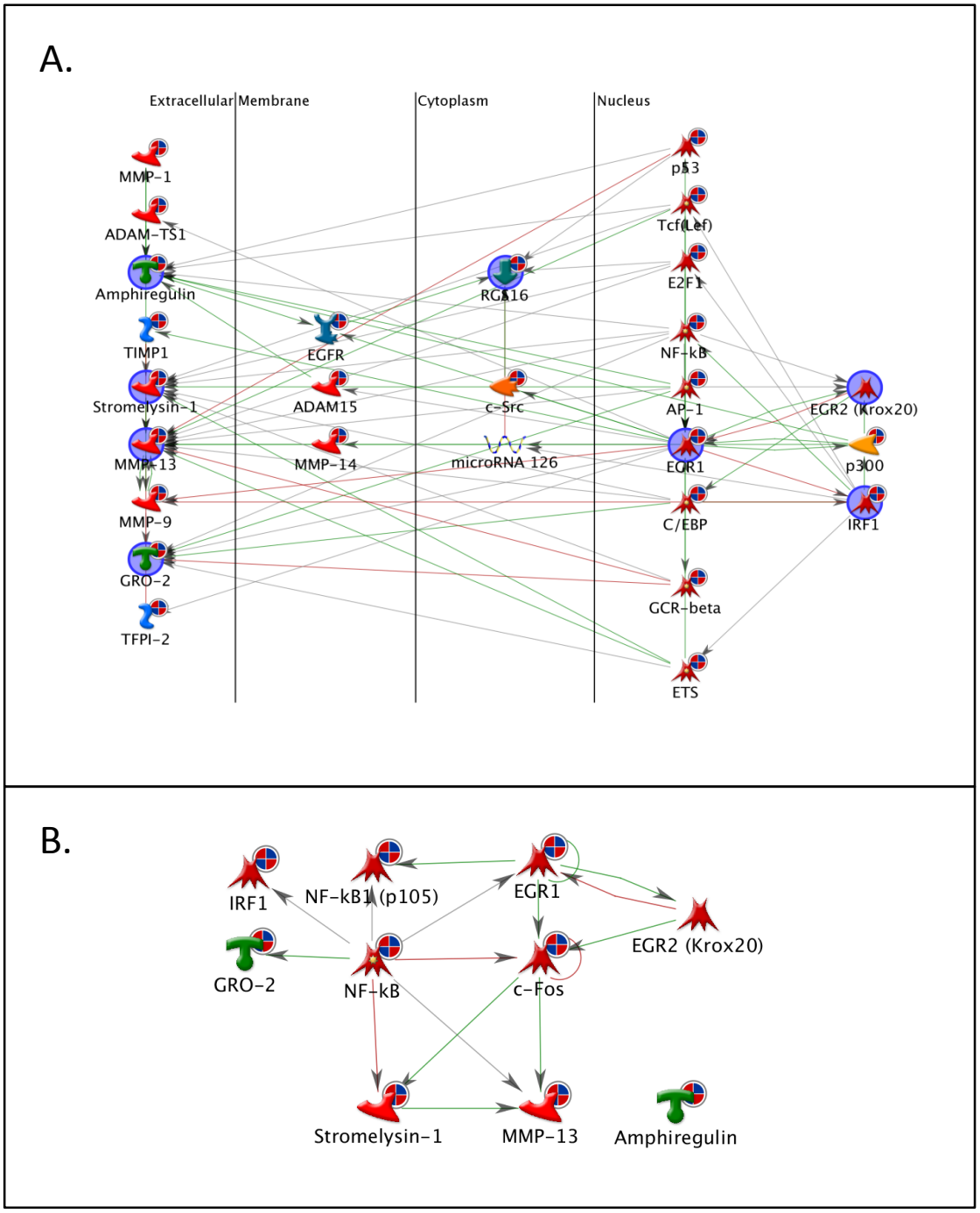

Figure 4.2.5.5 Gene linkage analysis of collated gene list. A. Network describing the interconnected regulation of the four key downstream effector genes as well as the 8 statistically significant genes from Figure 4.2.3.8. generated: shortest path, max 2 steps, excluding of canonical linkages Network is organised to cellular. B. Direct interaction informed by network in A showing the interactions of transcriptional regulators with the four key effector genes. Seed nodes are circled in navy blue. Thin lines are non-canonical interactions either transcriptional regulation or protein-protein association. Lines represent interaction: red=inhibition and green=activation.

transcription factors including AP-1 and NFκB. The generation of this network was significant because it was the first indication of a set of linked sublytic C responsive genes on which attention could be focussed.

To better display this network the highlighted downstream effectors were uploaded as a fresh entity list and network generation carried out as described above. The generated network is displayed in Figure 4.2.5.3.A.

Figure 4.2.5.4 A. shows the microarray gene expression data transformed and baseline adjusted to median as described in 4.2.2.2. Each of the genes highlighted by the network were upregulated at both 1 and 12 hours post exposure to pNHS compared to pNHS+OmCI. Both Mmp3 and Mmp13 were increased. They display similar expression patterns rising to ~0.2 above median levels but Mmp13 expression in controls at 0 and 1 hour were greatly below baseline. This is due to an increase in expression compared to the non-treated control in pNHS+OmCI at the 12 hour time point. Areg and Cxcl1 were also increased in response to pNHS in comparison to pNHS+OmCI by 0.5 above median at the 1 hour time points. The increase of Cxcl1 was reduced after 12 hours. At the 12 hour time point Areg is below baseline, -0.5 in control conditions but above baseline by ~0.2 in response to the treatment suggesting an overall drop in expression after 12 hours.

With these genes identified as important responsive genes to sublytic C it was of interest to correlate these with previous gene expression changes highlighted as the most statistically significant shown in Figure 4.2.3.7 and Figure 4.2.3.8. To understand the possible interconnectivity of these genes with those highlighted through network generation, they were combined to form a new gene list which was uploaded as seed nodes in a network selecting for shortest path with a maximum of 2 steps and canonical pathways excluded (Figure 4.2.5.5A). This analysis demonstrated the striking connectivity of the 4 downstream genes to AP-1 suggesting its crucial role in the observed response. In addition the association of EGFR with Rgs16 is evidence of Gαi-protein mediated trans-

activation of EGFR by phosphorylation (Derrien & Druey, 2001). Analysis was also repeated using the central interacting seed nodes plus NFκB to find direct interactions (Figure 4.2.5.5B). The interplay between EGR1, EGR2, IRF1, AP-1 and NFκB with the four previously described hits may go some way in informing a mechanism to explain the sequence of events leading to the observed response. Figure 4.2.5.5B makes clear that c-fos (AP-1) may be downstream of Egr1 and 2 and that Mmp3 and 13 may be controlled via this pathway. NFκB may be responsible for Cxcl1 induction but other interactions suggested are not backed up by the data, i.e. Irf1 was downregulated in the data. Areg is shown to be outside this network suggesting an independent mechanism. Taking the network data together a possible mechanism might be EGFR activation possibly via Gαi leading to transcription regulation primarily via AP-1 and NFκB.

4.3 Discussion

The aim of this chapter was to identify the gene expression profile induced by exposure of CT26 tumour cells to sublytic C using the conditions optimized in chapter 1. Specifically, the chapter aimed to identify gene expression changes which might be tumour promoting in nature. A microarray experiment was performed and bioinformatic analysis of expression data revealed a number of genes responsive to sublytic C attack which were sustained over 12 hours. Of these, 4 genes with roles in the extracellular space were identified as being co-regulated via network analysis. These had roles in extracellular matrix regulation, inflammation and proliferation acting to influence the interaction between a tumour cell and its environment. This is indirect evidence of a tumour promoting role for sublytic C.

4.3.1 **Data handling**

Data normalization was achieved using quantile method. Normalization methods were studied comparing complete methods which normalize based upon the signal data in its entirety with methods which make use of a baseline array (Bolstad et al, 2003). Within the

comparison the quantile method performed well in all the measures used. Quantile gave the smallest distance between arrays which was maintained across intensity data, scored well on bias and was the fastest to calculate. Quantile normalization is now considered the most robust method, performing well in reducing masking variation without affecting the biologically significant variation.

PCA analysis showed how the experimental groupings separated from each other initially revealing a batch effect, groupings were clearly seen once this was removed. Separation revealed influence of time and serum but crucially a difference between OmCI treated and untreated pNHS conditions. This gave a clear indication that a specific effect of terminal pathway competency could be detected in the gene expression response.

4.3.2 **ANOVA gene lists**

ANOVA statistics demonstrated that the main sources of variation as a factor of the error was serum exposure time contributing the majority of the variation. By comparison with this, the serum condition i.e. pNHS and pNHS+OmCI contributed much less variation. This was supported by the number of significant differentially expressed genes in the comparison between the 1 and 12 hour timepoints. Hierarchical clustering showed the main clustering effect to be time point dependent regardless of terminal complement competency further supporting the dominance of serum in this system.

Sublytic C attack experiments were designed in a way that focussed upon the terminal pathway of C. Serum isolated from human blood was used as a source of C and the terminal pathway controlled using OmCI, a specific inhibitor of C5 added to the same serum. Serum, with its complex mixture of growth factors, hormones and cytokines, can therefore be considered a dominant influence on gene expression changes. Cells respond to serum exposure by upregulating a number immediate early response genes which will have been detected by the hybridisation experiment as well as changes to genes downstream of these altered response genes. With such a high throughput technique it is

advisable to carefully formulate the experimental design. Complex and unpredictable effects such as those given by serum are not ideal. Eliminating such an effect could be achieved with a cleaner system such as reactive lysis (Abe et al, 2004). To do this C7 depleted serum could be treated with purified zymosan and the formed C5b6 complex then purified (Discipio et al, 1983).The C5b6 complex and C7 would be deposited on the membrane by co-incubation then the final components added separately (Wiedmer et al, 1987).

PCA analysis provided evidence that despite the substantial serum influence there was a sublytic complement effect that could be focused on using the ANOVA statistics.

ANOVA statistics facilitated the comparisons that yielded changes exclusive to terminal pathway activation. Among the responsive genes there were clues to the events induced by this activation. Genes involved in signal transduction (Itprip, Rgs16, Dusp2), transcription factors (Fos, Egr1, Egr2), proliferation (Areg, Bdnf) and inflammatory responses (Irf1, Socs4) were significantly altered.

Signalling involving G-protein, Ca^{2+} and MAPK activation were therefore implicated in agreement with reported signalling events associated with MAC deposition (Cole & Morgan, 2003). C-fos is well established to be upregulated rapidly in response to MAC deposition and may also uphold the possibility of Ca^{2+} and MAPK (particularly ERK) involvement (Badea et al, 2003).

A comparison of hits found in this study can be made to a microarray experiment where MAC deposition was shown to induce apoptosis in a Thy1N model (Liu et al, 2012). This was found to be through upregulation of Irf1 and induction of caspase 8 transcription and activation. Within the study by Liu et al (2012), microarray analysis of MAC deposition demonstrated upregulation of Irf1, Atf3, Egr1, C/EBPβ, Gadd45, connective tissue growth factor, IL-6, IL-1β, HO-1, schlafen 3, and cyclin L1. Of these, Egr1 upregulation was in agreement with data presented here but Irf1 and Gadd45ɣ were contrasting. Explanation

for this discrepancy may lie in the time scale used; RNA extraction of samples by the group was taken 40 minutes and 3 hours post-exposure and genes down regulated in the presented analysis may indicate the drop in expression of a gene which had previously been greatly upregulated, falling below basal levels. This is difficult to prove and it may be that the cell types respond to sublytic C differently. The observed down regulation of Irf1 and Gadd45ɣ at 1 hour may demonstrate a novel anti-apoptotic influence of sublytic C in CT26 cells.

4.3.3 **Enrichment analysis**

Gene list creation from ANOVA statistics allowed the comparison between conditions and provided indications of the systems and mechanisms that might be in play during exposure to sublytic C. These indications are significant but characterised by an assumption that a single or collectively significant gene expression change is indicative of a definite response. A more global and holistic view was therefore needed to take the entirety of the data and make informed correlations between groups of responsive genes and the systems they are involved with. This was achieved by enrichment analysis.

The implication of TGFβ, IL-1, CD137, and OSM pathway map enrichment by sublytic C are important leads to which some attention must be paid but interpretation requires consideration and caution. Their suggestion by enrichment analysis is likely due to common signalling pathway components and transcription regulation as set out in section 4.2.4.2.

Thrombospondin1 (TSP-1) and TGFβ was shown to be expressed in response to sublytic MAC deposition by GMCs via PI3K/Akt pathway activation, TSP-1 protein could then activate latent TGFβ1 (Gao et al, 2007). TGFβ (but not TSP-1) genes were upregulated after 12 hours as a serum response rather than as a consequence of sublytic C according to the microarray presented here. However it is conceivable that latent TGFβ secreted by the cells may have been cleaved by other factors expressed or activated by sublytic C.

IL-1β is reported to be released in response to sublytic MAC by several cell types and is associated with prostaglandin secretion (Schonermark et al, 1991). An IL-1β expression response is not shown in the microarray data but may still be involved in its pro form which can be cleaved to release the active cytokine (Black et al, 1988).

CD137 is a member of the TNF receptor super family, expressed primarily by T-cells as a co-stimulatory molecule and binds its ligand CD137L on target cells as a mechanism to regulate T-cell proliferation (Kwon et al, 2000). There is some evidence of expression change in the microarray data for both the CD137 and CD137L though it is most likely a serum response and the relevance of such a change is not clear.

As mentioned previously, it is the presence of common signalling component expression changes within each of the mentioned pathway maps which explains their significant enrichment scores. There is strong suggestion of mitogen activated protein kinase (MAPK) signalling cascade activation upon exposure to pNHS compared to pNHS+OmCI. MAPK signalling cascades are organised by a hierarchy of kinases starting from the triggering MAPK kinase kinase, which as its designation suggests phosphorylates the next component in the sequence, MAPK kinase which in turn phosphorylates MAPK. There are a number of MAPK modules in mammalian cells; they are the extracellular signal-regulated kinase 1 and 2 (ERK1/2) cascade, the c-Jun N-terminal kinase (JNK) and p38 MAPK pathways designated to refer to the main MAPK of the pathway. Each have their own specific kinase components that fit the described hierarchy and each component has close specificity to its substrate along the chain (Schaeffer & Weber, 1999). JNK cascade signalling is activated by cytokine and cell stress regulating transcription via phosphorylation of the AP-1 monomer c-jun (Davis, 2000). P38, like JNK, is responsive to stress stimuli such as LPS and osmolarity changes acting via c-jun and ATF-2 transcription factors (Han et al, 1994). ERK1/2 cascade is generally responsible for signal transduction from growth factor receptor triggers leading to cell activation and proliferation

as well as inhibition of apoptosis. Activated ERK1/2 regulates transcription via fos or Elk-1 (Mebratu & Tesfaigzi, 2009).

Within pathway maps there were common pathways which suggest activation of each of the three described MAPK cascades. A MEKK1/MEK3 or MEK4/JNK or p38 pathway implicates TRAF6/SITPEC activity.

TNF receptor associated factor 6 (TRAF6) is an adaptor protein involved in IL-1R, TLR and TNFR signalling pathways and is therefore a key component of innate immune signalling (Chung et al, 2002). In general TRAF mediated signalling involves the trimerization and recruitment of TRAF to receptor upon its activation (Ye & Wu, 2000). Association between receptor and TRAF6 is either direct, as with TNFR, or via IRAK adaptor proteins as with IL-1 and TLRs (Wu & Arron, 2003). TRAF6 can induce both MAPK (JNK, ERK, p38) and IKK pathways leading to activation of AP-1 and NFκB transcription factors. This requires TAK1 activation via adaptor proteins TAB1 and 2 a process which is now known to be regulated by k63 polyubiquitination (Ninomiya-Tsuji et al, 1999; Wang et al, 2001). TRAF6 is also capable of activating the PI3K/Akt signalling cascade (Wong et al, 1999; Yang et al, 2009). TRAF6 regulates signalling by way of its E3 ubiquitin ligase activity (Deng et al, 2000). It is through this activity that TRAF6 was shown to mediate PI3K/Akt activation in response to sublytic deposition of the MAC in Thy-1 GMCs (Qiu et al, 2012). It is therefore possible that activation induced by insertion of MAC into a cell membrane causes activation of pathways via TRAF6, indeed Qiu et. al. (2012) demonstrated direct binding between the MAC and TRAF6 through the immunoblotting of an anti-C5b-9 antibody immunoprecipitate, with anti-TRAF6.

Enrichment analysis of microarray data showed Oncostatin M (OSM) signalling via MAPK was strikingly enriched following pNHS treatment at both 1 and 12 hours. Two matrix metalloproteinases; 3 and 13 (Mmp13 and stromelysin-1 AKA Mmp3), were responsive to sublytic C. OSM is a multifunctional cytokine and a member of the interleukin 6 super-

family, signalling via the GP130 IL-6 signal transducer (Rose et al, 1994; Zhang et al, 1994). According to the microarray data OSM did not alter in response to pNHS treatment compared to pNHS+OmCI and so an association with OSM signalling shown in enrichment is likely indicative of the involvement of MAPK pathway signalling.

4.3.4 **Network analysis of genes upregulated at both time points**

Network analysis using a custom list of genes upregulated at both time points revealed possible co-regulated genes expressed into the extra-cellular compartment; Mmp3, Mmp13, Cxcl1 and Areg. Co-regulation is via canonical pathways including p38, JNK and ERK MAPK cascades controlling via AP-1 and NFκB, largely backing up the assertions made through enrichment analysis. However, in addition, the network points to EGFR involvement as well as possibly PI3K and PKC signalling cascades.

Epidermal growth factor receptor (EGFR) is a member of the erbB receptor tyrosine kinase family. erbB members are activated by ligand binding at the cell surface which leads to the phosphorylation of the intracellular tyrosine kinase domain. Phosphorylation causes homo/heterodimerization and auto/transphosphorylation of erbB RTKs which via adaptor molecules activate downstream signalling cascades (Lemmon & Schlessinger, 1994; Olayioye et al, 2000). Signalling cascades triggered are various including ERK1/2, PI3K/Akt and STAT pathways (Ono & Kuwano, 2006). Activation of the EGFR system has been described in response to UV, osmotic and oxidative stress via autophosphorylation of the receptor leading to the expression of EGFR ligands (Carpenter, 1999). UV and osmotic stress induction of EGFR responses was primarily mediated by a JNK pathway activation which also activated IL-1 and TNF receptors (Rosette & Karin, 1996). Additionally Oxidative stress can induce auto-phosphorylation of the EGFR tyrosine kinase domain (Gamou & Shimizu, 1995).

ErbB2 may link to the GP130 receptor in a constitutive association acting to regulate its phosphorylation and signalling indicating a possible link to OSM signalling (Grant et al, 2002)

MAC deposition is reported to be capable of activating of Gαi protein independent of receptor (Niculescu et al, 1994). Rgs16 expression suggests that EGFR activation is probably triggered by receptor coupled Gαi activation since Rgs16 has been shown to co-immunoprecipitate (Derrien & Druey, 2001) and gene expression is thought to be induced as a feedback mechanism for G-protein signalling (Beadling et al, 1999). This provides an indication that EGFR transactivation by tyrosine phosphorylation through activation of Gαi is part of the response by CT26 cells to sublytic C (Daub et al, 1997) Indeed such an effect has been observed in which MAC deposition activated EGFR signalling without ligand binding (Cybulsky et al, 1999). MAC is capable of transactivating several other RTKs such as fibroblast growth factor receptor-2 (FGFR2), and hepatocyte growth factor receptor (HGFR) which signal via ERK-2 tyrosine phosphorylation (Cybulsky et al, 1999).

Expression of both Mmp3 and 13 mRNAs can be induced by the EGF system and further regulated at the post-transcriptional level in fibroblasts (Delany & Brinckerhoff, 1992). Transactivation of the EGFR has been described by the MMP3 cleavage of pro-HB-EGF into the active HB-EGF which then ligates and activates the receptor providing a possible feedback mechanism (Suzuki et al, 1997). A similar mechanism has been reported for MMP13 induced EGFR transactivation but the cleavage substrate which mediated this effect was not discovered (possibly epiregulin) (Mukhin et al, 2006). Cxcl1 can also be expressed in response to EGFR activation through PI3K, through it can also be responsive to prostaglandin E2 release additionally involving MAPK signalling (Moscova et al, 2006; Wang et al, 2006). G-protein coupled receptor activation leads to the production of second messengers DAG and IP3 (Raghuwanshi et al, 2012). Activation of CXCR2 by CXCL1 triggers MEK and ERK MAPK pathways leading to an increase in c-fos expression (Shyamala & Khoja, 1998). Receptor activation can also transactivate EGFR

via MMP mediated cleavage of HB-EGF (Bolitho et al, 2010). Since a similar phenomenon involving EGFR transactivation by C5b-9 has been demonstrated previously (Cybulsky et al, 1999), it is possible that this is a central activator of signal transduction in response to MAC deposition thus mediating many of the reported sublytic C effects.

In addition to the EGFR, other systems responsive to stress stimuli might be considered. Mmp13 and mmp3 can be upregulated in response to oxidative stress via ERK1/2 and p38 pathways in RPE cells (Alge-Priglinger et al, 2009) and in response to osmotic stress via JNK (Li et al, 2004). IL-1β and TNFα are also shown to be inducers of Mmp3, Mmp13 and Cxcl1 gene expression through NFκB (Li et al, 2003; Liacini et al, 2002; Ribaux et al, 2007; Spiekstra et al, 2007) . This provides a possible link between stress induced EGFR/IL-1βR/TNFαR activation and expression of Mmp3, Mmp13, Cxcl1 and Areg and may provide a possible mechanism.

Mmp3 and Mmp13 upregulation has previously been associated with terminal C activation on chondrocytes in human disease and an experimental model of osteoarthritis (Wang et al, 2011). Deposition of MAC on cultured human chondrocytes induced expression of both Mmp3 and Mmp13 mRNA over the course of 72 hours in a reactive lysis system. Higher expression was also seen when comparing chondrocytes taken from $C5^{+/+}$ with $C5^{-/-}$ mice subjected to the destabilization of the medial meniscus (DMM) osteoarthritis model. The response by the Mmps was found to be mediated by ERK signalling. In addition to Mmp3 and Mmp13 the work also described the MAC mediated upregulation of c-jun. Though CT26 are epithelial in origin the data on their response to MAC presented in this section show some interesting similarities to the data published by Wang et. al. (2011) on chondrocytes, suggesting common response mechanisms.

4.3.5 **Summary and conclusion**

This chapter aimed to understand the gene expression effects of sublytic C membrane attack on tumour cells. Microarray data were generated from a carefully designed sublytic

C attack experiment and primary analysis of microarray data showed a dominant serum effect but that upon more careful and stringent analysis, including ANOVA statistics and gene list generation, the sublytic C effect and MAC dependence could be seen. Enrichment analysis revealed regulation pathways hidden within the data pointing to some key processes including ERK1/2, JNK and p38 MAPK signalling, IL-1, TNF and OSM signalling pathways and transcription regulation through AP-1, ATF-1 and NFκB. Network analysis revealed a small group of co-regulated genes upregulated at both time points with functions at the cell surface and ECM. With the benefit of enrichment analysis and network tools it was possible to propose mechanistic hypotheses regarding these expression changes which correlate with current knowledge of sublytic C and MAC effects. This revealed a number of possible feedback mechanisms, transcriptional and post-transcriptional regulatory connections and signalling activations which give an unprecedented perspective of the mechanisms involved in sublytic C induced cell activation.

Genes implicated here, including Areg, Cxcl1, Mmp3 and Mmp13, are strongly associated with carcinogenesis, tumour development and metastasis and so are candidate genes as mediators of a pro-tumour role for sublytic C attack.

5 Validation of microarray and interrogation of sublytic effects

5.1 Introduction

5.1.1 Validation

The validation of a microarray experiment is a crucial part of integrating this large dataset with an overall experimental approach. Chapter 4 set out the bioinformatic analyses and mining of microarray data which defined an influence on tumour cell gene expression after exposure to sublytic C. Several hits were in agreement with previously reported effects mediated by MAC deposition on nucleated cells, constituting an *in silico* validation and giving a degree of confidence in the results (Chuaqui et al, 2002).

The process of experimental validation is fundamental in dealing with concerns about false negatives and false positives and is required to confirm both the results of the microarray and the universality of those results, i.e. do the data reflect a biologically significant response to the treatment (Chuaqui et al, 2002; Rockett & Hellmann, 2004). The data can be confirmed using a corroborating method to assess transcript quantity such as quantitative PCR (qPCR) which has become a common validating technique for microarray studies. Microarray and qPCR data were shown to significantly correlate under certain criteria regarding statistical significance and fold change of chosen target genes (Morey et al, 2006).

Gene expression changes, defined as transcript level alterations may or may not translate into changes in level of expressed protein products and so in order to gauge the biological relevance of microarray hits, a protein level validation must also be sought.

5.1.2 **Candidate gene products**

5.1.2.1 Amphiregulin (AR)

The product of the Areg gene is the amphiregulin protein (AR) which has a 38% homology with EGF and, in a similar manner to EGF can trigger the erbB2 transmembrane receptor (Johnson et al, 1993). AR is expressed as a membrane anchored precursor which is cleaved at the cell surface to a soluble form by MMPs (Dong et al, 1999). Soluble AR is then able to act upon cognate receptors in autocrine or paracrine loops (Johnson et al, 1992). A disintegrin and metalloprotease (ADAM) 17 is the primary enzyme responsible for ectodomain cleavage and release of the AR at the membrane surface (Sahin et al, 2004). Oxidative and osmotic stress has been shown to stimulate activation of ADAM17 leading to shedding of EGFR ligands such as HB-EGF and AR (Fischer et al, 2004).

5.1.2.2 C-X-C motif ligand 1 (CXCL1)

CXCL1 is a potent chemoattractant of neutrophils in the event of infection and signals via the CXCR2; a G-protein coupled receptor (Chintakuntlawar & Chodosh, 2009).

5.1.2.3 Matrix metalloproteinases (MMPs) 3 and 13

MMPs have functions in extracellular matrix regulation, playing major roles in development, wounding, proliferation, inflammation and several disease processes including carcinogenesis and metastasis (Nagase et al, 2006). As the *metallo* designation suggests the proteins require a zinc ion bound to a HEXXHXXGXXH consensus sequence for catalytic activity (Stocker et al, 1995). MMP3 is a stromelysin enzyme and has ability to degrade several substrates, including collagens III, IV, V, IX, X, and XI, laminins, elastin, entactin, fibronectin, fibrin, fibrillins, fibulin, link protein, osteonectin, tenascin, vitronectin, ECM proteoglycans and latent IL-1. MMP13 is a collagenase enzyme which cleaves type II collagen preferentially to types I and III. All MMP enzymes are expressed in pro-forms and require cleavage by proteases or chemical activation to become enzymatically active (Visse & Nagase, 2003). MMP3 is capable of cleaving the

pro-form of itself and of MMP13, which in-turn is able to cleave its own pro-form (Lochter et al, 1997).

5.1.3 **Chapter Aims**

This chapter aims to provide validation of microarray data using qPCR and western blotting procedures. The chapter will also investigate the contributions made by the signalling cascades shown to inter-connect the downstream effectors revealed by network analysis. Finally, the chapter will investigate the roles of the terminal pathway products C5a and MAC in mediating the effects witnessed.

5.2 Methods

5.2.1 **Set up of qPCR for validation**

5.2.1.1 Housekeeping controls

Choosing genes which are expressed stably is key in the calculation of relative expression from qPCR data. The chosen gene must also be robust; unaffected by the experimental treatment. There are a number of genes suggested by the literature to be suitable for this purpose but the choice is context driven. Common housekeeping control genes include β-actin, GAPDH and 18s ribosomal RNA. In experiments described in the first results chapter, qPCR analysis was conducted using β-actin primers which were used in published data from our lab. In the search for suitable housekeeping controls the microarray dataset presented a unique opportunity to cross-check candidates for a stable expression profile across the dataset. β-actin was checked using GeneSpring and shown to be stable across the entire experiment. Literature searches of common housekeeping candidates and subsequent checking of microarray data found that a gene known as polymerase (RNA) II (DNA directed) polypeptide A (Pol2ra) was suitable (Saviozzi et al, 2006). Expression data from microarray for both β-actin and Polr2a are shown in Figure 5.2.1.1A. Using two housekeeping control genes

A.

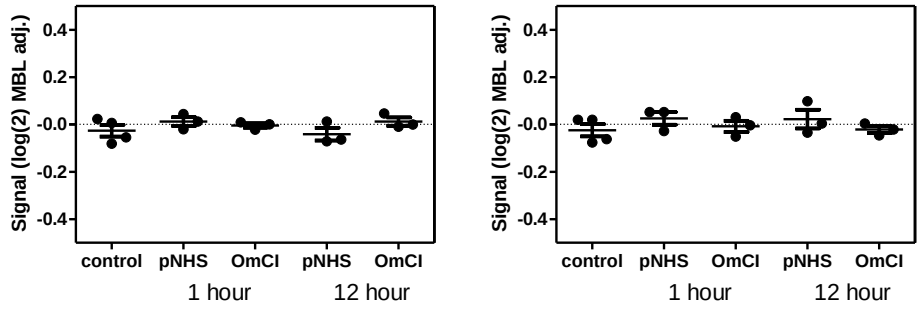

B.

Symbol	Accession Number	Description	Primer sequence	Length	Tm	Position	Fragment Length	Reference
Polr2A	NM_009089.2	polymerase (RNA) II (DNA directed) polypeptide A	CCCGCTGCGCACCATCAAGA	20	60.04	39-58	117	Primer-BLAST-Primer pair 1
			GGGCGACCTCCCTCCGTTGT	20	60.53	155-136		
Actb	NM_007393.3	Beta actin	ACGGCCAGGTCATCACTATTG	21	60.13	810-830	101	Donev et. al. (2008)
			AGTTTCATGGATGCCACAGGAT	20	60.02	910-889		

C.

Symbol	Accession Number	Description	Primer sequence	Length	Tm	Position	Fragment Length	Reference
Rgs16	NM_011267.3	regulator of G-protein signaling 16	GGTACTTGCTACTCGCTTTTCC	22	60.9	23-44	151	PrimerBank 29437173a1
			CAGCCGCGTCTTGAACTCT	19	62.3	173-155		
Fam110c	NM_027828.2	family with sequence similarity 110, member C	GGCCAAAGAAACCCCCAGCCAG	22	60.18	1297-1318	121	Primer-BLAST-Primer pair 1
			GGCTCTGGAGTTTCAGACGCCTA	23	58.16	1417-1395		
Irf1	NM_001159393.1	interferon regulatory factor 1	ATGCCAATCACTCGAATGCG	20	61.1	1-20	197	PrimerBank ID 6680467a1
			TTGTATCGGCCTGTGTGAATG	21	60.4	197-177		
Hbb-bh1	NM_008219.3	hemoglobin Z, beta-like embryonic chain	GAAACCCCCGGATTAGAGCC	20	62	170-189	93	PrimerBank ID 6680179a1
			GAGCAAAGGTCTCCTTGAGGT	21	61.4	262-242		

D.

Symbol	Accession Number	Description	Primer sequence	Length	Tm	Position	Fragment Length	Reference
Areg	NM_009704.3	amphiregulin	GGTCTTAGGCTCAGGCCATTA	21	61	48-68	137	Primer Bank 6753108a1
			CGCTTATGGTGGAAACCTCTC	21	60.4	184-164		
Cxcl1	NM_008176.3	chemokine (C-X-C motif) ligand 1	ACTGCACCCAAACCGAAGTC	20	60.04	39-58	114	Primer Bank 229577225b1
			TGGGGACACCTTTTAGCATCTT	22	60.53	155-136		
Mmp3	NM_010809.1	matrix metalloproteinase 3	ACATGGAGACTTTGTCCCTTTTG	23	60.7	507-529	192	Primer Bank 6754714a1
			TTGGCTGAGTGGTAGAGTCCC	21	62.9	698-678		
Mmp13	NM_008607.2	matrix metalloproteinase 13	TGTTTGCAGAGCACTACTTGAA	22	60.1	113-134	132	Primer Bank 291463259b1
			CAGTCACCTCTAAGCCAAAGAAA	23	60.2	244-222		

Figure 5.2.1.1 Validation primers for qPCR gene expression analysis of microarray hits. A. House keeping gene Polr2A and β-actin expression profiles from microarray data expressed as log2 transformed, median baseline adjusted signal. Summary of qPCR primers including gene information (NCBI accession number), primer sequence, primer length, melting temperature (Tm) position on transcript, fragment length and sequence design source (published, PrimerBLAST or PrimerBank). B. Housekeeping controls. C. Statistically significant hits. D. Network derived hits.

improves the validity of qPCR data produced as a relative expression value can be calculated from the mean Ct values given by β-actin and Polr2a.

All primers were designed as described in section 2.6.1 and the sequences along with summary information are shown in Figure 5.2.1.1, for housekeeping genes (B), statistically significant hits from microarray (C) and network derived hits from microarray (D).

5.2.1.2 Mapping primers to transcripts

To best visualize the primer pairs and their location on transcript sequences as well as their proximity to microarray probe sequence the sequences for each of the target genes were found within *Ensembl* MGI transcripts, where location of exons on the genomic material is displayed and exon sequence for each transcript variant described. Here the sequence along with the location of exon/exon boundaries (sites where intronic sequence has been removed during splicing) were used to create a colour coded sequence as shown in Figure 5.2.1.2, 3, 4 and 5.

Within the sequences displayed lower case is non-coding sequence and upper case is coding region. Exons were alternately coloured turquoise and green by text. Start codons were highlighted in green and stop coloured red. Primer pair sequence locations were highlighted as green and the probe sequence highlighted yellow.

5.2.1.3 Testing of qPCR primers

These primer pairs were tested by qPCR using cDNA reverse transcribed from RNA extracted from CT26 cells. The protocol described in section 2.6.2 was followed to test the primer pairs at a standard annealing temperature of 60°C. Melt curves taken from each primer pair reaction were scrutinized for signs of non-specific products and irregularities. Melt curves for each primer pair are shown in Figure 5.2.1.6 and 7. Each curve describes a peak at which the predominant dsDNA PCR product, which binds the fluorescent dye efficiently, is shown to dissociate and result in ssDNA which does not bind the dye. The

Figure 5.2.1.2 Mapping of qPCR primers and their products onto mRNA transcript sequence for Pol2ra and β-actin. Transcript sequence and exon/exon boundary information taken from Ensembl database was arranged and 5 and 3 prime non-coding shown in lower case and coding sequence in upper case. Sequence was also colour coded turquoise and blue so that exons were arranged alternately. Primer sequences were highlighted on the transcript in red and microarray probe in yellow. Start and stop codons were highlighted in green and red respectively.

Figure 5.2.1.3 Mapping of qPCR primers and their products onto mRNA transcript sequence for Irf1, Hbb-bh1, Rgs16, and Fam110c. Transcript sequence and exon/exon boundary information taken from Ensembl database was arranged and 5 and 3 prime non-coding shown in lower case and coding sequence in upper case. Sequence was also colour coded turquoise and blue so that exons were arranged alternately. Primer sequences were highlighted on the transcript in red and microarray probe in yellow. Start and stop codons were highlighted in green and red respectively.

Figure 5.2.1.4 Mapping of qPCR primers and their products onto mRNA transcript sequence for Mmp3 and Mmp13. Transcript sequence and exon/exon boundary information taken from Ensembl database was arranged and 5 and 3 prime non-coding shown in lower case and coding sequence in upper case. Sequence was also colour coded turquoise and blue so that exons were arranged alternately. Primer sequences were highlighted on the transcript in green and microarray probe in yellow. Start and stop codons were highlighted in green and red respectively.

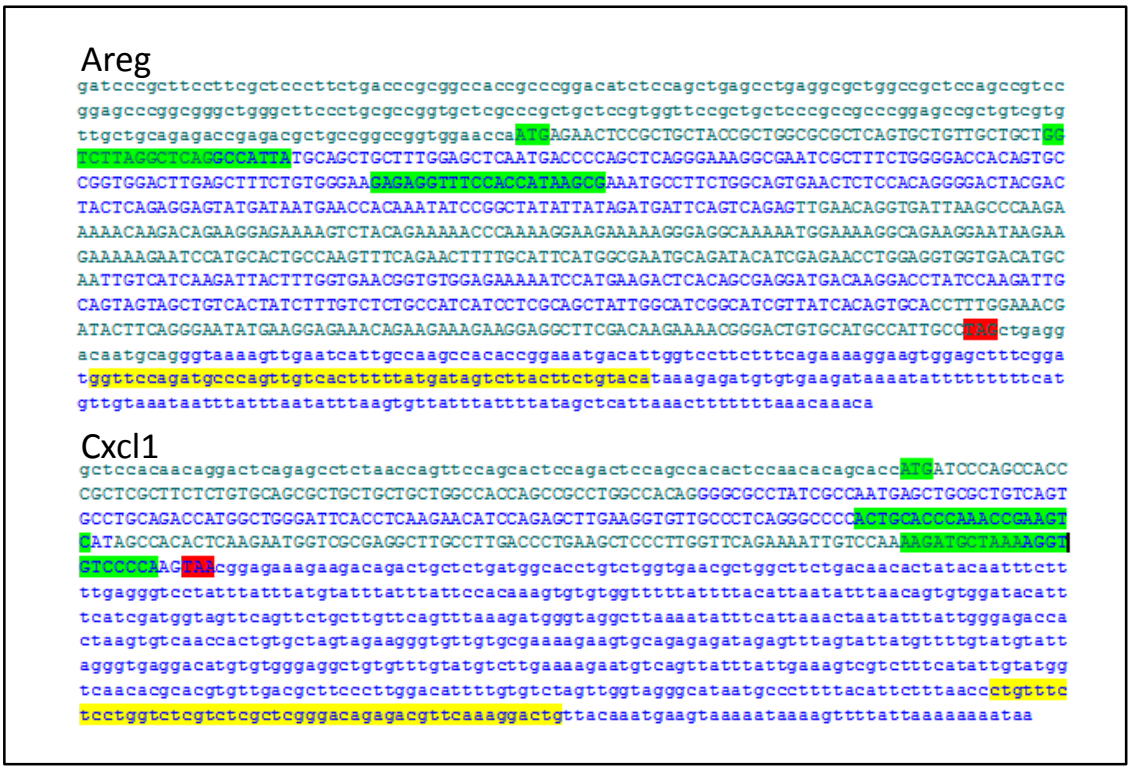

Figure 5.2.1.5 Mapping of qPCR primers and their products onto mRNA transcript sequence for Areg and Cxcl1. Transcript sequence and exon/exon boundary information was taken from Ensembl database was arranged and 5 and 3 prime non-coding shown in lower case and coding sequence in upper case. Sequence was also colour coded turquoise and blue so that exons were arranged alternately. Primer sequences were highlighted on the transcript in green and microarray probe in yellow. Start and stop codons were highlighted in green and red respectively.

temperature of this peak is directly related to the size of the fragment but is also influenced by other factors such as the % GC content of the sequence. The size of fragment and peak temperature largely correlates well for each of the shown melt curves, the greater the fragment size the higher the peak melt temperature. There are however a few exceptions.

Rgs16 PCR fragment of 151bp melted at 87°C which was higher than that for the 197bp fragment of Irf1 which melted at 84°C (Figure 5.2.1.6). The fragment generated by qPCR using the Rgs16 primers is rich in GC (62%) and thus has a much higher melting temperature compared to the Irf1 fragment which has a 50% GC. The same is true in the case of the fragments created by Areg and Mmp13 primers which were similar in size, 132 and 137bp respectively, but melted at 84.5°C and 81.5°C respectively (Figure 5.2.1.7). The higher Areg melting temperature was because of its higher GC content of 55% as compared to 47% for Mmp13. Melt curves demonstrated the specificity of each of the primer pairs for their intended targets and indicate that there were no issues with unintended products.

5.2.1.4 QPCR validation strategy

Primary qPCR corroboration of the expression changes was performed using RNA taken from samples prepared in parallel to that used in hybridisation experiment. Replicate 3 from each condition was therefore used as this was omitted from microarray analysis because of sample number restrictions. Control condition RNA was also replicate 3 regardless of its previous usage. This was further corroborated by performing a secondary validation involving an identical, independent sublytic C experiment to that used for microarray analysis. One microgram of sample RNA was reverse transcribed as described in section 2.5.4 then diluted 1/10 in upH_2O and subjected to qPCR analysis using primer pairs for Polr2a, β-actin and test gene specific primer pairs shown in section 2.1.2.

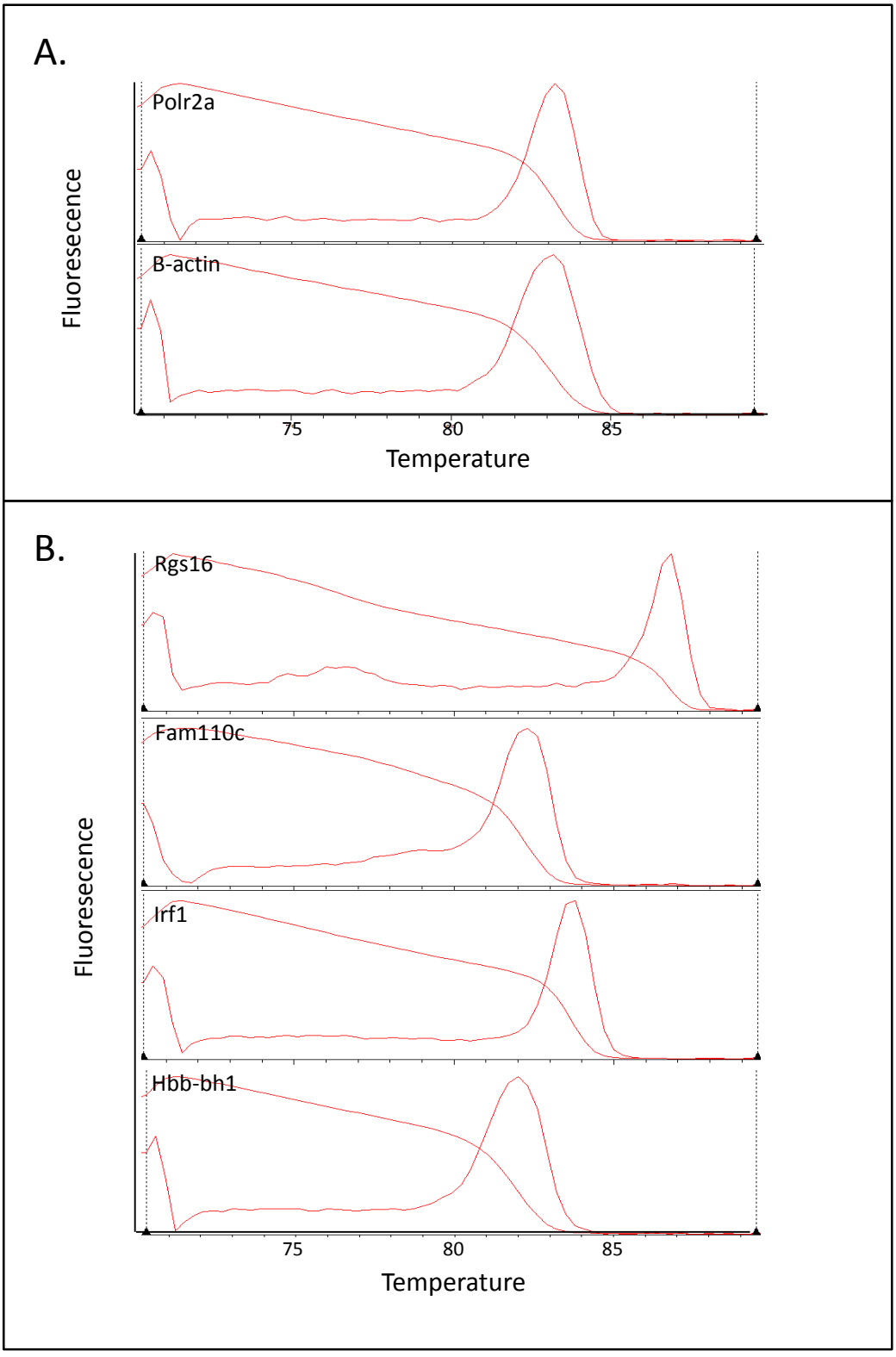

Figure 5.2.1.6 Melt curve analysis of qPCR products given by primers for housekeeping controls (Polr2A, β-actin) and top statistically significant changes from microarray analysis (Rgs16, Fam110c, Irf1, Hbb-bh1). RNA from CT26 cells under normal growth conditions was reverse transcribed and placed in qPCR reaction mixes and cycling program run as described in section 2.6.2. Melt curves taken post cycling program assessing SYBR Green fluorescence over temperature gradient from 70-90°C increasing by 0.3°C every second.

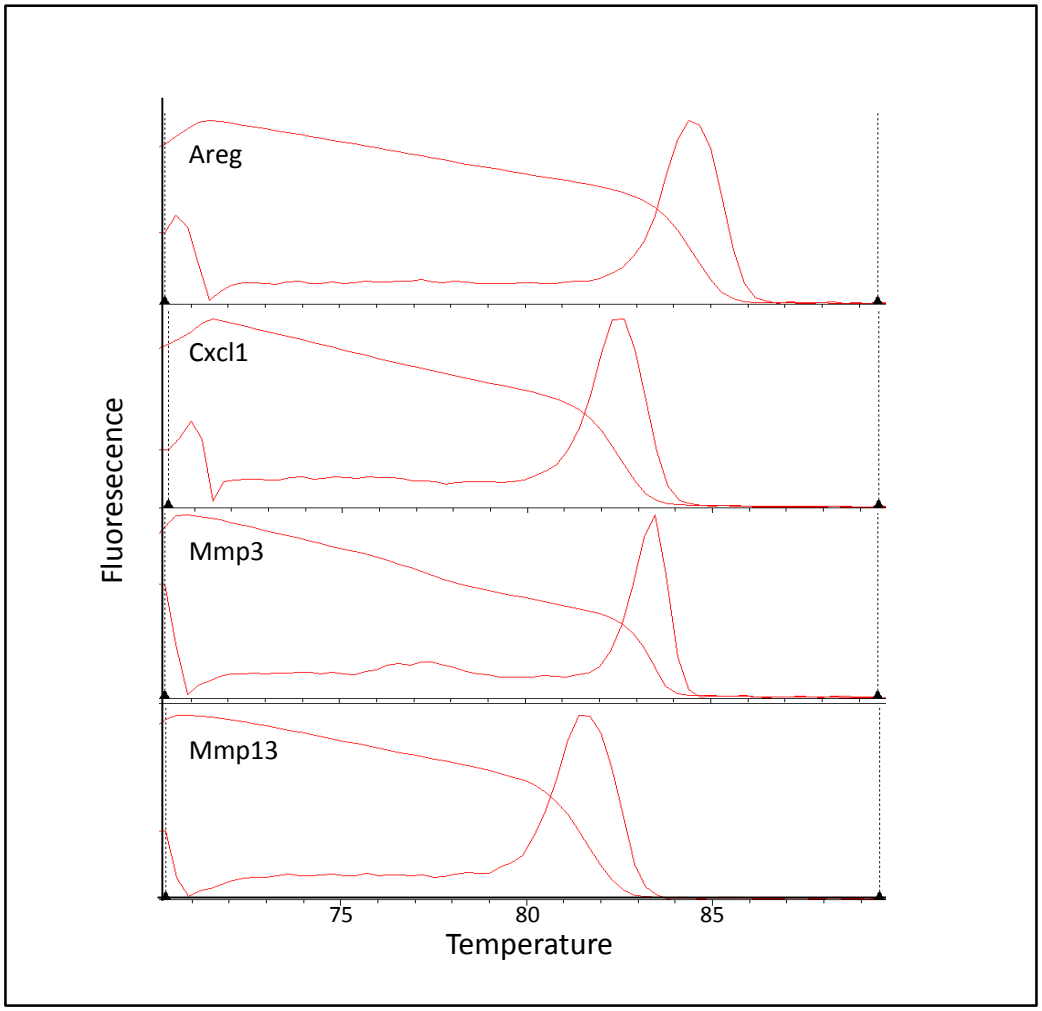

Figure 5.2.1.7 Melt curve analysis of qPCR products given by primers for network derived microarray hits (Areg, Cxcl1, Mmp3, Mmp13). RNA from CT26 cells under normal growth conditions was reverse transcribed and placed in qPCR reaction mixes and qPCR cycling program run as described in section 2.6.2. Melt curves taken post cycling program assessing SYBR Green fluorescence over temperature gradient from 70-90°C increasing by 0.3°C every 15 seconds.

5.2.2 **Protein Validation**

5.2.2.1 Conditioned medium (CM) preparation

CT26 cells were seeded at 5×10^5 per mL in normal growth medium and placed in three 75cm^2 tissue culture flasks (23 mL per flask) and incubated for 20 hours. Cell monolayers were exposed to pNHS, pNHS+OmCI or left untreated as a control. Cells were incubated for 1 hour at 37°C, then cell monolayers were washed in serum free medium only and 7.5 mL serum free medium added and incubated for 24 hours. Supernatant (CM) was centrifuged at 300×g to remove dead cells and debris then transferred to 50 mL falcon tubes ready for acetone precipitation of protein content.

5.2.2.2 Whole cell extract (WCE) preparation

Name	Contents
Whole Cell Extract (WCE) Buffer	0.5 M Tris, 0.1 mM EDTA, 125 mM $MgCl_2$, 100 mM KCl, 20% (v/v) Glycerol, 1% (v/v) Trition-X-100, pH8

Cell monolayers were washed in 10 mL ice cold PBS then cells detached using a cell scraper. The cell suspension was centrifuged at 300×g and the supernatant discarded. The cell pellet was resuspended in 1 mL WCE buffer (plus 100 mM PMSF, 1× Complete protease inhibitor cocktail from tablets (Roche, Welwyn Garden City, UK)) and the lysate incubated on ice for 5 minutes then centrifuged at 16,000×g, 4°C in a small refrigerated centrifuge. Supernatants were transferred to 15 mL falcon tubes ready for acetone precipitation of protein content.

5.2.2.3 Acetone protein precipitation

Conditioned media and whole cell extracts were mixed with 5× volume cold acetone and stored at -20°C for 1 hour. Precipitated protein was spun down by centrifugation at 4,400×g, 4°C for 20 minutes. Protein pellets were transferred carefully using a spatula to 2 mL screw cap eppendorf tubes then allowed to air dry. Screw caps were tightly closed to

prevent complete air drying of the protein pellet. Pellets were weighed by subtracting tube weights from that containing the pellet. Protein was resuspended in protein sample buffer volume relative to the least massive pellet (~100 µL- adjusting to mass in relation to smallest pellet).

5.2.3 **Pharmacological inhibitor preparation**

5.2.3.1 Inhibitors

LY294002, SP600125, PD0325901, inhibitors of PI3K, MEK and JNK pathways respectively, were purchased from Cambridge Biosciences (Cambridge, UK). SB202190, inhibitor of p38, was purchased from Stratech Scientific (Suffolk, UK). Inhibitors were received as crystalline powders and dissolved in dimethyl sulphoxide (DMSO) to create stock solutions of 1000× working concentration: LY294002 10mM, SB202190 1mM, SP600125 5 mM and PD0325901 0.5 mM. Aliquots of 10-20 µL of each drug were prepared and stored at -80°C. Drug stocks were thawed on ice prior to experiment and stored at 4°C for no more than a month.

5.2.3.2 Sublytic C with inhibitors

The sublytic C experimental procedure was modified as follows: seeded cells were washed in serum free medium and incubated for 1 hour with 1/1000 inhibitor solutions in normal growth media along with a carrier only control (DMSO) so that final concentrations were as shown in Table 5.2.3.1. Inhibitors and DMSO were also added to 5% pNHS and pNHS+OmCI solutions at the same final concentrations. Sublytic C experiment was proceeded as before.

Table 5.2.3.1 Pharmacological inhibitors used to investigate putative signalling cascades implicated by network generation.

Inhibitor	Inhibits	Dose	Reference
LY294002	PI3K	10 µM	(Zhang et al, 2011)
SB 202190	p38a/b MAPK	1 µM	(Manthey et al, 1998;
SP 600125	JNK1-3	5 µM	(Bennett et al, 2001)
PD 0325901	MEK/ERK	0.5 µM	(Lin et al, 2009)

5.2.4 **C5a, PMX53, C6D + C6**

C5a active protein was purchased from Abcam (Cambridge UK) as a lyophilized powder and was reconstituted to a concentration of 1 µg/mL in ice cold water containing 2.5 mg/mL BSA. 10 µL aliquots were stored at -80°C and thawed on ice prior to experiments. PMX53 (a kind gift from Queensland University, Australia) was prepared as a 100 µM in stock solution in upH_2O and 10 µL aliquots stored at -80°C and thawed on ice prior to experiments. C6D serum prepared as described in section 3.3.3.5 was used as serum in sublytic C experiments. C6D was diluted in serum free medium to 5% and C6 added back at 50 µg/mL of serum. Experiments were carried out in the same way as sublytic C experiments described in section 2.4.

5.3 Results

5.3.1 **QPCR validation of microarray**

Two sets of genes highlighted during bioinformatic analysis described in chapter 4, were brought forward for validation by qPCR. The first set were chosen as the 4 genes with the most statistically significant expression changes representing upregulation and down regulation at both 1 hour and 12 hour time points. These were Rgs16 and Fam110c which were upregulated at 1 hour, Irf1 which was downregulated at 1 hour and Hbb-bh1 which was upregulated at 12 hours. There were no genes significantly downregulated at 12 hours. The purpose of validating such gene expression changes is to demonstrate the capability of microarray in distinguishing gene expression changes and to ensure that no technical issues occurred at any stage of the sublytic C experiment used for microarray analysis, such as sample switching.

The second set of target genes were those highlighted by network analysis and therefore of particular interest in investigating the response to sublytic C, these were Areg, Cxcl1, Mmp3 and Mmp13. Validation of the expression profile of these genes was carried out to

confirm their involvement in the sublytic C response and provide grounds to further investigate these changes.

5.3.1.1 Top statistical changes

Upregulation of Fam110c and Rgs16 at 1 hour in response to pNHS in comparison to pNHS+OmCI was confirmed by qPCR in primary validation experiments with similar statistical significance. Expression profiles in secondary validation were largely reflective of microarray results for Fam110c but not for Rgs16. Although there was upregulation of Rgs16 after 1 hour it was also increased at 12 hours and by a greater degree suggesting a sustained and additive upregulation (Figure 5.3.1.1 and Figure 5.3.1.2).

Downregulation of Irf1 at 1 hour in response to pNHS compared to pNHS+OmCI was confirmed in both primary and secondary validation experiments; although in secondary validation the downregulation was not significant, it followed a similar trend to that outlined by microarray (Figure 5.3.1.3).

Upregulation of Hbb-bh1 at 12 hours in response to pNHS compared to pNHS+OmCI was confirmed very successfully in both primary and secondary qPCR validations. A significant comparative increase at 1 hour was observed in secondary validation which was not found in primary validation but actually reflected a similar expression pattern to that found in microarray data (Figure 5.3.1.4).

Primary validation reflected directly the expression profiles given in the microarray data, confirming them as true positives, and supporting the suitability of the statistical treatment. Despite the variability inevitable in a full biological repeat of the sublytic C experiment, the results of secondary validation were largely corroborative of microarray results.

5.3.1.2 Network generated genes

With the microarray experiment successfully validated by qPCR using a selection of key gene expression changes it was then possible to examine those genes highlighted as

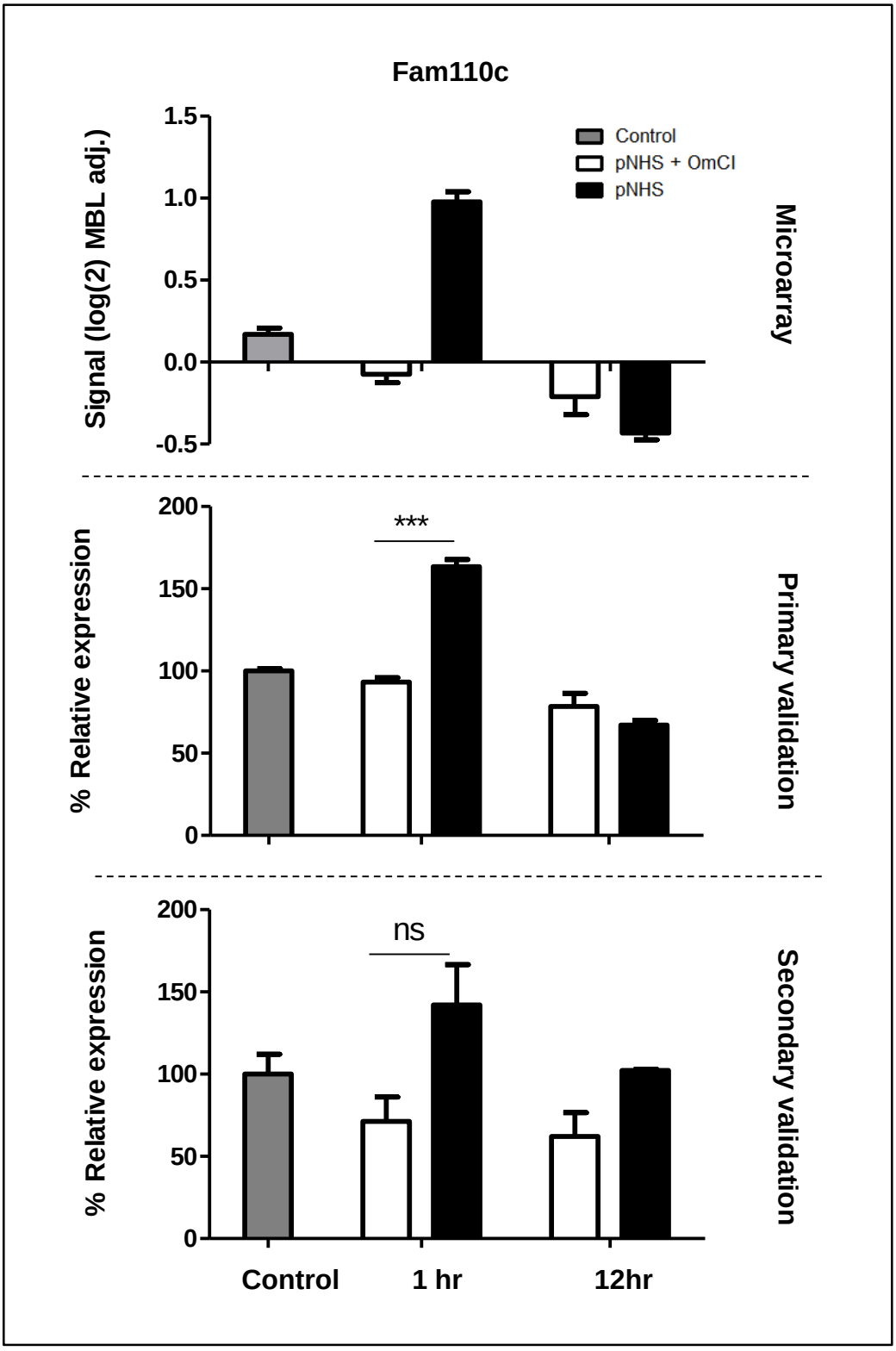

Figure 5.3.1.1 qPCR validation of Fam110c expression by CT26 cells in response to sublytic C. *Microarray*=original microarray data, *Primary Validation*=RNA extracted in parallel with that used in microarray, *Secondary validation*=RNA extracted in a fresh sublytic attack experiment. RNA was reverse transcribed and Fam110c gene expression analysed by qPCR and calculated as relative to β-actin and Pol2ra using the ΔΔCt calculation outlined in section 2.6.2 then presented as a % of untreated control . Results are mean n=3 +/- SEM (*p<0.001).**

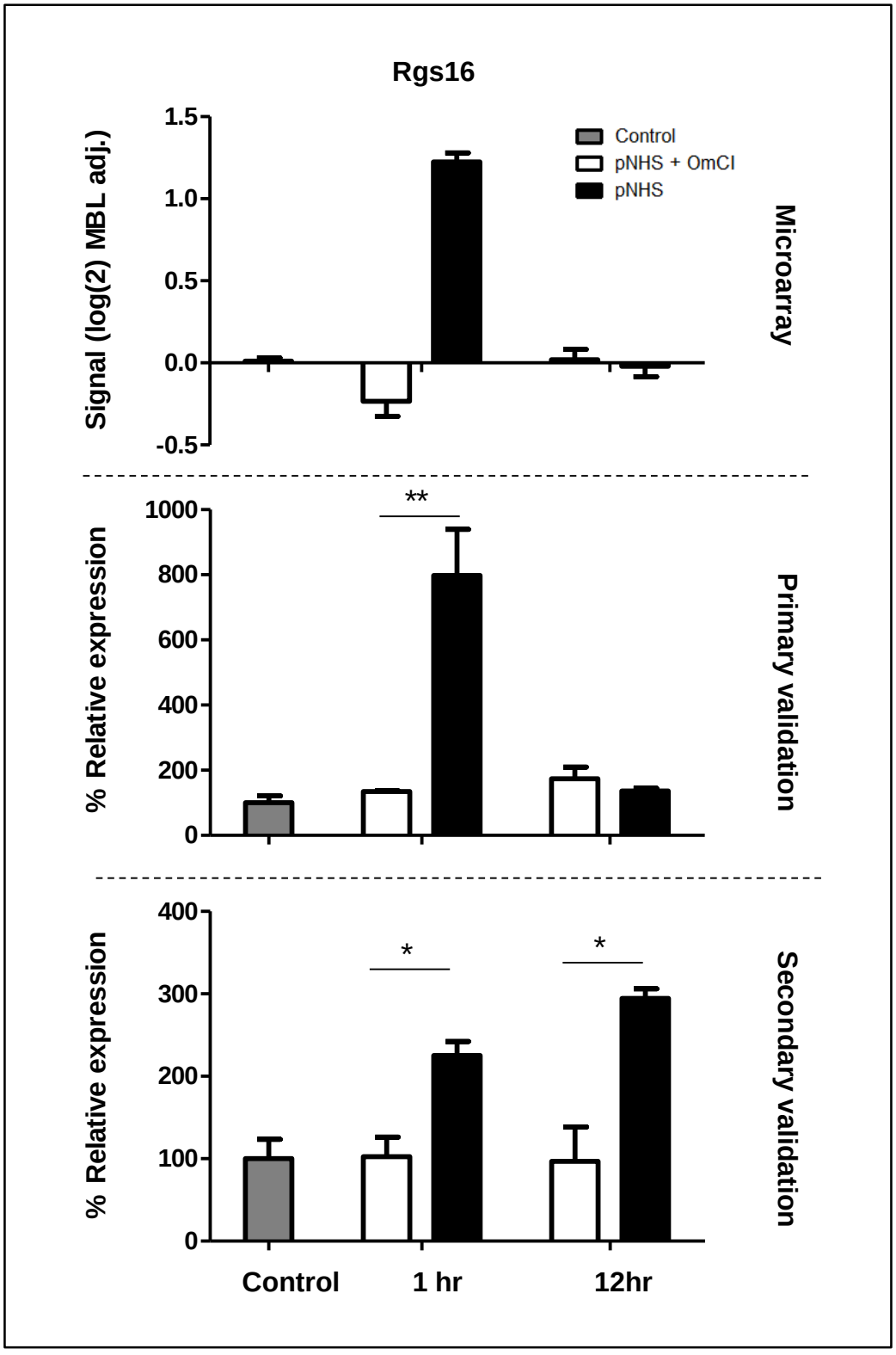

Figure 5.3.1.2 qPCR validation of Rgs16 expression by CT26 cells in response to sublytic C. *Microarray*=original microarray data, *Primary Validation*=RNA extracted in parallel with that used in microarray, *Secondary validation*=RNA extracted in a fresh sublytic attack experiment. RNA was reverse transcribed and Rgs16 gene expression analysed by qPCR and calculated as relative to β-actin and Pol2ra using the ΔΔCt calculation outlined in section 2.6.2 then presented as a % of untreated control. Results are mean n=3 +/- SEM (*p<0.05, **p<0.01).

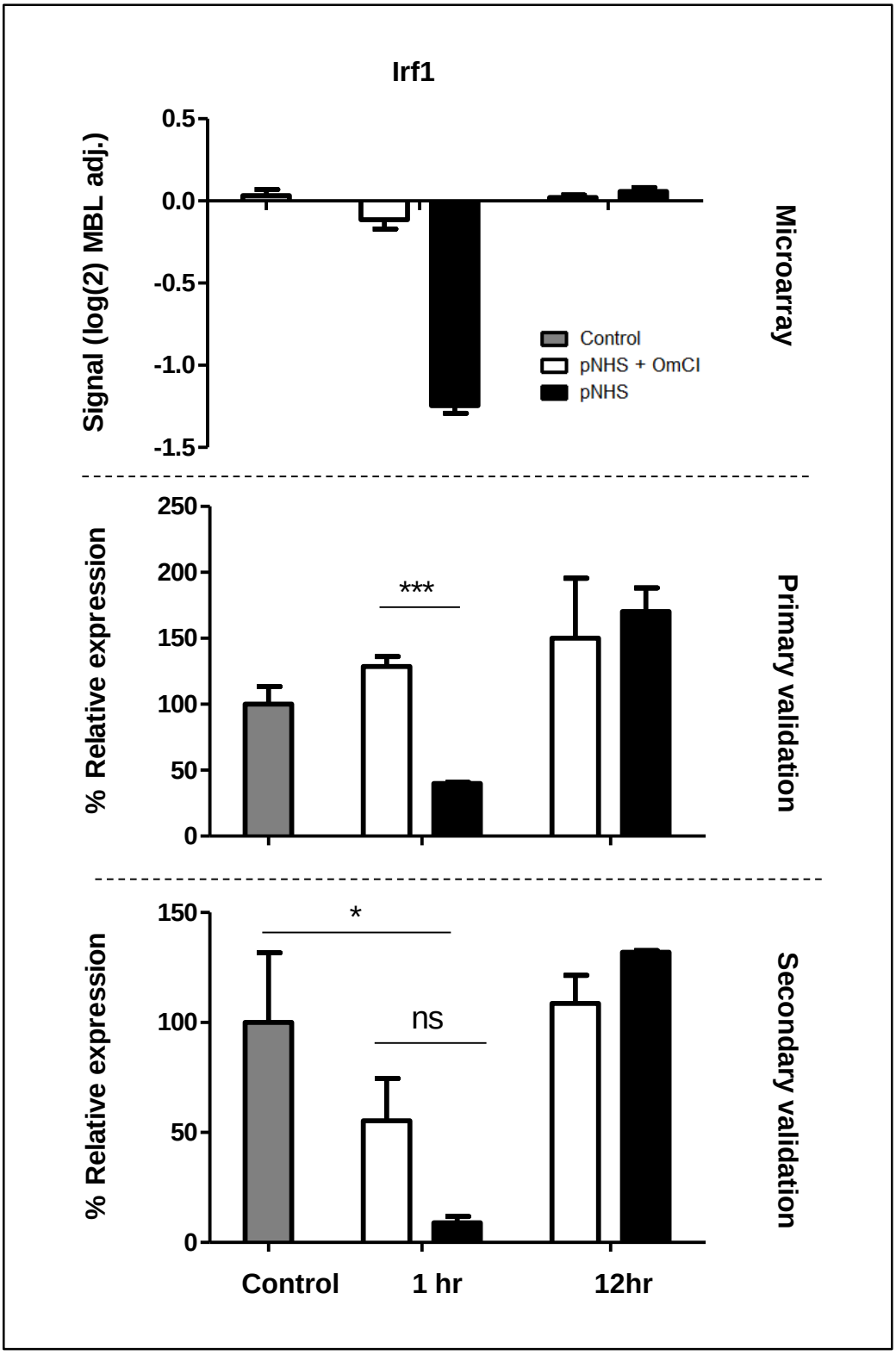

Figure 5.3.1.3 QPCR validation of Irf1 expression by CT26 cells in response to sublytic complement. *Microarray*=original microarray data, *Primary Validation*=RNA extracted in parallel with that used in microarray, *Secondary validation*=RNA extracted in a fresh sublytic attack experiment. RNA was reverse transcribed and Irf1 gene expression analysed by qPCR and calculated as relative to β-actin and Pol2ra using the ΔΔCt calculation outlined in section 2.6.2 then presented as a % of untreated control . Results are mean n=3 +/- SEM (ns=not significant, *p<0.05, ***p<0.001).

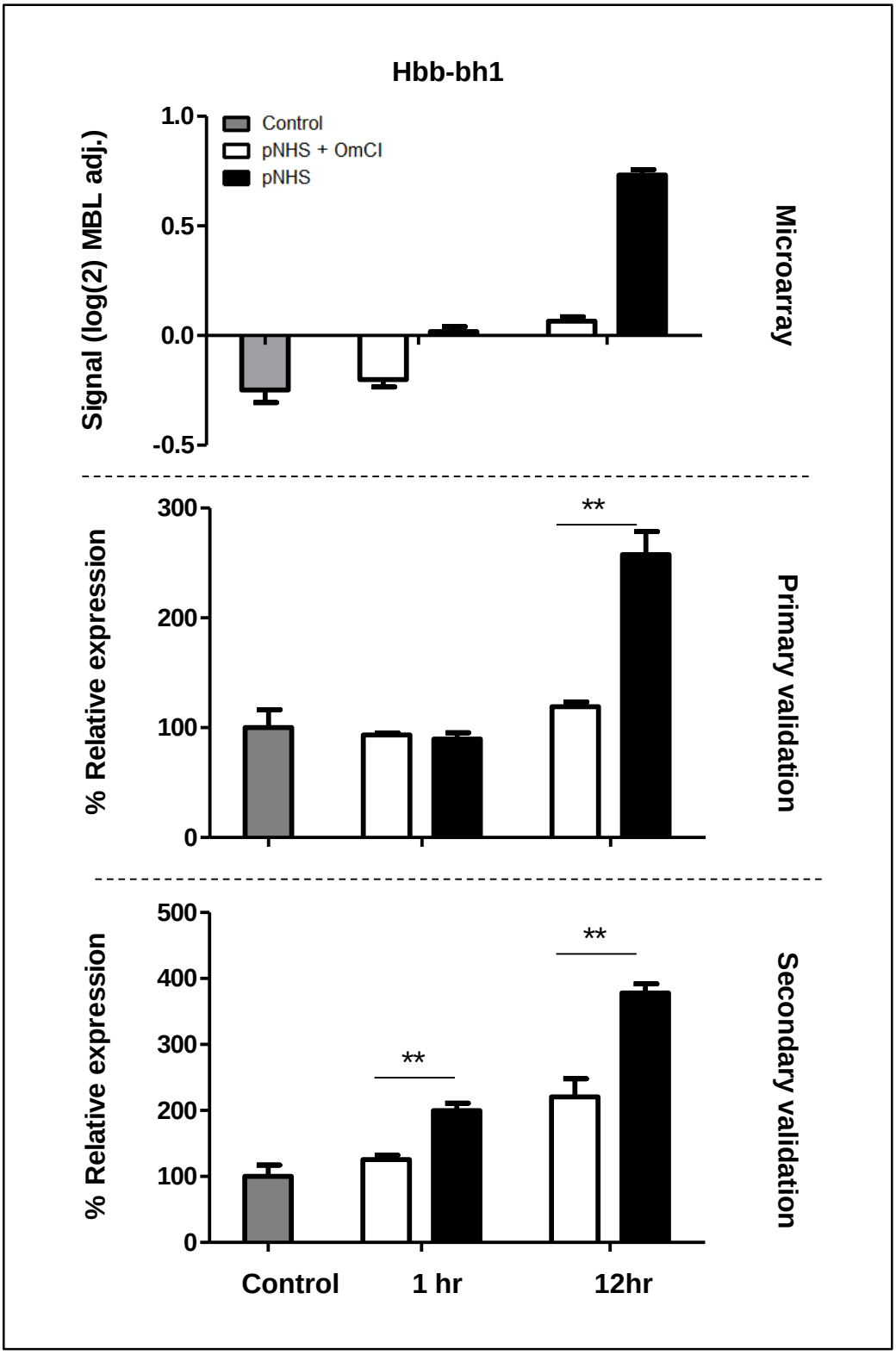

Figure 5.3.1.4 QPCR validation of Hbb-bh1 expression by CT26 cells in response to sublytic C. *Microarray*=original microarray data, *Primary Validation*=RNA extracted in parallel with that used in microarray, *Secondary validation*=RNA extracted in a fresh sublytic attack experiment. RNA was reverse transcribed and Hbb-bh1 gene expression analysed by qPCR and calculated as relative to β-actin and Pol2ra using the ΔΔCt calculation outlined in section 2.6.2 then presented as a % of untreated control. Results are mean n=3 +/- SEM (p<0.01).**

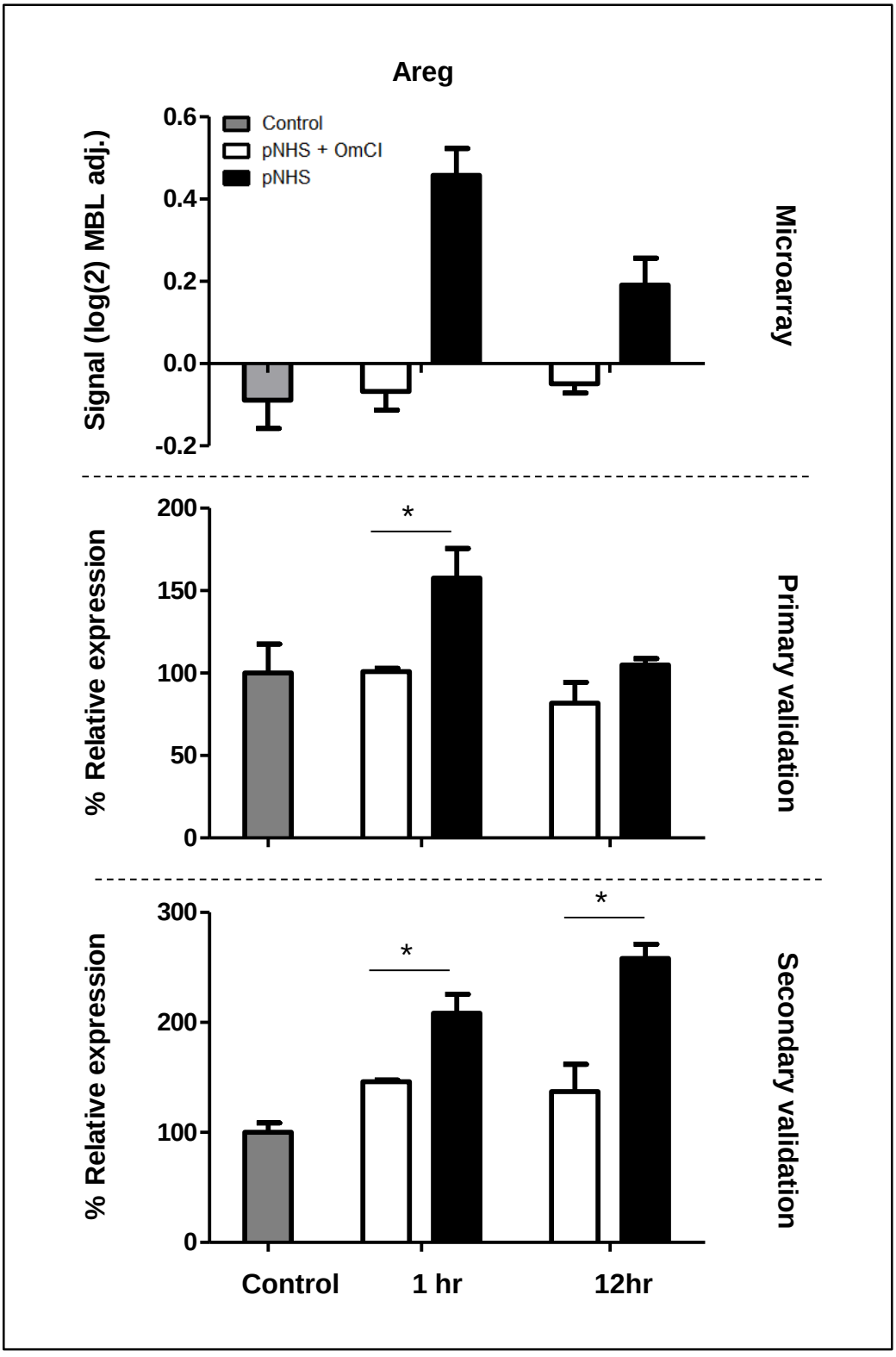

Figure 5.3.1.5 QPCR validation of Areg expression by CT26 cells in response to sublytic C. *Microarray*=original microarray data, *Primary Validation*=RNA extracted in parallel with that used in microarray, *Secondary validation*=RNA extracted in a fresh sublytic attack experiment. RNA was reverse transcribed and Areg gene expression analysed by qPCR and calculated as relative to β-actin and Pol2ra using the ΔΔCt calculation outlined in section 2.6.2 then presented as a % of untreated control . Results are mean n=3 +/- SEM (*p<0.05)

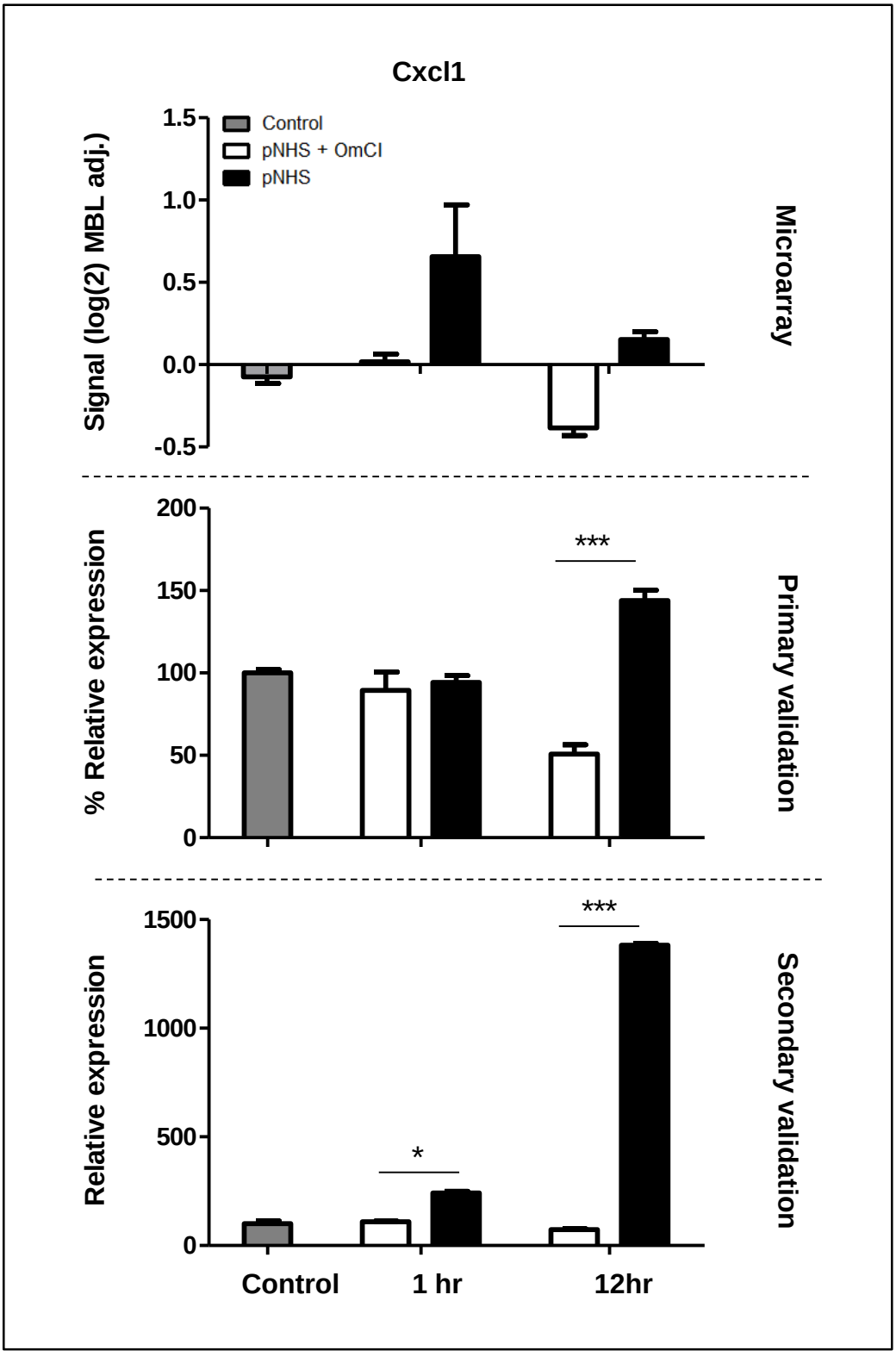

Figure 5.3.1.6 QPCR validation of Cxcl1 expression by CT26 cells in response to sublytic C. *Microarray*=original microarray data, *Primary Validation*=RNA extracted in parallel with that used in microarray, *Secondary validation*=RNA extracted in a fresh sublytic attack experiment. RNA was reverse transcribed and Cxcl1 gene expression analysed by qPCR and calculated as relative to β-actin and Pol2ra using the ΔΔCt calculation outlined in section 2.6.2 then presented as a % of untreated control. Results are mean n=3 +/- SEM (*p<0.05, ***p<0.001).

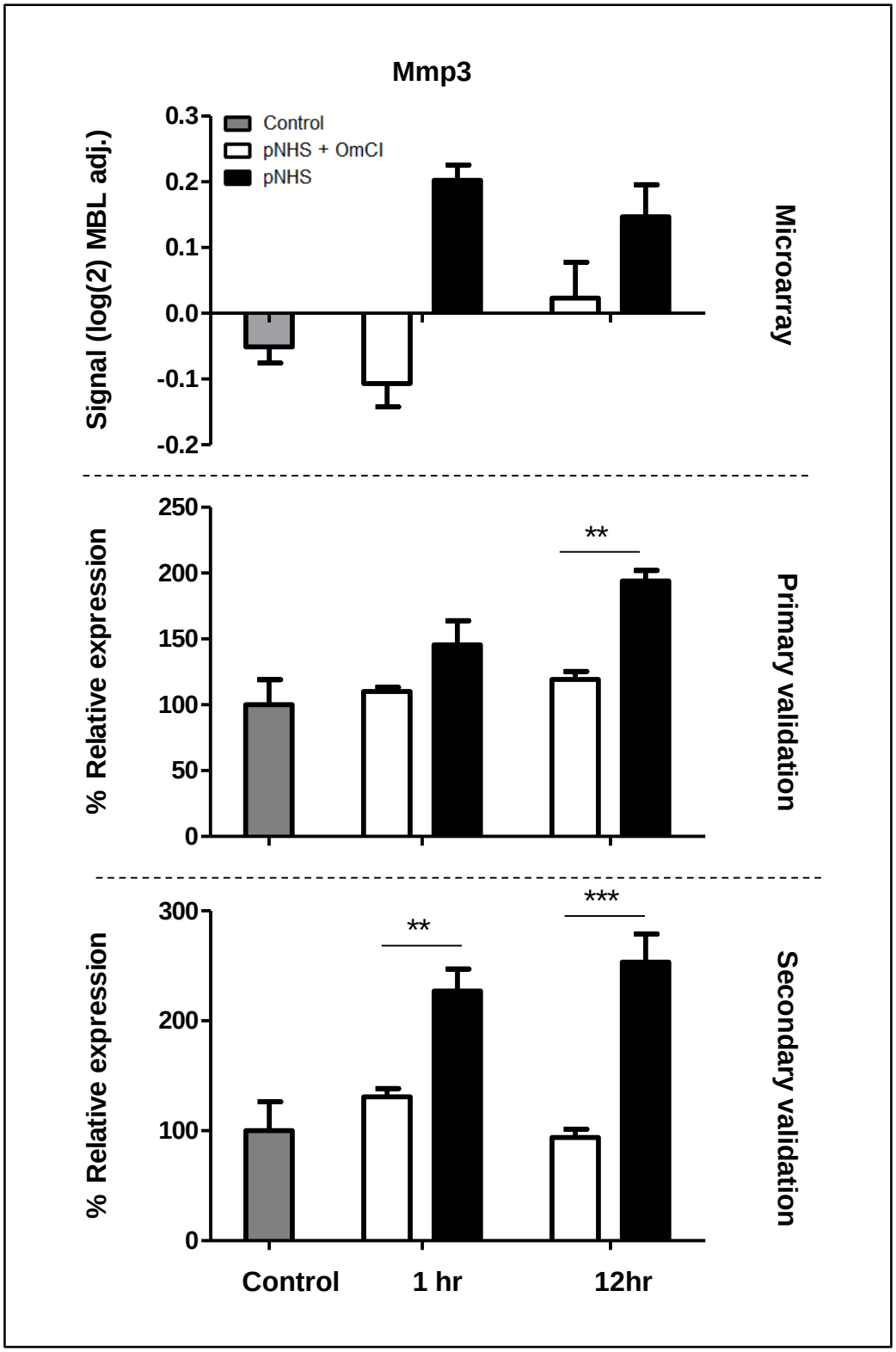

Figure 5.3.1.7 QPCR validation of Mmp3 expression by CT26 cells in response to sublytic C. *Microarray*=original microarray data, *Primary Validation*=RNA extracted in parallel with that used in microarray, *Secondary validation*=RNA extracted in a fresh sublytic attack experiment. RNA was reverse transcribed and Cxcl1 gene expression analysed by qPCR and calculated as relative to β-actin and Pol2ra using the ΔΔCt calculation outlined in section 2.6.2 then presented as a % of untreated control. Results are mean n=3 +/- SEM (p<0.01, ***p<0.001).**

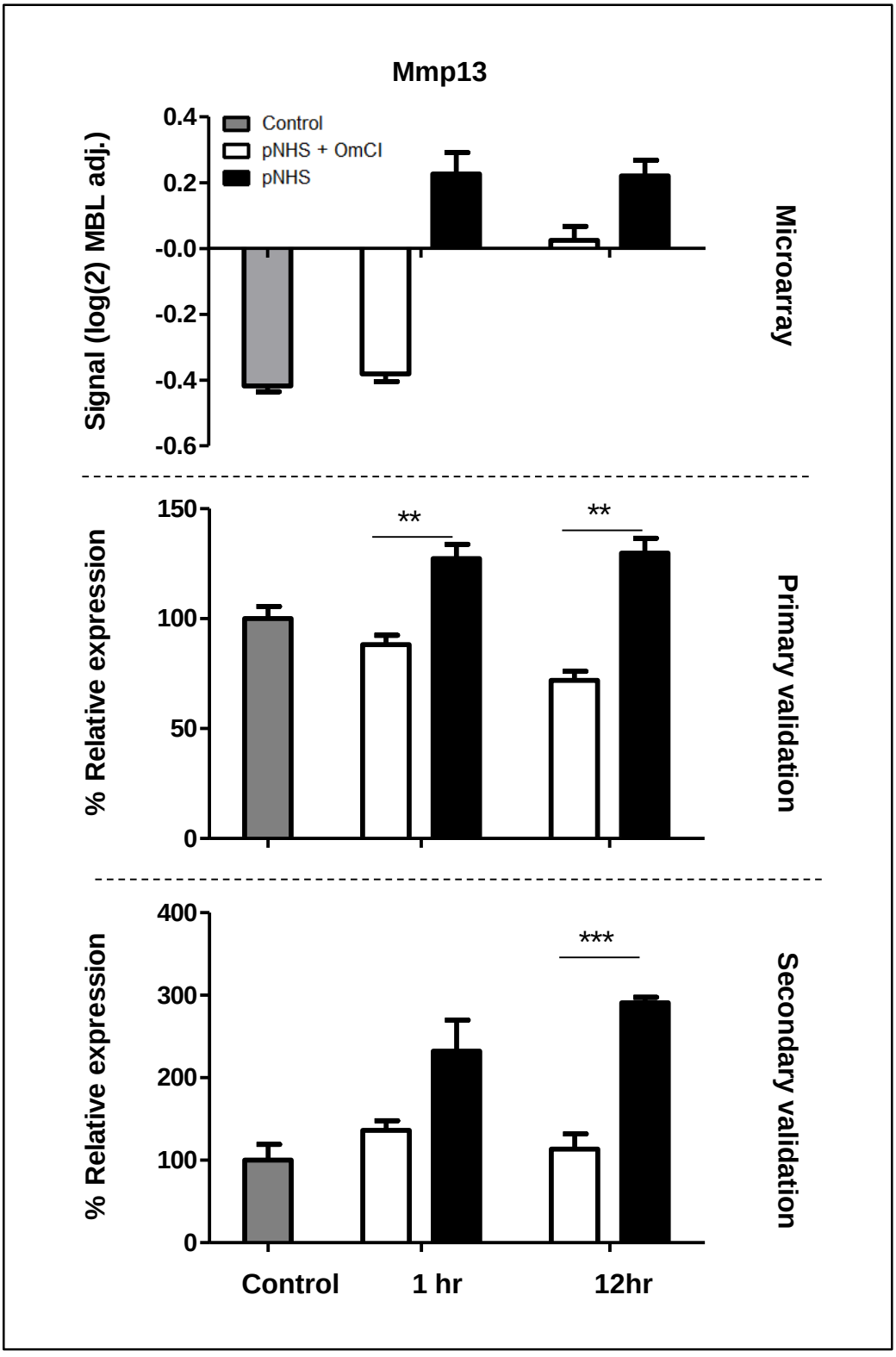

Figure 5.3.1.8 QPCR validation of Mmp13 expression by CT26 cells in response to sublytic C. *Microarray*=original microarray data, *Primary Validation*=RNA extracted in parallel with that used in microarray, *Secondary validation*=RNA extracted in a fresh sublytic attack experiment. RNA was reverse transcribed and Mmp13 gene expression analysed by qPCR and calculated as relative to β-actin and Pol2ra using the ΔΔCt calculation outlined in section 2.6.2 then presented as a % of untreated control. Results are mean n=3 +/- SEM (p<0.01, ***p<0.001).**

interesting by network analysis. Network analysis (section 4.2.5.2) revealed that within a list of genes upregulated at 1 and 12 hours there were four co-regulated downstream genes which represent a possible gene expression response to sublytic C; Areg, Cxcl1, Mmp3 and Mmp13.

Previously in this thesis I have described the significant interrelation of these genes through controlling receptor interactions, signalling cascades, transcription factors and biochemical interactions of the immature/mature protein products. These genes were validated by qPCR.

Areg

Areg expression data from the microarray was confirmed using primary and secondary validation qPCR (Figure 5.3.1.5). Microarray data showed an upregulation of Areg in response to pNHS compared to pNHS+OmCI at both 1 and 12 hour time points, with the largest increase happening at 1 hour. Primary validation qPCR confirmed this upregulation and showed a significant increase of 50% at 1 hour and a small, but not significant, increase at 12 hours. Areg upregulation was shown to be repeatable by secondary validation showing upregulation by 50% at 1 hour and 100% at 12 hour. OmCI controls had similar expression levels to untreated controls in all experiments.

Cxcl1

Cxcl1 expression data from the microarray was confirmed using primary and secondary validation qPCR (Figure 5.3.1.6). Expression of Cxcl1 was upregulated in the microarray experiment at both 1 hour and 12 hours in response to pNHS compared to pNHS+OmCI. Upregulation was greatest at 1 hour, as with the Areg microarray data.

Primary validation of Cxcl1 expression did not reflect this pattern. QPCR data showed no upregulation at 1 hour but a significant upregulation of 50% at 12 hours (Figure 5.3.1.6). Interestingly, although no change was detected at 1 hour between pNHS and

pNHS+OmCI, there was a decrease in expression of Cxcl1 in pNHS+OmCI at 12 hours compared to the untreated controls. This reflected a similar pattern in the microarray data. Secondary validation showed that expression at 1 hour increased in response to pNHS by comparison with pNHS+OmCI in a similar manner to the microarray data; however, at 12 hours upregulation was far higher than that shown by microarray and primary validation with increases in the order of 1500% of pNHS+OmCI. Both microarray and primary validation qPCR data showed a decrease in Cxcl1 expression in pNHS+OmCI at 12 hours compared to the untreated control but primary validation qPCR showed expression levels were more similar across the time points.

Mmp3

Mmp3 expression data from the microarray was confirmed using primary and secondary validation qPCR Figure 5.3.1.7. According to the microarray data Mmp3 expression was upregulated in response to pNHS at both 1 and 12 hours compared to pNHS+OmCI. Primary qPCR validation supported the microarray data in that it showed an upregulation in response to pNHS at both time points, however, upregulation was greatest at 12 hours being some 75% above pNHS+OmCI compared to an increase of 30% at 1 hour. Secondary validation confirmed this effect in a fresh experiment in which Mmp3 was upregulated by 100% in response to pNHS at both time points. Expression levels in pNHS+OmCI compared to untreated controls remained relatively similar and constant in all experiments.

Mmp13

The expression profile of Mmp13 from the microarray data shows some similarity to that of Mmp3, with significant increases over controls at both 1 and 12 hours (Figure 5.3.1.7 and Figure 5.3.1.8). Primary qPCR validation confirmed the findings of the microarray showing Mmp13 upregulation in response to pNHS by 50% at 1 hour and 75% at 12 hours compared to pNHS+OmCI (Figure 5.3.1.8). Secondary validation qPCR data confirmed

the pNHS induced Mmp13 upregulation at both time points showing an increase of 100% at 1 hour and 150% at 12 hours compared to pNHS+OmCI (Figure 5.3.1.8). Expression levels in pNHS+OmCI compared to untreated controls were generally similar except for microarray data which showed a decrease in Mmp13 expression at 12 hours.

5.3.2 **Protein validation**

Having confirmed by qPCR that the target genes Areg, Cxcl1, Mmp3 and Mmp13 were indeed responsive to sublytic C as the microarray had suggested, it was necessary to further confirm that these changes in transcript mRNA production correlated with increased protein levels. To achieve this western blotting was employed to detect the proteins in conditioned media (CM) and whole cell extracts (WCE).

Briefly, cells were seeded in 3× 75mm^2 TC flasks and 20 hours following initial seeding 2 flasks were removed, the cells washed then exposed to either 5% pNHS or 5% pNHS+OmCI as previously described (section 2.4) then incubated at 37°C for 1 hour. Cells were then washed, serum free media added to all three flasks and incubated for 24 hours to allow for the accumulation of expressed proteins. CM and WCEs were prepared as described in sections 5.2.2.1 and 5.2.2.2 and protein content precipitated with acetone as described in section 5.2.2.3. Protein pellets were weighed and reconstituted in loading buffer so that the volume corresponded to mass thus ensuring equal concentration and therefore equal loading. In each case roughly 8 mg of total protein was loaded per well. Samples were electrophoresed through 7.5 or 10% polyacrylamide gels (section 2.7) and proteins transferred to nitrocellulose membranes as described in section 2.8.1. Membranes were probed using anti- AR, CXCL1, MMP3 or MMP13 antibodies (section 2.8.2), detected by HRP conjugated secondary Ab and presence of positive staining revealed by chemiluminescence as described in section 2.8.3.

5.3.2.1 AR

Human AR is expressed as a transmembrane tethered 252 (248 murine protein) amino acid precursor glycoprotein. The soluble, active form is released by proteolytic cleavage (Plowman et al, 1990). Analysis of the multiple soluble forms of AR has demonstrated that the possible fragments depend on the location and sequence of cleavage (Brown et al, 1998; MartinezLacaci et al, 1996). From a 50 kDa pro-form, cleavage at a site proximal to the transmembrane domain results in 43 and 36 kDa high molecular weight fragments together with 21, 19 and 9 kDa lower molecular weight soluble forms. In addition 28, 26 and 16 kDa transmembrane forms can also result from cleavage (Brown et al, 1998). Murine AR shares a close amino acid homology with human AR and thus it is likely that similar active fragments are released upon cleavage.

Figure 5.3.2.1A shows a western blot of CM and WCE from pNHS and pNHS+OmCI treated cells probed for AR. In the lane containing the CM sample there are two clear bands located near the 36 and 50 kDa markers corresponding to the reported higher MW soluble forms of AR. These bands appeared weakly in CM sample from control and pNHS+OmCI treated cells but were much stronger in samples from cells that had undergone sublytic complement attack (pNHS). In addition to these bands there were also bands at approximately 100 kDa which could be non-specific primary or secondary Ab binding of aggregates, something which would have benefited from the inclusion of a secondary control. WCE from all conditions showed no discernible bands. From the available data it cannot be determined whether both the detected forms at 50 and 36 kDa are “active” fragments. The increased levels of soluble AR in CM induced by pNHS treatment agrees with qPCR data and suggests that increased transcription in response to sublytic complement results in increased protein secretion. The lack of signal in WCE suggests that the synthesised protein did not accumulate in the cytoplasm and implies it was secreted quickly upon expression.

5.3.2.2 CXCL1

The C-X-C motif ligand 1 (CXCL1) is a small cytokine of 107 amino acids. Within the amino acid sequence there are 4 cysteine residues of which two are separated by a single glutamine residue forming the C-X-C motif. Disulphide links between the cysteine residues of the motif with those dispersed in the sequence create a stable secondary structure encompassing antiparallel β-sheet with three β strands ending in C-terminal antiparallel α-helices, this structure couples to form homo-dimers. CXCL1 has a predicted mass of 11.5 kDa and typically migrates to 12 kDa on SDS-PAGE (Allen et al, 2007; Jin et al, 2005).

Figure 5.3.2.1B shows a western blot of CM and WCE from pNHS and pNHS+OmCI treated cells probed for CXCL1. This shows a band in CM lanes appearing at around the 36 kDa marker which is more prominent in pNHS compared to the OmCI control. A band at this molecular weight does not correspond to a reported CXCL1 fragment, thus no clear conclusion can be drawn from this data regarding the effect, if any, of sublytic complement attack on CXCL1 protein production. Of note, several commercially available antibodies raised against CXCL1 protein react with a protein of around 36 kDa in cell extracts (Thermo Scientific, Ab against human CXCL1: PA5-28822).

5.3.2.3 MMP3

Matrix metalloproteinase 3 (MMP3) is expressed as a single 477 polypeptide chain which folds to form a pro-form. Similar to other MMP proteins the MMP3 pro-enzyme contains an N-terminal propeptide, a catalytic domain of 180 amino acids and a C-terminal domain which contains the site for substrate recognition and inhibitor interaction (Becker et al, 1995). It is secreted as a 57 kDa protein as well as a minor 60 kDa glycosylated form.

Activation occurs by cleavage, which releases an 80 aa peptide and leaves the major active 48 and 45 kDa proteins (a minor fragment of 28 kDa has also been reported) (Koklitis et al, 1991). This information pertains to human MMP3, however cleavage and activation product sizes are likely to be similar in the mouse given sequence homology.

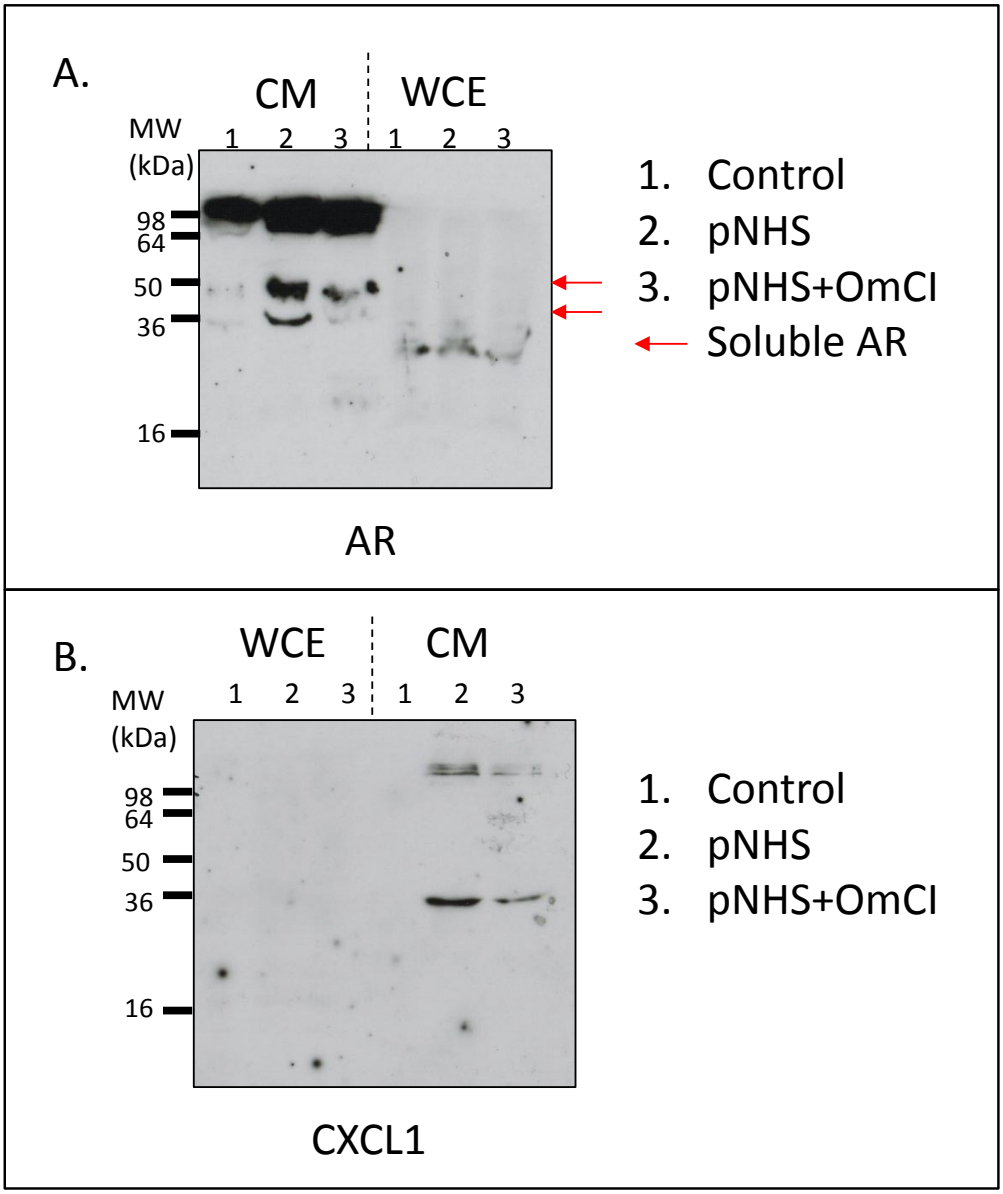

Figure 5.3.2.1 Protein validation of AR and CXCL1. Western blot analysis of CM and WCE of cells treated with pNHS or pNHS+OmCI for 1 hour, probed using antibodies raised against murine AR (A) and CXCL1 (B) proteins then developed using HRP conjugated secondary antibodies and the ECL system as described in section 2.8.

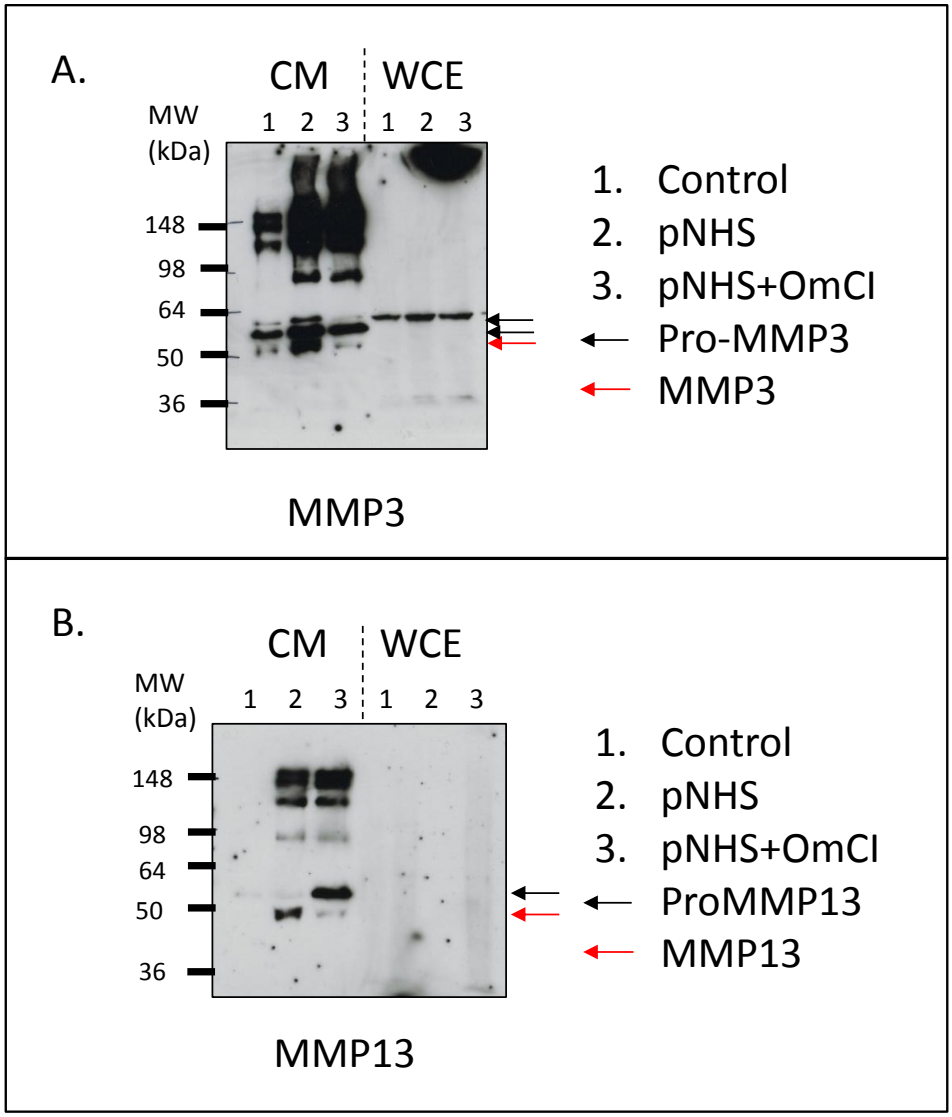

Figure 5.3.2.2 Protein validation of MMP3 and MMP13. Western blot analysis of CM and WCE of cells treated with pNHS or pNHS+OmCl for 1 hour, probed using antibodies raised against murine MMP3 (A) and MMP13 (B) proteins then developed using HRP conjugated secondary antibodies and the ECL system as described in section 2.8.

In Figure 5.3.2.2A, western blot analysis of CM obtained from CT26 cells exposed to pNHS shows increased expression of both pro-forms of MMP3 at 57 and 60 kDa, together with an apparent increase in the active form at 48 kDa, when compared to CM from both the untreated and pNHS+OmCI treated cells. WCE contained only the 60 kDa pro-MMP3 in all conditions with no apparent difference in levels between conditions. As with the AR western blots, there were several high molecular weight non-specific bands which are likely to be aggregated protein. The data is in agreement with the qPCR validation of Mmp3 mRNA levels and demonstrates that for Mmp3 increased levels of transcript correlate with protein production and secretion under conditions of sublytic C attack.

5.3.2.4 MMP13

MMP13 is expressed as a 427 amino acid (60 kDa) polypeptide chain pro-form which is activated by cleavage and removal of a pro-peptide sequence to yield a 48 kDa active form (Botos et al, 1999; Knauper et al, 1996).

Figure 5.3.2.2B shows an induction of MMP13 protein secretion by CT26 into the CM in response to pNHS with almost all induced protein in the 48 kDa active form while on exposure to pNHS+OmCI the 60 kDa pro-MMP13 predominated. Control conditions induced little MMP13 in either form. No MMP13 was detected in WCE suggesting the protein did not accumulate in the cytoplasm perhaps implying that the pro-form of the protein was secreted as soon as synthesised.

In summary, western blot analysis for each of the analyses, with the exception of CXCL1, demonstrated that upregulation at the mRNA level induced by sublytic complement attack correlated with changes in secreted protein levels in CM. This was most clearly seen with the blots for MMP3 and AR. Another effect of sublytic complement treatment on MMP13 protein production appeared to be an increased activation of the secreted pro-form.

5.3.3 **Pharmacological inhibition of signalling**

In sections 4.2.4 and 4.2.5 enrichment and network analyses implied that the gene expression response to sublytic C, largely validated at mRNA and protein expression levels in sections 5.3.1.2 and 5.3.2, were co-regulated by a number of signalling cascades. These included the PI3K and the MAPK pathways (p38, JNK, and ERK1/2). To discover the contributions made by each of these pathways in mediating the gene expression response pharmacological inhibition of each of the four pathways was attempted using pathway specific small molecule inhibitors.

The inhibitors used for investigation are shown in Table 5.2.3.1.

LY294002 is a morpholine derivative of quercetin (2-(4-morpholinyl)- 8-phenylchromone) and acts as a highly specific PI3K inhibitor by competing with ATP for its binding site (Vlahos et al, 1994). SB202190 is a pyridinyl-imidazole (4-(4-(4-fluorophenyl)-5-(pyridin-4-yl)-1H-imidazol-2-yl)phenol) compound shown to inhibit IL-1 and TNFα release by activated monocytes via inhibition of p38 kinase activity (Lee et al, 1994). SP600125 is an anthrapyrazolone (Anthra[1-9-cd]pyrazol-6(2H)-one) which is a kinase inhibitor capable of binding the ATP binding site on JNK with relative specificity for JNK1, 2 and 3. It prevents c-Jun mediated gene expression of inflammatory mediators including cytokines and MMPs (Bennett et al, 2001). PD 0325901 is benzhydroxamate (N-[(2R)-2,3-Dihydroxypropoxy]-3,4-difluoro-2-[(2-fluoro-4-iodophenyl)amino]-benzamide) which inhibits the ATP activation of MEK kinases preventing phosphorylation of ERK and continued transduction through the Raf/MEK/ERK pathway. It was shown to inhibit ERK phosphorylation in CT26 cells both *in vitro* and in an *in vivo* tumour model (Barrett et al, 2008).

5.3.3.1 Sublytic C experiment with inhibitors

In order to investigate the contribution made by each of the implicated signalling pathways the sublytic C experiments were repeated as described in section 2.4 in the presence of

pharmacological inhibitors of PI3K (LY294002), p38a/b (SB202190), JNK1-3 (SP 600125) and MEK/ERK (PD 0325901) at the doses shown in Table 5.2.3.1. Expression of Areg, Cxcl1, Mmp3 and Mmp13 was assessed by qPCR and compared to the carrier control (DMSO).

Figure 5.3.3.1 and Figure show the qPCR analysis of Areg, Cxcl1, Mmp3 and Mmp13 expression response to sublytic C under treatment with DMSO, LY294002, SB202190, PD0325901, and SP600125.

Areg

Areg gene expression was significantly upregulated at both time points in response to the sublytic C attack in the presence of the carrier control reflecting closely the validated data ($p<0.01$, Figure 5.3.3.1A). PI3K inhibition did nothing to suppress this effect, rather, it accelerated the response at the 12 hour time point. P38 inhibition had the effect of increasing the overall expression of Areg at both time points but did not suppress the comparative increase induced by sublytic C. Inhibition of MEK/ERK signalling suppressed Areg expression in all conditions representing both a reduction in overall expression and a suppression of the observed upregulation in response to sublytic C. JNK inhibition had no influence on the Areg expression response resulting in a similar profile to that of the control.

Cxcl1

Cxcl1 gene expression was upregulated at both time points in response to the sublytic C attack in the presence of the carrier control although this was not significant at the 1 hour time point but was at 12 thus reflecting the validated data (ns, $p<0.01$, Figure 5.3.3.1B). PI3K inhibition suppressed upregulation at 1 hour, but accelerated upregulation at the 12 hour time point suggesting a degree of redundancy in its control of Cxcl1 expression since PI3K inhibition could not permanently suppress an upregulatory response. P38 inhibition resulted in a significant ($p<0.05$) increase in overall expression at 1 hour and had an

acceleratory effect on the response to pNHS at 12 hours. However, it did not suppress the upregulation effect at either time point suggesting that p38 signalling has an inhibitory influence on Cxcl1 expression. Inhibition of MEK/ERK signalling suppressed the Cxcl1 expression response at 1 hour but did not affect it at 12 hours indicating a possible redundancy in MEK/ERK influence over Cxcl1 signalling. JNK inhibition had no influence on the Cxcl1 expression response resulting in a similar profile to that of the control.

Mmp3

Mmp3 gene expression was upregulated at both time points in response to the sublytic C attack in the presence of the carrier control, reflecting the validated data ($p<0.01$, $p<0.001$, Figure 5.3.3.2A). PI3K inhibition significantly reduced expression levels for both pNHS and pNHS+OmCI at 1 hour but appeared not to inhibit the upregulatory response to pNHS. In contrast PI3K inhibition significantly reduced the upregulatory response at 12 hours. P38 inhibition had the effect of increasing the overall expression of Mmp3 at the 1 hour time point but did not suppress the upregulatory response to pNHS compared to pNHS+OmCI at either time point. Inhibition of MEK/ERK signalling suppressed the Mmp3 expression response at both time points but had the effect of significantly increasing overall expression at 12 hours. JNK inhibition did not affect the expression response of Mmp3 at 1 hour but significantly reduced the upregulation at 12 hours.

Mmp13

Mmp13 gene expression was upregulated at both time points in response to the sublytic C attack in the presence of the carrier control, this was significant at 1 hour time point but not at 12 hours, overall, reflecting the validated data (Figure 5.3.3.2B). PI3K inhibition significantly increased overall Mmp13 at 1 hour but did not affect either overall levels or the upregulation at 12 hours, perhaps indicating a regulatory role for PI3K in Mmp13 expression. P38 inhibition had the effect of enhancing the expression response to sublytic C of Mmp13 at 1 hour but abolished the effect completely at 12 hours. Inhibition of

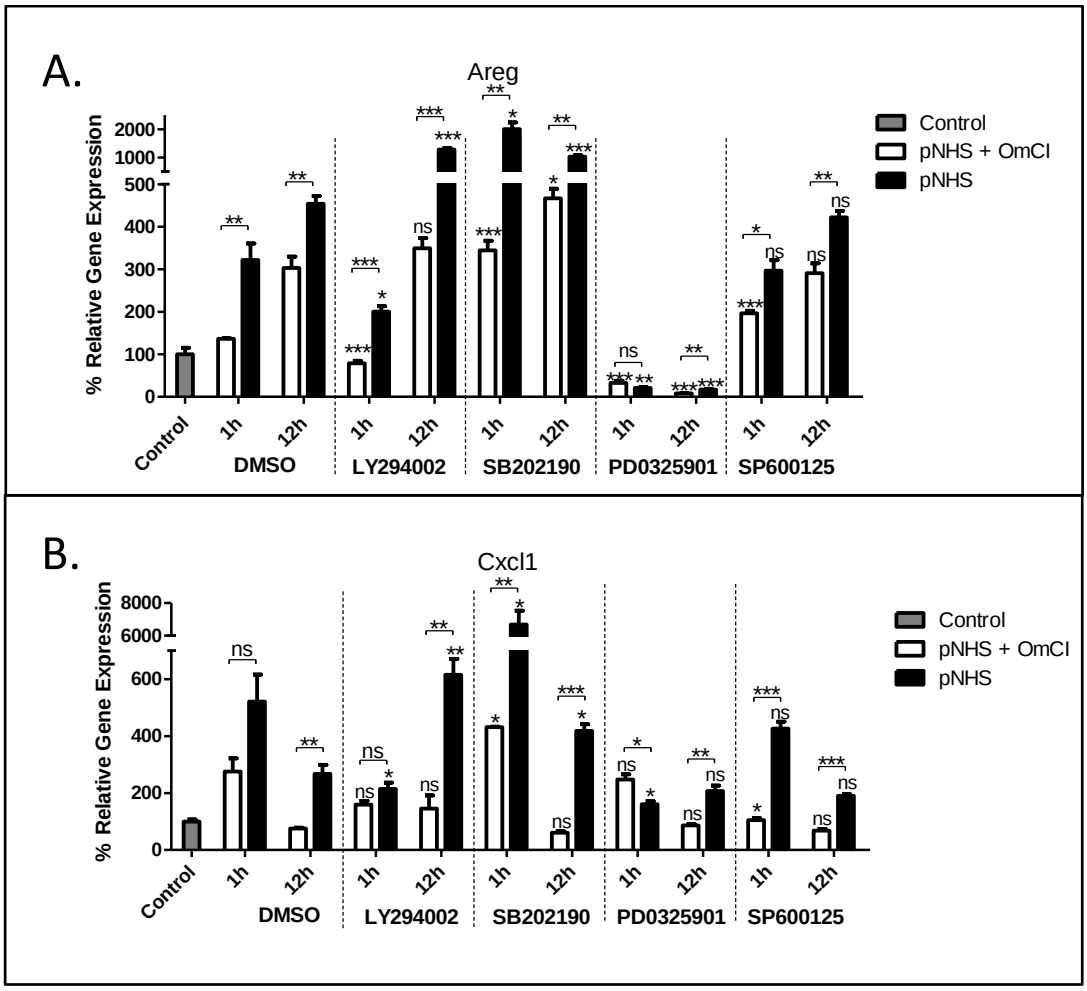

Figure 5.3.3.1 Effect of pharmacological inhibition of signalling pathways on Areg and Cxcl1 response to sublytic C attack. CT26 cells treated with LY294002, SB202190, PD0325901, SP600125 or a DMSO carrier control and exposed to pNHS and pNHS+OmCI for 1 and 12 hours. RNA was extracted from each including an untreated control. RNA was reverse transcribed then Areg (A.) and Cxcl1 (B.) gene expression analysed by qPCR and calculated as relative to β-actin using the ΔΔCt calculation outlined in section 2.6.2 then presented as a % of untreated control. Results are mean n=3 +/- SEM, statistics were calculated by ttest: comparing pNHS and pNHS+OmCI (displayed on comparative lines above) and comparing condition under inhibitor treatment with relevant DMSO control (displayed above individual bars) (ns=not significant *p<0.05, **p<0.01, ***p<0.001).

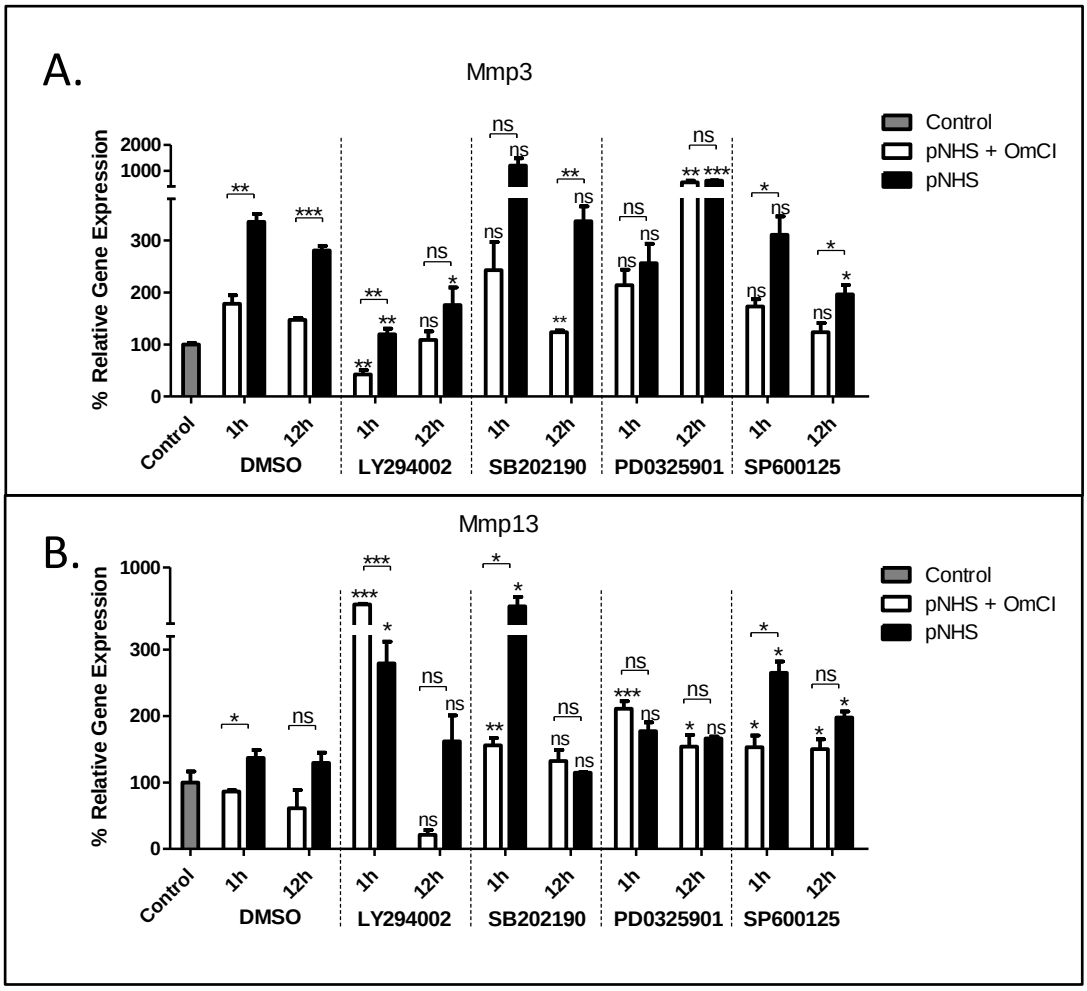

Figure 5.3.3.2 Effect of pharmacological inhibition of signalling pathways on Mmp3 and Mmp13 response to sublytic C attack. CT26 cells treated with LY294002, SB202190, PD0325901, SP600125 or a DMSO carrier control and exposed to pNHS and pNHS+OmCl for 1 and 12 hours. RNA was extracted from each including an untreated control. RNA was reverse transcribed then Mmp3 (A.) and Mmp13 (B.) gene expression analysed by qPCR and calculated as relative to β-actin using the ΔΔCt calculation outlined in section 2.6.2 then presented as a % of untreated control. Results are mean n=3 +/- SEM, statistics were calculated by ttest: comparing pNHS and pNHS+OmCl (displayed on comparative lines above) and comparing condition under inhibitor treatment with relevant DMSO control (displayed above individual bars) (ns=not significant *p<0.05, **p<0.01, ***p<0.001).

MEK/ERK signalling increased overall expression levels but suppressed the expression response at both time points suggesting a key role for MEK/ERK signalling in the Mmp13 expression response to sublytic C. JNK inhibition had no influence on the Mmp13 expression response resulting in a similar profile to that of the control although increasing expression levels overall.

5.3.4 **Roles of C5a and MAC**

Sublytic C experiments have so far been conducted using serum as a source of C and relied upon OmCI to switch off terminal pathway activation. Using OmCI in this way has obvious advantages that have been described in section 3.4.4 but by preventing C5 cleavage it removes not only MAC but also the highly active cleavage product C5a from the system which under the conditions used with pNHS would be released during activation. It is therefore possible that C5a plays a significant activatory role alongside the MAC in mediating the observed effects on gene expression.

5.3.4.1 C5a/C5aR axis

Involvement of C5a in the expression response requires the presence of a C5aR expressed on the surface of CT26 cells. The presence of the receptor was assessed by detecting levels of mRNA transcript using qPCR and protein by western blot. Cells were cultured to 80% confluency in normal growth conditions and either RNA extracted or a whole cell extract (WCE) prepared. RNA was reverse transcribed as described in section 2.5.4 and qPCR detection of C5aR performed by Dr Jack Ham (Institute of Molecular and Experimental Medicine Cardiff University) using a pre-existing qPCR primers and an optimized protocol (Figure 5.3.4.1A). WCE was prepared as described in section 5.2.2.2 and both the pellet and supernatant analysed by western blot alongside the murine macrophage cell line J774.2 WCE pellet as a positive control (Figure 5.3.4.1B). Western blotting was conducted by Dr Carmen Van den Berg (Institute of Molecular and

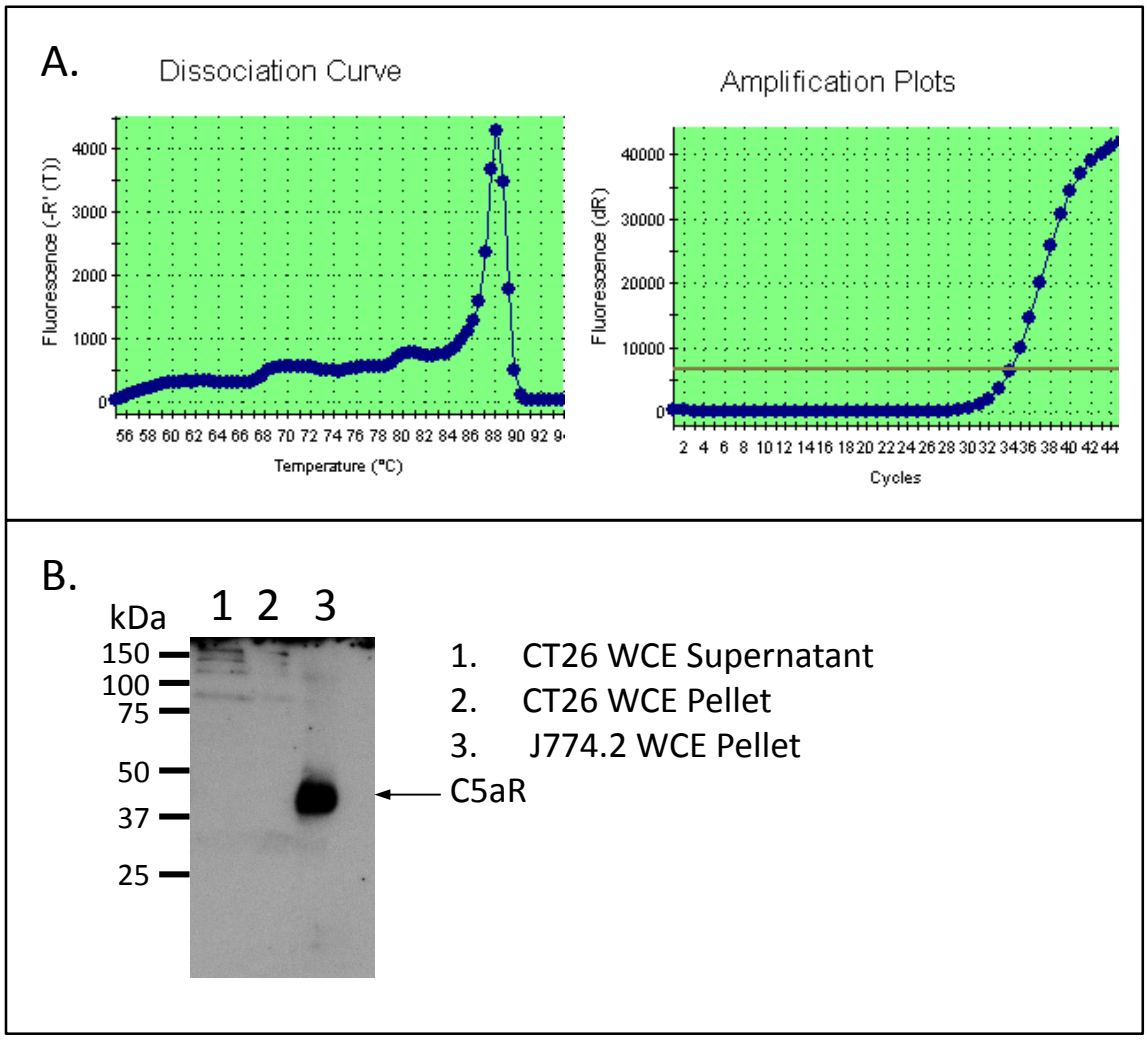

Figure 5.3.4.1 C5aR expression by CT26 cells. A. qPCR analysis of C5aR mRNA expression using specific primers showing melt curve and amplification plots. B. Western blot analysis of CT26 WCE (supernatant and pellet) and a J774.2 WCE (pellet only) for a positive control, probed using an antibody raised against murine C5aR then developed using HRP conjugated secondary antibodies and the ECL system as described in section 2.8.

Experimental Medicine Cardiff University) using a well established western blotting protocol for C5aR detection.

C5aR expression

CT26 were shown by qPCR analysis to express low levels of C5aR (Figure 5.3.4.1A). Expression level was not compared to a housekeeping or positive control instead qPCR analysis but was simply performed using 20 ng of cDNA (1 µg RNA reverse transcribed in 10 µL volume; cDNA diluted in qPCR reaction mix at a final concentration of 1 ng/µL in 20 µL).

Melt curve analysis demonstrated a clean amplification of C5aR transcript with amplification curve reaching the threshold at cycle 34 indicating low level expression. Western blot analysis suggested that the expressed transcript for C5aR was not translated into detectable protein (Figure 5.3.4.1B). The pellet of WCE taken from J774.2 macrophage cell line was clearly positive for C5aR protein giving a band between the 37 and 50 kDa markers. This band was absent in both supernatant and pellet of CT26 WCE.

C5aR inhibition and C5a treatment

The role of C5a and the C5aR signalling was investigated by two opposing strategies; treatment of cells with the C5aR inhibitor PMX53 and treatment with commercially obtained purified human C5a (Abcam) (Figure 5.3.4.2). PMX53 is a low molecular weight cyclic peptide, AcF-[OP(D-Cha)WR], developed to improve upon larger c-terminal C5a peptidic inhibitors (Finch et al, 1999). PMX53 competitively binds C5aR but does not trigger GPCR activation as demonstrated by myeloperoxidase (MPO) release from human PMNs which could be effectively inhibited by PMX53 at µM concentrations (Wong et al, 1998). Analogous to the pharmacological inhibitor experiments described in section 5.2.3.2, cells were treated for 1 hour with or without 100 nM PMX53 in normal growth medium. Cells were then exposed to 5% pNHS and pNHS+OmCI treatment as before (section 2.4), maintaining the PMX53 dose in relevant conditions.

To assess the effects of C5a present in the system with the absence of terminal pathway activation, C5a was added back to cells exposed to pNHS+OmCI. C5a was added at final concentration of 0.4 μM, an excess of physiological concentration equivalent to the molar concentration of C5 present in serum. In addition, the effects of C5a alone were tested with cells incubated with complete growth medium with or without the addition of C5a to the same concentration. Cells were incubated in their respective conditions for 1 hour at 37°C and RNA was extracted as before. RNA was reverse transcribed for qPCR analysis of Mmp3 expression response and presented as % of an untreated control (Figure 5.3.4.2). Mmp3 gene expression response to sublytic complement was used because it represented a reliable readout that had been confirmed at both transcript and protein levels.

Mmp3 was upregulated in untreated cells in response to pNHS treatment compared to pNHS+OmCI as in the validated data, though it did not reach significance (Figure 5.3.4.2). Under PMX53 inhibition of C5aR the effect was unaltered and upregulation in response to sublytic C reached significance ($p<0.01$). C5a added back to pNHS+OmCI condition did not reconstitute the upregulation observed in the pNHS condition and was not significantly different to pNHS+OmCI. Purified C5a added directly to medium induced a small upregulation compared to medium only control, though this was a much smaller increase compared to that provoked by pNHS and was not significant.

Taken together the data suggests that C5a is not responsible for the observed expression responses to terminal pathway activation at least for Mmp3 expression. With no detectable C5aR protein present on the cells it is unlikely that the cells can respond to C5a to any significant degree.

5.3.4.2 MAC

In order to ascertain the role played by MAC in the observed gene expression effects, C6 depleted serum (C6D) prepared in section 3.3.3.5 was employed. Cells were exposed to

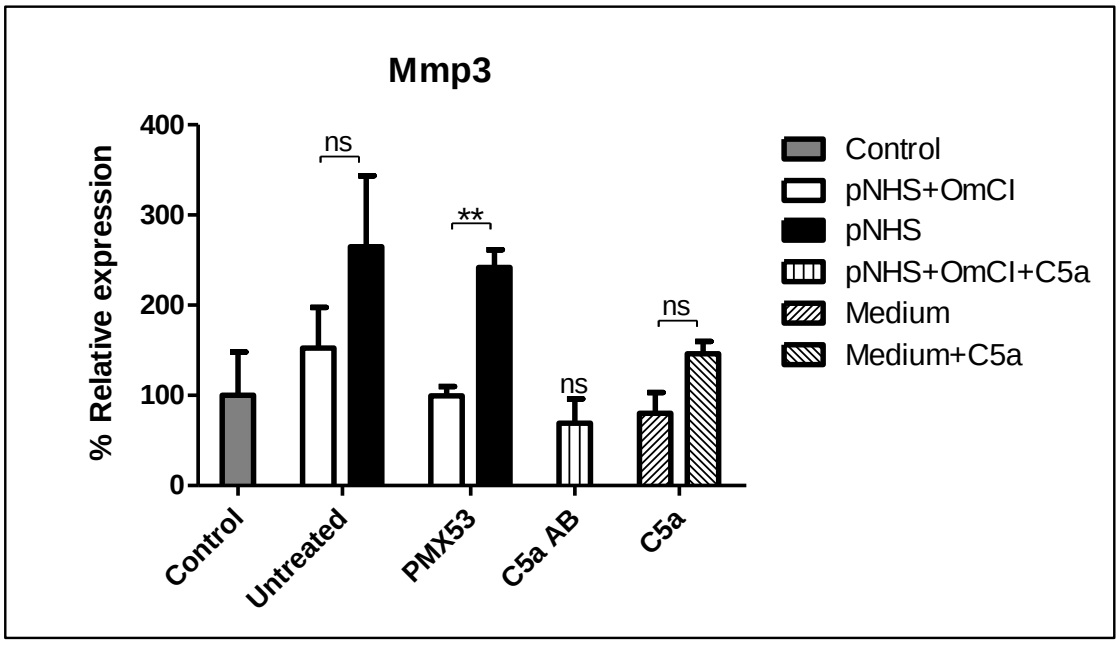

Figure 5.3.4.2 The role of the C5a/C5aR axis in the observed Mmp3 gene expression changes. Cells were treated with or without PMX53 for 1 hour and exposed to pNHS or pNHS+OmCI conditions. Purified C5a at 0.4 μM was added back to a separately prepared pNHS+OmCI condition to reconstitute C5a. C5a was also added to normal growth medium along with a medium only control. Treatments were incubated for 1 hour then RNA extracted from cells monolayers. RNA was reverse transcribed and Mmp3 gene expression analysed by qPCR and calculated as relative to β-actin using the ΔΔCt calculation outlined in section 2.6.2 then presented as a % of untreated control. Results are mean n=3 +/- SEM (p<0.01). C5aAB statistics compare to pNHS+OmCI.**

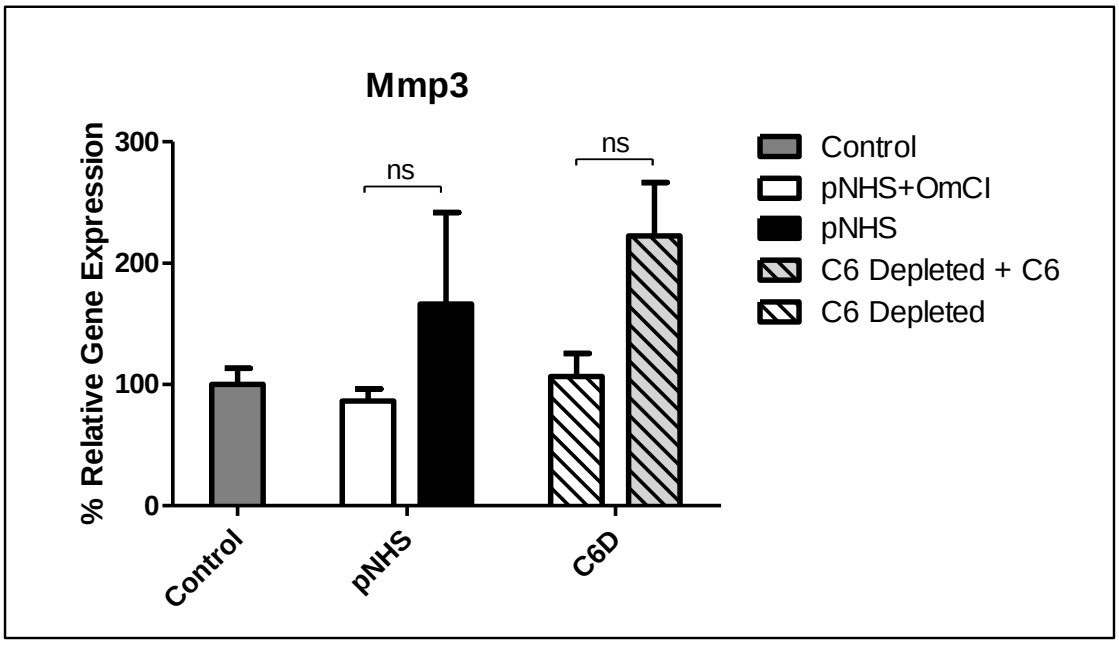

Figure 5.3.4.3 The role of MAC in the observed Mmp3 gene expression changes. Cells were exposed to pNHS or pNHS+OmCI conditions as well as C6D serum and C6D serum with C6 added back to 50 μg/mL of serum. Treatments were incubated for 1 hour then RNA extracted from cell monolayers. RNA was reverse transcribed and Mmp3 gene expression analysed by qPCR and calculated as relative to β-actin using the ΔΔCt calculation outlined in section 2.6.2 then presented as a % of untreated control. Results are mean n=3 +/- SEM.

C6D with or without C6 reconstituted to 50 µg/mL of serum alongside pNHS and pNHS+OmCI conditions as a comparison with the inclusion of an untreated control. Cells were incubated for 1 hour at 37°C and RNA was extracted as before and reverse transcribed for qPCR analysis of Mmp3 gene expression (

Figure 5.3.4.3). C6D serum reconstituted with C6 was able to produce upregulation of Mmp3 compared to the C6D serum alone resulting in a similar upregulation induced by pNHS compared to pNHS+OmCI though neither of these effects were significant. The data appears to suggest that the observed gene expression responses are due to the formation of MAC at least for Mmp3.

5.4 Discussion

5.4.1 **Validation of statistically significant changes**

Validation of the most significant expression changes selected allowed the microarray to be validated in an unbiased fashion. Genes were chosen so that upregulation and downregulation of the greatest significance and fold change values could be tested at each time point. Fam110c and Rgs16 representing upregulation at 1 hour, Irf1 representing downregulation at 1 hour and Hbb-bh1 representing upregulation at 12 hours, were each confirmed by qPCR analysis conducted on RNA extracted in parallel with that used for microarray (primary validation). In addition, qPCR was conducted using RNA extracted from an independent sublytic C experiment conducted in an identical manner (secondary validation). In all cases except for Rgs16, both primary and secondary validation qPCR data was in agreement with that of the microarray. This validation lends weight and confidence to the microarray data and the findings so far attributed to it.

5.4.2 **Validation of network analysis hits: qPCR**

Network analyses (section 4.2.5.2) suggested possible co-regulation of Areg, Cxcl1, Mmp3 and Mmp13 in response to sublytic C attack. Validation of these targets was

pursued using an identical strategy to that described above. In each case qPCR data confirmed the gene expression response described by microarray data i.e. an upregulation at both the 1 hour and the 12 hour time-points. There was some variation between the primary and secondary validation expression data especially for Cxcl1, and to some extent Areg, expression. For Mmp3 and Mmp13 both primary and secondary validations were in agreement. As discussed in chapter 4 their proposed interconnectivity and co-regulation make them interesting genes for further study given that there may be common mechanisms of control. Also, their roles as growth factors (Areg, Cxcl1) and extracellular matrix regulators (Mmp3 and Mmp13) make them possible candidates as tumour promoting genes expressed in response to sublytic C exposure.

5.4.3 **Validation variation**

Inevitably, there were discrepancies between microarray data and primary and secondary qPCR validation, most pronounced for Rgs16 and Cxcl1.

Rgs16 expression, which was shown by microarray and primary qPCR to be significantly upregulated at the 1h time point but not at 12h, was shown to be upregulated at both time points by secondary qPCR, with the increase greatest after 12 hours. Since secondary validation was an independent repeat of the experiment it is likely that biological variation arising from unknown experimental factors is the cause. This suggests that the observed Rgs16 expression response to sublytic C is less robust than for the other validated genes.

In the case of Cxcl1, array data showed a significant upregulation at both time points with the greatest increase at 1 hour. However, primary and secondary qPCR data showed upregulation of expression was most pronounced at 12 hours. In contrast with Areg validation, this discrepancy suggests a difference between microarray and qPCR methods for expression detection. *Ensembl* derived transcript sequences shown in section 5.2.1.2 with labelled microarray probes, demonstrate that Cxcl1 has no transcript variants and only 4 exons. If qPCR primers target this same transcript then differing levels of variants

cannot explain the difference between microarray and qPCR data. A more likely explanation is the location and proximity of the qPCR primers compared to the microarray probes since the two are designed to target opposite flanks of the transcript, indeed the forward primer is located on the 5'UTR and the probe on the 3'UTR. It has been demonstrated that the distance between the two is an important factor in the level of agreement between microarray and qPCR validation (Etienne et al, 2004).

Though the qPCR validation of Rgs16 and Cxcl1 did not perfectly match, validation of Fam110c, Irf1, Hbb-bh1, Areg, Mmp3 and Mmp13 data did closely match their microarray counterparts, indicating the overall suitability of qPCR a validation tool.

5.4.4 **Validation at protein level**

In order to assess whether the gene expression responses led to an increase in levels of translated proteins western blots were carried out on whole cell extracts and conditioned media using antibodies against each of the network generated protein targets. Despite the lack of a proper loading control efforts were made to load equal quantities of protein by calculating the mass of precipitated protein pellets and adjusting the volume of loading buffer added so that 8 mg could be loaded per sample.

AR

There was a clear increase upon exposure to sublytic C of two high molecular weight forms of AR at the 50 and 36 kDa markers secreted into the medium over 24 hours. AR at the 36 kDa marker is likely to correspond with the 36 kDa fragment produced by cleavage of the preferred distal position on the membrane anchored pre-cursor (Brown et al, 1998).

The 50 kDa AR band is likely the membrane tethered pro-form reported to be the dominant form by (Brown et al, 1998)). If this fragment was indeed the pro-form, its presence in CM suggests membrane fragment contamination which might have been eliminated by centrifugation or filtration. Another explanation is the release of vesicular bodies into CM, indeed sublytic C is known to induce production of MAC enriched vesicles

from mammalian cells as part of a C resistance strategy (Campbell & Morgan, 1985). In order to investigate whether this is the case, vesicular bodies of differing sizes can be isolated from the CM and run on a western blot to detect AR fragments.

CXCL1

CXCL1 in CM was not be seen by western blot under the described experimental conditions, no bands corresponded to the predicted 12 kDa mass. A higher molecular weight band of unknown identity at the 36 kDa marker was likely the result of non-specific binding or aggregates. Failure to detect the protein product suggested that abundance of the protein was below the limit of detection for western blot, therefore it is likely that ELISA would have been a more suitable method of detection.

MMP3

Western blotting for MMP3 showed that sublytic C attack induced increased expression and greater activation of secreted protein. The two bands at 57 and 60 kDa are likely to be the unglycosylated and glycosylated pro-forms of MMP3 respectively. Given that the 60 kDa form is dominant in WCE there is a possibility that, as was the case for the AR western blots, there were detached cells or vesicular bodies present in the CM. An MMP3 band at 50 kDa, corresponding to the activated form, was also increased in CM confirming that the expression pattern described by microarray and validated by qPCR translates into protein production.

MMP13

Expression of MMP13 protein was not increased comparing pNHS with pNHS+OmCI; however, expressed MMP13 from pNHS-exposed cells was mostly activated MMP13 (48 kDa) as opposed to the predominant pro-form found in control samples. Given that MMP3 is known to be an efficient activator of MMP13 it can be hypothesised that the shift of MMP13 into its active form during pNHS exposure may be due to expression and

activation of MMP3 (Lochter et al, 1997). In the same way MMP3, MMP13 or both active enzymes may be responsible for cleavage and solubilisation of an active AR cleavage product from the membrane anchored pro-AR, indeed cleavage of pro-AR is known to be inhibited by treatment with metalloprotease inhibitors (Brown et al, 1998). However ADAM17 is well characterised as a key component for pro-AR ectodomain shedding (Sahin et al, 2004).

Equality of protein loading was achieved by a crude method, less reliable than a protein assay or loading control such as β-actin staining. The latter was attempted but unfortunately failed to provide usable results within the time frame available. Obviously these limitations reduce the confidence in the protein expression changes. Also, again due to time pressures the presented blots were not confirmed by repeats, making interpretation of the data more difficult. This being said the data presented does provide some evidence that mRNA expression changes of Areg and Mmp3 are translated into changes in levels of expressed protein products. Interestingly, MMP13 expression was not increased but expressed protein was activated under sublytic C conditions. CXCL1 protein was not detected by WB.

5.4.5 **Pharmacological inhibition of signalling pathways**

Network analysis as described in section 4.2.5.2 implicated a number of signalling pathways which may co-regulate the validated responsive genes. The MAPK pathways, p38, JNK and MEK/ERK, as well as the PI3K pathway, were the four main implicated pathways. Pharmacological inhibition with small molecule drugs was used to ascertain the contributions made by each pathway. The results showed that overall p38 and JNK were not involved in the response but suggested involvement of MEK/ERK and PI3K pathways in some of the observed effects.

Areg expression was most affected by inhibition of MEK/ERK signalling. This pathway has been strongly associated with EGFR transactivation via the previously described

ectodomain shedding of pro-AR leading to proliferation (Kasina et al, 2009). The described response relied upon CXCL12 activation of ADAMs (or possibly MMPs) for the ectodomain cleavage. Given that Areg transcript expression was almost entirely knocked down by MEK inhibition in qPCR experiments, it may be that EGFR transactivation through ectodomain cleavage of an EGF family protein is responsible for the induction of Areg gene expression. Indeed Cxcl1 expression has been associated with EGFR transactivation via MMP mediated HB-EGF ectodomain cleavage, a process relying on MEK/ERK pathway (Bolitho et al, 2010).

The role for CXCL1 as a trigger for EGFR transactivation is challenged by the relative reduction in Cxcl1 expression during MEK inhibition especially at 1 hour post exposure which suggests that Cxcl1 response also relies in part upon MEK activation or perhaps the response is indirect via an unknown mechanism, able to recover at 12 hour in a way that Areg did not. Inhibition of Cxcl1 at the 1 hour time point by the PI3K inhibitor and subsequent recovery at 12 hours suggests both pathways may be involved. Cxcl1 expression is known to involve activation of ERK1/2 and p38 MAPK pathways (Yang et al, 2008), however while involvement of PI3K has not previously been described in endothelial derived cell types (from which CT26 are derived) it has been shown to be involved in Cxcl1 expression by macrophages (Pickens et al, 2011).

Potentiation of the Cxcl1 expression response by suppression of p38 suggests a role as a negative regulator, a phenomenon which has previously been described in hepatocytes, however the mechanism is as yet unclear (Wiechert et al, 2012). Areg gene expression response to sublytic C was also potentiated by inhibition of p38 signalling pathway. Precedent for p38 acting to inhibit gene expression, whilst ERK being required to activate it has been described during Ras activation and formation of growth factor autocrine loops in epithelial cells, this may explain the observed potentiation effects for both Areg and Cxcl1 under p38 inhibition (Pruitt et al, 2002).

PI3K signalling was implicated by pharmacology experiments in the sublytic C attack mediated Mmp3 upregulation, but not that of Mmp13. However, MEK/ERK was implicated in upregulation of both Mmp3 and Mmp13. EGFR activation has been shown to induce Mmp3 and Mmp13 via both MEK/ERK and PI3K signalling pathways in a number of contexts (Meierjohann et al, 2010; Shukla et al, 2006). This points to the key involvement of MEK/ERK and to a lesser extent PI3K in mediating Mmp3 and Mmp13 expression in response to sublytic C attack.

The phosphoinositide 3-kinase (PI3K) pathway refers to a signalling pathway which harnesses inositol phospholipid metabolism as a means of transduction. PI3Ks are a family of enzymes responsible for the phosphorylation of inositol phospholipids at the 3'-OH position. This leads to the generation of PtdIns(3)P, PtdIns(3,4)P_2 and PtdIns(3,4,5)P_3 which influence activation and localisation of several proteins possessing the pleckstrin homology domain (PH) (Rameh et al, 1997). PH domain containing proteins are generally signalling molecules and include protein kinases such as Akt (aka PKB or RAC) a serine/threonine kinase which is associated with receptor tyrosine kinase signal transduction (Burgering & Coffer, 1995). It is the PI3K/Akt pathway which has been most often associated with cellular responses to MAC deposition such as modulation of apoptosis and proliferation (Fosbrink et al, 2006; Soane et al, 2001).

The Raf/MEK/ERK MAPK pathway has previously been discussed in this thesis as being associated with growth factor cell activation, proliferation and protection from apoptosis (Mebratu & Tesfaigzi, 2009). Raf/MEK/ERK signalling has been demonstrated to be triggered in response to MAC deposition and was associated with a proliferative response in part through junD and c-fos gene upregulation (Rus et al, 1997). It has also been associated with the induced protection phenomenon (Kraus et al, 2001).

Overall the data suggests involvement of MEK/ERK and PI3K as the signalling pathways important in mediating the responses observed of upregulation upon exposure to sublytic

C. Indeed MEK/ERK appears to be the most important. MEK/ERK and PI3K are both key pathways involved in transduction of EGFR activation where they act to promote proliferation and survival respectively (Aksamitiene et al, 2010). MEK is the upstream effector of ERK1/2 phosphorylation and during growth factor signal transduction is activated through RTK/Ras sequential activation which initiates the Raf/MEK/ERK pathway (Chang et al, 2003). EGF treatment of cells has been demonstrated to increase ERK activity over several hours which coincided with a number of gene upregulations (Mullenbrock et al, 2011). The crosstalk of PI3K with MEK/ERK activation may explain their co-involvement since they appear to be activated in parallel and could be co-regulatory, indeed it could be hypothesised that PI3K promotes the MEK response through co-activation of Raf (Chang et al, 2003). This might explain why inhibition of PI3K did not fully suppress Mmp3 and Cxcl1 responses which for Cxcl1 recovered after 12 hours, perhaps indicative of MEK/ERK overcoming PI3K inhibition. In addition whilst PI3K inhibition was not sufficient to suppress the upregulation completely, MEK inhibition universally suppressed it.

These data provide some preliminary evidence of a central role for MEK/ERK activation in transduction of sublytic C induced signalling with possible involvement of PI3K. They also show that p38 and JNK pathways are not obviously involved. Within this a key role played by EGFR is suggested. Taken together, a possible hypothesis might be that EGFR is activated upon the event of a sublytic C attack, triggering MEK/ERK supported by PI3K signalling cascades. This is in agreement with the central segment of the network generated in section 4.2.5.2 which linked EGFR to PI3K and MEK/ERK. To confirm the involvement of EGFR in mediating the expression response an inhibitor of the EGFR receptor such as AG1478 could be used and the experiment repeated. If EGFR is a central effector in mediating the effects its inhibition would be expected to suppress the gene expression response.

5.4.6 **C5a/C5aR axis**

5.4.6.1 C5aR expression

Expression of the C5aR on the cell surface is required for C5a to exert influence on local cells. Sublytic C experiments described in this thesis have used human serum on a murine cell line, CT26 cells. Therefore when considering C5a/C5aR axis involvement it is important to consider that human C5a is known to be capable of ligating and activating murine C5aR (Gerard & Gerard, 1994). Expression data at transcript level suggested a low level expression in CT26 cells but western blot data suggested that this was not translated into protein. With no surface expression of C5aR it is less likely that C5a plays a central role in the observed sublytic C induced gene expression changes. Upon treatment with PMX53, a cyclical peptide inhibitor of C5aR, the repeatable expression response of Mmp3 was unaltered further ruling out the role played by C5aR

5.4.6.2 C5a

In experiments using commercially obtained purified human C5a protein on CT26 cells, no upregulation of Mmp3 was observed. C5a was added at a final concentration of 0.4 µM which was calculated as the concentration of C5 in serum. C5a was added at huge excess because the concentration was calculated for neat serum but erroneously added as a final concentration resulting in 20 fold excess. In addition the calculated quantity was based upon the concentration of C5, incorrectly assuming complete cleavage of all C5, however, in reality only 50% of available C5 is cleaved. As a result C5a was added at roughly 40 fold excess to physiologically relevant levels. C5a is often used in *in vitro* experiments at a concentration of 10 nM and a dose dependent effect can be seen in Ca^{2+} release by astrocytes during C5a treatment between 0.1 and 100 nm (Gasque et al, 1995). Given the excess of C5a added, if C5a was responsible for the changes in gene expression caused by pNHS, it would be expected that a significant response might have been observed but in reality there was little effect on Mmp3 expression.

Taken together the data suggests that a lack of C5aR expression on the cell surface prevents C5a from exerting an effect on CT26 cells under sublytic C conditions. This makes a role for C5a in mediating the observed gene expression responses unlikely, though it may contribute. Therefore the remaining terminal pathway components are implicated.

5.4.7 **MAC**

To further underline a role for the MAC in the observed effects C6D serum was used which retains the ability to activate complement, including the release of C5a, but is incapable of forming the MAC complex. C6D ability to form MAC was significantly reduced as shown in reduced haemolytic and CDC activity (section 3.3.3.5). These activities were reconstituted with the addition of C6. Expression data from Mmp3 showed that treatment with C6D serum resulted in similar expression levels to cells exposed to OmCI treated serum and untreated controls. This implies that the activation of C and the release of C5a is not enough to induce the expression response seen in pNHS treated cells. Indeed, upon the addition of C6 the cells responded in a similar manner to pNHS treatment and Mmp3 was upregulated. This is good evidence that MAC is required for the observed expression responses.

5.5 Summary and conclusions

Out of the 8 candidate genes 4 demonstrated the validity of the microarray experiment as a detector of expression change providing confidence in the discoveries made. The remaining genes were highlighted by network analysis as being possibly co-regulated and showing previous links in tumour progression/cancer cell growth therefore strong candidates for investigation. In addition to qPCR confirmation of a transcription response by Areg, Cxcl1, Mmp3 and Mmp13 these genes were confirmed at the protein level by western blot of which the response could be demonstrated for MMP3, MMP13 and AR protein levels and activation states but CXCL1 was not successfully corroborated. Further

investigation of the confirmed expression changes by pharmacological inhibition of PI3K and JNK, ERK and JNK MAPK pathways demonstrated that MEK/ERK and to a lesser extent PI3K activation were important in signalling the response triggered by sublytic C exposure. CT26 cells were shown to express small amounts of transcript but lacked C5aR on their surface. C5aR inhibitors did not inhibit, and addition of extrinsic C5a could not replicate the sublytic C response to pNHS compared to pNHS+OmCI. Treatment of cells with C6D+C6 compared to C6D alone induced an upregulation of Mmp3 which closely resembled that induced by pNHS compared to pNHS+OmCI strongly implicating the MAC complex as the central mediator of the effects.

6 Discussion

6.1 Hypothesis

This thesis has been concerned with the effects of the terminal pathway of C on tumour cells and in particular its effects on gene expression. The end product of terminal pathway activation, the MAC, is a potent activator of cells and influence on cell fate when deposited on nucleated cells, with a plethora of effects, including induction of expression of inflammatory mediators/cytokines (Cybulsky, 1991; Morgan, 1989; Schonermark et al, 1991), alterations in ECM components/regulators (Lueck et al, 2011; Torbohm et al, 1990), triggering entry into the cell cycle (Rus et al, 1996) protection from apoptosis (Rus et al, 1996) and induction of apoptosis ((Liu et al, 2012). It is through these effects on cell function that C promotes tumour formation and cause it to be considered a contributor to disease.

The hypothesis investigated was that tumour cells may respond to sublytic C membrane attack by up-regulating genes which bestow the tumour with a more metastatic and proliferative phenotype.

6.2 Summary of main findings

To investigate the above hypothesis, the murine colon carcinoma cell line CT26 was used as an *in vitro* model to study the sublytic effects of C attack. Pooled normal human serum was used as a C source which auto-activated on the cells, probably through the presence of natural antibodies; though this was never confirmed it is the most likely explanation. Cells were shown to be susceptible to C lysis and had a sublytic threshold, defined as that which caused less than 10% lysis, of 5% serum. The recombinant terminal pathway inhibitor OmCI, a C5-binding protein derived from the soft tick *Ornithodoros moubata*, served as a control allowing the terminal pathway specific effects to be deduced.

OPN and uPA which are known to increase metastatic potential in cells which express them, were upregulated in response to sublytic C (Wai et al, 2005). It was shown that CT26 cells expressed very low levels of the terminal pathway regulator CD59a. Sublytic C attack on CT26 cells overexpressing CD59a resulted in only a minor suppression of the effect on OPN and uPA seen in control cells. This indicates that these particular gene expression changes were little affected by increasing CD59a expression and were thus unlikely to be mediated via signalling shown previously to be caused by CD59 cross-linking (Murray & Robbins, 1998). The evidence suggests that MAC pore is responsible for the observed expression change and that inhibition of its formation effectively reduces the effect.

Expression of OPN mRNA by CT26 cells was then shown to increase steadily over the course of 12 hours exposure to sublytic C conditions. OPN upregulation by sublytic C has previously been reported as a marker for tubular injury in a study that suggested a key role for MAC (Nangaku et al, 1999). OPN expression is likely a stress response which for a forming tumour provides several advantages; it is capable of acting as a chemokine and promotes tumour-supporting local inflammation, can promote metastasis by acting as an adhesion molecule and can be anti-apoptotic through the ligation of receptors and stimulation of signalling cascades (Wang & Denhardt, 2008).

Following the successful establishment of an *in vitro* model of sublytic C attack on tumour cells, global gene expression analysis using microarray technology was used to identify an expression profile of genes reactive to sublytic C. Primary analysis was performed using Partek software. Data were quality checked by PCA and shown to be well separated by experimental grouping. The separation described through PCA was a significant observation showing that a definable gene expression response to sublytic C could be detected, giving clear evidence of an effect despite the substantial influence of serum factors. Using ANOVA statistics, lists were generated of the most differentially expressed genes responsive to C. This analysis highlighted a number of genes with products

involved in Ca^{2+}, G-protein, and MAPK signal regulation, c-fos, Egr1 and Egr2 transcription factors, Areg and Bdnf growth factors, and inflammatory signal regulators. Representative genes were found for upregulation and downregulation at 1 and 12 hours; Fam110c, Rgs16, Irf1 and Hbb-bh1, for validation.

Pathway and network analysis was performed using a systems biology approach with GeneGo MetaCore software. Enrichment analysis of the data further crystallized the involvement of MAPK signalling. Network analysis of genes upregulated in the test conditions at both time points revealed four key downstream genes which were apparently co-regulated through a number of canonical pathways converging on the EGFR receptor. The four network derived genes were Areg, Cxcl1, Mmp3, and Mmp13. Network analysis also suggested the involvement of the MAPK, PI3K signalling cascades leading to gene expression control via AP-1 and NFκB.

The data derived from the microarray analysis was in agreement with published literature describing the effects of MAC deposition on nucleated cells, including causing Ca^{2+} fluxes, G-protein activation together with PI3K and MAPK signalling (Campbell et al, 1979; Dashiell et al, 2000; Fosbrink et al, 2006; Rus et al, 1997). Further reported effects which could influence broad changes in gene expression include induction of expression of c-fos, a member of the AP-1 family of transcription factors (Rus et al, 1996). Involvement of the EGFR in mediating intracellular signalling by MAC has been previously described, proposed to be by transactivation via G-protein coupled receptors (Cybulsky et al, 1999). Induction of Mmp3 and Mmp13 gene expression in response to sublytic C has also previously been reported in chondrocytes but responses involving Areg and Cxcl1 are novel (Wang et al, 2011).

Microarray data were validated experimentally by qPCR analysis conducted using both RNA extracted in parallel with that used for the microarray experiment (primary) and an independent experimental repeat (secondary). Primary and secondary validation of

statistically significant changes and the network derived hits showed a high degree of agreement, confirming the biological relevance of the microarray data. The upregulation of Areg and Mmp3 gene expression was further examined at the protein level by western blotting to confirm whether the changes seen at mRNA level were translated into changes in levels of expressed protein. For both protein products I showed that sublytic C stimulated increases in protein level. Overall levels of Mmp13 protein product were not increased, however the balance between the pro-form and the activated form of the protein shifted dramatically towards the latter. Cxcl1 protein could not be detected by western blot with the available reagents and so the changes seen in the mRNA could not be confirmed at protein level.

Various pharmacological inhibitors were used to investigate the involvement of PI3K and the three MAPK pathways implicated by network analysis. JNK and p38 signalling pathways were shown not to be involved in the observed responses, however, p38 was shown to have an overall inhibitory influence on gene expression of the four network derived genes. MEK/ERK signalling appeared to play a central role in the upregulation of Areg, Cxcl1, Mmp3 and Mmp13 gene expression responses with PI3K acting as a co-activator.

Since use of OmCI blocks release of C5a as well as MAC formation, the role of the C5aR/C5a axis in the observed gene expression responses was investigated. C5aR transcript expression was present in CT26 cells but surface expression was not detectable. Addition of C5a to CT26 cells had no effect on Mmp3 expression and PMX53, a C5aR inhibitor did not suppress the upregulation of Mmp3 in cells attacked by sublytic C. Therefore, C5a through the binding of C5aR, could be ruled out as the key terminal pathway component responsible for mediating the response.

To further define the role of the MAC in mediating the effects seen, C6D serum was used. C6D is capable of C activation up to and including C5a release but lacks the capacity to

form MAC. The ability to produce the MAC was restored by the addition of C6. C6D serum failed to elicit any increase in Mmp3 expression whereas C6D with C6 added induced a similar increase in Mmp3 expression to those shown by pNHS when compared to pNHS+OmCI controls. This was compelling evidence that MAC is the key mediator of the observed effect and further discounted the role of C5a.

6.3 Tumour promoting MAC

Each of the four key genes identified during the expression studies in this thesis as responsive to sublytic MAC encode proteins reported to possess tumour promoting properties and are strongly associated with several tumorigenic disease processes. MAC deposition was shown here to induce the expression of Areg (AR), Cxcl1(CXCL1), Mmp3 (MMP3) and Mmp13 (MMP13) in tumour cells, which have known roles in proliferation and metastatic potential. The changes in expression caused by sublytic MAC on this particular set of genes may thus represent a possible mechanism by which low level MAC deposition and the chronic inflammatory context it engenders benefits the cells of a forming tumour.

Expression of AR has been shown to be increased, at mRNA and protein levels, in a number of human cancer tissues including breast, colon, liver, ovary and pancreas compared to healthy counterparts (Castillo et al, 2006; Ciardiello et al, 1991; D'Antonio et al, 2002; Ebert et al, 1994; Lejeune et al, 1993). AR has been shown to play a role in tumorigenesis via its function as a growth factor through the development of autocrine or juxtacrine loops in hepatocellular carcinoma (Castillo et al, 2006), colon carcinoma (Johnson et al, 1992), pancreatic cancer (Murphy et al, 2001) and breast cancer (Willmarth & Ethier, 2006) cells. AR loops are self-sustaining, self-stimulating AR expression which acts through the EGFR receptor to support proliferation of transformed cells (Castillo et al, 2006). AR stimulation can also support cell survival through protection from apoptosis through Akt and STAT3 pathways and upregulation of Bcl-xl (Berasain et

al, 2005). AR has been shown to induce increased motility and invasion as part of its wound healing and tissue development roles in healthy tissue through upregulation of a number of associated genes (Willmarth & Ethier, 2006).

The described roles define a gene product which can bestow several advantages to forming tumours and indeed this translates into patient outcome and survival. (Fontanini et al, 1998; McBryan et al, 2008). A strong correlation between AR expression and survival has been demonstrated in lung, breast and colon cancers and high expression levels in colon carcinoma have been shown to be predictive of disease aggression and liver metastasis development (Fontanini et al, 1998; McBryan et al, 2008; MichiyoYamada et al, 2008).

CXCL1 expression at the transcript and protein level has been shown to be increased in colorectal, gastric, bladder and ovarian cancers when compared to healthy tissue (Junnila et al, 2010; Kawanishi et al, 2008; Rubie et al, 2008; Yang et al, 2006). CXCL1 production at inflammatory sites is required to recruit immune cells such as neutrophils but in the tumour microenvironment of mouse breast cancer cells, it is capable of recruiting myeloid derived suppressor cells (MDSCs) which are shown to support tumour growth and metastasis as well as suppress the local immune response (Acharyya et al, 2012; Diaz-Montero et al, 2009; Yang et al, 2004). CXCL1 can also exert autocrine growth signals directly on tumour cells via binding of CXCR2 thus promoting their proliferation (Bordoni et al, 1990). In addition CXCL1 can support tumour growth through directly promoting angiogenesis and metastasis in autocrine/paracrine loops (Acharyya et al, 2012; Strieter et al, 1995; Wang et al, 2006). A role in tumour self-seeding has also been proposed in which CXCL1 expression by tumour mass helps homing of tumour derived cells from circulation where they can contribute to tumour invasion and metastasis (Kim et al, 2009).

Like AR, the tumour promoting functions of CXCL1 mean that expression by tumour tissue is correlated with patient outcomes. This is true for gastric cancer patients where

expression levels correlate with disease stage, likelihood of metastatic development and number of lymph node metastases (Jung et al, 2010). CXCL1 expression has also been shown to correlate with poorer relapse free survival in stage III colorectal cancer (Oladipo et al, 2011).

Matrix metalloproteinases (MMPs) have long been associated with tumour development and progression primarily through their role in degrading and remodelling the ECM (Egeblad & Werb, 2002). MMPs contribute to tumour progression through their ability to promote angiogenesis, tumour invasion and metastasis (Deryugina & Quigley, 2006). In addition to these functions, MMPs can cleave and activate molecules in ECM with various tumour promoting roles such as inducing proliferation, motility and alterations in adhesion (Lukashev & Werb, 1998). Increased expression of MMPs is associated with poor tumour differentiation, increased invasiveness, poor prognosis, increased likelihood of metastasis and shorter survival time (Deryugina & Quigley, 2006).

MMP3 proteolytic cleavage can release E-cadherin, L-selectin, HB-EGF and TNFα as well as activate MMPs, proteases and protease inhibitors (Sternlicht et al, 1999). It has been proposed that by releasing/activating these factors, MMP3 acts as a central mediator of mammary tumorigenesis as a subversion to its role during normal tissue development (Sternlicht et al, 1999). MMP3 can induce a stable change from an epithelial to mesenchymal phenotype (epithelial to mesenchymal transition (EMT)) a process which is closely linked to tumour development (Lochter et al, 1997).

MMP13 in the tumour microenvironment has a number of roles in promoting tumour development, growth and metastasis. Activities key to this role are its collagenase and angiogenic activities. In a melanoma model MMP13 promoted angiogenesis, though expression did not to correlate with VEGF levels, suggesting an independent mechanism which contributed to organ specific metastasis (Zigrino et al, 2009). The angiogenic properties of MMP13 were investigated on HUVECs, though in opposition to the

melanoma model, VEGF was shown to be partly responsible for the promotion of tube formation and did not require protease activity, suggesting a direct and indirect influence (Kudo et al, 2012). In this same report MMP13 expression was shown to correlate with vascular density in human cancers.

MMP13 is overexpressed at transcript and protein levels in colon and breast cancers (Chang et al, 2009; Mori et al, 2005; Roeb et al, 2004). MMP13 expression is also associated with poor prognosis in colorectal and head and neck cancer and is proposed as a predictive marker for patient outcome (Huang et al, 2010; Leeman et al, 2002; Luukkaa et al, 2006). Indeed in prostate and oesophageal cancer patients MMP13 correlates to tumour metastasis and poor outcome, and thus may be used as a biomarker for metastatic spread (Morgia et al, 2005; Ye et al, 2011).

The process of EMT is characterised by loss of cell-cell contact, disruption of epithelial cell polarity, cytoskeletal organization, cell adhesion and production of ECM (Turley et al, 2008). It is associated with development and wound healing as well as disease processes such as driving tumour development and metastasis (Kalluri, 2009). CXCL1, MMP3 and MMP13 are each shown to be upregulated in, and therefore considered markers for, EMT (Lim et al, 2011; Radisky et al, 2005; Toh et al, 2011). The contribution made by upregulation of CXCL1, MMPs and EGFR ligands to EMT and metastasis may extend to the preparation of target organ tissue to create premetastatic niches (Kaplan et al, 2006; Minn et al, 2005)

Increased gene expression of Cxcl1, Areg, Mmp3 and Mmp13 upon MAC deposition therefore presents a novel mechanism by which C activation may lead to tumour promotion through alterations to the tumour:stroma interaction, bestowing cells of the tumour with proliferative, anti-apoptotic and angiogenic signals as well as the capability to degrade local ECM and metastasise.

6.4 Mechanism of MAC signalling

A great many signalling pathways have been described to be triggered upon MAC deposition onto mammalian cells, including Ca^{2+}, PKC, PI3K as well as the three MAPK pathways; p38, JNK and ERK (Aoudjit et al, 2003; Campbell et al, 1979; Cybulsky et al, 1995; Cybulsky et al, 1998; Niculescu et al, 1999; Rus et al, 1997).The exact mechanism by which MAC triggers signalling, if indeed it is specific and consistent, has eluded many investigators but Gαi, Gβɣ, receptor tyrosine kinase (EGFR, PDGFR) activation have all been implicated (Cybulsky et al, 1999; Niculescu et al, 1997; Soane et al, 2001). Evidence presented in this thesis from microarray analysis and pharmacology experiments, has pointed towards an EGFR mediated activation of MEK/ERK supported by PI3K in response to deposition of MAC resulting in the upregulation of Areg, Cxcl1, Mmp3 and Mmp13.

Cross-talk between PI3K and MEK/ERK is a well established phenomenon but the distinct mechanisms and nature of this interaction are not well defined. Focussing on the Ras/Raf/MEK/ERK pathway an interaction with PI3K has been described post Ras-GTP since PI3K can bind and be activated by it (Rodriguezviciana et al, 1994). However in the EGFR activated Ras/Raf/MEK/ERK pathway, PI3K was shown to support activation both pre and post-Ras, but this was only observed under low level EGFR activation and so the importance of PI3K in this pathway is highly context dependent (Wennstrom & Downward, 1999). EGF receptor signalling through PI3K and ERK may be coupled through regulation of Gab1 scaffold protein and this interaction has the ability to sustain MEK/ERK activation (Kiyatkin et al, 2006). This interaction is therefore complex and difficult to pin down with the available data and so is ripe for further interrogation.

EGFR activation by MAC is hypothesised as a transactivation via ligand independent induction of tyrosine phosphorylation of EGFR RTK via GPCRs (Cybulsky et al, 1999; Daub et al, 1997; Daub et al, 1996). This transactivation may be due to Ca^{2+} influx, the well characterised first cellular response to sublytic MAC, shown to induce EGFR

activation of MAPK signalling in vascular endothelial cells (Campbell et al, 1979; Eguchi et al, 1998).

Both MEK/ERK and PI3K pathways are associated with tumour survival and proliferation signals. Indeed Raf activation has been shown to induce autocrine expression of the EGF-like growth factors including AR in sustained Raf/MAPK pathway stimulation as part of a tumour promoting mechanism (Schulze et al, 2001). The two pathways are also shown to contribute to survival through caspase 9 inactivation and inhibition of apoptosis (Cardone et al, 1999).

Taken together, MAC induced EGFR transactivation, possibly via Ca^{2+} influx, mediating activation of MEK/ERK alongside PI3K is a compelling explanation for the observed gene expression responses. This may be the initial trigger for Areg upregulation which goes on to form a feedback loop sustaining activation and promoting the upregulation of Cxcl1, Mmp3 and Mmp13. MAC stimulation of EGFR-Ras/Raf/MEK/ERK can therefore be considered a possible mechanism of tumorigenesis driven by sublytic C.

6.5 Future work

To investigate the role of the EGFR triggered activation of the PI3K and MEK/ERK pathways, vector expressed siRNA transfected for specific knock down of early and late pathway members could be used to determine their roles in signalling. This has an advantage over pharmacology in that it is highly specific and controlled so that effects on phosphorylation of downstream controllers such as ERK can be quantified using western blot stained using phosphorylation state specific antibodies. Furthermore, transcription factor activity could be assess using EMSA or CHiP techniques.

The work described in this thesis demonstrates a mechanism by which activation of the C terminal pathway might promote tumour development and metastasis. To confirm the impact of the gene upregulation cell motility and invasiveness as measurements of

metastatic potential, a transwell experiment could be performed using a matrigel insert. Cells exposed to pNHS and pNHS+OmCI would be placed in the upper chamber and serum used as a chemoattractant. Cells exposed to sublytic C would be expected to have increased capacity to degrade and migrate through the matrigel by virtue of upregulated MMP3 and 13 expression. Conditioned medium used in place of serum, as the chemoattractant would demonstrate whether expression of CXCL1 influences the migratory potential, this could be performed with or without matrigel. Proliferation could also be measured to ascertain the influence of Areg and Cxcl1 upregulation on growth potential.

The work presented in this thesis makes use of a murine cell line, CT26 colon carcinoma cells. These were used in anticipation of using them to create an animal model to confirm the *in vitro* results *in vivo*. CT26 cells would be injected into WT and C3, C6 or C5 knockout BALB/c mice and tumour growth monitored over ~30 days (Current knockout mice held at Cardiff animal house are C57BL/6 and so it may be necessary to use the B16 cell line instead of CT26). Tumours would then be resected and analysed for Areg, Cxcl1, Mmp3 and Mmp13 gene expression by qPCR and protein expression assessed by immunostaining of fixed tissue. It would be expected that tumour promoting gene expression would occur in increased tumour growth rate and reduced survival in C sufficient mice compared to C knockouts. Tumours could also be assessed for tumour infiltrating leukocytes including the possible presence of MDSCs using FACS analysis. In addition to primary tumour analysis the formation of lung metastasis could be quantified and assessed for gene expression. Metastatic nodes would be expected to be more frequent in C sufficient WT mice and their tumour cells would be expected to be higher expressors of the four genes.

The described model could also be used to test the efficacy of therapeutic strategies. Using C6 anti-sense oligonucleotides (RNAi) delivered via a lentiviral system C6 could be knocked down in the tumour cells and used in the WT mice in an injectable model.

Treatment would be compared to a nonsense oligo and readouts repeated as above. Also, an available anti-C5 reagent BB5.1, commonly used in C driven disease research, could be used in the WT injectable model and compared to an IgG control. The mouse mAb BB5.1 binds mouse C5 and prevents it's cleavage, effectively blocking terminal pathway activation. Treatment with BB5.1 would determine the effect of MAC and C5a on tumour development *in vivo* and may provide information on the relationship between the two and whether this is additive or synergistic. BB5.1 is homologous to the human mAb eculizumab which will be discussed in the following section. C intervention would be expected to reduce gene expression responses in tumour cells and reduce development and metastasis formation in a manner homologous to KO models. These investigations would inform treatment regimens which could be adapted for cancer patients.

A confounding factor in KO, RNAi and inhibitor treatment experiments is the expression of terminal pathway components by the injected cells. This would result in C sufficiency in the tumour microenvironment serving to make the KO/RNAi/inhibitor strategy ineffectual in the relevant context. In order to address this problem it might be necessary to perform additional experiments in which terminal pathway component expression by injected cells is knocked down using RNAi. This could be performed in the same way as described for above experiments in WT and KO mice as well as RNAi knock down and inhibitor treatments, providing information on the importance of local vs. systemic sources of C terminal pathway components.

6.6 Treatment strategies

The findings of this thesis have demonstrated the pro-tumour role for C and shown that low level activation can be a contributor to tumour development, growth and metastasis. This forms part of the contribution to tumorigenesis made by inflammation. Importantly the use of anti-tumour mAb in immunotherapy which harness C activation for efficacy may require cautious administration since sub-effective doses, analogous to antibiotic

resistance, may promote tumour development and resistance to treatment through sublytic levels of MAC.

Treatment of cancer patients using C therapeutics to reduce this contribution might target C terminal pathway activation. Eculizumab could be used, a humanized monoclonal anti-C5 antibody which binds to C5 and prevents it's cleavage. Eculizumab is licensed for use in paroxysmal nocturnal haemoglobinuria (Hillmen et al, 2006). This prevents release of C5a and formation of MAC. In addition to reduction in MAC mediated effect, C5a release would be reduced, shown to have potential pro-tumour roles through recruitment and activation of suppressive MDSCs to the tumour micro-environment (Markiewski et al, 2008).

Alternatively, to inhibit MAC formation alone a soluble form of CD59 (sCD59) which is able to tether to membrane could be used, a strategy which has been developed for use in PNH (Hill et al, 2006). An alternative to this would be systemic knockdown of C6 using anti-sense oligonucleotides (RNAi) delivered by viral vector system to the liver (Fluiter et al, 2011). Removal of MAC formation would prevent any pro-tumour influence of MAC deposition but leave the remaining C functions intact including opsonization and anaphylatoxin release. Ability to control infection would be retained but increased susceptibility to *Neisseria* infection would necessitate monitoring.

Since tumours often express high levels of membrane bound C regulatory proteins (mCregs), tumour localised sublytic C may be the result of robust activation on well protected cells (Fishelson et al, 2003; Jurianz et al, 2001). Evidence for which is shown by the deposition of C products and increased activation characteristics (Niculescu et al, 1992). It might be possible to reduce CD59 expression through tumour cell targeted knockdown (Shi et al, 2009). By removing regulation during immunotherapy perhaps C activation could shift towards lytic levels and become anti-tumour.

Strategies to prevent tumour promoting sublytic C effects would best be deployed in the early stages of development. Recently transformed or pre-malignant cells may require certain triggers for transition and C activation may be a key component in this switch. Indeed the pre-malignant state might itself be assisted through inflammatory processes as is the case in breast cancer and mesothelioma (Dostert et al, 2008; Lochter et al, 1997).

6.7 Concluding remarks

A role for C in tumour promoting inflammation has only very recently gained substantive recognition. The work presented in this thesis provides evidence to suggest that MAC deposition which does not result in cell lysis is a potent tumour cell activator leading to significant changes in gene expression. Indeed the work suggests that a gene expression response might be indicative of a shift in tumour behaviour through induction of proliferative, migratory and survival pathways. The work also suggested that sublytic MAC may trigger the EGFR system. This phenomenon has been shown before but by exploiting microarray technology and systems biology this work provides more evidence of its role and the possible consequences of this activation. A role for sublytic MAC in tumour development therefore presents a therapeutic opportunity which no doubt could benefit from the C terminal pathway targeting drugs currently available.

7 References

Abe K, Li K, Sacks SH, Sheerin NS (2004) The membrane attack complex, C5b-9, up regulates collagen gene expression in renal tubular epithelial cells. *Clinical and Experimental Immunology* **136:** 60-66

Acharyya S, Oskarsson T, Vanharanta S, Malladi S, Kim J, Morris PG, Manova-Todorova K, Leversha M, Hogg N, Seshan VE, Norton L, Brogi E, Massague J (2012) A CXCL1 Paracrine Network Links Cancer Chemoresistance and Metastasis. *Cell* **150:** 165-178

Ahmed AA, Mills AD, Ibrahim AEK, Temple J, Blenkiron C, Vias M, Massie CE, Iyer NG, McGeoch A, Crawford R, Nicke B, Downward J, Swanton C, Bell SD, Earl HM, Laskey RA, Caldas C, Brenton JD (2007) The extracellular matrix protein TGFBI induces microtubule stabilization and sensitizes ovarian cancers to paclitaxel. *Cancer Cell* **12:** 514-527

Aksamitiene E, Kholodenko BN, Kolch W, Hoek JB, Kiyatkin A (2010) PI3K/Akt-sensitive MEK-independent compensatory circuit of ERK activation in ER-positive PI3K-mutant T47D breast cancer cells. *Cellular Signalling* **22:** 1369-1378

Alge-Priglinger CS, Kreutzer T, Obholzer K, Wolf A, Mempel M, Kernt M, Kampik A, Priglinger SG (2009) Oxidative Stress-Mediated Induction of MMP-1 and MMP-3 in Human RPE Cells. *Investigative Ophthalmology & Visual Science* **50:** 5495-5503

Allen SJ, Crown SE, Handel TM (2007) Chemokine: Receptor structure, interactions, and antagonism. *Annual Review of Immunology* **25:** 787-820

Altschul SF, Gish W, Miller W, Myers EW, Lipman DJ (1990) BASIC LOCAL ALIGNMENT SEARCH TOOL. *Journal of Molecular Biology* **215:** 403-410

Andreasen PA, Kjoller L, Christensen L, Duffy MJ (1997) The urokinase-type plasminogen activator system in cancer metastasis: a review. *Int J Cancer* **72:** 1-22

Aoudjit L, Stanciu M, Li HP, Lemay S, Takano T (2003) p38 Mitogen-activated protein kinase protects glomerular epithelial cells from complement-mediated cell injury. *American Journal of Physiology-Renal Physiology* **285:** F765-F774

Baalasubramanian S, Harris CL, Donev RM, Mizuno M, Omidvar N, Song WC, Morgan BP (2004) CD59a is the primary regulator of membrane attack complex assembly in the mouse. *Journal of Immunology* **173**

Badea T, Niculescu F, Soane L, Fosbrink M, Sorana H, Rus V, Shin ML, Rus H (2002) RGC-32 increases p34(CDC2) kinase activity and entry of aortic smooth muscle cells into S-phase. *Journal of Biological Chemistry* **277:** 502-508

Badea TC, Niculescu FI, Soane L, Shin ML, Rus H (1998) Molecular cloning and characterization of RGC-32, a novel gene induced by complement activation in oligodendrocytes. *Journal of Biological Chemistry* **273:** 26977-26981

Badea TD, Park JH, Soane L, Niculescu T, Niculescu F, Rus H, Shin ML (2003) Sublytic terminal complement attack induces c-fos transcriptional activation in myotubes. *Journal of Neuroimmunology* **142:** 58-66

Ballard LL, Bora NS, Yu GH, Atkinson JP (1988) BIOCHEMICAL-CHARACTERIZATION OF MEMBRANE COFACTOR PROTEIN OF THE COMPLEMENT-SYSTEM. *Journal of Immunology* **141:** 3923-3929

Barde YA, Edgar D, Thoenen H (1982) PURIFICATION OF A NEW NEUROTROPHIC FACTOR FROM MAMMALIAN BRAIN. *Embo Journal* **1:** 549-553

Barrett SD, Bridges AJ, Dudley DT, Saltiel AR, Fergus JH, Flamme CM, Delaney AM, Kaufman M, LePage S, Leopold WR, Przybranowski SA, Sebolt-Leopold J, Van Becelaere K, Doherty AM, Kennedy RM, Marston D, Howard WA, Smith Y, Warmus JS, Tecle H (2008) The discovery of the benzhydroxamate MEK inhibitors CI-1040 and PD 0325901. *Bioorganic & Medicinal Chemistry Letters* **18:** 6501-6504

Beadling C, Druey KM, Richter G, Kehrl JW, Smith KA (1999) Regulators of G protein signaling exhibit distinct patterns of gene expression and target G protein specificity in human lymphocytes. *Journal of Immunology* **162:** 2677-2682

Becker C, Fantini MC, Schramm C, Lehr HA, Wirtz S, Nikolaev A, Burg J, Strand S, Kiesslich R, Huber S, Ito H, Nishimoto N, Yoshizaki K, Kishimoto T, Galle PR, Blessing M, Rose-John S, Neurath MF (2004) TGF-beta suppresses tumor progression in colon cancer by inhibition of IL-6 trans-signaling. *Immunity* **21:** 491-501

Becker JW, Marcy AI, Rokosz LL, Axel MG, Burbaum JJ, Fitzgerald PMD, Cameron PM, Esser CK, Hagmann WK, Hermes JD, Springer JP (1995) STROMELYSIN-1 - 3-DIMENSIONAL STRUCTURE OF THE INHIBITED CATALYTIC DOMAIN AND OF THE C-TRUNCATED PROENZYME. *Protein Science* **4:** 1966-1976

Ben-Izhak O, Bar-Chana M, Sussman L, Dobiner V, Sandbank J, Cagnano M, Cohen H, Sabo E (2002) Ki67 antigen and PCNA proliferation markers predict survival in anorectal malignant melanoma. *Histopathology* **41:** 519-525

Benjamini Y, Hochberg Y (1995) CONTROLLING THE FALSE DISCOVERY RATE - A PRACTICAL AND POWERFUL APPROACH TO MULTIPLE TESTING. *Journal of the Royal Statistical Society Series B-Methodological* **57:** 289-300

Bennett BL, Sasaki DT, Murray BW, O'Leary EC, Sakata ST, Xu WM, Leisten JC, Motiwala A, Pierce S, Satoh Y, Bhagwat SS, Manning AM, Anderson DW (2001) SP600125, an anthrapyrazolone inhibitor of Jun N-terminal kinase. *Proceedings of the National Academy of Sciences of the United States of America* **98:** 13681-13686

Benzaquen LR, Nicholsonweller A, Halperin JA (1994) TERMINAL COMPLEMENT PROTEINS C5B-9 RELEASE BASIC FIBROBLAST GROWTH-FACTOR AND PLATELET-DERIVED GROWTH-FACTOR FROM ENDOTHELIAL-CELLS. *Journal of Experimental Medicine* **179:** 985-992

Berasain C, Garcia-Trevijano ER, Castillo J, Erroba E, Santamaria M, Lee DC, Prieto J, Avila MA (2005) Novel role for amphiregulin in protection from liver injury. *Journal of Biological Chemistry* **280:** 19012-19020

Berman DM, Wilkie TM, Gilman AG (1996) GAIP and RGS4 are GTPase-activating proteins for the G(i) subfamily of G protein alpha subunits. *Cell* **86:** 445-452

Bexborn F, Andersson PO, Chen H, Nilsson B, Ekdahl KN (2008) The tick-over theory revisited: formation and regulation of the soluble alternative complement C3 convertase (C3(H2O)Bb). *Mol Immunol* **45:** 2370-2379

Billings PC, Whitbeck JC, Adams CS, Abrams WR, Cohen AJ, Engelsberg BN, Howard PS, Rosenbloom J (2002) The transforming growth factor-beta-inducibie matrix protein beta ig-h3 interacts with fibronectin. *Journal of Biological Chemistry* **277:** 28003-28009

Bjorge L, Hakulinen J, Vintermyr OK, Jarva H, Jensen TS, Iversen OE, Meri S (2005) Ascitic complement system in ovarian cancer. *Br J Cancer* **92:** 895-905

Black RA, Kronheim SR, Cantrell M, Deeley MC, March CJ, Prickett KS, Wignall J, Conlon PJ, Cosman D, Hopp TP, Mochizuki DY (1988) GENERATION OF BIOLOGICALLY-ACTIVE INTERLEUKIN-1-BETA BY PROTEOLYTIC CLEAVAGE OF THE INACTIVE PRECURSOR. *Journal of Biological Chemistry* **263:** 9437-9442

Blom AM, Villoutreix BO, Dahlbäck B (2004) Functions of human complement inhibitor C4b-binding protein in relation to its structure. *Arch Immunol Ther Exp (Warsz)* **52:** 83-95

Bolitho C, Hahn MA, Baxter RC, Marsh DJ (2010) The chemokine CXCL1 induces proliferation in epithelial ovarian cancer cells by transactivation of the epidermal growth factor receptor. *Endocrine-Related Cancer* **17:** 929-940

Bollrath J, Phesse TJ, von Burstin VA, Putoczki T, Bennecke M, Bateman T, Nebelsiek T, Lundgren-May T, Canli O, Schwitalla S, Matthews V, Schmid RM, Kirchner T, Arkan MC, Ernst M, Greten FR (2009) gp130-mediated Stat3 activation in enterocytes regulates cell survival and cell-cycle progression during colitis-associated tumorigenesis. *Cancer Cell* **15:** 91-102

Bolstad BM, Irizarry RA, Astrand M, Speed TP (2003) A comparison of normalization methods for high density oligonucleotide array data based on variance and bias. *Bioinformatics* **19:** 185-193

Bordoni R, Fine R, Murray D, Richmond A (1990) CHARACTERIZATION OF THE ROLE OF MELANOMA GROWTH STIMULATORY ACTIVITY (MGSA) IN THE GROWTH OF NORMAL MELANOCYTES, NEVOCYTES, AND MALIGNANT MELANOCYTES. *Journal of Cellular Biochemistry* **44:** 207-219

Botos I, Meyer E, Swanson SM, Lemaitre V, Eeckhout Y, Meyer EF (1999) Structure of recombinant mouse collagenase-3 (MMP-13). *Journal of Molecular Biology* **292:** 837-844

Boyle MD, Ohanian SH, Borsos T (1976) Studies on the terminal stages of antibody-complement-mediated killing of a tumor cell. II. Inhibition of transformation of T to dead cells by 3'5' cAMP. *J Immunol* **116:** 1276-1279

Brandt J, Pippin J, Schulze M, Hänsch GM, Alpers CE, Johnson RJ, Gordon K, Couser WG (1996) Role of the complement membrane attack complex (C5b-9) in mediating experimental mesangioproliferative glomerulonephritis. *Kidney Int* **49:** 335-343

Brattain MG, Strobelstevens J, Fine D, Webb M, Sarrif AM (1980) ESTABLISHMENT OF MOUSE COLONIC-CARCINOMA CELL-LINES WITH DIFFERENT METASTATIC PROPERTIES. *Cancer Research* **40:** 2142-2146

Brown CL, Meise KS, Plowman GD, Coffey RJ, Dempsey PJ (1998) Cell surface ectodomain cleavage of human amphiregulin precursor is sensitive to a metalloprotease inhibitor - Release of a predominant N-glycosylated 43-kDa soluble form. *Journal of Biological Chemistry* **273:** 17258-17268

Bugrim A, Nikolskaya T, Nikolsky Y (2004) Early prediction of drug metabolism and toxicity: systems biology approach and modeling. *Drug Discovery Today* **9:** 127-135

Bullock AN, Rodriguez MC, Debreczeni JE, Songyang Z, Knapp S (2007) Structure of the SOCS4-ElonginB/C complex reveals a distinct SOCS box interface and the molecular basis for SOCS-dependent EGFR degradation. *Structure* **15:** 1493-1504

Burgering BMT, Coffer PJ (1995) PROTEIN-KINASE-B (C-AKT) IN PHOSPHATIDYLINOSITOL-3-OH INASE SIGNAL-TRANSDUCTION. *Nature* **376:** 599-602

Campbell AK, Daw RA, Hallett MB, Luzio JP (1981) Direct measurement of the increase in intracellular free calcium ion concentration in response to the action of complement. *Biochem J* **194:** 551-560

Campbell AK, Daw RA, Luzio JP (1979) Rapid increase in intracellular free Ca2+ induced by antibody plus complement. *FEBS Lett* **107:** 55-60

Campbell AK, Hallett MB (1983) MEASUREMENT OF INTRACELLULAR CALCIUM-IONS AND OXYGEN RADICALS IN POLYMORPHONUCLEAR LEUKOCYTE-ERYTHROCYTE GHOST HYBRIDS. *Journal of Physiology-London* **338**

Campbell AK, Morgan BP (1985) Monoclonal antibodies demonstrate protection of polymorphonuclear leukocytes against complement attack. *Nature* **317:** 164-166

Cardone MH, Roy N, Stennicke HR, Salvesen GS, Franke T, Stanbridge E, Frisch S, Reed JC (1999) Regulation of cell death protease caspase-9 by phosphorylation. *Proceedings of the American Association for Cancer Research Annual Meeting* **40:** 307-307

Carney DF, Hammer CH, Shin ML (1986) Elimination of terminal complement complexes in the plasma membrane of nucleated cells: influence of extracellular Ca2+ and association with cellular Ca2+. *J Immunol* **137:** 263-270

Carney DF, Koski CL, Shin ML (1985) Elimination of terminal complement intermediates from the plasma membrane of nucleated cells: the rate of disappearance differs for cells carrying C5b-7 or C5b-8 or a mixture of C5b-8 with a limited number of C5b-9. *J Immunol* **134:** 1804-1809

Carpenter G (1999) Employment of the epidermal growth factor receptor in growth factor-independent signaling pathways. *Journal of Cell Biology* **146:** 697-702

Carroll MC (2000) The role of complement in B cell activation and tolerance. *Advances in immunology* **74:** 61-88

Castillo J, Erroba E, Perugorria MJ, Santamaria M, Lee DC, Prieto J, Avila MA, Berasain C (2006) Amphiregulin contributes to the transformed phenotype of human hepatocellular carcinoma cells. *Cancer Research* **66:** 6129-6138

Cavalieri D, De Filippo C (2005) Bioinformatic methods for integrating whole-genome expression results into cellular networks. *Drug Discovery Today* **10:** 727-734

Chang F, Steelman LS, Lee JT, Shelton JG, Navolanic PM, Blalock WL, Franklin RA, McCubrey JA (2003) Signal transduction mediated by the Ras/Raf/MEK/ERK pathway

from cytokine receptors to transcription factors: potential targeting for therapeutic intervention. *Leukemia* **17:** 1263-1293

Chang H-J, Yang M-J, Yang Y-H, Hou M-F, Hsueh E-J, Lin S-R (2009) MMP13 is potentially a new tumor marker for breast cancer diagnosis. *Oncology Reports* **22:** 1119-1127

Cheung NK, Walter EI, Smith-Mensah WH, Ratnoff WD, Tykocinski ML, Medof ME (1988) Decay-accelerating factor protects human tumor cells from complement-mediated cytotoxicity in vitro. *J Clin Invest* **81:** 1122-1128

Cheung VG, Morley M, Aguilar F, Massimi A, Kucherlapati R, Childs G (1999) Making and reading microarrays. *Nat Genet* **21:** 15-19

Chintakuntlawar AV, Chodosh J (2009) Chemokine CXCL1/KC and its Receptor CXCR2 Are Responsible for Neutrophil Chemotaxis in Adenoviral Keratitis. *Journal of Interferon and Cytokine Research* **29:** 657-666

Chuaqui RF, Bonner RF, Best CJM, Gillespie JW, Flaig MJ, Hewitt SM, Phillips JL, Krizman DB, Tangrea MA, Ahram M, Linehan WM, Knezevic V, Emmert-Buck MR (2002) Post-analysis follow-up and validation of microarray experiments. *Nature Genetics* **32:** 509-514

Chung JY, Park YC, Ye H, Wu H (2002) All TRAFs are not created equal: common and distinct molecular mechanisms of TRAF-mediated signal transduction. *Journal of Cell Science* **115:** 679-688

Churchil.Wh, Weintrau.Rm, Borsos T, Rapp HJ (1967) MOUSE COMPLEMENT - EFFECT OF SEX HORMONES AND CASTRATION ON 2 OF LATE-ACTING COMPONENTS. *Journal of Experimental Medicine* **125:** 657-&

Ciardiello F, Kim N, Saeki T, Dono R, Persico MG, Plowman GD, Garrigues J, Radke S, Todaro GJ, Salomon DS (1991) DIFFERENTIAL EXPRESSION OF EPIDERMAL GROWTH FACTOR-RELATED PROTEINS IN HUMAN COLORECTAL TUMORS. *Proceedings of the National Academy of Sciences of the United States of America* **88:** 7792-7796

Cikes M, Friberg S (1971) Expression of H-2 and Moloney leukemia virus-determined cell-surface antigens in synchronized cultures of a mouse cell line. *Proc Natl Acad Sci U S A* **68:** 566-569

Cole DS, Morgan BP (2003) Beyond lysis: how complement influences cell fate. *Clinical Science* **104:** 455-466

Cooper NR, Polley MJ, Oldstone MB (1974) Failure of terminal complement components to induce lysis of Moloney virus transformed lymphocytes. *J Immunol* **112:** 866-868

Corbett TH, Griswold DP, Roberts BJ, Peckham JC, Schabel FM (1975) TUMOR INDUCTION RELATIONSHIPS IN DEVELOPMENT OF TRANSPLANTABLE CANCERS OF COLON IN MICE FOR CHEMOTHERAPY ASSAYS, WITH A NOTE ON CARCINOGEN STRUCTURE. *Cancer Research* **35:** 2434-2439

Cornacoff JB, Hebert LA, Smead WL, Vanaman ME, Birmingham DJ, Waxman FJ (1983) PRIMATE ERYTHROCYTE-IMMUNE COMPLEX-CLEARING MECHANISM. *Journal of Clinical Investigation* **71:** 236-247

Coussens LM, Werb Z (2001) Inflammatory cells and cancer: Think different! *Journal of Experimental Medicine* **193:** F23-F26

Coussens LM, Werb Z (2002) Inflammation and cancer. *Nature* **420:** 860-867

Cragg MS, Glennie MJ (2004) Antibody specificity controls in vivo effector mechanisms of anti-CD20 reagents. *Blood* **103:** 2738-2743

Cudrici C, Niculescu F, Jensen T, Zafranskaia E, Fosbrink M, Rus V, Shin ML, Rus H (2006) C5b-9 terminal complex protects oligodendrocytes from apoptotic cell death by inhibiting caspase-8 processing and up-regulating FLIP. (vol 176, pg 3173, 2006). *Journal of Immunology* **176**

Curtis RK, Oresic M, Vidal-Puig A (2005) Pathways to the analysis of microarray data. *Trends in Biotechnology* **23:** 429-435

Cybulsky AV (1991) RELEASE OF ARACHIDONIC-ACID BY COMPLEMENT C5B-9 COMPLEX IN GLOMERULAR EPITHELIAL-CELLS. *American Journal of Physiology* **261:** F427-F427

Cybulsky AV, Monge JC, Papillon J, McTavish AJ (1995) COMPLEMENT C5B-9 ACTIVATES CYTOSOLIC PHOSPHOLIPASE A(2) IN GLOMERULAR EPITHELIAL-CELLS. *American Journal of Physiology-Renal Fluid and Electrolyte Physiology* **269**

Cybulsky AV, Papillon J, McTavish AJ (1998) Complement activates phospholipases and protein kinases in glomerular epithelial cells. *Kidney International* **54:** 360-372

Cybulsky AV, Takano T, Papillon J, McTavish AJ (1999) Complement C5b-9 induces receptor tyrosine kinase transactivation in glomerular epithelial cells. *American Journal of Pathology* **155:** 1701-1711

D'Antonio A, Losito S, Pignata S, Grassi M, Perrone F, De Luca A, Tambaro R, Bianco C, Gullick WJ, Johnson GR, Iaffaioli VR, Salomon DS, Normanno N (2002) Transforming growth factor alpha, amphiregulin and cripto-1 are frequently expressed in advanced human ovarian carcinomas. *International Journal of Oncology* **21:** 941-948

Daffern PJ, Pfeifer PH, Ember JA, Hugli TE (1995) C3a is a chemotaxin for human eosinophils but not for neutrophils. I. C3a stimulation of neutrophils is secondary to eosinophil activation. *J Exp Med* **181:** 2119-2127

Daha MR, van Es LA (1980) Relative resistance of the F-42-stabilized classical pathway C3 convertase to inactivation by C4-binding protein. *J Immunol* **125:** 2051-2054

Dashiell SM, Rus H, Koski CL (2000) Terminal complement complexes concomitantly stimulate proliferation and rescue of Schwann cells from apoptosis. *Glia* **30:** 187-198

Daub H, Wallasch C, Lankenau A, Herrlich A, Ullrich A (1997) Signal characteristics of G protein-transactivated EGF receptor. *Embo Journal* **16:** 7032-7044

Daub H, Weiss FU, Wallasch C, Ullrich A (1996) Role of transactivation of the EGF receptor in signalling by G-protein-coupled receptors. *Nature* **379:** 557-560

Davies A, Simmons DL, Hale G, Harrison RA, Tighe H, Lachmann PJ, Waldmann H (1989) CD59, an LY-6-like protein expressed in human lymphoid cells, regulates the

action of the complement membrane attack complex on homologous cells. *J Exp Med* **170:** 637-654

Davis AE (1981) The C3b inactivator of the human complement system: homology with serine proteases. *FEBS Lett* **134:** 147-150

Davis AE, Mejia P, Lu F (2008) Biological activities of C1 inhibitor. *Mol Immunol* **45:** 4057-4063

Davis RJ (2000) Signal transduction by the JNK group of MAP kinases. *Cell* **103:** 239-252

Davitz MA, Low MG, Nussenzweig V (1986) RELEASE OF DECAY-ACCELERATING FACTOR (DAF) FROM THE CELL-MEMBRANE BY PHOSPHATIDYLINOSITOL-SPECIFIC PHOSPHOLIPASE-C (PIPLC) - SELECTIVE MODIFICATION OF A COMPLEMENT REGULATORY PROTEIN. *Journal of Experimental Medicine* **163:** 1150-1161

De Ambrosis A, Casciano I, Croce M, Pagnan G, Radic L, Banelli B, Di Vinci A, Allemanni G, Tonini GP, Ponzoni M, Romani M, Ferrini S (2007) An interferon-sensitive response element is involved in constitutive caspase-8 gene expression in neuroblastoma cells. *International Journal of Cancer* **120:** 39-47

de Martel C, Franceschi S (2009) Infections and cancer: established associations and new hypotheses. *Crit Rev Oncol Hematol* **70:** 183-194

Delany AM, Brinckerhoff CE (1992) POSTTRANSCRIPTIONAL REGULATION OF COLLAGENASE AND STROMELYSIN GENE-EXPRESSION BY EPIDERMAL GROWTH-FACTOR AND DEXAMETHASONE IN CULTURED HUMAN FIBROBLASTS. *Journal of Cellular Biochemistry* **50:** 400-410

Deng L, Wang C, Spencer E, Yang LY, Braun A, You JX, Slaughter C, Pickart C, Chen ZJ (2000) Activation of the I kappa B kinase complex by TRAF6 requires a dimeric ubiquitin-conjugating enzyme complex and a unique polyubiquitin chain. *Cell* **103:** 351-361

Derrien A, Druey KM (2001) RGS16 function is regulated by epidermal growth factor receptor-mediated tyrosine phosphorylation. *Journal of Biological Chemistry* **276:** 48532-48538

Deryugina EI, Quigley JP (2006) Matrix metalloproteinases and tumor metastasis. *Cancer and Metastasis Reviews* **25:** 9-34

Di Gaetano N, Cittera E, Nota R, Vecchi A, Grieco V, Scanziani E, Botto M, Introna M, Golay J (2003) Complement activation determines the therapeutic activity of rituximab in vivo. *J Immunol* **171:** 1581-1587

Diaz-Montero CM, Salem ML, Nishimura MI, Garrett-Mayer E, Cole DJ, Montero AJ (2009) Increased circulating myeloid-derived suppressor cells correlate with clinical cancer stage, metastatic tumor burden, and doxorubicin-cyclophosphamide chemotherapy. *Cancer Immunology Immunotherapy* **58:** 49-59

Discipio RG, Hugli TE (1989) THE MOLECULAR ARCHITECTURE OF HUMAN-COMPLEMENT COMPONENT-C6. *Journal of Biological Chemistry* **264:** 16197-16206

Discipio RG, Smith CA, Mullereberhard HJ, Hugli TE (1983) THE ACTIVATION OF HUMAN-COMPLEMENT COMPONENT-C5 BY A FLUID PHASE C5-CONVERTASE. *Journal of Biological Chemistry* **258:** 629-636

Donev RM, Sivasankar B, Mizuno M, Morgan BP (2008) The mouse complement regulator CD59b is significantly expressed only in testis and plays roles in sperm acrosome activation and motility. *Molecular Immunology* **45:** 534-542

Dong JY, Opresko LK, Dempsey PJ, Lauffenburger DA, Coffey RJ, Wiley HS (1999) Metalloprotease-mediated ligand release regulates autocrine signaling through the epidermal growth factor receptor. *Proceedings of the National Academy of Sciences of the United States of America* **96:** 6235-6240

Donin N, Jurianz K, Ziporen L, Schultz S, Kirschfink M, Fishelson Z (2003) Complement resistance of human carcinoma cells depends on membrane regulatory proteins, protein kinases and sialic acid. *Clin Exp Immunol* **131:** 254-263

Dostert C, Pétrilli V, Van Bruggen R, Steele C, Mossman BT, Tschopp J (2008) Innate immune activation through Nalp3 inflammasome sensing of asbestos and silica. *Science* **320:** 674-677

Dunkelberger JR, Song W-C (2010) Role and mechanism of action of complement in regulating T cell immunity. *Molecular Immunology* **47:** 2176-2186

Ebanks RO, Isenman DE (1996) Mouse complement component C4 is devoid of classical pathway C5 convertase subunit activity. *Molecular Immunology* **33:** 297-309

Ebert M, Yokoyama M, Kobrin MS, Friess H, Lopez ME, Buchler MW, Johnson GR, Korc M (1994) INDUCTION AND EXPRESSION OF AMPHIREGULIN IN HUMAN PANCREATIC-CANCER. *Cancer Research* **54:** 3959-3962

Egeblad M, Werb Z (2002) New functions for the matrix metalloproteinases in cancer progression. *Nature Reviews Cancer* **2:** 161-174

Eguchi S, Numaguchi K, Iwasaki H, Matsumoto T, Yamakawa T, Utsunomiya H, Motley ED, Kawakatsu H, Owada KM, Hirata Y, Marumo F, Inagami T (1998) Calcium-dependent epidermal growth factor receptor transactivation mediates the angiotensin II-induced mitogen-activated protein kinase activation in vascular smooth muscle cells. *Journal of Biological Chemistry* **273:** 8890-8896

Ehrenreich A (2006) DNA microarray technology for the microbiologist: an overview. *Applied Microbiology and Biotechnology* **73:** 255-273

Eisenhart C (1947) THE ASSUMPTIONS UNDERLYING THE ANALYSIS OF VARIANCE. *Biometrics* **3:** 1-21

Ekbom A, Helmick C, Zack M, Adami HO (1990a) Increased risk of large-bowel cancer in Crohn's disease with colonic involvement. *Lancet* **336:** 357-359

Ekbom A, Helmick C, Zack M, Adami HO (1990b) Ulcerative colitis and colorectal cancer. A population-based study. *N Engl J Med* **323:** 1228-1233

Ellison BS, Zanin MK, Boackle RJ (2007) Complement susceptibility in glutamine deprived breast cancer cells. *Cell Div* **2:** 20

Elsner J, Oppermann M, Czech W, Dobos G, Schöpf E, Norgauer J, Kapp A (1994a) C3a activates reactive oxygen radical species production and intracellular calcium transients in human eosinophils. *Eur J Immunol* **24:** 518-522

Elsner J, Oppermann M, Czech W, Kapp A (1994b) C3a activates the respiratory burst in human polymorphonuclear neutrophilic leukocytes via pertussis toxin-sensitive G-proteins. *Blood* **83:** 3324-3331

Ember JA, Sanderson SD, Taylor SM, Kawahara M, Hugli TE (1992) Biologic activity of synthetic analogues of C5a anaphylatoxin. *J Immunol* **148:** 3165-3173

Etienne W, Meyer MH, Peppers J, Meyer RA (2004) Comparison of mRNA gene expression by RT-PCR and DNA microarray. *Biotechniques* **36:** 618-+

Fallman M, Andersson R, Andersson T (1993) SIGNALING PROPERTIES OF CR3 (CD11B/CD18) AND CR-1 (CD35) IN RELATION TO PHAGOCYTOSIS OF COMPLEMENT-OPSONIZED PARTICLES. *Journal of Immunology* **151:** 330-338

Farace MG, Brown BA, Raschella G, Alexander J, Gambari R, Fantoni A, Hardies SC, Hutchison CA, Edgell MH (1984) THE MOUSE BETA-H1 GENE CODES FOR THE Z-CHAIN OF EMBRYONIC HEMOGLOBIN. *Journal of Biological Chemistry* **259:** 7123-7128

Fearon DT (1980) IDENTIFICATION OF THE MEMBRANE GLYCOPROTEIN THAT IS THE C3B RECEPTOR OF THE HUMAN-ERYTHROCYTE, POLYMORPHONUCLEAR LEUKOCYTE, LYMPHOCYTE-B, AND MONOCYTE. *Journal of Experimental Medicine* **152:** 20-30

Fearon DT, Austen KF, Ruddy S (1973) Formation of a hemolytically active cellular intermediate by the interaction between properdin factors B and D and the activated third component of complement. *J Exp Med* **138:** 1305-1313

Ferreira A, Weiszcarrington P, Nussenzweig V (1978) TESTOSTERONE CONTROL OF SERUM LEVELS OF C4-BINDING PROTEIN IN MICE. *Journal of Immunology* **121:** 1213-1215

Finch AM, Wong AK, Paczkowski NJ, Wadi SK, Craik DJ, Fairlie DP, Taylor SM (1999) Low-molecular-weight peptidic and cyclic antagonists of the receptor for the complement factor C5a. *Journal of Medicinal Chemistry* **42:** 1965-1974

Fischer OM, Hart S, Gschwind A, Prenzel N, Ullrich A (2004) Oxidative and osmotic stress signaling in tumor cells is mediated by ADAM proteases and heparin-binding epidermal growth factor. *Molecular and Cellular Biology* **24:** 5172-5183

Fishelson Z, Donin N, Zell S, Schultz S, Kirschfink M (2003) Obstacles to cancer immunotherapy: expression of membrane complement regulatory proteins (mCRPs) in tumors. *Mol Immunol* **40:** 109-123

Fishelson Z, Pangburn MK, Müller-Eberhard HJ (1984) Characterization of the initial C3 convertase of the alternative pathway of human complement. *J Immunol* **132:** 1430-1434

Fluiter K, Ramaglia V, Baas F (2011) INHIBITION OF COMPLEMENT C6 SYNTHESIS IN THE LIVER USING ANTISENSE OLIGONUCLEOTIDES AFFECTS NEURO-REGENERATION. *Nucleic Acid Therapeutics* **21:** A8-A8

Fontanini G, De Laurentiis M, Vignati S, Chine S, Lucchi M, Silvestri V, Mussi A, De Placido S, Tortora G, Bianco AR, Gullick W, Angeletti CA, Bevilacqua G, Ciardiello F (1998) Evaluation of epidermal growth factor-related growth factors and receptors and of neoangiogenesis in completely resected stage I-IIIA non-small-cell lung cancer: Amphiregulin and microvessel count are independent prognostic indicators of survival. *Clinical Cancer Research* **4:** 241-249

Fosbrink M, Niculescu F, Rus V, Shin ML, Rus H (2006) C5b-9-induced endothelial cell proliferation and migration are dependent on Akt inactivation of forkhead transcription factor FOXO1. *Journal of Biological Chemistry* **281:** 19009-19018

Franco AT, Johnston E, Krishna U, Yamaoka Y, Israel DA, Nagy TA, Wroblewski LE, Piazuelo MB, Correa P, Peek RM, Jr. (2008) Regulation of gastric carcinogenesis by helicobacter pylori virulence factors. *Cancer Research* **68:** 379-387

Fredslund F, Laursen NS, Roversi P, Jenner L, Oliveira CLP, Pedersen JS, Nunn MA, Lea SM, Discipio R, Sottrup-Jensen L, Andersen GR (2008) Structure of and influence of a tick complement inhibitor on human complement component 5. *Nature Immunology* **9**

Fu MG, Zhu XJ, Zhang JF, Liang J, Lin YM, Zhao LN, Ehrengruber MU, Chen YQE (2003) Egr-1 target genes in human endothelial cells identified by microarray analysis. *Gene* **315:** 33-41

Fujita T, Gigli I, Nussenzweig V (1978) Human C4-binding protein. II. Role in proteolysis of C4b by C3b-inactivator. *J Exp Med* **148:** 1044-1051

Fujita T, Inoue T, Ogawa K, Iida K, Tamura N (1987) THE MECHANISM OF ACTION OF DECAY-ACCELERATING FACTOR (DAF) DAF INHIBITS THE ASSEMBLY OF C-3 CONVERTASES BY DISSOCIATING C2A AND BB. *Journal of Experimental Medicine* **166:** 1221-1228

Gamou S, Shimizu N (1995) HYDROGEN-PEROXIDE PREFERENTIALLY ENHANCES THE TYROSINE PHOSPHORYLATION OF EPIDERMAL GROWTH-FACTOR RECEPTOR. *Febs Letters* **357:** 161-164

Gao H, Neff TA, Guo RF, Speyer CL, Sarma JV, Tomlins S, Man Y, Riedemann NC, Hoesel LM, Younkin E, Zetoune FS, Ward PA (2005) Evidence for a functional role of the second C5a receptor C5L2. *FASEB J* **19:** 1003-1005

Gao L, Qiu W, Wang Y, Xu W, Xu J, Tong J (2007) Sublytic complement C5b-9 complexes induce thrombospondin-1 production in rat glomerular mesangial cells via PI3-k/Akt: Association with activation of latent transforming growth factor-beta1. *Molecular Immunology* **44:** 174-174

Gao LJ, Guo SY, Cai YQ, Gu PQ, Su YJ, Gong H, Liu Y, Chen C (2009) Cooperation of decay-accelerating factor and membrane cofactor protein in regulating survival of human cervical cancer cells. *BMC Cancer* **9:** 384

Gasque P, Chan P, Fontaine M, Ischenko A, Lamacz M, Gotze O, Morgan BP (1995) IDENTIFICATION AND CHARACTERIZATION OF THE COMPLEMENT C5A ANAPHYLATOXIN RECEPTOR ON HUMAN ASTROCYTES. *Journal of Immunology* **155:** 4882-4889

Gerard C, Gerard NP (1994) C5A anaphylatoxin and its seven transmembrane-segment receptor. *Annu Rev Immunol* **12:** 775-808

Gigli I, Fujita T, Nussenzweig V (1979) Modulation of the classical pathway C3 convertase by plasma proteins C4 binding protein and C3b inactivator. *Proc Natl Acad Sci U S A* **76:** 6596-6600

Gimmi ER, Soprano KJ, Rosenberg M, Reff ME (1988) DELETIONS IN THE SV40 LATE POLYADENYLATION REGION DOWNSTREAM OF THE AATAAA MEDIATE SIMILAR EFFECTS ON EXPRESSION IN VARIOUS MAMMALIAN-CELL LINES. *Nucleic Acids Research* **16:** 8977-8997

Gorter A, Blok VT, Haasnoot WH, Ensink NG, Daha MR, Fleuren GJ (1996) Expression of CD46, CD55, and CD59 on renal tumor cell lines and their role in preventing complement-mediated tumor cell lysis. *Lab Invest* **74:** 1039-1049

Grant SL, Hammacher A, Douglas AM, Goss GA, Mansfield RK, Heath JK, Begley CG (2002) An unexpected biochemical and functional interaction between gp130 and the EGF receptor family in breast cancer cells. *Oncogene* **21:** 460-474

Greten FR, Eckmann L, Greten TF, Park JM, Li ZW, Egan LJ, Kagnoff MF, Karin M (2004) IKKbeta links inflammation and tumorigenesis in a mouse model of colitis-associated cancer. *Cell* **118:** 285-296

Grivennikov S, Karin E, Terzic J, Mucida D, Yu GY, Vallabhapurapu S, Scheller J, Rose-John S, Cheroutre H, Eckmann L, Karin M (2009) IL-6 and Stat3 are required for survival of intestinal epithelial cells and development of colitis-associated cancer. *Cancer Cell* **15:** 103-113

Gunderson KL, Kruglyak S, Graige MS, Garcia F, Kermani BG, Zhao CF, Che DP, Dickinson T, Wickham E, Bierle J, Doucet D, Milewski M, Yang R, Siegmund C, Haas J, Zhou LX, Oliphant A, Fan JB, Barnard S, Chee MS (2004) Decoding randomly ordered DNA arrays. *Genome Research* **14:** 870-877

Halperin JA, Taratuska A, Nicholson-Weller A (1993a) Terminal complement complex C5b-9 stimulates mitogenesis in 3T3 cells. *J Clin Invest* **91:** 1974-1978

Halperin JA, Taratuska A, Rynkiewicz M, Nicholson-Weller A (1993b) Transient changes in erythrocyte membrane permeability are induced by sublytic amounts of the complement membrane attack complex (C5b-9). *Blood* **81:** 200-205

Han J, Lee JD, Bibbs L, Ulevitch RJ (1994) A MAP KINASE TARGETED BY ENDOTOXIN AND HYPEROSMOLARITY IN MAMMALIAN-CELLS. *Science* **265:** 808-811

Hansch GM, Seitz M, Betz M (1987) EFFECT OF THE LATE COMPLEMENT COMPONENTS-C5B-9 ON HUMAN-MONOCYTES - RELEASE OF PROSTANOIDS, OXYGEN RADICALS AND OF A FACTOR INDUCING CELL-PROLIFERATION. *International Archives of Allergy and Applied Immunology* **82:** 317-320

Harjunpaa A, Junnikkala S, Meri S (2000) Rituximab (anti-CD20) therapy of B-cell lymphomas: direct complement killing is superior to cellular effector mechanisms. *Scand J Immunol* **51:** 634-641

Harris CL, Rushmere NK, Morgan BP (1999) Molecular and functional analysis of mouse decay accelerating factor (CD55). *Biochemical Journal* **341:** 821-829

Harris MA, Clark J, Ireland A, Lomax J, Ashburner M, Foulger R, Eilbeck K, Lewis S, Marshall B, Mungall C, Richter J, Rubin GM, Blake JA, Bult C, Dolan M, Drabkin H, Eppig JT, Hill DP, Ni L, Ringwald M, Balakrishnan R, Cherry JM, Christie KR, Costanzo MC, Dwight SS, Engel S, Fisk DG, Hirschman JE, Hong EL, Nash RS, Sethuraman A, Theesfeld CL, Botstein D, Dolinski K, Feierbach B, Berardini T, Mundodi S, Rhee SY, Apweiler R, Barrell D, Camon E, Dimmer E, Lee V, Chisholm R, Gaudet P, Kibbe W, Kishore R, Schwarz EM, Sternberg P, Gwinn M, Hannick L, Wortman J, Berriman M, Wood V, de la Cruz N, Tonellato P, Jaiswal P, Seigfried T, White R, Gene Ontology C (2004) The Gene Ontology (GO) database and informatics resource. *Nucleic Acids Research* **32:** D258-D261

Hattori R, Hamilton KK, McEver RP, Sims PJ (1989) COMPLEMENT PROTEINS C5B-9 INDUCE SECRETION OF HIGH MOLECULAR-WEIGHT MULTIMERS OF ENDOTHELIAL VONWILLEBRAND-FACTOR AND TRANSLOCATION OF GRANULE MEMBRANE-PROTEIN GMP-140 TO THE CELL-SURFACE. *Journal of Biological Chemistry* **264:** 9053-9060

Heinen S, Hartmann A, Lauer N, Wiehl U, Dahse H-M, Schirmer S, Gropp K, Enghardt T, Wallich R, Haelbich S, Mihlan M, Schloetzer-Schrehardt U, Zipfel PF, Skerka C (2009) Factor H-related protein 1 (CFHR-1) inhibits complement C5 convertase activity and terminal complex formation. *Blood* **114**

Hepburn NJ, Williams AS, Nunn MA, Chamberlain-Banoub JC, Hamer J, Morgan BP, Harris CL (2007) In vivo characterization and therapeutic efficacy of a C5-specific inhibitor from the soft tick Ornithodoros moubata. *Journal of Biological Chemistry* **282:** 8292-8299

Hila S, Soane L, Koski CL (2001) Sublytic C5b-9-stimulated Schwann cell survival through PI 3-kinase-mediated phosphorylation of BAD. *Glia* **36**

Hill A, Ridley SH, Esser D, Oldroyd RG, Cullen MJ, Kareclas P, Gallagher S, Smith GP, Richards SJ, White J, Smith RAG, Hillmen P (2006) Protection of erythrocytes from human complement-mediated lysis by membrane-targeted recombinant soluble CD59: a new approach to PNH therapy. *Blood* **107:** 2131-2137

Hillmen P, Young NS, Schubert J, Brodsky RA, Socie G, Muus P, Roeth A, Szer J, Elebute MO, Nakamura R, Browne P, Risitano AM, Hill A, Schrezenmeier H, Fu C-L, Maciejewski J, Rollins SA, Mojcik CF, Rother RP, Luzzatto L (2006) The complement inhibitor eculizumab in paroxysmal nocturnal hemoglobinuria. *New England Journal of Medicine* **355:** 1233-1243

Holers VM, Kinoshita T, Molina H (1994) Identification and analysis of functional domains of mouse complement receptors 1 and 2. *Journal of Cellular Biochemistry Supplement* **0:** 297-297

Holguin MH, Wilcox LA, Bernshaw NJ, Rosse WF, Parker CJ (1990) ERYTHROCYTE-MEMBRANE INHIBITOR OF REACTIVE LYSIS - EFFECTS OF PHOSPHATIDYLINOSITOL-SPECIFIC PHOSPHOLIPASE-C ON THE ISOLATED AND CELL-ASSOCIATED PROTEIN. *Blood* **75**

Hsiung L, Barclay AN, Brandon MR, Sim E, Porter RR (1982) Purification of human C3b inactivator by monoclonal-antibody affinity chromatography. *Biochem J* **203:** 293-298

Huang M-Y, Chang H-J, Chung F-Y, Yang M-J, Yang Y-H, Wang J-Y, Lin S-R (2010) MMP13 is a potential prognostic marker for colorectal cancer. *Oncology Reports* **24:** 1241-1247

Hughes J, Nangaku M, Alpers CE, Shankland SJ, Couser WG, Johnson RJ (2000) C5b-9 membrane attack complex mediates endothelial cell apoptosis in experimental glomerulonephritis. *American Journal of Physiology-Renal Physiology* **278:** F747-F757

Hughes TR, Mao M, Jones AR, Burchard J, Marton MJ, Shannon KW, Lefkowitz SM, Ziman M, Schelter JM, Meyer MR, Kobayashi S, Davis C, Dai HY, He YDD, Stephaniants SB, Cavet G, Walker WL, West A, Coffey E, Shoemaker DD, Stoughton R, Blanchard AP, Friend SH, Linsley PS (2001) Expression profiling using microarrays fabricated by an ink-jet oligonucleotide synthesizer. *Nature Biotechnology* **19:** 342-347

Hugli TE (1984) Structure and function of the anaphylatoxins. *Springer Semin Immunopathol* **7:** 193-219

Hussain SP, Hofseth LJ, Harris CC (2003) Radical causes of cancer. *Nat Rev Cancer* **3:** 276-285

IARC (2012) Arsenic, metals, fibres, and dusts. *IARC Monogr Eval Carcinog Risks Hum* **100:** 11-465

Ikeda J, Morii E, Liu Y, Qiu Y, Nakamichi N, Jokoji R, Miyoshi Y, Noguchi S, Aozasa K (2008) Prognostic significance of CD55 expression in breast cancer. *Clin Cancer Res* **14:** 4780-4786

Ishida M, Chang K-T, Hirabayashi K, Nishihara M, Takahashi M (1999) Cloning of mouse 20alpha-hydroxysteroid dehydrogenase cDNA and its mRNA localization during pregnancy. *Journal of Reproduction and Development* **45:** 321-329

Jeong HW, Kim IS (2004) TGF-beta 1 enhances beta ig-h3-mediated keratinocyte cell migration through the alpha 3 beta 1 integrin and PI3K. *Journal of Cellular Biochemistry* **92:** 770-780

Jiang H, Wagner E, Zhang H, Frank MM (2001) Complement 1 inhibitor is a regulator of the alternative complement pathway. *J Exp Med* **194:** 1609-1616

Jin HJ, Hayes GL, Darbha NS, Meyer E, LiWang PJ (2005) Investigation of CC and CXC chemokine quaternary state mutants. *Biochemical and Biophysical Research Communications* **338:** 987-999

Johnsen JI, Lindskog M, Ponthan F, Pettersen I, Elfman L, Orrego A, Sveinbjörnsson B, Kogner P (2004) Cyclooxygenase-2 is expressed in neuroblastoma, and nonsteroidal anti-inflammatory drugs induce apoptosis and inhibit tumor growth in vivo. *Cancer Res* **64:** 7210-7215

Johnson GR, Kannan B, Shoyab M, Stromberg K (1993) AMPHIREGULIN INDUCES TYROSINE PHOSPHORYLATION OF THE EPIDERMAL GROWTH-FACTOR RECEPTOR AND P185(ERBB2) - EVIDENCE THAT AMPHIREGULIN ACTS EXCLUSIVELY THROUGH THE EPIDERMAL GROWTH-FACTOR RECEPTOR AT THE SURFACE OF HUMAN EPITHELIAL-CELLS. *Journal of Biological Chemistry* **268:** 2924-2931

Johnson GR, Saeki T, Gordon AW, Shoyab M, Salomon DS, Stromberg K (1992) AUTOCRINE ACTION OF AMPHIREGULIN IN A COLON-CARCINOMA CELL-LINE AND IMMUNOCYTOCHEMICAL LOCALIZATION OF AMPHIREGULIN IN HUMAN COLON. *Journal of Cell Biology* **118:** 741-751

Joisel F, Lerouxnicollet I, Lebreton JP, Fontaine M (1983) A HEMOLYTIC ASSAY FOR CLINICAL INVESTIGATION OF HUMAN-C2. *Journal of Immunological Methods* **59:** 229-235

Jokiranta TS, Zipfel PF, Hakulinen J, Kuhn S, Pangburn MK, Tamerius JD, Meri S (1996) Analysis of the recognition mechanism of the alternative pathway of complement by monoclonal anti-factor H antibodies: Evidence for multiple interactions between H and surface bound C3b. *Febs Letters* **393**

Jolliffe IT (2002) *Springer Series in Statistics: Principal Component Analysis*, 2nd edn. New York: Springer.

Joseph LJ, Lebeau MM, Jamieson GA, Acharya S, Shows TB, Rowley JD, Sukhatme VP (1988) MOLECULAR-CLONING, SEQUENCING, AND MAPPING OF EGR2, A HUMAN EARLY GROWTH-RESPONSE GENE ENCODING A PROTEIN WITH ZINC-BINDING FINGER STRUCTURE. *Proceedings of the National Academy of Sciences of the United States of America* **85:** 7164-7168

Jung J-J, Noh S, Jeung H-C, Jung M, Kim TS, Noh SH, Roh JK, Chung HC, Rha SY (2010) Chemokine growth-regulated oncogene 1 as a putative biomarker for gastric cancer progression. *Cancer Science* **101:** 2200-2206

Junnila S, Kokkola A, Mizuguchi T, Hirata K, Karjalainen-Lindsberg ML, Puolakkainen P, Monni O (2010) Gene Expression of Analysis Identifies Over-expression of CXCL1, SPARC, SPP1, and SULF1 in Gastric Cancer. *Genes Chromosomes & Cancer* **49:** 28-39

Jurianz K, Ziegler S, Donin N, Reiter Y, Fishelson Z, Kirschfink M (2001) K562 erythroleukemic cells are equipped with multiple mechanisms of resistance to lysis by complement. *Int J Cancer* **93:** 848-854

Kafatos FC, Jones CW, Efstratiadis A (1979) DETERMINATION OF NUCLEIC-ACID SEQUENCE HOMOLOGIES AND RELATIVE CONCENTRATIONS BY A DOT HYBRIDIZATION PROCEDURE. *Nucleic Acids Research* **7:** 1541-1552

Kaliner M, Austen KF (1974) Adenosine 3'5'-monophosphate: inhibition of complement-mediated cell lysis. *Science* **183:** 659-661

Kalluri R (2009) EMT: When epithelial cells decide to become mesenchymal-like cells. *Journal of Clinical Investigation* **119:** 1417-1419

Kanehisa M, Goto S, Kawashima S, Okuno Y, Hattori M (2004) The KEGG resource for deciphering the genome. *Nucleic Acids Research* **32:** D277-D280

Kaplan RN, Rafii S, Lyden D (2006) Preparing the "Soil": The premetastatic niche. *Cancer Research* **66:** 11089-11093

Karin M, Liu ZG, Zandi E (1997) AP-1 function and regulation. *Current Opinion in Cell Biology* **9:** 240-246

Kasina S, Scherle PA, Hall CL, Macoska JA (2009) ADAM-mediated amphiregulin shedding and EGFR transactivation. *Cell Proliferation* **42:** 799-812

Kawanishi H, Matsui Y, Ito M, Watanabe J, Takahashi T, Nishizawa K, Nishiyama H, Kamoto T, Mikami Y, Tanaka Y, Jung G, Akiyama H, Nobumasa H, Guilford P, Reeve A,

Okuno Y, Tsujimoto G, Nakamura E, Ogawa O (2008) Secreted CXCL1 is a potential mediator and marker of the tumor invasion of bladder cancer. *Clinical Cancer Research* **14:** 2579-2587

Kelman Z (1997) PCNA: structure, functions and interactions. *Oncogene* **14:** 629-640

Kennedy AD, Beum PV, Solga MD, DiLillo DJ, Lindorfer MA, Hess CE, Densmore JJ, Williams ME, Taylor RP (2004) Rituximab infusion promotes rapid complement depletion and acute CD20 loss in chronic lymphocytic leukemia. *J Immunol* **172:** 3280-3288

Kerjaschki D, Schulze M, Binder S, Kain R, Ojha PP, Susani M, Horvat R, Baker PJ, Couser WG (1989) Transcellular transport and membrane insertion of the C5b-9 membrane attack complex of complement by glomerular epithelial cells in experimental membranous nephropathy. *J Immunol* **143:** 546-552

Kerr FK, Thomas AR, Wijeyewickrema LC, Whisstock JC, Boyd SE, Kaiserman D, Matthews AY, Bird PI, Thielens NM, Rossi V, Pike RN (2008) Elucidation of the substrate specificity of the MASP-2 protease of the lectin complement pathway and identification of the enzyme as a major physiological target of the serpin, C1-inhibitor. *Mol Immunol* **45:** 670-677

Kilgore KS, Flory CM, Miller BF, Evans VM, Warren JS (1996) The membrane attack complex of complement induces interleukin-8 and monocyte chemoattractant protein-1 secretion from human umbilical vein endothelial cells. *American Journal of Pathology* **149:** 953-961

Kilgore KS, Schmid E, Shanley TP, Flory CM, Maheswari V, Tramontini NL, Cohen H, Ward PA, Friedl HP, Warren JS (1997) Sublytic concentrations of the membrane attack complex of complement induce endothelial interleukin-8 and monocyte chemoattractant protein-1 through nuclear factor-kappa B activation. *American Journal of Pathology* **150:** 2019-2031

Kilgore KS, Shen JP, Miller BF, Ward PA, Warren JS (1995) ENHANCEMENT BY THE COMPLEMENT MEMBRANE ATTACK COMPLEX OF TUMOR NECROSIS FACTOR-ALPHA-INDUCED ENDOTHELIAL-CELL EXPRESSION OF E-SELECTIN AND ICAM-1. *Journal of Immunology* **155:** 1434-1441

Kim M-Y, Oskarsson T, Acharyya S, Nguyen DX, Zhang XHF, Norton L, Massague J (2009) Tumor Self-Seeding by Circulating Cancer Cells. *Cell* **139:** 1315-1326

Kim PKM, Armstrong M, Liu Y, Yan P, Bucher B, Zuckerbraun BS, Gambotto A, Billiar TR, Yim JH (2004) IRF-1 expression induces apoptosis and inhibits tumor growth in mouse mammary cancer cells in vitro and in vivo. *Oncogene* **23:** 1125-1135

Kim YU, Kinoshita T, Molina H, Hourcade D, Seya T, Wagner LM, Holers VM (1995) MOUSE COMPLEMENT REGULATORY PROTEIN CRRY/P65 USES THE SPECIFIC MECHANISMS OF BOTH HUMAN DECAY-ACCELERATING FACTOR AND MEMBRANE COFACTOR PROTEIN. *Journal of Experimental Medicine* **181:** 151-159

Kimberley FC, Sivasankar B, Morgan BP (2007) Alternative roles for CD59. *Molecular Immunology* **44:** 73-81

Kinoshita T, Lavoie S, Nussenzweig V (1985) REGULATORY PROTEINS FOR THE ACTIVATED 3RD AND 4TH COMPONENTS OF COMPLEMENT (C3B AND C4B) IN

MICE .2. IDENTIFICATION AND PROPERTIES OF COMPLEMENT RECEPTOR TYPE-1 (CR-1). *Journal of Immunology* **134:** 2564-2570

Kiyatkin A, Aksamitiene E, Markevich NI, Borisov NM, Hoek JB, Kholodenko BN (2006) Scaffolding protein Grb2-associated binder 1 sustains epidermal growth factor-induced mitogenic and survival signaling by multiple positive feedback loops. *Journal of Biological Chemistry* **281:** 19925-19938

Klickstein LB, Wong WW, Smith JA, Weis JH, Wilson JG, Fearon DT (1987) HUMAN C3B/C4B RECEPTOR (CR-1) DEMONSTRATION OF LONG HOMOLOGOUS REPEATING DOMAINS THAT ARE COMPOSED OF THE SHORT CONSENSUS REPEATS CHARACTERISTIC OF C3/C4 BINDING-PROTEINS. *Journal of Experimental Medicine* **165:** 1095-1112

Knauper V, Will H, LopezOtin C, Smith B, Atkinson SJ, Stanton H, Hembry RM, Murphy G (1996) Cellular mechanisms for human procollagenase-3 (MMP-13) activation - Evidence that MT1-MMP (MMP-14) and gelatinase A (MMP-2) are able to generate active enzyme. *Journal of Biological Chemistry* **271:** 17124-17131

Kohler PF, Müller-Eberhard HJ (1967) Immunochemical quantitation of the third, fourth and fifth components of human complement: concentrations in the serum of healthy adults. *J Immunol* **99:** 1211-1216

Koklitis PA, Murphy G, Sutton C, Angal S (1991) PURIFICATION OF RECOMBINANT HUMAN PROSTROMELYSIN - STUDIES ON HEAT ACTIVATION TO GIVE HIGH-MR AND LOW-MR ACTIVE FORMS, AND A COMPARISON OF RECOMBINANT WITH NATURAL STROMELYSIN ACTIVITIES. *Biochemical Journal* **276:** 217-221

Koski CL, Ramm LE, Hammer CH, Mayer MM, Shin ML (1983) Cytolysis of nucleated cells by complement: cell death displays multi-hit characteristics. *Proc Natl Acad Sci U S A* **80:** 3816-3820

Kozak M (1987) AT LEAST 6 NUCLEOTIDES PRECEDING THE AUG INITIATOR CODON ENHANCE TRANSLATION IN MAMMALIAN-CELLS. *Journal of Molecular Biology* **196:** 947-950

Kraus S, Seger R, Fishelson Z (2001) Involvement of the ERK mitogen-activated protein kinase in cell resistance to complement-mediated lysis. *Clinical and Experimental Immunology* **123:** 366-374

Krych M, Clemenza L, Howdeshell D, Hauhart R, Hourcade D, Atkinson JP (1994) ANALYSIS OF THE FUNCTIONAL DOMAINS OF COMPLEMENT RECEPTOR-TYPE-1 (C3B/C4B RECEPTOR, CD35) BY SUBSTITUTION MUTAGENESIS. *Journal of Biological Chemistry* **269:** 13273-13278

Krych M, Hourcade D, Atkinson JP (1991) SITES WITHIN THE COMPLEMENT C3B C4B RECEPTOR IMPORTANT FOR THE SPECIFICITY OF LIGAND-BINDING. *Proceedings of the National Academy of Sciences of the United States of America* **88:** 4353-4357

Krych-Goldberg M, Hauhart RE, Subramanian VB, Yurcisin BM, Crimmins DL, Hourcade DE, Atkinson JP (1999) Decay accelerating activity of complement receptor type 1 (CD35) - Two active sites are required for dissociating C5 convertases. *Journal of Biological Chemistry* **274:** 31160-31168

Kudo Y, Iizuka S, Yoshida M, Tsunematsu T, Kondo T, Subarnbhesaj A, Deraz EM, Siriwardena SBSM, Tahara H, Ishimaru N, Ogawa I, Takata T (2012) Matrix Metalloproteinase-13 (MMP-13) Directly and Indirectly Promotes Tumor Angiogenesis. *Journal of Biological Chemistry* **287:** 38716-38728

Kuhn K, Baker SC, Chudin E, Lieu MH, Oeser S, Bennett H, Rigault P, Barker D, McDaniel TK, Chee MS (2004) A novel, high-performance random array platform for quantitative gene expression profiling. *Genome Research* **14:** 2347-2356

Kuraya M, Yefenof E, Klein G, Klein E (1992) Expression of the complement regulatory proteins CD21, CD55 and CD59 on Burkitt lymphoma lines: their role in sensitivity to human serum-mediated lysis. *Eur J Immunol* **22:** 1871-1876

Kwon B, Moon CH, Kang SW, Seo SK, Kwon BS (2000) 4-1BB: Still in the midst of Darkness. *Molecules and Cells* **10:** 119-126

Lachmann PJ (2009) The amplification loop of the complement pathways. *Adv Immunol* **104:** 115-149

Lambris JD (1988) The multifunctional role of C3, the third component of complement. *Immunol Today* **9:** 387-393

Lambris JD, Müller-Eberhard HJ (1986) The multifunctional role of C3: structural analysis of its interactions with physiological ligands. *Mol Immunol* **23:** 1237-1242

Lashner BA, Shapiro BD, Husain A, Goldblum JR (1999) Evaluation of the usefulness of testing for p53 mutations in colorectal cancer surveillance for ulcerative colitis. *Am J Gastroenterol* **94:** 456-462

Lau LF, Nathans D (1987) EXPRESSION OF A SET OF GROWTH-RELATED IMMEDIATE EARLY GENES IN BALB-C 3T3 CELLS - COORDINATE REGULATION WITH C-FOS OR C-MYC. *Proceedings of the National Academy of Sciences of the United States of America* **84:** 1182-1186

Laudes IJ, Chu JC, Huber-Lang M, Guo RF, Riedemann NC, Sarma JV, Mahdi F, Murphy HS, Speyer C, Lu KT, Lambris JD, Zetoune FS, Ward PA (2002) Expression and function of C5a receptor in mouse microvascular endothelial cells. *J Immunol* **169:** 5962-5970

Laurell AB (1990) Jules Bordet--a giant in immunology. *Scand J Immunol* **32:** 429-432

Lee JC, Laydon JT, McDonnell PC, Gallagher TF, Kumar S, Green D, McNulty D, Blumenthal MJ, Heys JR, Landvatter SW, Strickler JE, McLaughlin MM, Siemens IR, Fisher SM, Livi GP, White JR, Adams JL, Young PR (1994) A PROTEIN-KINASE INVOLVED IN THE REGULATION OF INFLAMMATORY CYTOKINE BIOSYNTHESIS. *Nature* **372:** 739-746

Leeman MF, McKay JA, Murray GI (2002) Matrix metalloproteinase 13 activity is associated with poor prognosis in colorectal cancer. *Journal of Clinical Pathology* **55:** 758-762

Lejeune S, Leek R, Horak E, Plowman G, Greenall M, Harris AL (1993) AMPHIREGULIN, EPIDERMAL GROWTH-FACTOR RECEPTOR, AND ESTROGEN-RECEPTOR EXPRESSION IN HUMAN PRIMARY BREAST-CANCER. *Cancer Research* **53:** 3597-3602

Lemmon MA, Schlessinger J (1994) REGULATION OF SIGNAL-TRANSDUCTION AND SIGNAL DIVERSITY BY RECEPTOR OLIGOMERIZATION. *Trends in Biochemical Sciences* **19:** 459-463

Lengyel E, Gum R, Stepp E, Juarez J, Wang H, Boyd D (1996) Regulation of urokinase-type plasminogen activator expression by an ERK1-dependent signaling pathway in a squamous cell carcinoma cell line. *J Cell Biochem* **61:** 430-443

Li DQ, Chen Z, Song XJ, Luo LH, Pflugfelder SC (2004) Stimulation of matrix metalloproteinases by hyperosmolarity via a JNK pathway in human corneal epithelial cells. *Investigative Ophthalmology & Visual Science* **45:** 4302-4311

Li DQ, Shang TY, Kim HS, Solomon A, Lokeshwar BL, Pflugfelder SC (2003) Regulated expression of collagenases MMP-1,-8, and-13 and stromelysins MMP-3,-10, and-11 by human corneal epithelial cells. *Investigative Ophthalmology & Visual Science* **44:** 2928-2936

Liacini A, Sylvester J, Li WQ, Zafarullah M (2002) Inhibition of interleukin-1-stimulated MAP kinases, activating protein-1 (AP-1) and nuclear factor kappa B (NF-kappa B) transcription factors down-regulates matrix metalloproteinase gene expression in articular chondrocytes. *Matrix Biology* **21:** 251-262

Lim M, Chuong C-M, Roy-Burman P (2011) PI3K, Erk Signaling in BMP7-Induced Epithelial-Mesenchymal Transition (EMT) of PC-3 Prostate Cancer Cells in 2-and 3-Dimensional Cultures. *Hormones & Cancer* **2:** 298-309

Lin EY, Nguyen AV, Russell RG, Pollard JW (2001) Colony-stimulating factor 1 promotes progression of mammary tumors to malignancy. *Journal of Experimental Medicine* **193:** 727-739

Lin TX, Ambasudhan R, Yuan X, Li WL, Hilcove S, Abujarour R, Lin XY, Hahm HS, Hao E, Hayek A, Ding S (2009) A chemical platform for improved induction of human iPSCs. *Nature Methods* **6:** 805-U824

Liszewski M, Fang C, Atkinson J (2008) Inhibiting complement activation on cells at the step of C3 cleavage. *Vaccine* **26 Suppl 8:** I22-27

Liu LS, Qiu W, Wang H, Li Y, Zhou JB, Xia M, Shan K, Pang RR, Zhou Y, Zhao D, Wang YW (2012) Sublytic C5b-9 Complexes Induce Apoptosis of Glomerular Mesangial Cells in Rats with Thy-1 Nephritis through Role of Interferon Regulatory Factor-1-dependent Caspase 8 Activation. *Journal of Biological Chemistry* **287:** 16410-16423

Lo TN, Boyle MD (1979) Relationship between the intracellular cyclic adenosine 3':5'-monophosphate level of tumor cells and their sensitivity to killing by antibody and complement. *Cancer Res* **39:** 3156-3162

Loberg RD, Day LL, Dunn R, Kalikin LM, Pienta KJ (2006) Inhibition of decay-accelerating factor (CD55) attenuates prostate cancer growth and survival in vivo. *Neoplasia* **8:** 69-78

Lochter A, Galosy S, Muschler J, Freedman N, Werb Z, Bissell MJ (1997) Matrix metalloproteinase stromelysin-1 triggers a cascade of molecular alterations that leads to stable epithelial-to-mesenchymal conversion and a premalignant phenotype in mammary epithelial cells. *Journal of Cell Biology* **139:** 1861-1872

Lozada C, Levin RI, Huie M, Hirschhorn R, Naime D, Whitlow M, Recht PA, Golden B, Cronstein BN (1995) IDENTIFICATION OF CLQ AS THE HEAT-LABILE SERUM COFACTOR REQUIRED FOR IMMUNE-COMPLEXES TO STIMULATE ENDOTHELIAL EXPRESSION OF THE ADHESION MOLECULES E-SELECTIN AND INTERCELLULAR AND VASCULAR CELL-ADHESION MOLECULES-1. *Proceedings of the National Academy of Sciences of the United States of America* **92:** 8378-8382

Lu Y, Liu X, Shi S, Su H, Bai X, Cai G, Yang F, Xie Z, Zhu Y, Zhang Y, Zhang S, Li X, Wang S, Wu D, Zhang L, Wu J, Xie Y, Chen X (2012) Bioinformatics Analysis of Proteomic Profiles During the Process of Anti-Thy1 Nephritis. *Molecular & Cellular Proteomics* **11**

Lublin DM, Atkinson JP (1989) Decay-accelerating factor: biochemistry, molecular biology, and function. *Annu Rev Immunol* **7:** 35-58

Lucas SD, Karlsson-parra A, Nilsson BO, Grimelius L, Rastad J, Juhlin C (1996) Tumor-Specific Deposition of Immunoglobulin G and Complement in Papillary Thyroid Carcinoma. *Human Pathology***:** 1329-1335

Lueck K, Wasmuth S, Williams J, Hughes TR, Morgan BP, Lommatzsch A, Greenwood J, Moss SE, Pauleikhoff D (2011) Sub-lytic C5b-9 induces functional changes in retinal pigment epithelial cells consistent with age-related macular degeneration. *Eye* **25**

Lukashev ME, Werb Z (1998) ECM signalling: orchestrating cell behaviour and misbehaviour. *Trends in Cell Biology* **8:** 437-441

Luo X, Popov S, Bera AK, Wilkie TM, Muallem S (2001) RGS proteins provide biochemical control of agonist-evoked Ca2+ (i) oscillations. *Molecular Cell* **7:** 651-660

Luukkaa M, Vihinen P, Kronqvist P, Vahlberg T, Pyrhonen S, Kahari VM, Grenman R (2006) Association between high collagenase-3 expression levels and poor prognosis in patients with head and neck cancer. *Head and Neck-Journal for the Sciences and Specialties of the Head and Neck* **28:** 225-234

Lynen R, Brade V, Wolf A, Vogt W (1973) PURIFICATION AND SOME PROPERTIES OF A HEAT LABILE SERUM FACTOR (UF) - IDENTITY WITH GLYCINE-RICH BETA-GLYCOPROTEIN AND PROPERDIN FACTOR B. *Hoppe-Seylers Zeitschrift Fur Physiologische Chemie* **354:** 37-47

Maeda S, Kamata H, Luo JL, Leffert H, Karin M (2005) IKKbeta couples hepatocyte death to cytokine-driven compensatory proliferation that promotes chemical hepatocarcinogenesis. *Cell* **121:** 977-990

Manthey CL, Wang SW, Kinney SD, Yao ZB (1998) SB202190, a selective inhibitor of p38 mitogen-activated protein kinase, is a powerful regulator of LPS-induced mRNAs in monocytes. *Journal of Leukocyte Biology* **64:** 409-417

Marder SR, Chenoweth DE, Goldstein IM, Perez HD (1985) Chemotactic responses of human peripheral blood monocytes to the complement-derived peptides C5a and C5a des Arg. *J Immunol* **134:** 3325-3331

Markiewski MM, DeAngelis RA, Benencia F, Ricklin-Lichtsteiner SK, Koutoulaki A, Gerard C, Coukos G, Lambris JD (2008) Modulation of the antitumor immune response by complement. *Nature Immunology* **9:** 1225-1235

Marmur J, Doty P (1961) THERMAL RENATURATION OF DEOXYRIBONUCLEIC ACIDS. *Journal of Molecular Biology* **3:** 585-&

MartinezLacaci I, Johnson GR, Salomon DS, Dickson RB (1996) Characterization of a novel amphiregulin-related molecule in 12-O-tetradecanoylphorbol-13-acetate-treated breast cancer cells. *Journal of Cellular Physiology* **169:** 497-508

Mayer MM, Miller JA, Shin HS (1970) A specific method for purification of the second component of guinea pig complement and a chemical evaluation of the one-hit theory. *J Immunol* **105:** 327-341

McBryan J, Howlin J, Napoletano S, Martin F (2008) Amphiregulin: Role in mammary gland development and breast cancer. *Journal of Mammary Gland Biology and Neoplasia* **13:** 159-169

McConnell I, Klein G, Lint TF, Lachmann PJ (1978) Activation of the alternative complement pathway by human B cell lymphoma lines is associated with Epstein-Barr virus transformation of the cells. *Eur J Immunol* **8:** 453-458

McNearney T, Ballard L, Seya T, Atkinson JP (1989) MEMBRANE COFACTOR PROTEIN OF COMPLEMENT IS PRESENT ON HUMAN FIBROBLAST, EPITHELIAL, AND ENDOTHELIAL-CELLS. *Journal of Clinical Investigation* **84:** 538-545

Mebratu Y, Tesfaigzi Y (2009) How ERK1/2 activation controls cell proliferation and cell death is subcellular localization the answer? *Cell Cycle* **8:** 1168-1175

Medof ME, Kinoshita T, Nussenzweig V (1984) INHIBITION OF COMPLEMENT ACTIVATION ON THE SURFACE OF CELLS AFTER INCORPORATION OF DECAY-ACCELERATING FACTOR (DAF) INTO THEIR MEMBRANES. *Journal of Experimental Medicine* **160:** 1558-1578

Meierjohann S, Hufnagel A, Wende E, Kleinschmidt MA, Wolf K, Friedl P, Gaubatz S, Schartl M (2010) MMP13 mediates cell cycle progression in melanocytes and melanoma cells: in vitro studies of migration and proliferation. *Molecular Cancer* **9**

Meri S, Morgan BP, Davies A, Daniels RH, Olavesen MG, Waldmann H, Lachmann PJ (1990) Human protectin (CD59), an 18,000-20,000 MW complement lysis restricting factor, inhibits C5b-8 catalysed insertion of C9 into lipid bilayers. *Immunology* **71:** 1-9

Mi Z, Guo H, Wai PY, Gao C, Wei J, Kuo PC (2004) Differential osteopontin expression in phenotypically distinct subclones of murine breast cancer cells mediates metastatic behavior. *J Biol Chem* **279:** 46659-46667

Michael KL, Taylor LC, Schultz SL, Walt DR (1998) Randomly ordered addressable high-density optical sensor arrays. *Analytical Chemistry* **70:** 1242-1248

Michaels DW, Abramovitz AS, Hammer CH, Mayer MM (1976) Increased ion permeability of planar lipid bilayer membranes after treatment with the C5b-9 cytolytic attack mechanism of complement. *Proc Natl Acad Sci U S A* **73:** 2852-2856

MichiyoYamada, Ichikawa Y, Yarnagishi S, Momiyama N, Ota M, Fujii S, Tanaka K, Togo S, Ohki S, Shimadal H (2008) Amphiregulin is a promising prognostic marker for liver metastases of colorectal cancer. *Clinical Cancer Research* **14:** 2351-2356

Miller MB, Tang Y-W (2009) Basic Concepts of Microarrays and Potential Applications in Clinical Microbiology. *Clinical Microbiology Reviews* **22:** 611-+

Minn AJ, Gupta GP, Siegel PM, Bos PD, Shu WP, Giri DD, Viale A, Olshen AB, Gerald WL, Massague J (2005) Genes that mediate breast cancer metastasis to lung. *Nature* **436:** 518-524

Minta JO, Fung M, Paramaswara B (1998) Transcriptional and post-transcriptional regulation of complement factor I (CFI) gene expression in Hep G2 cells by interleukin-6. *Biochim Biophys Acta* **1442:** 286-295

Miyamoto M, Fujita T, Kimura Y, Maruyama M, Harada H, Sudo Y, Miyata T, Taniguchi T (1988) REGULATED EXPRESSION OF A GENE ENCODING A NUCLEAR FACTOR, IRF-1, THAT SPECIFICALLY BINDS TO IFN-BETA-GENE REGULATORY ELEMENTS. *Cell* **54:** 903-913

Molina H (2002) The murine complement regulator Crry: new insights into the immunobiology of complement regulation. *Cellular and Molecular Life Sciences* **59:** 220-229

Mollnes TE, Brekke OL, Fung M, Fure H, Christiansen D, Bergseth G, Videm V, Lappegård KT, Köhl J, Lambris JD (2002) Essential role of the C5a receptor in E coli-induced oxidative burst and phagocytosis revealed by a novel lepirudin-based human whole blood model of inflammation. *Blood* **100:** 1869-1877

Monje P, Hernandez-Losa J, Lyons RJ, Castellone MD, Gutkind JS (2005) Regulation of the transcriptional activity of c-Fos by ERK: A novel role for the prolyl isomerase Pin1. *Journal of Biological Chemistry* **280:** 35081-35084

Monk PN, Scola AM, Madala P, Fairlie DP (2007) Function, structure and therapeutic potential of complement C5a receptors. *Br J Pharmacol* **152:** 429-448

Monsinjon T, Gasque P, Chan P, Ischenko A, Brady JJ, Fontaine MC (2003) Regulation by complement C3a and C5a anaphylatoxins of cytokine production in human umbilical vein endothelial cells. *FASEB J* **17:** 1003-1014

Monsinjon T, Gasque P, Ischenko A, Fontaine M (2001) C3A binds to the seven transmembrane anaphylatoxin receptor expressed by epithelial cells and triggers the production of IL-8. *FEBS Lett* **487:** 339-346

Morey JS, Ryan JC, Van Dolah FM (2006) Microarray validation: factors influencing correlation between oligonucleotide microarrays and real-time PCR. *Biological Procedures Online* **8:** 175-193

Morgan BP (1989) COMPLEMENT MEMBRANE ATTACK ON NUCLEATED CELLS - RESISTANCE, RECOVERY AND NON-LETHAL EFFECTS. *Biochemical Journal* **264**

Morgan BP, Campbell AK (1985) The recovery of human polymorphonuclear leucocytes from sublytic complement attack is mediated by changes in intracellular free calcium. *Biochem J* **231:** 205-208

Morgan BP, Dankert JR, Esser AF (1987) Recovery of human neutrophils from complement attack: removal of the membrane attack complex by endocytosis and exocytosis. *J Immunol* **138:** 246-253

Morgan BP, Harris CL (1999) *Complement regulatory proteins*, San Diego ; London: Academic Press.

Morgan BP, Imagawa DK, Dankert JR, Ramm LE (1986) Complement lysis of U937, a nucleated mammalian cell line in the absence of C9: effect of C9 on C5b-8 mediated cell lysis. *J Immunol* **136:** 3402-3406

Morgan BP, van den Berg CW, Harris CL (2005) "Homologous restriction" in complement lysis: roles of membrane complement regulators. *Xenotransplantation* **12:** 258-265

Morgan BP, Vandenberg CW, Davies EV, Hallett MB, Horejsi V (1993) CROSS-LINKING OF CD59 AND OF OTHER GLYCOSYL PHOSPHATIDYLINOSITOL-ANCHORED MOLECULES ON NEUTROPHILS TRIGGERS CELL ACTIVATION VIA TYROSINE KINASE. *European Journal of Immunology* **23:** 2841-2850

Morgia G, Falsaperla M, Malaponte G, Madonia M, Indelicato M, Travali S, Mazzarino M (2005) Matrix metalloproteinases as diagnostic (MMP-13) and prognostic (MMP-2, MMP-9) markers of prostate cancer. *Urological Research* **33:** 44-50

Mori D, Nakafusa Y, Miyazaki K, Tokunaga O (2005) Differential expression of Janus kinase 3 (JAK3), matrix metalloproteinase 13 (MMP13), heat shock protein 60 (HSP60), and mouse double minute 2 (MDM2) in human colorectal cancer progression using human cancer cDNA microarrays. *Pathology Research and Practice* **201:** 777-789

Morley BJ, Walport MJ (2000) The Complement Facts Book.

Moscova M, Marsh DJ, Baxter RC (2006) Protein chip discovery of secreted proteins regulated by the phosphatidylinositol 3-kinase pathway in ovarian cancer cell lines. *Cancer Research* **66:** 1376-1383

Moskovich O, Fishelson Z (2007) Live cell imaging of outward and inward vesiculation induced by the complement c5b-9 complex. *J Biol Chem* **282:** 29977-29986

Mukhin YV, Gooz M, Raymond JR, Garnovskaya MN (2006) Collagenase-2 and-3 mediate epidermal growth factor receptor transactivation by bradykinin B-2 receptor in kidney cells. *Journal of Pharmacology and Experimental Therapeutics* **318:** 1033-1043

Mullenbrock S, Shah J, Cooper GM (2011) Global Expression Analysis Identified a Preferentially Nerve Growth Factor-induced Transcriptional Program Regulated by Sustained Mitogen-activated Protein Kinase/Extracellular Signal-regulated Kinase (ERK) and AP-1 Protein Activation during PC12 Cell Differentiation. *Journal of Biological Chemistry* **286:** 45131-45145

Murakami Y, Imamichi T, Nagasawa S (1993) Characterization of C3a anaphylatoxin receptor on guinea-pig macrophages. *Immunology* **79:** 633-638

Murphy LO, Cluck MW, Lovas S, Otvos F, Murphy RF, Schally AV, Permert J, Larsson J, Knezetic JA, Adrian TE (2001) Pancreatic cancer cells require an EGF receptor-mediated autocrine pathway for proliferation in serum-free conditions. *British Journal of Cancer* **84:** 926-935

Murray EW, Robbins SM (1998) Antibody cross-linking of the glycosylphosphatidylinositol-linked protein CD59 on hematopoietic cells induces signaling pathways resembling activation by complement. *Journal of Biological Chemistry* **273:** 25279-25284

Müller-Eberhard HJ (1986) The membrane attack complex of complement. *Annu Rev Immunol* **4:** 503-528

Müller-Eberhard HJ (1988) Molecular organization and function of the complement system. *Annu Rev Biochem* **57:** 321-347

Müller-Eberhard HJ, Polley MJ, Calcott MA (1967) Formation and functional significance of a molecular complex derived from the second and the fourth component of human complement. *J Exp Med* **125:** 359-380

Nagase H, Visse R, Murphy G (2006) Structure and function of matrix metalloproteinases and TIMPs. *Cardiovascular Research* **69:** 562-573

Nangaku M, Pippin J, Couser WG (1999) Complement membrane attack complex (C5b-9) mediates interstitial disease in experimental nephrotic syndrome. *Journal of the American Society of Nephrology* **10:** 2323-2331

Nguyen H, Hiscott J, Pitha PM (1997) The growing family of interferon regulatory factors. *Cytokine and Growth Factor Reviews* **8:** 293-312

Nicholsonweller A, Burge J, Fearon DT, Weller PF, Austen KF (1982) ISOLATION OF A HUMAN-ERYTHROCYTE MEMBRANE GLYCOPROTEIN WITH DECAY-ACCELERATING ACTIVITY FOR C-3 CONVERTASES OF THE COMPLEMENT-SYSTEM. *Journal of Immunology* **129**

Niculescu F, Badea T, Rus H (1999) Sublytic C5b-9 induces proliferation of human aortic smooth muscle cells - Role of mitogen activated protein kinase and phosphatidylinositol 3-kinase. *Atherosclerosis* **142:** 47-56

Niculescu F, Rus H, Shino ML (1994) RECEPTOR-INDEPENDENT ACTIVATION OF GUANINE-NUCLEOTIDE-BINDING REGULATORY PROTEINS BY TERMINAL COMPLEMENT COMPLEXES. *Journal of Biological Chemistry* **269:** 4417-4423

Niculescu F, Rus H, vanBiesen T, Shin ML (1997) Activation of Ras and mitogen-activated protein kinase pathway by terminal complement complexes is G protein dependent. *Journal of Immunology* **158:** 4405-4412

Niculescu F, Rus HG, Retegan M, Vlaicu R (1992) Persistent complement activation on tumor cells in breast cancer. *Am J Pathol* **140:** 1039-1043

Nilsson G, Johnell M, Hammer CH, Tiffany HL, Nilsson K, Metcalfe DD, Siegbahn A, Murphy PM (1996) C3a and C5a are chemotaxins for human mast cells and act through distinct receptors via a pertussis toxin-sensitive signal transduction pathway. *J Immunol* **157:** 1693-1698

Ninomiya-Tsuji J, Kishimoto K, Hiyama A, Inoue J, Cao ZD, Matsumoto K (1999) The kinase TAK1 can activate the NIK-I kappa B as well as the MAP kinase cascade in the IL-1 signalling pathway. *Nature* **398:** 252-256

Nunn MA, Sharma A, Paesen GC, Adamson S, Lissina O, Willis AC, Nuttall PA (2005) Complement inhibitor of C5 activation from the soft tick Ornithodoros moubata. *Journal of Immunology* **174:** 2084-2091

Oglesby TJ, Allen CJ, Liszewski MK, White DJG, Atkinson JP (1992) MEMBRANE COFACTOR PROTEIN (CD46) PROTECTS CELLS FROM COMPLEMENT-MEDIATED

ATTACK BY AN INTRINSIC MECHANISM. *Journal of Experimental Medicine* **175:** 1547-1551

Ohanian SH, Borsos T (1975) Lysis of tumor cells by antibody and complement. II. Lack of correlation between amount of C4 and C3 fixed and cell lysis. *J Immunol* **114:** 1292-1295

Ohanian SH, Schlager SI (1981) Humoral immune killing of nucleated cells: mechanisms of complement-mediated attack and target cell defense. *Crit Rev Immunol* **1:** 165-209

Okinaga S, Slattery D, Humbles A, Zsengeller Z, Morteau O, Kinrade MB, Brodbeck RM, Krause JE, Choe HR, Gerard NP, Gerard C (2003) C5L2, a nonsignaling C5A binding protein. *Biochemistry* **42:** 9406-9415

Oladipo O, Conlon S, O'Grady A, Purcell C, Wilson C, Maxwell PJ, Johnston PG, Stevenson M, Kay EW, Wilson RH, Waugh DJJ (2011) The expression and prognostic impact of CXC-chemokines in stage II and III colorectal cancer epithelial and stromal tissue. *British Journal of Cancer* **104:** 480-487

Olayioye MA, Neve RM, Lane HA, Hynes NE (2000) The ErbB signaling network: receptor heterodimerization in development and cancer. *Embo Journal* **19:** 3159-3167

Ono M, Kuwano M (2006) Molecular mechanisms of epidermal growth factor receptor (EGFR) activation and response to gefitinib and other EGFR-targeting drugs. *Clinical Cancer Research* **12:** 7242-7251

Ooi YM, Colten HR (1979) GENETIC DEFECT IN SECRETION OF COMPLEMENT-C5 IN MICE. *Nature* **282:** 207-208

Orren A, Wurzner R, Potter PC, Fernie BA, Coetzee S, Morgan BP, Lachmann PJ (1992) PROPERTIES OF A LOW-MOLECULAR-WEIGHT COMPLEMENT COMPONENT C6 FOUND IN HUMAN-SUBJECTS WITH SUBTOTAL C6 DEFICIENCY. *Immunology* **75:** 10-16

Owens DM, Keyse SM (2007) Differential regulation of MAP kinase signalling by dual-specificity protein phosphatases. *Oncogene* **26:** 3203-3213

Pabon C, Modrusan Z, Ruvolo MV, Coleman IM, Daniel S, Yue H, Arnold LJ, Reynolds MA (2001) Optimized T7 amplification system for microarray analysis. *Biotechniques* **31:** 874-879

Pangburn MK, Müller-Eberhard HJ (1983) Kinetic and thermodynamic analysis of the control of C3b by the complement regulatory proteins factors H and I. *Biochemistry* **22:** 178-185

Pangburn MK, Schreiber RD, Mullereberhard HJ (1977) HUMAN COMPLEMENT C3B INACTIVATOR - ISOLATION, CHARACTERIZATION, AND DEMONSTRATION OF AN ABSOLUTE REQUIREMENT FOR SERUM-PROTEIN BETA-1H FOR CLEAVAGE OF C3B AND C4B IN SOLUTION. *Journal of Experimental Medicine* **146:** 257-270

Parkin DM (2006) The global health burden of infection-associated cancers in the year 2002. *Int J Cancer* **118:** 3030-3044

Pickens SR, Chamberlain ND, Volin MV, Gonzalez M, Pope RM, Mandelin AM, II, Kolls JK, Shahrara S (2011) Anti-CXCL5 therapy ameliorates IL-17-induced arthritis by decreasing joint vascularization. *Angiogenesis* **14:** 443-455

Pilzer D, Fishelson Z (2005) Mortalin/GRP75 promotes release of membrane vesicles from immune attacked cells and protection from complement-mediated lysis. *Int Immunol* **17:** 1239-1248

Pilzer D, Saar M, Koya K, Fishelson Z (2010) Mortalin inhibitors sensitize K562 leukemia cells to complement-dependent cytotoxicity. *Int J Cancer* **126:** 1428-1435

Plowman GD, Green JM, McDonald VL, Neubauer MG, Disteche CM, Todaro GJ, Shoyab M (1990) THE AMPHIREGULIN GENE ENCODES A NOVEL EPIDERMAL GROWTH FACTOR-RELATED PROTEIN WITH TUMOR-INHIBITORY ACTIVITY. *Molecular and Cellular Biology* **10:** 1969-1981

Plummer M, van Doorn LJ, Franceschi S, Kleter B, Canzian F, Vivas J, Lopez G, Colin D, Muñoz N, Kato I (2007) Helicobacter pylori cytotoxin-associated genotype and gastric precancerous lesions. *J Natl Cancer Inst* **99:** 1328-1334

Podack ER, Esser AF, Biesecker G, Mullereberhard HJ (1980) MEMBRANE ATTACK COMPLEX OF COMPLEMENT - STRUCTURAL-ANALYSIS OF ITS ASSEMBLY. *Journal of Experimental Medicine* **151:** 301-313

Ponthan F, Wickström M, Gleissman H, Fuskevåg OM, Segerström L, Sveinbjörnsson B, Redfern CP, Eksborg S, Kogner P, Johnsen JI (2007) Celecoxib prevents neuroblastoma tumor development and potentiates the effect of chemotherapeutic drugs in vitro and in vivo. *Clin Cancer Res* **13:** 1036-1044

Popivanova BK, Kitamura K, Wu Y, Kondo T, Kagaya T, Kaneko S, Oshima M, Fujii C, Mukaida N (2008) Blocking TNF-alpha in mice reduces colorectal carcinogenesis associated with chronic colitis. *J Clin Invest* **118:** 560-570

Post TW, Liszewski MK, Adams EM, Tedja I, Miller EA, Atkinson JP (1991) MEMBRANE COFACTOR PROTEIN OF THE COMPLEMENT-SYSTEM - ALTERNATIVE SPLICING OF SERINE THREONINE PROLINE RICH EXONS AND CYTOPLASMIC TAILS PRODUCES MULTIPLE ISOFORMS THAT CORRELATE WITH PROTEIN PHENOTYPE. *Journal of Experimental Medicine* **174:** 93-102

Powell MB, Marchbank KJ, Rushmere NK, vandenBerg CW, Morgan BP (1997) Molecular cloning, chromosomal localization, expression, and functional characterization of the mouse analogue of human CD59. *Journal of Immunology* **158:** 1692-1702

Pruitt K, Pruitt WM, Bilter GK, Westwick JK, Der CJ (2002) Raf-independent deregulation of p38 and JNK mitogen-activated protein kinases are critical for Ras transformation. *Journal of Biological Chemistry* **277:** 31808-31817

Qian YM, Qin XB, Miwa T, Sun XJ, Halperin JA, Song WC (2000) Identification and functional characterization of a new gene encoding the mouse terminal complement inhibitor CD59. *Journal of Immunology* **165:** 2528-2534

Qiu W, Zhang Y, Liu X, Zhou J, Li Y, Zhou Y, Shan K, Xia M, Che N, Feng X, Zhao D, Wang Y (2012) Sublytic C5b-9 complexes induce proliferative changes of glomerular mesangial cells in rat Thy-1 nephritis through TRAF6-mediated PI3K-dependent Akt1 activation. *Journal of Pathology* **226:** 619-632

Quackenbush J (2002) Microarray data normalization and transformation. *Nature Genetics* **32:** 496-501

Qureshi SA, Saldittgeorgieff M, Darnell JE (1995) TYROSINE-PHOSPHORYLATED STAT1 AND STAT2 PLUS A 48-KDA PROTEIN ALL CONTACT DNA IN FORMING INTERFERON-STIMULATED-GENE FACTOR-3. *Proceedings of the National Academy of Sciences of the United States of America* **92:** 3829-3833

Radisky DC, Levy DD, Littlepage LE, Liu H, Nelson CM, Fata JE, Leake D, Godden EL, Albertson DG, Nieto MA, Werb Z, Bissell MJ (2005) Rac1b and reactive oxygen species mediate MMP-3-induced EMT and genomic instability. *Nature* **436:** 123-127

Raghuwanshi SK, Su YJ, Singh V, Haynes K, Richmond A, Richardson RM (2012) The Chemokine Receptors CXCR1 and CXCR2 Couple to Distinct G Protein-Coupled Receptor Kinases To Mediate and Regulate Leukocyte Functions. *Journal of Immunology* **189:** 2824-2832

Rameh LE, Arvidsson AK, Carraway KL, Couvillon AD, Rathbun G, Crompton A, VanRenterghem B, Czech MP, Ravichandran KS, Burakoff SJ, Wang DS, Chen CS, Cantley LC (1997) A comparative analysis of the phosphoinositide binding specificity of pleckstrin homology domains. *Journal of Biological Chemistry* **272:** 22059-22066

Ramm LE, Whitlow MB, Koski CL, Shin ML, Mayer MM (1983) Elimination of complement channels from the plasma membranes of U937, a nucleated mammalian cell line: temperature dependence of the elimination rate. *J Immunol* **131:** 1411-1415

Rasmuson A, Kock A, Fuskevåg OM, Kruspig B, Simón-Santamaría J, Gogvadze V, Johnsen JI, Kogner P, Sveinbjörnsson B (2012) Autocrine prostaglandin E2 signaling promotes tumor cell survival and proliferation in childhood neuroblastoma. *PLoS One* **7:** e29331

Rassool FV, Gaymes TJ, Omidvar N, Brady N, Beurlet S, Pla M, Reboul M, Lea N, Chomienne C, Thomas NS, Mufti GJ, Padua RA (2007) Reactive oxygen species, DNA damage, and error-prone repair: a model for genomic instability with progression in myeloid leukemia? *Cancer Res* **67:** 8762-8771

Rawal N, Pangburn MK (2001) Structure/function of C5 convertases of complement. *Int Immunopharmacol* **1:** 415-422

Reiter Y, Ciobotariu A, Fishelson Z (1992) Sublytic complement attack protects tumor cells from lytic doses of antibody and complement. *Eur J Immunol* **22:** 1207-1213

Reiter Y, Ciobotariu A, Jones J, Morgan BP, Fishelson Z (1995) COMPLEMENT MEMBRANE ATTACK COMPLEX, PERFORIN, AND BACTERIAL EXOTOXINS INDUCE IN K562 CELLS CALCIUM-DEPENDENT CROSS-PROTECTION FROM LYSIS. *Journal of Immunology* **155:** 2203-2210

Ribaux P, Ehses JA, Lin-Marq N, Carrozzino F, Boni-Schnetzler M, Hammar E, Irminger J-C, Donath MY, Halban PA (2007) Induction of CXCL1 by extracellular matrix and autocrine enhancement by interleukin-1 in rat pancreatic beta-cells. *Endocrinology* **148:** 5582-5590

Richter R, Becker M, Harlozinska A, Golubska B (1977) HETEROLOGOUS REACTIVITY OF INVITRO CULTURED MOUSE CELLS WITH NATURAL HUMAN-SERUM ANTIBODIES. *Archivum Immunologiae Et Therapiae Experimentalis* **25:** 93-99

Riedemann NC, Guo RF, Sarma VJ, Laudes IJ, Huber-Lang M, Warner RL, Albrecht EA, Speyer CL, Ward PA (2002) Expression and function of the C5a receptor in rat alveolar epithelial cells. *J Immunol* **168:** 1919-1925

Ripoche J, Day AJ, Harris TJR, Sim RB (1988) THE COMPLETE AMINO-ACID SEQUENCE OF HUMAN-COMPLEMENT FACTOR-H. *Biochemical Journal* **249**

Rockett JC, Hellmann GM (2004) Confirming microarray data - is it really necessary? *Genomics* **83:** 541-549

Rodriguezviciana P, Warne PH, Dhand R, Vanhaesebroeck B, Gout I, Fry MJ, Waterfield MD, Downward J (1994) PHOSPHATIDYLINOSITOL-3-OH KINASE AS A DIRECT TARGET OF RAS. *Nature* **370:** 527-532

Roeb E, Arndt M, Jansen B, Schumpelick V, Matern S (2004) Simultaneous determination of matrix metalloproteinase (MMP)-7, MMP-1,-3, and-13 gene expression by multiplex PCR in colorectal carcinomas. *International Journal of Colorectal Disease* **19:** 518-524

Rose TM, Weiford DM, Gunderson NL, Bruce AG (1994) ONCOSTATIN-M (OSM) INHIBITS THE DIFFERENTIATION OF PLURIPOTENT EMBRYONIC STEM-CELLS IN-VITRO. *Cytokine* **6:** 48-54

Rosette C, Karin M (1996) Ultraviolet light and osmotic stress: Activation of the JNK cascade through multiple growth factor and cytokine receptors. *Science* **274:** 1194-1197

Ross GD, Newman SL, Lambris JD, Devery-Pocius JE, Cain JA, Lachmann PJ (1983) Generation of three different fragments of bound C3 with purified factor I or serum. II. Location of binding sites in the C3 fragments for factors B and H, complement receptors, and bovine conglutinin. *J Exp Med* **158:** 334-352

Rozen S, Skaletsky H (2000) Primer3 on the WWW for general users and for biologist programmers. *Methods in molecular biology (Clifton, NJ)* **132:** 365-386

Rubie C, Frick VO, Wagner M, Schuld J, Graeber S, Brittner B, Bohle RM, Schilling MK (2008) ELR plus CXC chemokine expression in benign and malignant colorectal conditions. *Bmc Cancer* **8**

Rus H, Niculescu F, Badea T, Shin ML (1997) Terminal complement complexes induce cell cycle entry in oligodendrocytes through mitogen activated protein kinase pathway. *Immunopharmacology* **38:** 177-187

Rus HG, Niculescu F, Shin ML (1996) Sublytic complement attack induces cell cycle oligodendrocytes - S phase induction is dependent on c-jun activation. *Journal of Immunology* **156:** 4892-4900

Ruseva MM, Hughes TR, Donev RM, Sivasankar B, Pickering MC, Wu X, Harris CL, Morgan BP (2009) Crry deficiency in complement sufficient mice: C3 consumption occurs without associated renal injury. *Molecular Immunology* **46:** 803-811

Sacks T, Moldow CF, Craddock PR, Bowers TK, Jacob HS (1978) Oxygen radicals mediate endothelial cell damage by complement-stimulated granulocytes. An in vitro model of immune vascular damage. *J Clin Invest* **61:** 1161-1167

Sahin U, Weskamp G, Kelly K, Zhou HM, Higashiyama S, Peschon J, Hartmann D, Saftig P, Blobel CP (2004) Distinct roles for ADAM10 and ADAM17 in ectodomain shedding of six EGFR ligands. *Journal of Cell Biology* **164:** 769-779

Saiki RK, Walsh PS, Levenson CH, Erlich HA (1989) GENETIC-ANALYSIS OF AMPLIFIED DNA WITH IMMOBILIZED SEQUENCE-SPECIFIC OLIGONUCLEOTIDE PROBES. *Proceedings of the National Academy of Sciences of the United States of America* **86:** 6230-6234

Sakurai T, He G, Matsuzawa A, Yu GY, Maeda S, Hardiman G, Karin M (2008) Hepatocyte necrosis induced by oxidative stress and IL-1 alpha release mediate carcinogen-induced compensatory proliferation and liver tumorigenesis. *Cancer Cell* **14:** 156-165

Saviozzi S, Cordero F, Lo Iacono M, Novello S, Scagliotti GV, Calogero RA (2006) Selection of suitable reference genes for accurate normalization of gene expression profile studies in non-small cell lung cancer. *BMC cancer* **6:** 200-200

Schaeffer HJ, Weber MJ (1999) Mitogen-activated protein kinases: Specific messages from ubiquitous messengers. *Molecular and Cellular Biology* **19:** 2435-2444

Schafer DP, Lehrman EK, Kautzman AG, Koyama R, Mardinly AR, Yamasaki R, Ransohoff RM, Greenberg ME, Barres BA, Stevens B (2012) Microglia Sculpt Postnatal Neural Circuits in an Activity and Complement-Dependent Manner. *Neuron* **74:** 691-705

Schena M, Shalon D, Davis RW, Brown PO (1995) QUANTITATIVE MONITORING OF GENE-EXPRESSION PATTERNS WITH A COMPLEMENTARY-DNA MICROARRAY. *Science* **270:** 467-470

Schlager SI, Ohanian SH, Borsos T (1978) Stimulation of the synthesis and release of lipids in tumor cells under attack by antibody and C. *J Immunol* **120:** 895-901

Scholzen T, Gerdes J (2000) The Ki-67 protein: from the known and the unknown. *J Cell Physiol* **182:** 311-322

Schonermark M, Deppisch R, Riedasch G, Rother K, Hansch GM (1991) INDUCTION OF MEDIATOR RELEASE FROM HUMAN GLOMERULAR MESANGIAL CELLS BY THE TERMINAL COMPLEMENT COMPONENTS C5B-9. *International Archives of Allergy and Applied Immunology* **96:** 331-337

Schreibe.Ad, Frank MM (1972) ROLE OF ANTIBODY AND COMPLEMENT IN IMMUNE CLEARANCE AND DESTRUCTION OF ERYTHROCYTES .1. IN-VIVO EFFECTS OF IGG AND IGM COMPLEMENT-FIXING SITES. *Journal of Clinical Investigation* **51:** 575-&

Schulze A, Lehmann K, Jefferies HBJ, McMahon M, Downward J (2001) Analysis of the transcriptional program induced by Raf in epithelial cells. *Genes & Development* **15:** 981-994

Schumacher WA, Fantone JC, Kunkel SE, Webb RC, Lucchesi BR (1991) The anaphylatoxins C3a and C5a are vasodilators in the canine coronary vasculature in vitro and in vivo. *Agents Actions* **34:** 345-349

Schwaeble WJ, Reid KB (1999) Does properdin crosslink the cellular and the humoral immune response? *Immunol Today* **20:** 17-21

Scolding NJ, Morgan BP, Houston WA, Linington C, Campbell AK, Compston DA (1989) Vesicular removal by oligodendrocytes of membrane attack complexes formed by activated complement. *Nature* **339:** 620-622

Sekine H, Takahashi M, Iwaki D, Fujita T (2013) The Role of MASP-1/3 in Complement Activation. *Adv Exp Med Biol* **734:** 41-53

Seya T, Ballard LL, Bora NS, Kumar V, Cui WY, Atkinson JP (1988) DISTRIBUTION OF MEMBRANE COFACTOR PROTEIN OF COMPLEMENT ON HUMAN PERIPHERAL-BLOOD CELLS - AN ALTERED FORM IS FOUND ON GRANULOCYTES. *European Journal of Immunology* **18:** 1289-1294

Seya T, Turner JR, Atkinson JP (1986) PURIFICATION AND CHARACTERIZATION OF A MEMBRANE-PROTEIN (GP45-70) THAT IS A COFACTOR FOR CLEAVAGE OF C3B AND C4B. *Journal of Experimental Medicine* **163**

Shi XX, Zhang B, Zang JL, Wang GY, Gao MH (2009) CD59 silencing via retrovirus-mediated RNA interference enhanced complement-mediated cell damage in ovary cancer. *Cell Mol Immunol* **6:** 61-66

Shoyab M, Plowman GD, McDonald VL, Bradley JG, Todaro GJ (1989) STRUCTURE AND FUNCTION OF HUMAN AMPHIREGULIN - A MEMBER OF THE EPIDERMAL GROWTH-FACTOR FAMILY. *Science* **243:** 1074-1076

Shreffler DC (1976) S REGION OF MOUSE MAJOR HISTOCOMPATIBILITY COMPLEX (H-2) - GENETIC-VARIATION AND FUNCTIONAL ROLE IN COMPLEMENT-SYSTEM. *Transplantation Reviews* **32:** 140-167

Shukla A, Barrett TF, Nakayama KI, Nakayama K, Mossman BT, Lounsbury KM (2006) Transcriptional up-regulation of MMP12 and MMP13 by asbestos occurs via a PKC delta-dependent pathway in murine lung. *Faseb Journal* **20:** 997-+

Shyamala V, Khoja H (1998) Interleukin-8 receptors R1 and R2 activate mitogen-activated protein kinases and induce c-fos, independent of Ras and Raf-1 in Chinese hamster ovary cells. *Biochemistry* **37:** 15918-15924

Silvers AL, Bachelor MA, Bowden GT (2003) The role of JNK and p38 MAPK activities in UVA-induced signaling pathways leading to AP-1 activation and c-fos expression. *Neoplasia* **5:** 319-329

Silversmith RE, Nelsestuen GL (1986) INTERACTION OF COMPLEMENT PROTEIN-C5B-6 AND PROTEIN-C5B-7 WITH PHOSPHOLIPID-VESICLES - EFFECTS OF PHOSPHOLIPID STRUCTURAL FEATURES. *Biochemistry* **25:** 7717-7725

Sim RB, Discipio RG (1982) PURIFICATION AND STRUCTURAL STUDIES ON THE COMPLEMENT-SYSTEM CONTROL PROTEIN BETA-1H (FACTOR-H). *Biochemical Journal* **205:** 285-293

Sims PJ, Wiedmer T (1986) Repolarization of the membrane potential of blood platelets after complement damage: evidence for a Ca++ -dependent exocytotic elimination of C5b-9 pores. *Blood* **68:** 556-561

Skonier J, Neubauer M, Madisen L, Bennett K, Plowman GD, Purchio AF (1992) CDNA CLONING AND SEQUENCE-ANALYSIS OF BETA-IG-H3, A NOVEL GENE INDUCED IN

A HUMAN ADENOCARCINOMA CELL-LINE AFTER TREATMENT WITH TRANSFORMING GROWTH-FACTOR-BETA. *DNA and Cell Biology* **11:** 511-522

Soane L, Cho HJ, Niculescu F, Rus H, Shin ML (2001) C5b-9 terminal complement complex protects oligodendrocytes from death by regulating bad through phosphatidylinositol 3-kinase/Akt pathway. *Journal of Immunology* **167:** 2305-2311

Soane L, Rus H, Niculescu F, Shin ML (1999) Inhibition of oligodendrocyte apoptosis by sublytic C5b-9 is associated with enhanced synthesis of Bcl-2 and mediated by inhibition of caspase-3 activation. *Journal of Immunology* **163**

Southern EM (2001) DNA microarrays. History and overview. *Methods Mol Biol* **170:** 1-15

Spandidos A, Wang X, Wang H, Seed B (2010) PrimerBank: a resource of human and mouse PCR primer pairs for gene expression detection and quantification. *Nucleic Acids Research* **38:** D792-D799

Spiekstra SW, Breetveld M, Rustemeyer T, Scheper RJ, Gibbs S (2007) Wound-healing factors secreted by epidermal keratinocytes and dermal fibroblasts in skin substitutes. *Wound Repair and Regeneration* **15:** 708-717

Sternlicht MD, Lochter A, Sympson CJ, Huey B, Rougler JP, Gray JW, Pinkel D, Bissell MJ, Werb Z (1999) The stromal proteinase MMP3/stromelysin-1 promotes mammary carcinogenesis. *Cell* **98:** 137-146

Stocker W, Grams F, Baumann U, Reinemer P, Gomisruth FX, McKay DB, Bode W (1995) THE METZINCINS - TOPOLOGICAL AND SEQUENTIAL RELATIONS BETWEEN THE ASTACINS, ADAMALYSINS, SERRALYSINS, AND MATRIXINS (COLLAGENASES) DEFINE A SUPERFAMILY OF ZINC-PEPTIDASES. *Protein Science* **4:** 823-840

Strieter RM, Polverini PJ, Kunkel SL, Arenberg DA, Burdick MD, Kasper J, Dzuiba J, Vandamme J, Walz A, Marriott D, Chan SY, Roczniak S, Shanafelt AB (1995) THE FUNCTIONAL-ROLE OF THE ELR MOTIF IN CXC CHEMOKINE-MEDIATED ANGIOGENESIS. *Journal of Biological Chemistry* **270:** 27348-27357

Sukhatme VP, Cao XM, Chang LC, Tsaimorris CH, Stamenkovich D, Ferreira PCP, Cohen DR, Edwards SA, Shows TB, Curran T, Lebeau MM, Adamson ED (1988) A ZINC FINGER-ENCODING GENE COREGULATED WITH C-FOS DURING GROWTH AND DIFFERENTIATION, AND AFTER CELLULAR DEPOLARIZATION. *Cell* **53:** 37-43

Suzuki M, Raab G, Moses MA, Fernandez CA, Klagsbrun M (1997) Matrix metalloproteinase-3 releases active heparin-binding EGF-like growth factor by cleavage at a specific juxtamembrane site. *Journal of Biological Chemistry* **272:** 31730-31737

Takabayashi T, Vannier E, Burke JF, Tompkins RG, Gelfand JA, Clark BD (1998) Both C3a and C3a(desArg) regulate interleukin-6 synthesis in human peripheral blood mononuclear cells. *J Infect Dis* **177:** 1622-1628

Takabayashi T, Vannier E, Clark BD, Margolis NH, Dinarello CA, Burke JF, Gelfand JA (1996) A new biologic role for C3a and C3a desArg: regulation of TNF-alpha and IL-1 beta synthesis. *J Immunol* **156:** 3455-3460

Takahashi H, Ogata H, Nishigaki R, Broide DH, Karin M (2010) Tobacco smoke promotes lung tumorigenesis by triggering IKKbeta- and JNK1-dependent inflammation. *Cancer Cell* **17:** 89-97

Takano T, Cybulsky AV (2000) Complement C5b-9-mediated arachidonic acid metabolism in glomerular epithelial cells - Role of cyclooxygenase-1 and-2. *American Journal of Pathology* **156:** 2091-2101

Tamhane AC, Dunlop DD (2000) *Statistics and data analysis : from elementary to intermediate*, Upper Saddle River, N.J.: Prentice Hall ; London : Prentice-Hall International (UK).

Tanaka S, Suzuki T, Sakaizumi M, Harada Y, Matsushima Y, Miyashita N, Fukumori Y, Inai S, Moriwaki K, Yonekawa H (1991) GENE RESPONSIBLE FOR DEFICIENT ACTIVITY OF THE BETA-SUBUNIT OF C8, THE 8TH COMPONENT OF COMPLEMENT, IS LOCATED ON MOUSE CHROMOSOME-4. *Immunogenetics* **33:** 18-23

Tarca AL, Romero R, Draghici S (2006) Analysis of microarray experiments of gene expression profiling. *American Journal of Obstetrics and Gynecology* **195:** 373-388

Tedesco F, Pausa M, Nardon E, Introna M, Mantovani A, Dobrina A (1997) The cytolytically inactive terminal complement complex activates endothelial cells to express adhesion molecules and tissue factor procoagulant activity. *Journal of Experimental Medicine* **185:** 1619-1627

Thiel S (2007) Complement activating soluble pattern recognition molecules with collagen-like regions, mannan-binding lectin, ficolins and associated proteins. *Mol Immunol* **44:** 3875-3888

Thomas J, Webb W, Davitz MA, Nussenzweig V (1987) DECAY ACCELERATING FACTOR DIFFUSES RAPIDLY ON HELAAE CELL-SURFACES. *Biophysical Journal* **51:** A522-A522

Tian H, Qian GW, Li W, Chen FF, Di JH, Zhang BF, Pei DS, Ma P, Zheng JN (2010) A critical role of Sp1 transcription factor in regulating the human Ki-67 gene expression. *Tumour Biol* **32:** 273-283

Tirosh R, Degani H, Berke G (1984) Prelytic reduction of high-energy phosphates induced by antibody and complement in nucleated cells. 31P-NMR study. *Complement* **1:** 207-212

Toh B, Wang X, Keeble J, Sim WJ, Khoo K, Wong W-C, Kato M, Prevost-Blondel A, Thiery J-P, Abastado J-P (2011) Mesenchymal Transition and Dissemination of Cancer Cells Is Driven by Myeloid-Derived Suppressor Cells Infiltrating the Primary Tumor. *Plos Biology* **9**

Toprak NU, Yagci A, Gulluoglu BM, Akin ML, Demirkalem P, Celenk T, Soyletir G (2006) A possible role of Bacteroides fragilis enterotoxin in the aetiology of colorectal cancer. *Clin Microbiol Infect* **12:** 782-786

Torbohm I, Schonermark M, Wingen AM, Berger B, Rother K, Hansch GM (1990) C5B-8 AND C5B-9 MODULATE THE COLLAGEN RELEASE OF HUMAN GLOMERULAR EPITHELIAL-CELLS. *Kidney International* **37:** 1098-1104

Tsujimura A, Shida K, Kitamura M, Nomura M, Takeda J, Tanaka H, Matsumoto M, Matsumiya K, Okuyama A, Nishimune Y, Okabe M, Seya T (1998) Molecular cloning of a murine homologue of membrane cofactor protein (CD46): preferential expression in testicular germ cells. *Biochemical Journal* **330:** 163-168

Turley EA, Veiseh M, Radisky DC, Bissell MJ (2008) Mechanisms of disease: epithelial-mesenchymal transition - does cellular plasticity fuel neoplastic progression? *Nature Clinical Practice Oncology* **5:** 280-290

van de Wiel MA, Costa JL, Smid K, Oudejans CBM, Bergman AM, Meijer GA, Peters GJ, Ylstra B (2005) Expression microarray analysis and oligo array comparative genomic hybridization of acquired gemcitabine resistance in mouse colon reveals selection for chromosomal aberrations. *Cancer Research* **65:** 10208-10213

van Rossum DB, Patterson RL, Cheung K-H, Barrow RK, Syrovatkina V, Gessell GS, Burkholder SG, Watkins DN, Foskett JK, Snyder SH (2006) DANGER, a novel regulatory protein of inositol 1,4,5-trisphosphate-receptor activity. *Journal of Biological Chemistry* **281:** 37111-37116

Vandenberg CW, Cinek T, Hallett MB, Horejsi V, Morgan BP (1995) EXOGENOUS GLYCOSYL PHOSPHATIDYLINOSITOL-ANCHORED CD59 ASSOCIATES WITH KINASES IN MEMBRANE CLUSTERS ON U937 CELLS AND BECOMES CA2+-SIGNALING COMPETENT. *Journal of Cell Biology* **131:** 669-677

Vangelder RN, Vonzastrow ME, Yool A, Dement WC, Barchas JD, Eberwine JH (1990) AMPLIFIED RNA SYNTHESIZED FROM LIMITED QUANTITIES OF HETEROGENEOUS CDNA. *Proceedings of the National Academy of Sciences of the United States of America* **87:** 1663-1667

Viedt C, Hansch GM, Brandes RP, Kubler W, Kreuzer J (2000) The terminal complement complex C5b-9 stimulates interleukin-6 production in human smooth muscle cells through activation of transcription factors NF-kappa B and AP-1. *Faseb Journal* **14:** 2370-2372

Virchow R, Chance F (1971) *Cellular pathology : as based on physiological and pathological histology*, [1st ed., reprinted] / with a new introductory essay by L.J. Rather. edn. New York: Dover Publications ; London : Constable.

Visse R, Nagase H (2003) Matrix metalloproteinases and tissue inhibitors of metalloproteinases - Structure, function, and biochemistry. *Circulation Research* **92:** 827-839

Vlahos CJ, Matter WF, Hui KY, Brown RF (1994) A SPECIFIC INHIBITOR OF PHOSPHATIDYLNOSITOL 3-KINASE, 2-(4-MORPHOLINYL)-8-PHENYL-4H-1-BENZOPYRAN-4-ONE (LY294002). *Journal of Biological Chemistry* **269:** 5241-5248

Vogt W (1986) Anaphylatoxins: possible roles in disease. *Complement* **3:** 177-188

Vorup-Jensen T, Jensenius JC, Thiel S (1998) MASP-2, the C3 convertase generating protease of the MBLectin complement activating pathway. *Immunobiology* **199:** 348-357

Wagner C, Braunger M, Beer M, Rother K, Hansch GM (1994) INDUCTION OF MATRIX PROTEIN-SYNTHESIS IN HUMAN GLOMERULAR MESANGIAL CELLS BY THE TERMINAL COMPLEMENT COMPLEX. *Experimental Nephrology* **2:** 51-56

Wai PY, Mi Z, Guo H, Sarraf-Yazdi S, Gao C, Wei J, Marroquin CE, Clary B, Kuo PC (2005) Osteopontin silencing by small interfering RNA suppresses in vitro and in vivo CT26 murine colon adenocarcinoma metastasis. *Carcinogenesis* **26:** 741-751

Walport MJ (2001a) Complement. First of two parts. *New England Journal of Medicine* **344:** 1058-1066

Walport MJ (2001b) Complement. Second of two parts. *New England Journal of Medicine* **344:** 1140-1144

Wang C, Deng L, Hong M, Akkaraju GR, Inoue J, Chen ZJJ (2001) TAK1 is a ubiquitin-dependent kinase of MKK and IKK. *Nature* **412:** 346-351

Wang DZ, Wang HB, Brown J, Daikoku T, Ning W, Shi Q, Richmond A, Strieter R, Dey SK, DuBois RN (2006) CXCL1 induced by prostaglandin E-2 promotes angiogenesis in colorectal cancer. *Journal of Experimental Medicine* **203:** 941-951

Wang KX, Denhardt DT (2008) Osteopontin: Role in immune regulation and stress responses. *Cytokine & Growth Factor Reviews* **19:** 333-345

Wang Q, Rozelle AL, Lepus CM, Scanzello CR, Song JJ, Larsen DM, Crish JF, Bebek G, Ritter SY, Lindstrom TM, Hwang IY, Wong HDH, Punzi L, Encarnacion A, Shamloo M, Goodman SB, Wyss-Coray T, Goldring SR, Banda NK, Thurman JM, Gobezie R, Crow MK, Holers VM, Lee DM, Robinson WH (2011) Identification of a central role for complement in osteoarthritis. *Nature Medicine* **17:** 1674-U1196

Wang XW, Seed B (2003a) A PCR primer bank for quantitative gene expression analysis. *Nucleic Acids Research* **31**

Wang XW, Seed B (2003b) Selection of oligonucleotide probes for protein coding sequences. *Bioinformatics* **19:** 796-802

Watson JD, Crick FH (1974) Molecular structure of nucleic acids: a structure for deoxyribose nucleic acid. J.D. Watson and F.H.C. Crick. Published in Nature, number 4356 April 25, 1953. *Nature* **248:** 765-765

Watson NF, Durrant LG, Madjd Z, Ellis IO, Scholefield JH, Spendlove I (2006) Expression of the membrane complement regulatory protein CD59 (protectin) is associated with reduced survival in colorectal cancer patients. *Cancer Immunol Immunother* **55:** 973-980

Weiler JM, Daha MR, Austen KF, Fearon DT (1976) CONTROL OF AMPLIFICATION CONVERTASE OF COMPLEMENT BY PLASMA-PROTEIN BETA-1H. *Proceedings of the National Academy of Sciences of the United States of America* **73:** 3268-3272

Wennstrom S, Downward J (1999) Role of phosphoinositide 3-kinase in activation of Ras and mitogen-activated protein kinase by epidermal growth factor. *Molecular and Cellular Biology* **19:** 4279-4288

Whaley K, Ruddy S (1976) MODULATION OF C3B HEMOLYTIC ACTIVITY BY A PLASMA-PROTEIN DISTINCT FROM C3B INACTIVATOR. *Science* **193:** 1011-1013

Wiechert L, Nemeth J, Pusterla T, Bauer C, De Ponti A, Manthey S, Marhenke S, Vogel A, Klingmueller U, Hess J, Angel P (2012) Hepatocyte-specific S100a8 and S100a9 transgene expression in mice causes Cxcl1 induction and systemic neutrophil enrichment. *Cell Communication and Signaling* **10**

Wiedmer T, Ando B, Sims PJ (1987) Complement C5b-9-stimulated platelet secretion is associated with a Ca2+-initiated activation of cellular protein kinases. *J Biol Chem* **262:** 13674-13681

Willmarth NE, Ethier SP (2006) Autocrine and juxtacrine effects of amphiregulin on the proliferative, invasive, and migratory properties of normal and neoplastic human. *Journal of Biological Chemistry* **281:** 37728-37737

Wilson JG, Tedder TF, Fearon DT (1983) CHARACTERIZATION OF HUMAN LYMPHOCYTES-T THAT EXPRESS THE C3B-RECEPTOR. *Journal of Immunology* **131:** 684-689

Wong AK, Finch AM, Pierens GK, Craik DJ, Taylor SM, Fairlie DP (1998) Small molecular probes for G-protein-coupled C5a receptors: Conformationally constrained antagonists derived from the C terminus of the human plasma protein C5a. *Journal of Medicinal Chemistry* **41:** 3417-3425

Wong BR, Besser D, Kim N, Arron JR, Vologodskaia M, Hanafusa H, Choi Y (1999) TRANCE, a TNF family member, activates Akt/PKB through a signaling complex involving TRAF6 and c-Src. *Molecular Cell* **4:** 1041-1049

Wu H, Arron JR (2003) TRAF6, a molecular bridge spanning adaptive immunity, innate immunity and osteoimmunology. *Bioessays* **25:** 1096-1105

Wu S, Rhee KJ, Albesiano E, Rabizadeh S, Wu X, Yen HR, Huso DL, Brancati FL, Wick E, McAllister F, Housseau F, Pardoll DM, Sears CL (2009) A human colonic commensal promotes colon tumorigenesis via activation of T helper type 17 T cell responses. *Nat Med* **15:** 1016-1022

Wu X, Spitzer D, Mao D, Peng SL, Molina H, Atkinson JP (2008) Membrane protein Crry maintains homeostasis of the complement system. *Journal of Immunology* **181:** 2732-2740

Wurzner R, Orren A, Potter P, Morgan BP, Ponard D, Spath P, Brai M, Schulze M, Happe L, Gotze O (1991) FUNCTIONALLY ACTIVE COMPLEMENT PROTEINS C6 AND C7 DETECTED IN C6-DEFICIENT AND C7-DEFICIENT INDIVIDUALS. *Clinical and Experimental Immunology* **83:** 430-437

Yamakawa M, Yamada K, Tsuge T, Ohrui H, Ogata T, Dobashi M, Imai Y (1994) PROTECTION OF THYROID-CANCER CELLS BY COMPLEMENT-REGULATORY FACTORS. *Cancer* **73:** 2808-2817

Yamamoto KI, Gewurz G (1978) The complex of C5b and C6: isolation, characterization, and identification of a modified form of C5b consisting of three polypeptide chains. *J Immunol* **120:** 2008-2015

Yan J, Allendorf DJ, Li B, Yan R, Hansen R, Donev R (2008) The role of membrane complement regulatory proteins in cancer immunotherapy. *Adv Exp Med Biol* **632:** 159-174

Yang G, Roser DG, Zhang Z, Bast RC, Jr., Mills GB, Colacino JA, Mercado-Uribe I, Liu J (2006) The chemokine growth-regulated oncogene 1 (Gro-1) links RAS signaling to the senescence of stromal fibroblasts and ovarian tumorigenesis. *Proceedings of the National Academy of Sciences of the United States of America* **103:** 16472-16477

Yang HT, Cohen P, Rousseau S (2008) IL-1 beta-stimulated activation of ERK1/2 and p38 alpha MAPK mediates the transcriptional up-regulation of IL-6, IL-8 and GRO-alpha in HeLa cells. *Cellular Signalling* **20:** 375-380

Yang L, DeBusk LM, Fukuda K, Fingleton B, Green-Jarvis B, Shyr Y, Matrisian LM, Carbone DP, Lin PC (2004) Expansion of myeloid immune suppressor Gr+CD11b+cells in tumor-bearing host directly promotes tumor angiogenesis. *Cancer Cell* **6:** 409-421

Yang W-L, Wang J, Chan C-H, Lee S-W, Campos AD, Lamothe B, Hur L, Grabiner BC, Lin X, Darnay BG, Lin H-K (2009) The E3 Ligase TRAF6 Regulates Akt Ubiquitination and Activation. *Science* **325:** 1134-1138

Ye H, Wu H (2000) Thermodynamic characterization of the interaction between TRAF2 and tumor necrosis factor receptor peptides by isothermal titration calorimetry. *Proceedings of the National Academy of Sciences of the United States of America* **97:** 8961-8966

Ye Q, Yan Z, Liao X, Li Y, Yang J, Sun J, Kawano T, Wang X, Cao Z, Wang Z, Huang L (2011) MUC1 induces metastasis in esophageal squamous cell carcinoma by upregulating matrix metalloproteinase 13. *Laboratory Investigation* **91:** 778-787

Ytting H, Jensenius JC, Christensen IJ, Thiel S, Nielsen HJ (2004) Increased activity of the mannan-binding lectin complement activation pathway in patients with colorectal cancer. *Scand J Gastroenterol* **39:** 674-679

Zhang GX, Zhao ZQ, Wang HD, Hao B (2004) Enhancement of osteopontin expression in HepG2 cells by epidermal growth factor via phosphatidylinositol 3-kinase signaling pathway. *World J Gastroenterol* **10:** 205-208

Zhang Q-X, Nakhaei-Nejad M, Haddad G, Wang X, Loutzenhiser R, Murray AG (2011) Glomerular endothelial PI3 kinase-alpha couples to VEGFR2, but is not required for eNOS activation. *American Journal of Physiology-Renal Physiology* **301:** F1242-F1250

Zhang XG, Gu JJ, Lu ZY, Yasukawa K, Yancopoulos GD, Turner K, Shoyab M, Taga T, Kishimoto T, Bataille R, Klein B (1994) CILIARY NEUROTROPIC FACTOR, INTERLEUKIN-11, LEUKEMIA INHIBITORY FACTOR, AND ONCOSTATIN-M ARE GROWTH-FACTORS FOR HUMAN MYELOMA CELL-LINES USING THE INTERLEUKIN-6 SIGNAL TRANSDUCER GP130. *Journal of Experimental Medicine* **179:** 1337-1342

Zhao WP, Zhu B, Duan YZ, Chen ZT (2009) Neutralization of complement regulatory proteins CD55 and CD59 augments therapeutic effect of herceptin against lung carcinoma cells. *Oncol Rep* **21:** 1405-1411

Zhou W (2012) The new face of anaphylatoxins in immune regulation. *Immunobiology* **217:** 225-234

Zhou X, Hu W, Qin X (2008) The role of complement in the mechanism of action of rituximab for B-cell lymphoma: implications for therapy. *Oncologist* **13:** 954-966

Ziccardi RJ (1981) Activation of the early components of the classical complement pathway under physiologic conditions. *J Immunol* **126:** 1769-1773

Zigrino P, Kuhn I, Bauerle T, Zamek J, Fox JW, Neumann S, Licht A, Schorpp-Kistner M, Angel P, Mauch C (2009) Stromal Expression of MMP-13 Is Required for Melanoma Invasion and Metastasis. *Journal of Investigative Dermatology* **129:** 2686-2693

8 Appendices